Memory Consolidation during Sleep. On the Function of Neuronal Oscillations in Brain Plasticity.

Dissertation

zur Erlangung des Doktorgrades
der Philosophischen Fakultät
der Christian-Albrechts-Universität
zu Kiel

vorgelegt von
Til Ole Bergmann

Kiel 2010

Erstgutachter: Prof. Dr. Roman Ferstl
Zweitgutachter: Prof. Dr. Hartwig R. Siebner
Drittgutachter: Prof. Dr. Udo Konradt
Tag der mündlichen Prüfung: 12.05.2010
Durch den Prodekan Prof. Dr. Rainer Zaiser
zum Druck genehmigt am: 28.05.2010

It may turn out that the rhythms of the brain are also the rhythms of the mind.

– György Buzsáki

Acknowledgements

First and foremost I wish to thank my supervisor Prof. Hartwig R. Siebner who gave me the opportunity to work in this fascinating field of research. He taught me much of what I know about neuroscience, its methods, its mechanisms, and its community and supported me generously in numerous ways.

I am further greatly thankful to Prof. Roman Ferstl who not only aroused my interest for neuroscience early during my course of studies, but also kindly sponsored my dissertation project from the very beginning until its completion.

For their scientific support, I wish to thank Dr. Matthias Mölle who patiently introduced me into the world of sophisticated EEG analyses as well as PD Dr. Lisa Marshall who by her pioneering work on slow oscillatory stimulation provided the basis for a part of this thesis.

Many thanks to Prof. Jan Born who as a leading expert in the field of sleep-dependent memory consolidation gave helpful advice to my projects and welcomed me in his lab were I enjoyed my education on polysomnography and sleep scoring.

I am also grateful to Prof. Günther Deuschl for affiliating me in his department and providing the infrastructure for my scientific development.

For continuous scientific and methodological discussion as well as enjoyable every day office life I thank my friends and colleagues from Kiel: Oliver Granert (special thanks to your programming skills!), Gesa Hartwigsen, Christoph Ritter, Dr. Sergiu Groppa, Tanja Kassuba, Arne Knutzen, Anke Hoff (thanks for keeping the lab running!), Dr. Michael Weiss, and Dr. Martin Peller.

I am also grateful to my friends and colleagues from Lübeck for interesting discussions on sleep and memory and for making my time in there a personally enriching experience: Dr. Björn Rasch (now in Basel, CH), Susanne Diekelmann, Ines Wilhelm, Dr. Ulrich Wagner (now in Bangor, UK), Sabine Groch, Manfred Hallschmid, Dr. Christian Benedict (now in Uppsala, SE), Prof. Kerstin Oltmanns, and Anja Otterbein.

For their tremendous help with conducting the experiments and data preprocessing I am very thankful to (in alphabetical order): Alexander Nowak, Christoph Lindner, David Witzki, Janina von Borstel, Jens Diedrichs, Juliane Döhring, Katharina Benz,

Lena Jacobsen, Leval Kaja-Yildiz, Markus Seeger, Marlit Schmidt, Regina Fischer, and Thorsten Holstad.

Further, I wish to thank Stephan Wolff who introduced me into the handling of the MRI scanner and gave helpful technical support, Dr. PD Stephan Ulmer who more than once provided neuroradiological consultation, and Prof. Olaf Jansen who kindly gave me access to the 3T MRI scanner during the nights, thus making my sleep fMRI-EEG experiments possible.

Beyond any professional acknowledgements, I wish to express my gratitude to my parents for their personal support and confidence and to all my friends preserving me from complete social isolation during the times of extensive data collection.

Finally and most important, my very special thanks go to Christin Haselbeck, the woman I love. She gave me so much emotional support and understanding when once again my free time was running short and sleep experiments kept me away from home during the nights. Thank you so much for sharing life with me!

Til Ole Bergmann

The research presented in this thesis received financial support from the German Scientific Society: *SFB 654 „Plasticity and Sleep“*, *Project A6 „Neocortical processing modes of the sleeping brain as a neuronal substrate for memory consolidation in humans”*

List of Relevant Publications

This thesis is based on the following research papers:

I. Siebner, H. R., **Bergmann, T. O.**, Bestmann, S., Massimini, M., Johansen-Berg, H., Mochizuki, H., Bohning, D. E., Boorman, E. D., Groppa, S., Miniussi, C., Pascual-Leone, A., Huber, R., Taylor, P. C., Ilmoniemi, R. J., De Gennaro, L., Strafella, A. P., Kähkönen, S., Klöppel, S., Frisoni, G. B., George, M. S., Hallett, M., Brandt, S. A., Rushworth, M. F., Ziemann, U., Rothwell, J. C., Ward, N., Cohen, L. G., Baudewig, J., Paus, T., Ugawa, Y., Rossini, P. M. (2009). Consensus paper: Combining transcranial stimulation with neuroimaging. *Brain Stimulation*, 2(2), 58-80.

II. **Bergmann, T. O.,** Molle, M., Marshall, L., Kaya-Yildiz, L., Born, J., & Siebner, H. R. (2008). A local signature of LTP- and LTD-like plasticity in human NREM sleep. *European Journal of Neuroscience, 27*(9), 2241-2249.

III. Mölle, M., **Bergmann, T. O.**, Marshall, L., & Born, J. (in prep). Slow and fast spindles grouped in opposite phase during slow sleep oscillations.

IV. **Bergmann, T. O.**, Mölle, M., Diedrichs, J., Born, J., & Siebner, H. R. (in prep). Sleep spindles drive learning-specific hippocampo-neocortical reactivation.

V. **Bergmann, T. O.**, Groppa, S., Seeger, M., Mölle, M., Marshall, L., & Siebner, H. R. (2009). Acute changes in motor cortical excitability during slow oscillatory and constant anodal transcranial direct current stimulation. *Journal of Neurophysiology*, 102(4): 2303-2311.

VI. Groppa, S., **Bergmann, T. O.**, Siems, C., Mölle, M., Marshall, L., & Siebner, H. R. (2010). Slow-oscillatory transcranial DC stimulation can induce bidirectional shifts in motor cortical excitability in awake humans. *Neuroscience*, 166(4): 1219-1225.

Contents

1 Introduction

Why do we sleep? This seemingly simple question is actually among the most intriguing ones in contemporary neuroscience. Given the fact that sleep comes with the total loss of consciousness, it makes us completely vulnerable to any dangers of the environment for a third of our life time. As the state of sleep has developed in presumably all species (Cirelli & Tononi, 2008; but see Siegel, 2008) it must yield a strong evolutionary advantage by serving an essential function for the organism that compensates for its tremendous costs (for an alternative perspective see Siegel, 2009).

But what exactly is this critical function? Although the entire body may benefit from sleep in terms of metabolic restoration and recovery of muscles from preceding activities, this could be achieved just as well by periods of quiet wakefulness without sleep's most hazardous drawback of loosing consciousness. However, since falling asleep is inevitably accompanied by the fading of consciousness, it is obviously the brain for which it is indispensable to periodically shift its state to one incompatible with conscious information processing. This notion is corroborated by the fact that sleep deprivation is associated with massive cognitive impairments and cannot be prolonged indefinitely, as after some time sleeplike brain activity unavoidably intrudes into wakefulness and as sleep-specific neuronal patterns are even more pronounced during subsequent recovery sleep (Cirelli & Tononi, 2008).

So what happens in the sleeping brain that cannot be achieved during wakefulness? To begin with, during sleep compared to wakefulness the brain state is markedly altered regarding gene transcription (Cirelli, Gutierrez, & Tononi, 2004), immunological factors (Marshall & Born, 2002), endocrine and neurochemical levels (Kalia, 2006; Siegel, 2004) and electrophysiological processes (Steriade, Timofeev, & Grenier, 2001), providing a beneficial environment for a variety of brain functions. However, not all these functions were necessarily critical to the ontogenetic emergence of sleep but may have been allocated to that state after or during its evolutionary development. For example, there might be some adventitious metabolic functions, such as restoring depleted neuronal resources (Benington & Heller, 1995) or removing neurotoxic substances that have accumulated during wakefulness (Reimund, 1994). However, the most intriguing option for a core function of sleep be-

ing mostly favored in the last decades is that sleep serves brain plasticity (Born, Rasch, & Gais, 2006; Diekelmann & Born, 2010; Hobson & Pace-Schott, 2002; Maquet, 2001; Sejnowski & Destexhe, 2000; Steriade & Timofeev, 2003; Stickgold, 2005; Tononi & Cirelli, 2006).

Brain plasticity refers to the capability of the brain to change its own structure based on past experience in order to adapt its function to future challenges. It is thus one of the brain's most essential features and of vital importance to the organism, justifying the high costs of sleep. While brain plasticity on a cellular level refers to the strengthening or weakening of synaptic connections between individual neurons, it results on the system level in the modification of neuronal networks composed of numerous interconnected neurons from various brain regions. The exact configuration of these networks is generally considered to make up the neuronal representations constituting our memories.

The two major aspects of sleep-dependent brain plasticity currently proposed are (i) on a synaptic level, the homeostatic regulation of synaptic weights to maintain a functional level of plasticity throughout life (Tononi & Cirelli, 2006) and (ii) on a systemic level, the consolidation of initially labile newly acquired memory traces and their integration into existing memory representations (Born et al., 2006; Diekelmann & Born, 2010). While the existence of these beneficial effects of sleep on brain plasticity is nowadays scarcely raised to question (but see Siegel, 2001; Vertes, 2004), its underlying neuronal mechanisms are still poorly understood. However, promising models have emerged in the last few years, pointing out the critical role of sleep-specific *neuronal oscillations* in brain plasticity (Born et al., 2006; Diekelmann & Born, 2010; Marshall & Born, 2007; Rasch & Born, 2007; Tononi & Cirelli, 2006). *Neuronal oscillations* refer to rhythmically reverberating neuronal activity. A hierarchy of these brain rhythms with different origin, propagation, and frequency, mostly emerging from the interaction of distributed neuronal populations, is organizing the timing of information processing of the brain (for an excellent review of this topic see Buzsaki, 2006).

These models are gaining more and more empirical evidence but are still in need of bridging some substantial explanatory gaps. Nevertheless, they have already set the ground for pioneering attempts to use emerging neuromodulatory techniques (like oscillatory transcranial direct current stimulation; tDCS) to interact with the ongoing oscillatory activity during sleep and facilitate memory consolidation (Marshall,

Helgadottir, Mölle, & Born, 2006). This promising approach has to be refined and set on a more elaborated neurophysiological basis to become a possible therapeutic tool in the future. The work presented in this thesis is therefore part of the scientific endeavor to uncover the neuronal processes mediating sleep-dependent brain plasticity on both the synaptic and the systemic level, thus also providing the basis for neuromodulatory developments.

In the further course of the introduction, I will first outline the neuronal mechanisms of synaptic plasticity (Section 1.1.1) and shortly describe the most established concepts of human memory systems as well as the *standard theory of memory consolidation* (Section 1.1.2). I will then briefly review the current knowledge about sleep-specific neuronal oscillations and their specific features and interactions (Section 1.2). Finally, both topics will be linked by introducing the *synaptic homeostasis hypothesis* (Tononi & Cirelli, 2003, 2006) (Section 1.3.1) and the idea of a sleep-dependent *active system consolidation* through reactivation and redistribution of memories (Born et al., 2006; Diekelmann & Born, 2010; Marshall & Born, 2007; Rasch & Born, 2007) (Section 1.3.2). Both theories will be substantiated by empirical evidence and will be set into correspondence with each other (Section 1.3.3). Hereafter, I will make some general methodological considerations regarding the applied multimodal neuroscientific approach (Section 2). I will then outline the results of my own empirical studies (Section 3) which can be found in greater detail in the original papers included in the appendix. I will end up with a general discussion of my empirical findings in the context of the existing literature and their implications for future research (Section 4), and close with the main conclusions (Section 5).

1.1 The Neuronal Basis of Memory Consolidation

Memory generally refers to the ability of an organism's neuronal system to encode, maintain, and retrieve information. Though maintenance is often taken for granted, it actually requires a process of active consolidation. The term "*consolidation"* was first introduced by Müller & Pilzecker more than a century ago (G. E. Müller & Pilzecker, 1900) and refers to the idea that learning does not instantaneously induce permanent memories but that newly acquired memory traces are initially labile and take time to get stabilized (or consolidated). Therefore, memories remain vulnerable to disruption

by psychological (e.g. *retroactive interference*) or biological factors (e.g. *protein synthesis inhibitors*) for a certain time window after learning. During the last century of psychological and neuroscientific research this idea has become sort of a fact (for recent comments see Lechner, Squire, & Byrne, 1999; McGaugh, 2000). However, the term *consolidation* commonly refers to two different types of processes: (i) *synaptic consolidation*, taking place within minutes to hours on the level of single neurons and (ii) *system consolidation*, taking much longer (from hours do years) and depending on the reorganization and redistribution of memory engrams across distant brain regions (Figure 1-1) (Dudai, 2004).

Although nature and complexity of memory systems vary strongly across as within species, they all rely more or less on the same molecular and cellular mechanisms. An understanding of these basic principles of learning and memory at single neurons is of crucial importance also for gaining insight into the functioning of more complex large-scale memory systems. I shall therefore provide a brief summary of some major features of synaptic plasticity and its consolidation before turning to the idea of system consolidation in higher-order memory systems with a focus on hippocampus-dependent declarative memory.

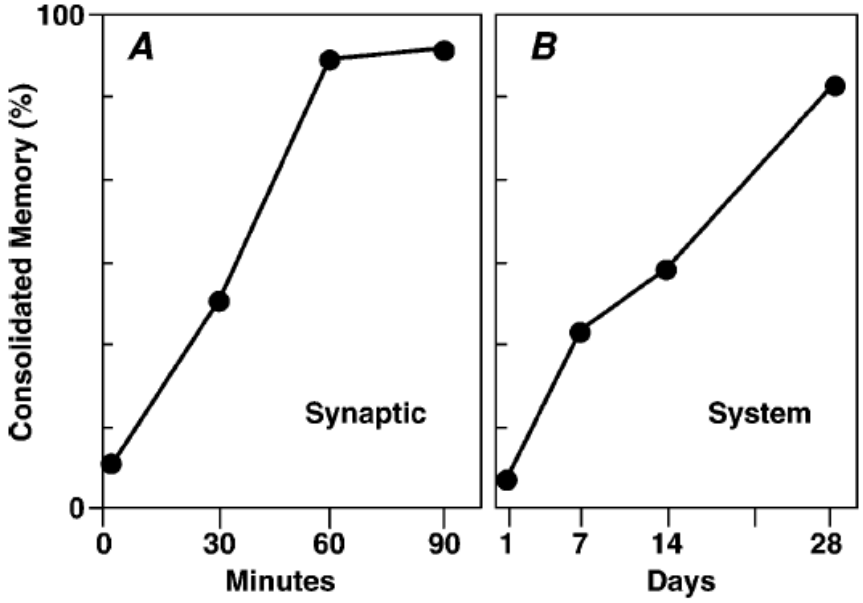

Figure 1-1: Types of consolidation. (A) The time course of *synaptic consolidation* had been determined by probing the sensitivity of memory to the inhibition of protein synthesis in the goldfish. **(B)** The time course of *system consolidation* was derived from measuring the sensitivity of long-term fear memory in contextual conditioning in the rat. (Taken from Dudai, 2004).

1.1.1 Synaptic Level

What is memory on a synaptic level? It can mainly be seen as the initial functional strengthening and weakening of synaptic connections between individual neurons which is potentially followed by structural changes including the formation or elimination of synapses, changing the impact of one neuron's firing on that of another. The very conditions under which synapses are shortly (learning) or long-lastingly (synaptic consolidation) altered in their function and structure make up the rules of synaptic plasticity. Although additional forms of plasticity have been discovered, the most important ones are still considered to be the N-methyl D-aspartate (NMDA)-receptor-dependent long-term synaptic potentiation and depression of fast glutamatergic excitatory postsynaptic potentials (EPSPs) (Kim & Linden, 2007). I will thus refrain from taking into account other e.g. metabotropic glutamate receptors (mGluR)-mediated forms, as an exhaustive review of the topic is far beyond the scope of this thesis.

1.1.1.1 Long-term Potentiation (LTP)

Since the initial discovery of long-term potentiation (LTP) by high-frequency tetanic stimulation of hippocampal neurons in the anaesthetized rabbit in 1973 by Bliss and Lømo (Bliss & Lømo, 1973), the phenomenon has been intensively studied in a variety of species and neuronal structures. It has been found to be a ubiquitous but not a unitary phenomenon, being mediated by numerous different mechanisms (Malenka & Bear, 2004). However, focusing on the most widely studied form found in the adult CA1 region of the mammalian hippocampus, LTP is roughly based on the following processes (Citri & Malenka, 2008; Kandel, 2001; Lynch, 2004; Malenka & Bear, 2004; Sweatt, 1999) which can be divided into an early (E-LTP) and a late phase (L-LTP). Roughly, E-LTP and L-LTP could be considered as *synaptic learning* and *synaptic consolidation*, respectively.

The induction of E-LTP occurs when the amount of calcium (Ca^{2+}) in the postsynaptic cell exceeds a certain threshold. The influx of extracellular calcium, however, requires the activation of NMDA-receptor controlled Ca^{2+}-conducting ion channels, opening only when two conditions are fulfilled. First, a sufficient amount of postsynaptic depolarization has to be achieved by sodium influx due to the activation of glutamate-dependent α-amino-3-hydroxyl-5-methyl-4-isoxazole-propionate (AMPA)

receptors, which relieves a magnesium blockade from the NMDA receptor. Second, the NMDA-receptor itself has to be activated by presynaptic glutamate release. This is why the NMDA receptor is called a “coincidence detector”, as it initiates LTP only at those synapses which received a presynaptic input temporarily tightly coupled to an EPSP strong enough for actually resulting in postsynaptic firing of the neuron. Now, the increased Ca^{2+} concentration activates a series off enzymes including calcium/calmodulin-dependent protein kinase II (CaMKII), protein kinase C (PKC), protein kinase A (PKA), and mitogen-activated protein kinase (MAPK). CaMKII and PKC in turn phosphorylate existing AMPA receptors to increase their activity and mediate the integration of stored AMPA receptors into the postsynaptic membrane, a process termed *AMPA receptor trafficking* (Figure 1-2). In addition to these postsynaptic processes, retrograde messengers are synthesized, traveling across the synaptic cleft and triggering a cascade of presynaptic processes such as increasing the number and facilitating the release of neurotransmitter vesicles. Together these post- and presynaptic processes of E-LTP, which are completely independent of protein synthesis, cause a functional increase in the synaptic efficacy.

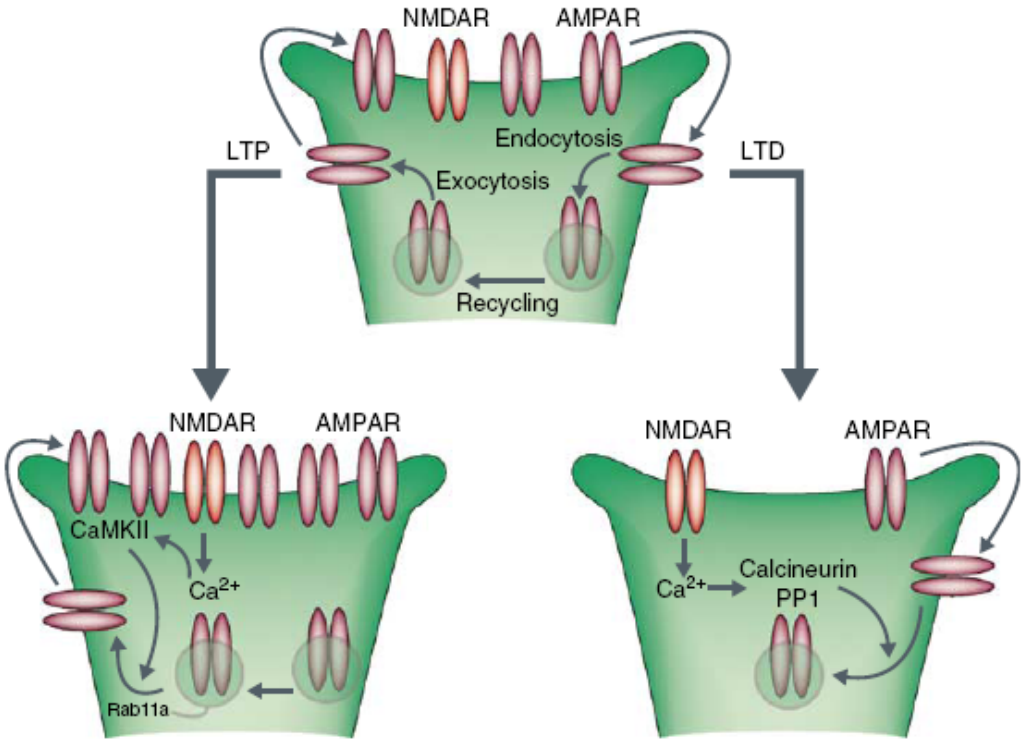

Figure 1-2: Functional changes during the early phases of long-term potentiation (E-LTP) and depression (E-LTD). AMPA receptors (AMPAR) are incorporated (LTP) or removed (LTD) from the postsynaptic membrane, thereby increasing (LTP) or decreasing (LTD) synaptic efficacy. (Taken from Citri & Malenka, 2008)

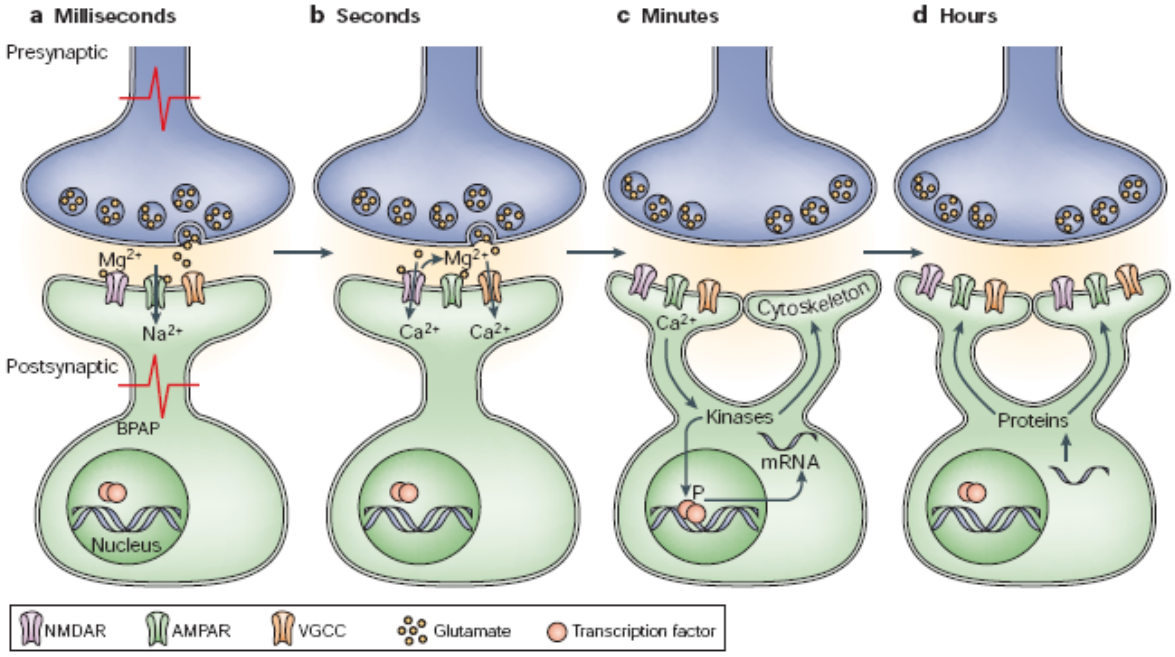

Figure 1-3: Structural changes during the late phase of long-term potentiation (L-LTP). Initial functional strengthening within seconds is followed by a long-lasting structural modification of the synapse and growth of new dendritic spines. (Taken from Lamprecht & LeDoux, 2004).

During the subsequent phase of L-LTP, the persistent activation of certain kinases, e.g. MAPK, causes the phosphorylation of numerous transcription factors like the cAMP response element binding protein (CREB). These in turn cause gene transcription and the synthesis of various proteins, eventually leading to structural modifications including enlargement of the postsynaptic membrane and even the growth of new dendritic spines (Figure 1-3). Additionally, also presynaptic modifications in the axon bouts are triggered, presumably via signaling of retrograde messengers. Thus, during L-LTP existing synapses grow in size and new synapses can be formed (Lamprecht & LeDoux, 2004).

1.1.1.2 Long-term Depression (LTD)

Long-term depression (LTD) can be considered as the complement of LTP. Although much less is known about its exact mechanisms, it mainly follows the same but reversed principles as LTP (Citri & Malenka, 2008; Malenka & Bear, 2004), with analog early (E-LTD) and late phases (L-LTD). It has however to be distinguished from a phenomenon termed *depotentiation* (Barrionuevo, Schottler, & Lynch, 1980), in which merely previous potentiation of synapses is disrupted or reversed. Again neglecting

e.g. mGluR- or endocanabinoid-mediated forms, LTD is the NMDA receptor-dependent novel induction of a long-lasting decrease in EPSPs. It has first been shown by Dudek and Bear in 1992 for low-frequency stimulation of the Schaffer collaterals in the CA1 region of hippocampal slices (Dudek & Bear, 1992).

Like with LTP, the initiation of LTD is dependent on NMDA receptor mediated Ca^{2+} influx into the postsynaptic dendrites, although the influx is prolonged and considerably lower than for LTP. Regardless of the yet unknown precise mechanisms it seems to be the case that Ca^{2+} activated protein phosphatases dephosphorylate existing AMPA receptors (Figure 1-2), causing their inactivation as well as their internalization into the postsynaptic cytoplasm. Presumably, the maintenance of LTD also requires protein synthesis which leads to structural changes, i.e. the reduction in size and number of existing synapses (Citri & Malenka, 2008; Malenka & Bear, 2004).

1.1.1.3 Spike Timing-Dependent Plasticity (STDP)

The above described neuronal mechanisms of LTP and LTD provide the biological basis for a principle already proposed in 1949 by Donald Hebb and summarized in the simplified statement "*what fires together, wires together*". Unbeknown to the biochemical findings of today's neuroscience he stated what later has become famous as "Hebb's rule":

"*When an axon of cell A is near enough to excite a cell B and repeatedly or persistently takes part in firing it, some growth process or metabolic change takes place in one or both cells such that A's efficiency, as one of the cells firing B, is increased*." (Hebb, 1949, p. 50).

By thoroughly investigating the exact timing of action potentials in connected neurons later research (Levy & Steward, 1983) could refine his ideas by adding important temporal information, thereby defining the rules of spike timing-dependent plasticity (STDP, for a recent review see Caporale & Dan, 2008). While Hebb's original rule focused on the mere coincidence of two neurons firing, STDP adds causality to the equation. That is, LTP is induced when the postsynaptic neuron fires in close temporal vicinity (i.e. in the order of milliseconds) after the presynaptic neuron (*pre-post spiking*). Conversely, LTD is induced when the postsynaptic neuron fires already before it has obtained input from the presynaptic one (*post-pre spiking*) (Figure 1-4).

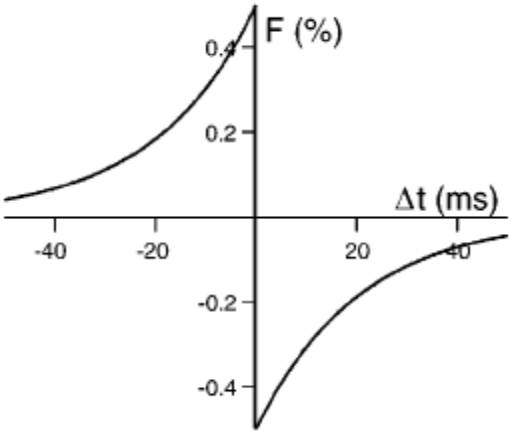

Figure 1-4: The spike timing-dependent plasticity (STDP) modification function. The diagram displays percent change in synaptic strength (F%) as a function of the time delay between pre- and postsynaptic spiking (Δt, pre minus post). (Taken from Song, Miller, & Abbott, 2000).

Thereby, STDP reflects the fact that in the first case activation of the presynaptic neuron could have causally contributed to the excitation of the postsynaptic neuron, while it could not have in the latter. STDP also appears to rely on NMDS receptors and Ca^{2+} influx characteristics, but the understanding of its exact mechanisms is less clear. However, the interaction of NMDA receptor kinetics with the backpropagation of action potentials from the axon hillock to the postsynaptic dendrites by means of voltage-gated Ca^{2+}-channels might be of particular importance (Caporale & Dan, 2008).

1.1.1.4 Homeostatic Metaplasticity

Together, these activity-dependent mechanisms of synaptic plasticity are a powerful means for modulating the response properties and association of individual neurons and thereby presumably provide the very basis of learning and memory. However, there comes a danger with it. For neuronal networks to remain stable and efficient over time, plasticity has to be coordinated appropriately to avoid the dysfunctional and excessive growth or shrinkage of synapses and of accompanied reverberating activity (Abbott & Nelson, 2000; Abraham, 2008). And indeed, there seem to be certain cellular mechanisms that, depending on the activation history of a neuron, prevent the saturation of LTP and LTD by inhibiting repeated plasticity of the same direction. This form of plasticity regularization has been termed "*metaplasticity*" (Abraham

& Bear, 1996; Abraham & Tate, 1997) or "*homeostatic metaplasticity*" (Abraham, 2008; Ziemann & Siebner, 2008). While "*meta*" refers to the higher-order nature of the plasticity, i.e. plasticity of synaptic plasticity, the term "*homeostatic*" indicates that plasticity, i.e. the bidirectional inducibility of both LTP and LTD, is kept in a certain functional range.

One of the most influential models of homeostatic metaplasticity is the Bienenstock-Cooper-Munro (BCM) model of bidirectional plasticity (Bienenstock, Cooper, & Munro, 1982). This model has two principal features. First, resembling a modified form of Hebb's rule, it describes the extend of LTP or LTD as a function of postsynaptic firing relative to the presynaptic input (Figure 1-5). If presynaptic input is delivered while the postsynaptic neuron fires, LTP is induced, while presynaptic input during low postsynaptic activity induces LTD. Second, the crossover point between LTP and LTD, termed *modification threshold*, is sliding and can be modified by previous postsynaptic activity. That is, previously high postsynaptic firing rates shift the modification threshold to the right, thereby increasing the threshold for LTP induction, while LTD is facilitated. Conversely, prolonged inactivation of the postsynaptic neuron shifts the threshold to the left, thus making LTP more likely to occur, while decreasing the probability of further LTD induction.

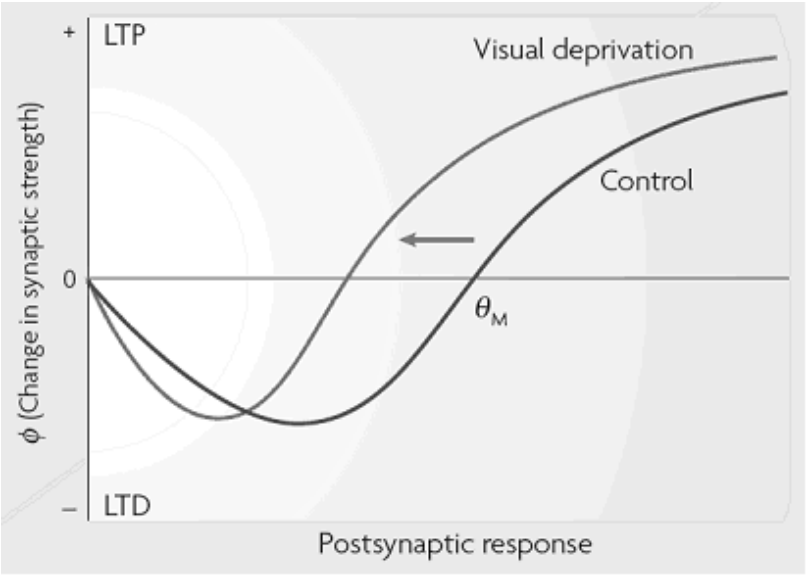

Figure 1-5: The Bienenstock-Cooper-Munro (BCM) model of bidirectional plasticity. The extend of induced LTP or LTD (Φ) is modeled as function of the postsynaptic response, with the *modification threshold* (θ_M) marking the transition from potentiation to depression. The diagram shows the shifting of θ_M (from dark to light grey line) in direction of LTP facilitation due to prolonged low postsynaptic activity (visual deprivation). See text for a more detailed description. (Taken from Abraham, 2008).

Later, the intracellular postsynaptic Ca^{2+} level has been proposed as the crucial parameter constituting the threshold between LTP and LTD (Gold & Bear, 1994) as CA^{2+} is a key trigger for both LTP and LTD induction. Although the exact mechanisms underlying the shifting of the modification threshold are still under investigation, empirical evidence supporting the BCM model predictions has accumulated (Abraham, 2008).

1.1.2 Systems Level

Processes of synaptic plasticity as described above (or similar to those) are most likely the very basis of and a necessary prerequisite for all types of memory. However, the complexity of human memory can certainly not be understood without taking into account the systemic features of involved large-scale neuronal networks. In the last decades, a general taxonomy (Figure 1-6) of different, though interacting, memory systems has been constructed (Squire & Zola, 1996).

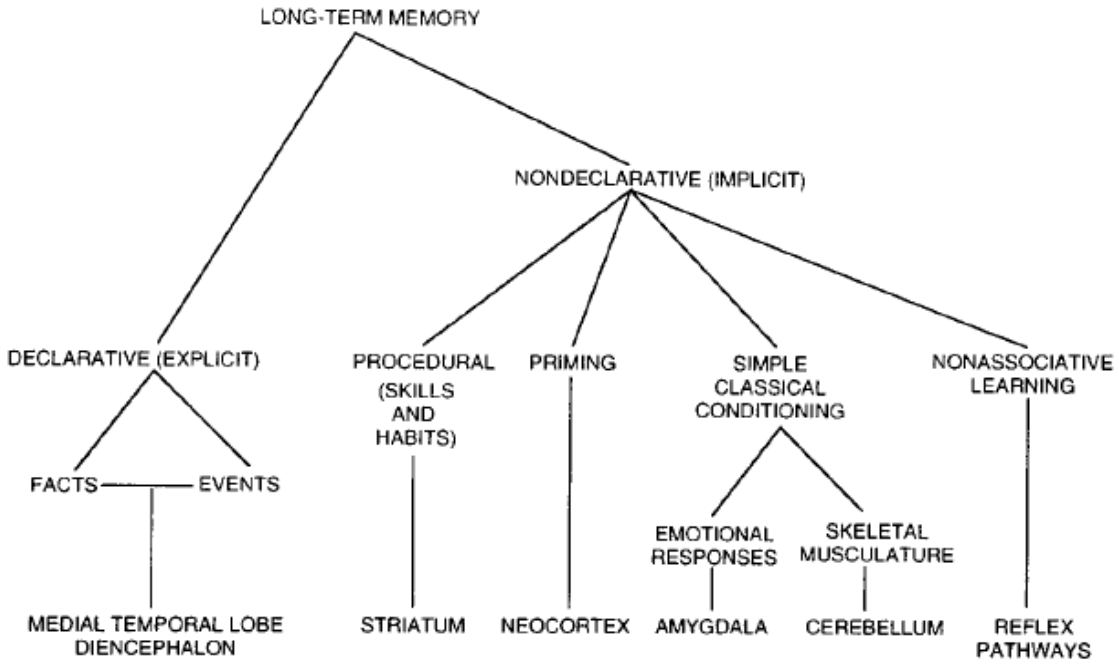

Figure 1-6: Traditional taxonomy of human memory systems. The various forms of human memory have been organized in a hierarchical system with declarative and non-declarative memory as major divisions. Though maybe oversimplified from today's perspective, a rough assignment of responsible brain structures has already been provided more than a decade ago. (Taken from Squire & Zola, 1996).

In the following, I will mainly focus on the declarative memory system, however, with respect to its importance in research on sleep-dependent memory consolidation, I will also briefly introduce the procedural memory system, responsible for the acquisition of motor skills.

1.1.2.1 Declarative Memory

Declarative memories are those of verbalizable content and can be separated into knowledge of facts (*semantic memory*) and memories for events of mostly autobiographic nature (*episodic memory*) (Tulving, 1972). As cases of amnestic patients have repeatedly shown (Kopelman & Kapur, 2001), encoding of declarative memories in general and at least retrieval of episodic memories essentially relies on the functional integrity of the medial temporal lobe, especially the hippocampal system (Squire, Stark, & Clark, 2004; Tulving, 2002).

The hippocampal system, located in the medial temporal lobe (Figure 1-7), is specialized on associating neuronal representations distributed throughout the entire brain (Greenberg & Rubin, 2003). Receiving its main inputs from unimodal and polymodal association areas, the tightly interconnected perirhinal and parahippocampal cortices preprocess the information and pass it on to the entorhinal cortex which is the major informational backbone of the hippocampal system. It provides in- and output for the hippocampal region (dentate gyrus, CA1 and CA3 fields of the hippocampus proper, and subiculum) and connects it to prefrontal areas involved in the organization of memory encoding and retrieval (Eichenbaum, 2000; Squire et al., 2004; Squire & Zola-Morgan, 1991). Due to its functional architecture, the hippocampal system is therefore capable of both the encoding of episodic memories by indexing neuronal representations of perceptual, motor, and cognitive information involved in the original experience of a given situation and subsequent reconstitution by simultaneous reactivation of the associated engrams (Teyler & DiScenna, 1986). The hippocampal system is therefore not believed to be the actual storage site of the remembered episodes but rather links the appropriate representations stored at their respective processing sites, such as higher-order sensory areas as well as prefrontal, temporal and parietal association cortices (Greenberg & Rubin, 2003).

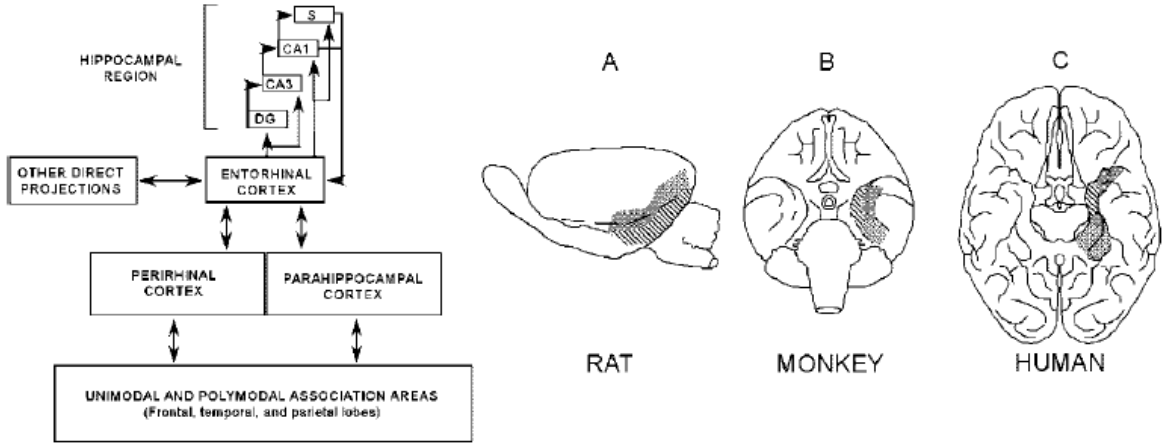

Figure 1-7: The medial temporal lobe memory system. (Left) A rough connection scheme of medial temporal lobe structures important for declarative memory. S = subiculum; DG = dentate gyrus; CA = cornu ammonis. **(Right)** Location of the perirhinal cortex (gray), entorhinal cortex (diagonal stripes), and parahippocampal cortex (mottled shading) in **(A)** rat, **(B)** monkey , and **(C)** human. (Taken from Squire et al., 2004).

Moreover, various subregions of the prefrontal cortex subserve the initiation, monitoring, and assessment of declarative memory retrieval (Fletcher & Henson, 2001; Simons & Spiers, 2003), while the posterior cingulate gyrus (Burgess, 2008; Maddock, 1999), the adjacent precuneus (Cavanna & Trimble, 2006), and the lateral parietal lobes (Wagner, Shannon, Kahn, & Buckner, 2005) are probably involved in the visuospatial reconstruction during memory recollection.

Memories do not remain static but their neuronal representations seem to be reorganized with time when they mature from recent to remote memories. This was noted because the older a memory, the more resistant it becomes against brain injury (Ribot, 1882), specifically against damage of the medial temporal lobes (Rempel-Clower, Zola, Squire, & Amaral, 1996), a fact also termed *Ribot's law*. Initial findings in human patients were replicated in large number of animal experiments were hippocampal lesions could be experimentally induced (for a review on these studies see Frankland & Bontempi, 2005). The still most influential idea about consolidation in the declarative memory system, nowadays termed the *standard consolidation model*, argues for the existence of complementary learning systems in hippocampus and neocortex (McClelland, McNaughton, & O'Reilly, 1995). While the hippocampus is a fast learner, able to rapidly adapt its synaptic weights for representation of newly acquired information, the neocortex is much slower and needs multiple repetitions to

encode new information. Thus, the hippocampus makes one-trial learning possible, whereas the neocortex has to incorporate new information carefully without interfering with existing representations. The core idea is that new information is transferred from the hippocampus to the neocortex by repeated reactivation of those neocortical representations that were initially bound by the hippocampus (Buzsaki, 1989; Frankland & Bontempi, 2005; McClelland et al., 1995; Squire & Alvarez, 1995). With time, new cortico-cortical connections are formed while hippocampo-neocortical connections are weakened, and eventually the memory becomes independent of the hippocampus (Figure 1-8). During the course of hippocampo-neocortical memory transfer the prefrontal cortex might partly take over the integrating role of the hippocampus, indexing the neocortical representations of remote memories. As mentioned previously, it is therefore in an ideal position to trigger, monitor, assess, and regulate the retrieval of remote memories (Frankland & Bontempi, 2005). By now, the standard consolidation model as well as its extension regarding the role of the prefrontal cortex have gained accumulating evidence also from functional imaging studies (Frankland & Bontempi, 2006; Takashima et al., 2009; Takashima et al., 2006) and animal research (Peyrache, Khamassi, Benchenane, Wiener, & Battaglia, 2009; Ribeiro et al., 2004).

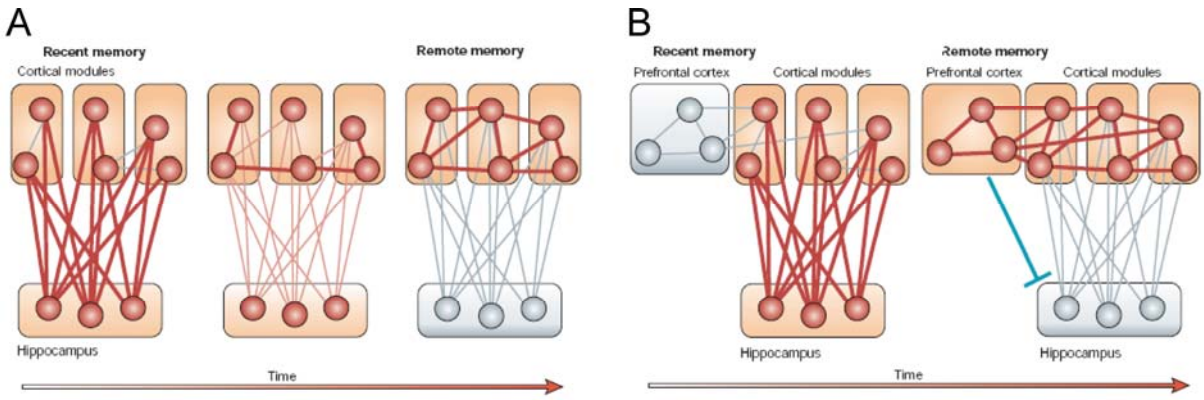

Figure 1-8: Reorganization of hippocampo-neocortical memory representations. (A) The standard consolidation model. Initially, the hippocampus binds the neocortical representations forming a certain memory. With time repeated joint reactivations of neocortical representations build up new cortico-cortical connections, hippocampo-neocortical connections are weakened, and the memory eventually becomes independent of the hippocampus. **(B)** Potential role of the prefrontal cortex. When memories mature the prefrontal cortex might partially take over the integrative role of the hippocampus. The prefrontal cortex not only triggers the retrieval of remote information but also regulates the uptake of new memories, e.g. preventing the encoding of redundant information. (Modified after Frankland & Bontempi, 2005).

The standard model of consolidation has however not remained unchallenged. Most prominent is the so called *multiple trace theory of consolidation* (Nadel & Moscovitch, 1997), assuming that the standard model holds true for semantic memories, as the process of hippocampo-neocortical transfer might also be one of abstraction and episodic-to-semantic conversion, whereas the vivid and self-referenced nature of episodic memories remains dependent of the hippocampus throughout life. It is argued that each reactivation takes place in another experiential context, thus making up a new hippocampo-neocortical memory trace. With time, mediated by the increased number of reactivations, a certain episodic memory has become represented by multiple traces. The theory therefore predicts that a (very rare) complete hippocampal lesion would also result in a complete loss of episodic memory, while (mostly studied) partial lesions would only affect some of the traces with a higher probability for remote memories to survive. As there is also neuroimaging data in support of this hypothesis (Bosshardt, Degonda et al., 2005; Bosshardt, Schmidt et al., 2005), it is an ongoing debate on how Ribot's law is best explained.

1.1.2.2 Procedural Memory

Procedural memory represents a non-declarative type of memory which also relies on large-scale circuits, consisting of neocortical (primary and secondary motor and sensory cortices, premotor cortex, supplementary motor area), cerebellar, and subcortical structures (thalamus and basal ganglia). Despite the natural variety of motor skills (be it in sports, playing a musical instrument, or typewriting), laboratory experiments can essentially be divided into two major paradigms, that is (1) the acquisition of new motor sequences and (ii) the adaptation of well established movements to changed environmental conditions (Doyon & Benali, 2005).

Learning of motor skills initially requires effort and attention, but after repeated practice becomes effortless and unconsciously available. Moreover, beside overt training, performance of motor skills seems to strongly benefit from the mere passage of time (Krakauer & Shadmehr, 2006). Thus, following the initial phase of comparably fast skill acquisition, also procedural memory undergoes a slow process of reorganization in which parts of the circuit become dispensable and new circuits are incorporated that were not involved during initial encoding (Dudai, 2004). According

to Doyon and Ungerleider, initial acquisition of new motor skills relies on the interaction of cortico-striatal and cortico-cerebellar systems (Doyon & Ungerleider, 2002). During the subsequent phase of slow consolidation, the basal ganglia are proposed to be crucial for motor sequence learning, while the cerebellum is more important for adaptive motor skills. Recent neuroimaging evidence had led to a refinement of the model, now taking also into account the involvement of the hippocampus in motor sequence learning (Albouy et al., 2008; Doyon & Benali, 2005). However, while the existence of system consolidation in procedural memory is generally accepted, much less is known about its exact mechanisms than it is the case for declarative memory.

Although early models of system consolidation were not explicit about an active function of sleep, it has always been considered a brain state beneficial for the reactivation of memory traces, as was quite wakefulness (McClelland et al., 1995). However, beside the mere lack of sensory interference, sleep might also offer features actively subserving processes of system consolidation in both declarative and procedural memory. The following chapter will therefore outline the neurochemical environment and the prominent sleep-specific neuronal oscillations, rendering it a unique environment for brain plasticity and the reactivation of memories.

1.2 Oscillations of the Sleeping Brain

What is so special about sleep? First and foremost, it is not a state of neuronal inactivity, as initially thought, giving rise to the phrase "*death's little brother*". The opposite is the case: the sleeping brain is highly active. Although cerebral energy metabolism slightly decreases (5-10%) with the deepening of sleep (Hobson & Pace-Schott, 2002; Kalia, 2006), mean neuronal firing rates are sometimes comparable to wakefulness (Destexhe, Hughes, Rudolph, & Crunelli, 2007; Steriade et al., 2001). Nevertheless, sleep is the most fundamental yet physiological shift in the brain's neuronal processing mode. I will briefly outline the regulatory mechanisms of sleep and its architecture before elaborating the specific neuronal oscillations, representing the electrophysiological hallmarks of sleep.

1.2.1 Regulation and Architecture of Sleep

The nature of sleep appears as an hierarchical nesting of oscillatory patterns on different time scales. To begin on the most macroscopic level, phases of sleep and wakefulness are usually alternating on a circadian basis, driven by internal clock genes and entrained by external signals of night and day (Cirelli, 2009; Franken & Dijk, 2009). In Borbély's famous *two-process model of sleep regulation* (Figure 1-9) (Borbely, 2009; Borbély, 1980; Borbely & Achermann, 1999) this circadian rhythm is termed the *Process C*. It is complemented by the homeostatic *Process S*, rising during wakefulness and declining during sleep, which is expressed through increasing sleep propensity with prolonged wakefulness and intensified subsequent recovery sleep. Notably, Process S is quantified based on an electrophysiological measure termed *slow wave activity* (SWA, i.e. the EEG power between 0.5 and 4.5 Hz).

However, also periods of sleep are not homogeneous, but composed of alternating sleep stages, each with a characteristic pattern of neuronal activity and peripheral physiological parameters (Figure 1-10). Using polysomnography (PSG), comprising electroencephalography (EEG) at central electrodes C3 and C4, electromyography (EMG) at the chin, and electrooculography (EOG), sleep stages can be visually distinguished in 30 s epochs, based on standard sleep scoring criteria (Rechtschaffen & Kales, 1968). The most fundamental division is that into rapid-eye movement (REM) and Non-rapid eye movement (NREM) sleep, with the latter being subdivided into four stages (NREM stage 1 to 4). A full sleep cycle (~ 1.5 h duration), of which we have four to six per night, is constituted as follows.

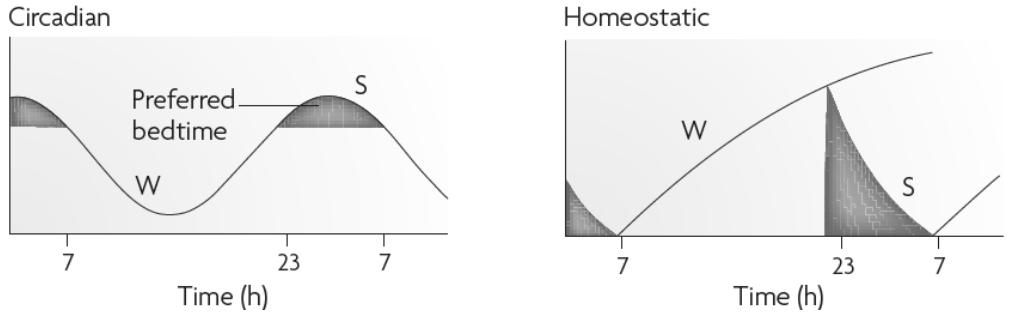

Figure 1-9: Borbély's two-process model of sleep regulation. (Left) The circadian *Process C* is driven by internal clocks and entrained by external signals. **(Right)** The independent homeostatic *Process S* accumulates sleep need during wakefulness which is reduced during subsequent sleep. (Taken from Cirelli, 2009).

During quiet wakefulness with closed eyes, alpha activity (8-12 Hz) dominates the EEG, muscle tone is relatively high and spontaneous fast eye movements are frequent. Then during the transition to light sleep (*NREM stage 1*), the EEG is slowing, EMG becomes less, and the eyes show a characteristic rolling. After a few minutes sleep consolidates, eye movements diminish, and spindles (burst of 12-14 Hz with a duration > 0.5 s) and K-complexes (high-amplitude sharp negative waves followed by slow positive deflections) begin to occur, resembling the hallmarks of *NREM stage 2*. When sleep deepens further, delta activity (0.5-4 Hz) becomes stronger and more prominent slow waves (high-amplitude waves > 75 µV, duration > 0.5 s) emerge, defining the so called *slow wave sleep (SWS).* SWS can be subdivided in *NREM stages 3 and 4*, depending on whether more than 20% or 50% of a 30 s epoch are constituted of slow waves. After a while, sleep becomes lighter again, passing through NREM stages 3 and 2 and eventually converting to REM sleep. The EEG pattern during this sleep stage is similar to that of wakefulness, hence also called *paradoxical sleep*, and is marked by predominant theta (4-7 Hz) and some intermittent alpha activity as well as the lack of slow waves, spindles, and K-complexes. More important, however, is the periodic occurrence of the name-giving rapid saccadic eye movements and the pronounced muscle atonia. During the course of the night, periods of SWS become less and shorter while REM period become longer and more frequent.

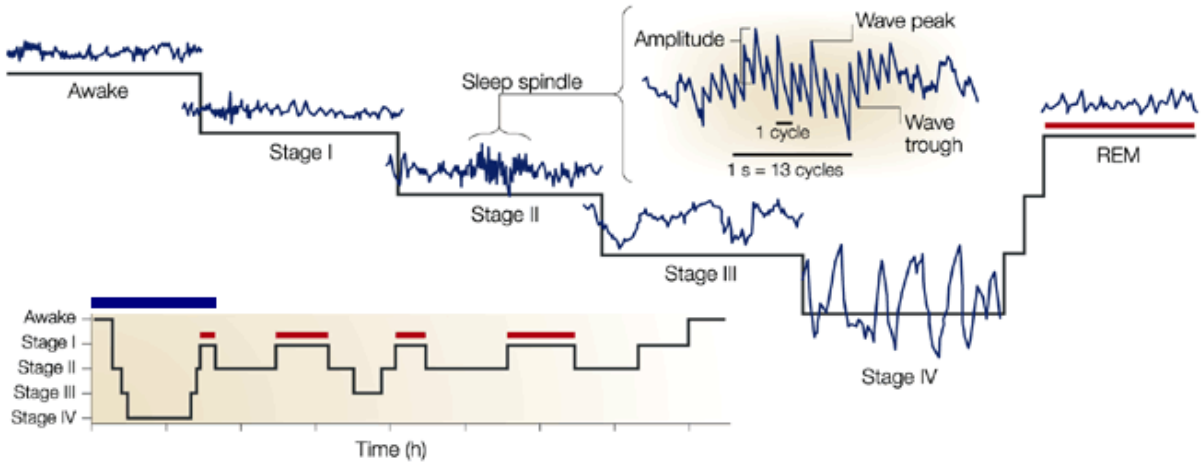

Figure 1-10: The alternation of sleep stages and their electroencephalographic (EEG) pattern. (Lower part) Hypnogram depicting the cycling of sleep stages across a typical night. REM sleep is indicated by red bars. **(Upper part)** Characteristic EEG patterns are shown for the different sleep stages included in a full sleep cycle (~1.5 h) indicated as blue bar in the hypnogram. See text for details. (Modified after Pace-Schott & Hobson, 2002).

The mechanisms controlling the transition from wakefulness to sleep and the alternation of REM and NREM episodes are not yet completely understood but matter of ongoing research. They presumably involve neuromodulatory neurons of the hypothalamus, the basal forebrain, and several brainstem nuclei (Kalia, 2006). Moreover, so called *REM-on* and *REM-off* neurons located in pontine brainstem nuclei have been found to play a major role in switching between REM and NREM sleep (Fuller, Saper, & Lu, 2007). Also, the release of neuromodulators regulating the activity of the cortico-thalamic system differs markedly between REM and NREM sleep. During NREM sleep, levels of acetylcholine, serotonin, and noradrenaline are generally lowerd compared to wakefulness. During REM sleep, however, serotonin and noradrenalin reach their minimum while acetylcholine now almost achieves a wake-like level (Pace-Schott & Hobson, 2002). These neuromodulatory changes also have impact on the direction of information flow within hippocampo-neocortical circuits, favoring neocortico-hippocampal inputs during high cholinergic levels in wakefulness and REM sleep, while allowing reversed hippocampo-neocortical feedback during low cholinergic tone in SWS (Gais & Born, 2004).

In the following sections, I will exclusively discuss the neuronal oscillations mediated by the thalamo-cortical system during NREM sleep (neglecting REM sleep) as this phase of sleep is in the major focus of current theories of sleep-dependent memory consolidation and subject of my own research (for a recent attempt to re-integrate REM sleep by reviving the 'sequential hypothesis of sleep-dependent memory consolidation' see Diekelmann & Born, 2010).

1.2.2 Sleep Oscillations in the Thalamo-Cortical System

The thalamo-cortical system resembles the central processing unit of the mammalian central nervous system. The thalamus, deeply located in the very center of the brain, is its major hub and the gate for almost the entire neocortex. All afferent sensory signals (be it visual, auditory, somatosensory or visceral, with an exception of the olfactory system) have to pass the thalamus to be projected to the corresponding primary sensory cortices. Even signals originating from the neocortex that have been sent through subcortical parallel processing loops, such as the basal ganglia or the cerebellum, have to take their way back to the cortex via the thalamus. Therefore, despite

the cortex maintains a high number of short-, mediate-, and long-range cortico-cortico connections “to talk to itself”, the thalamus provides its link to the outside world. During sleep, this connection is interrupted by suppression of incoming sensory information in the thalamus through prolonged phases of hyperpolarization in thalamo-cortical neurons. Disconnected from the environment, the thalamo-cortical system mainly (re-)processes internal information by means of oscillatory activity that is based on the very nature of its functional anatomy.

As shortly addressed above, oscillatory brain activity during NREM sleep is dominated by three major rhythms (Figure 1-11): (i) sleep spindles, (ii) delta waves, and (iii) slow oscillations (Steriade, 2003), that shall be described in the next paragraphs. K-complexes as another defining element of NREM sleep will be discussed together with the slow oscillation, as I share the opinion of many researchers that both are expressions of the same underlying neuronal mechanism.

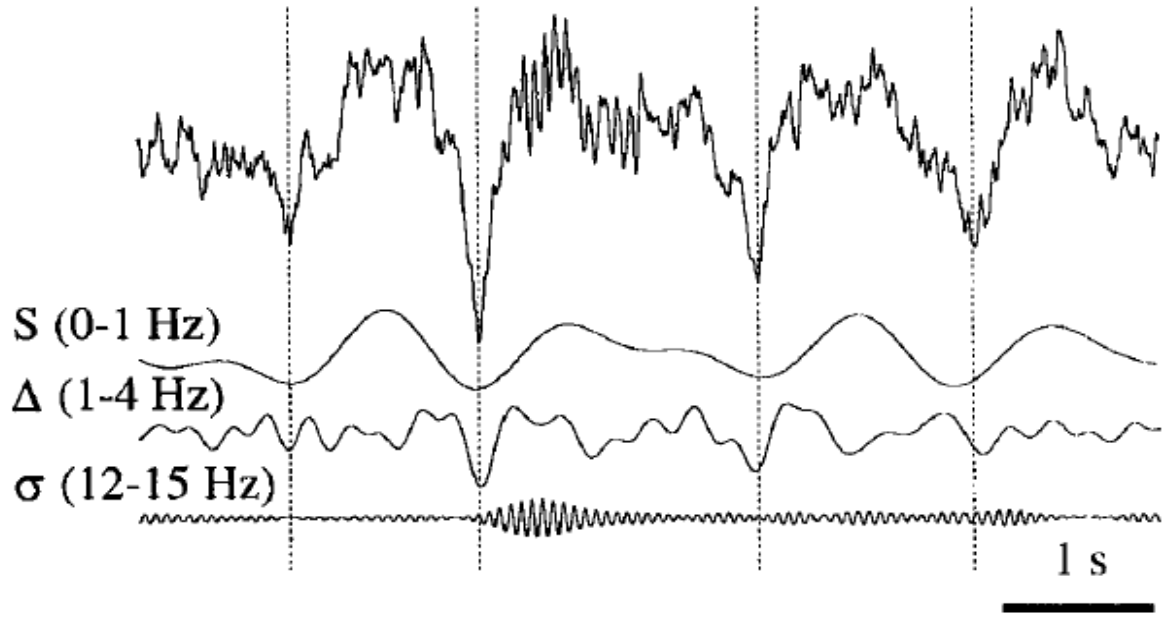

Figure 1-11: The three major rhythms of NREM sleep. (Upper row) typical surface EEG signal of human NREM sleep. **(Lower rows)** Decomposition of the raw EEG signal into three components: (S) slow oscillation < 1 Hz, (Δ) delta with 1-4 Hz, and (σ) sigma or spindle frequency with 12-15 Hz. Please note, that exact frequency ranges differ markedly in the literature. (Taken from Amzica & Steriade, 1997).

1.2.2.1 Sleep Spindles

In the surface EEG, *sleep spindles* appear as an oscillatory pattern of waxing and waning amplitudes with a duration of about 0.5-3 s. Formally confined to frequencies of 12-16 Hz (Rechtschaffen & Kales, 1968), recent research has put forth the concept of two types of spindles with either ~10-13 Hz (slow spindles) or ~13-16 Hz (fast spindles) peaking at frontal and centro-parietal cortical sites, respectively. However, the boundaries of the spindle frequency (sometimes also referred to as *sigma band*) as well as of the two spindle subtypes are not consistently confined (for a comprehensive review see De Gennaro & Ferrara, 2003).

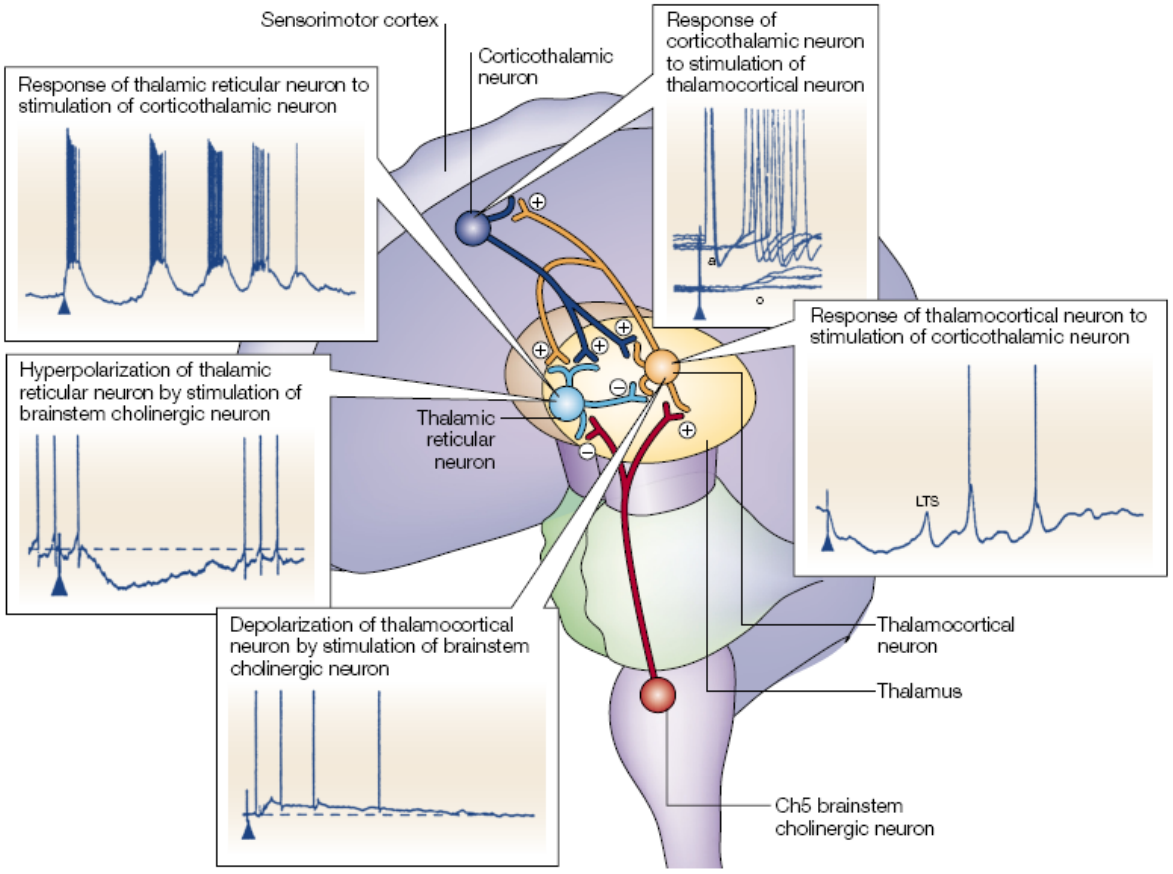

Figure 1-12: The thalamo-cortical system generating the oscillations of NREM sleep. Spindles are projected from thalamo-cortical neurons (TC, yellow) to the neocortex, from where cortico-thalamic neurons (CT, dark blue) project back to the thalamus. Inhibitory thalamic neurons from the reticular nucleus (RE, light blue) are driven by both TC and CT neurons and by recurrently suppressing the activity of TC neurons cause the oscillatory pattern of sleep spindles. Brainstem nuclei (red) can alter the network effects of the thalamo-cortical system by differentially driving RE and TC neurons during sleep. Single neuron firing patterns are depicted for the different contributing neuron populations. (Taken from Hobson & Pace-Schott, 2002).

Sleep spindles are conjointly generated by different parts of the thalamo-cortical system (Steriade, 2000, 2003). They are composed of repetitive short bursts of neuronal firing originating in thalamo-cortical neurons (TC) and projected to the neocortex by a bunch of partly specific, partly diffuse radiant fibers. The spindle-like character is created by means of a negative feedback loop of glutamatergic excitatory TC neurons and gamma-aminobutyric acid (GABA)-ergic inhibitory neurons from the reticular thalamic nucleus (RE). Sleep spindles are, however, synchronized and can even be initiated via projections from cortico-thalamic (CT) neurons. See Figure 1-12 for a graphical summary. In humans, thalamic involvement in sleep spindle generation has also been demonstrated by means of functional neuroimaging (Paper IV, Bergmann, Mölle, Diedrichs, Born, & Siebner, in preparation; Schabus et al., 2007).

As will be discussed later, by means of their augmenting pattern of massive firing, sleep spindles might play a major role in the induction of cortical plasticity during sleep (Steriade & Timofeev, 2003). However, it is still unclear whether slow frontal and fast centro-parietal spindles are merely an expression of neuroanatomical diversity in thalamic source and/or cortical target areas (Schabus et al., 2007) or whether they actually serve separate functions, e.g. in brain plasticity (Paper II, Bergmann et al., 2008; Paper III, Mölle, Bergmann, Marshall, & Born, in prep.).

1.2.2.2 Delta Waves

Steriade distinguishes two subtypes of *delta waves* (Steriade, 2003): (i) clock-like waves generated in TC neurons and (ii) cortical waves surviving thalamectomy. This differentiation might actually elucidate some of the inconsistencies found in current terminology. Since all EEG frequencies below 4 or 4.5 Hz have originally been summarized as *delta band*, the discovery of the slow oscillation (Steriade, Contreras, Curro Dossi, & Nunez, 1993; Steriade, Nunez, & Amzica, 1993a, 1993b) has led to some confusion in the nomenclature. Some authors refer to *slow oscillations* and *delta waves* as frequencies of ~0.5-1 Hz and ~2-4 Hz, respectively (Achermann & Borbely, 1997; Steriade, 2006), while others now use the term *slow waves* for all cortical frequencies between 0.5-4.5 Hz (Tononi & Cirelli, 2006). Presumably, the former is reasonable when referring to thalamo-cortical delta waves and the latter when

speaking of those with cortical origin. I will, however, use either of these classifications, depending on the authors I am currently referring to.

1.2.2.3 Slow Oscillations

The *slow oscillation* is the hallmark rhythm of NREM sleep and its most important organizing feature. The neocortical fluctuation with a frequency below 1 Hz was first observed in the cat *(Steriade, Contreras et al., 1993; Steriade, Nunez et al., 1993a, 1993b)* but could later also be demonstrated in humans, there peaking at a frequency of 0.7-0.8 Hz (Achermann & Borbely, 1997). The rhythm could be recorded in all major types of neocortical neurons (excitatory as inhibitory), consisting of alternating phases of hyperpolarization (*down state*) where most cortical neurons are silent and subsequent phases of depolarization (*up state*) with rebounds of massive synchronous firing (Figure 1-13). The slow oscillation has certain features rendering it of particular importance for the organization of oscillatory activity in the thalamo-cortical system during NREM sleep, which shall be covered below.

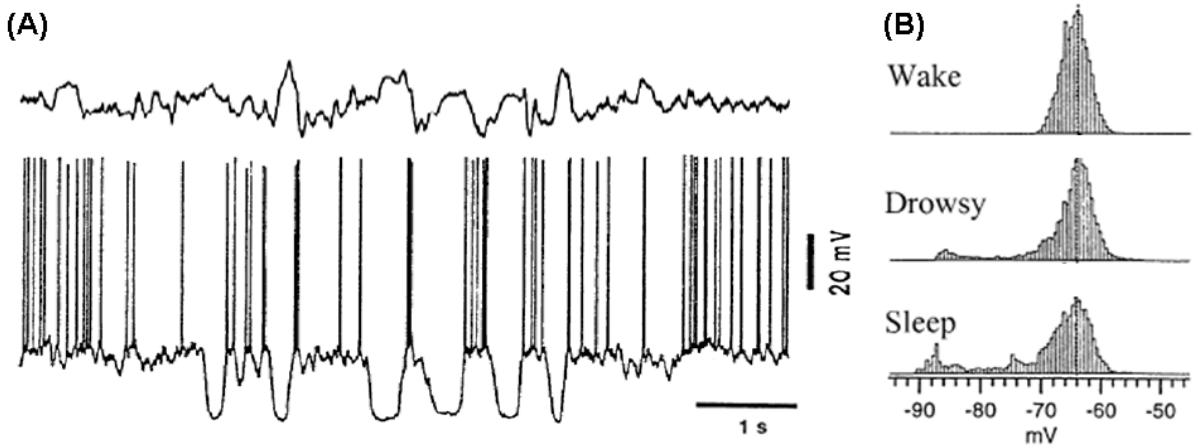

Figure 1-13: The slow oscillation during natural slow wave sleep in the chronically implanted cat. (A) The top panel depicts recordings of intracortical EEG from deep cortical layers. Note that polarities are reversed compared to surface EEG recordings: here, positive deflections indicate hyperpolarization (*down state*) and negative deflections indicate depolarization (*up state*). The bottom panel shows intracellular recordings from a single cortical neuron, revealing the underlying oscillation of the neuronal membrane potential which is accompanied by the complete lack of firing during hyperpolarization phases and rapid neuronal spiking during subsequent phases of depolarization. **(B)** Histograms of membrane potentials for different vigilance states. Please note, that the average membrane potential becomes more and more hyperpolarized during the transition from wakefulness over drowsiness to sleep.

The first important feature of the slow oscillation is its spontaneous cortical origin. It has been observed not only during natural sleep but also *in vivo* during anesthesia (Steriade, Nunez et al., 1993b), after cortical deafferentation (i.e. dissection of cortico-cortical and thalamo-cortical projections of isolated cortical slabs, Timofeev, Grenier, Bazhenov, Sejnowski, & Steriade, 2000) or thalamectomy (i.e. destruction or removal of the thalamus, Steriade, Nunez et al., 1993a), and even *in vitro* in cortical slices (Sanchez-Vives & McCormick, 2000). The up state of the slow oscillation mainly consists of non-NMDA-mediated EPSPs, fast prepotentials, voltage-dependent persistent inward directed NA^+ currents, and also fast inhibitory postsynaptic potentials (IPSPs) of GABAergic inhibitory interneurons. The down state is thus probably not produced by GABAergic inhibitory interneurons but is due to disfacilitation, that is the removal of excitatory synaptic inputs possibly through extracellular Ca^{2+} depletion, and NA^+-induced outward directed K^+ currents (Steriade, 2006; Steriade & Timofeev, 2003). Although the neocortex is apparently able to produce slow oscillations spontaneously, under physiological circumstances many slow oscillations may in fact be triggered by clock-like thalamo-cortical firing or sometimes even by afferent sensory signals that survived thalamic suppression (cf. evoked K-complexes). In fact, it has recently been argued that the full manifestation of the slow oscillation during natural NREM sleep requires the interaction of a synaptically based cortical and two intrinsic thalamic oscillators (Crunelli & Hughes, 2009). However, it is probably also true that every depolarization being strong enough to shift the bistable activity mode of cortical neurons during NREM sleep, evokes a slow oscillation (Massimini, Tononi, & Huber, 2009), which could in fact be demonstrated by intracortical electrical stimulation in rats (Vyazovskiy, Faraguna, Cirelli, & Tononi, 2009) and by transcranial magnetic stimulation in humans (Massimini et al., 2007).

The second important feature of the slow oscillation is its travelling nature. As could be shown by high-density EEG recordings (Massimini, Huber, Ferrarelli, Hill, & Tononi, 2004), each individual slow oscillation cycle originates from a definite cortical site and travels with an estimated speed of 1.2-7.0 m/s across the entire cortex. Although slow oscillations can originate at any cortical site and travel in any possible direction, they most frequently emerge in prefrontal regions and spread in an anterior to posterior direction (Figure **1-14**A&B). Source localization analyses (Murphy et al., 2009) recently revealed that most slow oscillations in fact emerge at left insular and

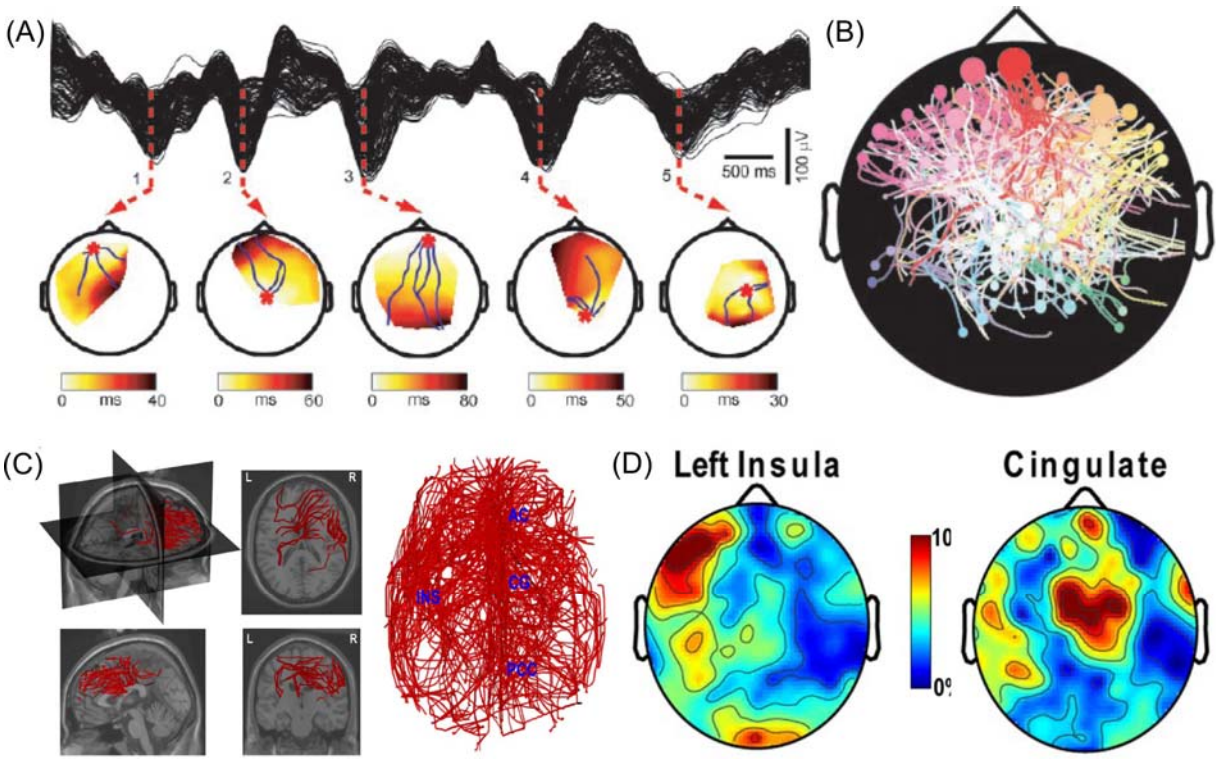

Figure 1-14: The slow oscillation as a travelling wave. (A) Origin and main direction of cortical spread for individual cycles of the slow oscillation in high-density (256 channel) EEG recordings estimated from delays between negative peaks of slow oscillation down states at the various recording sites. **(B)** Streamline map from the first hour of sleep in a single subject. Dot size is proportional to the number if slow oscillations originating at the respective site, color codes different sites of origin. (A & B taken from Massimini et al., 2004). **(C)** Slow oscillation streamline maps derived from source localization analyses, indicating that **(D)** most slow oscillations actually origin in left insular and anterior cingulate cortex. (C & D taken from Murphy et al., 2009).

anterior cingulate cortex and travel along the cingulate gyrus, characterizing it the major connectional backbone of the cortex. (Figure 1-14C&D). The traveling nature of slow oscillations also held true for those externally evoked by intracortical electrical (Vyazovskiy, Faraguna et al., 2009) or transcranial magnetic stimulation (Massimini et al., 2007). However, externally evoked slow oscillations were highly stereotypic regarding their origin, propagation and involvement of cortical regions, depending on the respective site of stimulation (Murphy et al., 2009).

The third and may be most important feature of the slow oscillation is its grouping function for faster oscillations such as (thalamo-cortical) delta waves, sleep spindles, gamma activity, and hippocampal sharp wave-ripples (Figure **1-15**). The wide-spread cortical hyperpolarization followed by massive simultaneous firing seems to me an ideal mechanism for resetting and entraining the oscillatory activity

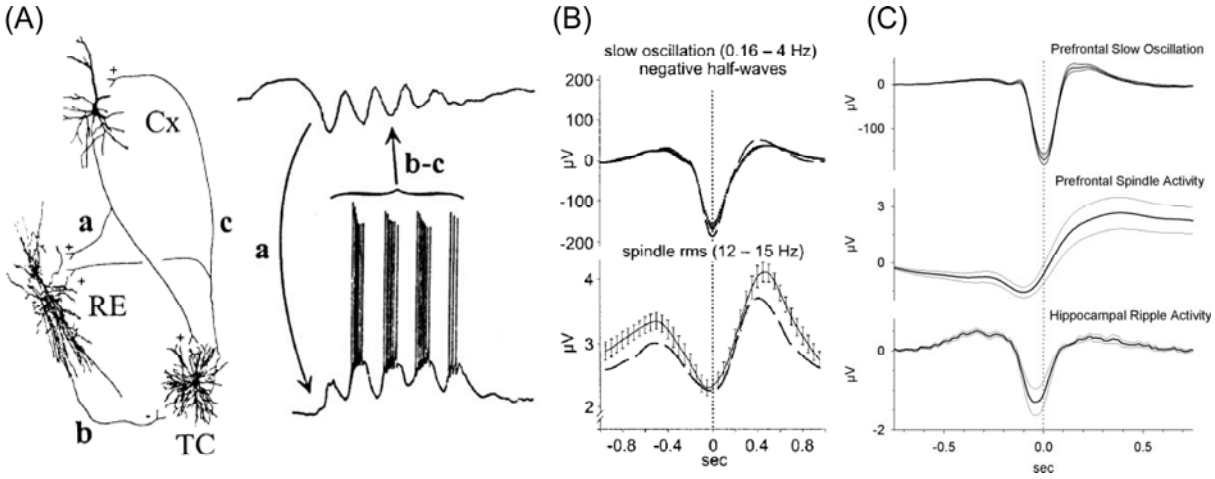

Figure 1-15: Grouping of faster brain rhythms by the slow oscillation. The slow oscillation groups oscillatory activity generated in the thalamo-cortical system (sleep spindles, delta waves, gamma activity) and the hippocampus (sharp wave-ripples). **(A)** The schematic wiring of the thalamo-cortical circuit (left) shows exemplarily how the slow oscillation up state from cortical (Cx) neurons by means of cortico-thalamic projections (a) triggers the generation of sleep spindles in reticular thalamic (RE) and thalamo-cortical (TC) neurons. Spindle activity is then transferred back to the neocortex (b-c) where it shapes the tail of the slow oscillatory cycle (right). (Taken from Steriade, 2006). **(B)** Grouping of sleep spindles (lower row) time-locked to the down state of the slow oscillation (upper row) in the human EEG. (Modified after Mölle, Marshall, Gais, & Born, 2002). **(C)** Synchronization of EEG spindle activity (middle row) and hippocampal sharp wave-ripple activity in CA1 local field potentials (lower row) by the slow oscillation down state (prefrontal EEG, upper row) in the rat. (Taken from Mölle, Yeshenko, Marshall, Sara, & Born, 2006).

generated in thalamic or limbic structures. As shown in Figure 1-15A, the slow oscillation up state triggers the thalamic generation of sleep spindles by means of cortico-thalamic projections, while the slow oscillation down state effectively suppresses spindle expression. This grouping was initially shown in the cat (Steriade, 2006; Steriade, Nunez et al., 1993b) but could also be demonstrated in rat (Mölle et al., 2006) and human (Figure 1-15B) (Mölle et al., 2002). It is by the slow oscillatory synchronization that sleep spindles mainly appear simultaneously at distant cortical sites while being desynchronized when thalamo-cortical connections are disrupted (Destexhe, Contreras, & Steriade, 1999; Sejnowski & Destexhe, 2000). As also wake-like gamma activity (> 30 Hz) is found to be grouped in the slow oscillation up states, these periods have been referred to as *fragments of wakefulness* (Destexhe et al., 2007). In parallel, the slow oscillation also synchronizes the so called sharp wave-ripple activity of hippocampal CA1 neurons (Figure 1-15C) (Clemens et al., 2007; Mölle et al., 2006), presumably marking the read out of information from the

medial temporal lobe memory system. The idea that slow oscillations initiate hippocampal activity has also been corroborated by recent human neuroimaging findings, demonstrating that the slow oscillation is in fact driving hippocampal activity (Dang-Vu et al., 2008). As the next chapter will show, slow oscillations play a crucial role in system memory consolidation as well as in homeostatic metaplasticity during sleep.

1.2.2.4 The K-complex

Although the K-complex is a prominent and defining feature of light NREM sleep, its distinction from slow waves during deep sleep is likely to be an artificial one as both oscillations seem to be based on the same mechanisms (Amzica & Steriade, 1997; Colrain, 2005). Like the slow oscillation, whose precursor it may be during the deepening of sleep, the K-complex is characterized by a sharp high-amplitude hyperpolarization phase followed by moderate depolarization which is often accompanied by pronounced spindle activity. Moreover, recent intracortical recordings in humans with chronically implanted micro-electrodes for epilepsy diagnostics could demonstrate that the K-complex is indeed a kind of isolated slow oscillation downstate (Cash et al., 2009).

1.3 Sleep-Dependent Neuronal Plasticity

As already mentioned, sleep may provide the ideal state for a variety of plastic brain processes to occur. Due to the above described sleep-specific oscillations of the thalamo-cortical system, the neocortex is mainly decoupled from the environment and thereby protected from sensory interference. Additionally, also endogenous sources of interference, like memory recollection, problem solving, or future planning are prevented by a complete loss of consciousness. In this environment internal representations can be reactivated and reprocessed without interrupting with ongoing cognitive processing and vice versa. In the following sections, I will describe the two currently most influential models linking specific oscillations to distinct process of neuronal plasticity during sleep and review empirical evidence corroborating them. First, I will outline the *synaptic homeostasis hypothesis (Tononi & Cirelli, 2003, 2006)* which focuses on the role of slow waves in metaplastic downscaling mechanisms on the cel-

lular level. Second, I will describe the mechanistic model of a sleep-dependent *active system consolidation* proposed by Born and coworkers (Born et al., 2006; Diekelmann & Born, 2010; Marshall & Born, 2007; Rasch & Born, 2007) which is mainly built on the interaction of cortical slow oscillatory, thalamic spindle, and hippocampal sharp wave-ripple activity, subserving the hippocampo-neocortical transfer of declarative memory traces. Both models are not mutually exclusive but rather describe complementary processes.

1.3.1 Synaptic Homeostasis

Based on Borbély's *two-process model of sleep regulation* (described in Section 1.2.1), Tononi and Cirelli formulated their *synaptic homeostasis hypothesis (Tononi & Cirelli, 2003, 2006)*. The main idea is that the neuronal mechanism of the homeostatic *Process S*, which is responsible for the buildup of sleep pressure with prolonged wakefulness, relies on the accumulating induction of synaptic potentiation. Unlimited synaptic potentiation, however, comes with increasing costs in energy (metabolism due to synaptic activity), space (sprouting of new synaptic connections), and with the risk of saturation in the plastic capacity of neuronal networks (see Section 1.1.1.4). Therefore, the net increase in synaptic strength has to be downregulated again while the information coded in the relative synaptic weights on a given neuron has to remain intact. According to the *synaptic homeostasis hypothesis*, this regulation is implemented by means of so called *synaptic downscaling*. Although the detailed neuronal mechanisms underlying this process have not yet been fully determined, it is thought to reduce all synaptic weights of a given neuron with respect to their relative contribution to the neuron's net synaptic input. Thereby its information processing characteristics are preserved. Sleep slow waves itself, their power serving as a reliable biomarker for sleep pressure, are also believed to mediate synaptic downscaling. See Figure 1-16 for a detailed description of a full cycle of day and night comprising synaptic potentiation and synaptic downscaling.

The synaptic downscaling hypothesis has already gained empirical evidence from a variety of experiments. In a series of studies using high-density EEG recordings in humans, Huber and colleagues could show local slow wave activity

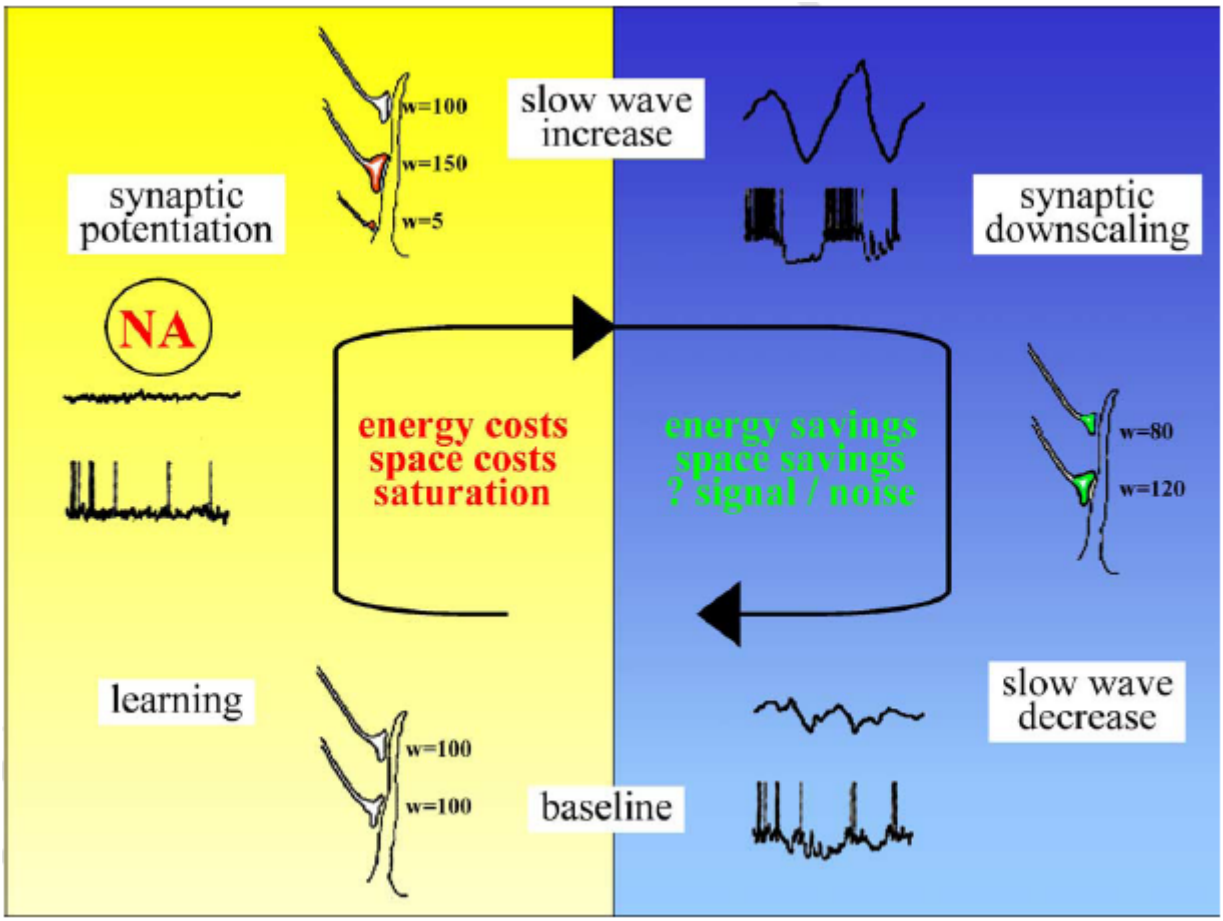

Figure 1-16: The synaptic homeostasis hypothesis. The diagram visualizes the proposed cycle of synaptic potentiation during wakefulness (left side) and synaptic downscaling during subsequent sleep (right side). In the cartoon-like simplified example a model neuron starts the day with two synaptic connections on its dendrite, each with an arbitrary weight (w) of 100. In the course of the day strengthening of synaptic weights (LTP) occurs due to learning and facilitated by neuromodulators like noradrenaline (NA). This net increase in synaptic strength comes with extra costs in energy and space, and with the risk of saturation. At the evening one of the synaptic weights is increased to 150 and even a new weak synaptic connection has evolved. Due to its strengthened synaptic connections to other neurons the model neuron is now more easily recruited to join the collective firing pattern of spontaneous slow oscillations. Thereby it not only contributes to increased local slow wave activity (SWA) but its synaptic weights are coincidently downscaled by means of the slow oscillatory firing pattern itself. The downscaling is proportional, thus while decreasing the total synaptic input of a given neuron, proportions between synaptic weights remain roughly the same (here 80 and 120). Particularly weak synapses are even removed completely, reducing the consumption of energy and space. The net decrease in synaptic weights is in turn accompanied by decreasing SWA across the course of sleep. The next morning the model neuron starts again with a total synaptic weight of 200 but with a changed synaptic configuration, representing what was learned the day before, however, with an increased signal-to-noise ratio. (Taken from Tononi & Cirelli, 2006).

(SWA) to be increased in those brain areas where synaptic potentiation (LTP) has previously evolved during wakefulness. This was demonstrated after learning of a visuomotor task (Huber, Ghilardi, Massimini, & Tononi, 2004) as well as after application of high-frequency repetitive transcranial magnetic stimulation (rTMS) to the left primary motor cortex (Huber et al., 2007). Conversely, local SWA decreased in the contralateral sensorimotor cortex after 12 hours of arm immobilization which is thought to induce synaptic depression (LTD) due to reduced neuronal activity (Huber et al., 2006). Moreover, the amount of SWA increase also correlated with an increase in task performance after sleep, which was attributed to an enhanced signal-to-noise ratio (Huber et al., 2004).

In the rat, Vyazovskiy and colleagues could demonstrate that electrical cortex stimulation evoked stronger responses after wakefulness than after sleep, suggesting a reduction of synaptic weights during sleep (Vyazovskiy, Cirelli, Pfister-Genskow, Faraguna, & Tononi, 2008). As they found AMPA receptor levels in the rat hippocampus and cortex to be decreased during sleep relative to wakefulness, they argued that synapses had been potentiated during wakefulness and downscaled during subsequent sleep. Recently, it was also shown hat extracellular glutamate concentration (Dash, Douglas, Vyazovskiy, Cirelli, & Tononi, 2009) and spontaneous neuronal firing rates (Vyazovskiy, Olcese et al., 2009) follow the same pattern. Possibly, cortical expression of the brain-derived neurotrophic factor (BDNF) is driving the homeostatic downregulation (Faraguna, Vyazovskiy, Nelson, Tononi, & Cirelli, 2008).

While it is still unclear how slow waves could actively downscale synaptic weights, computational modeling of the thalamo-cortical system (for a detailed description see Hill & Tononi, 2005) has convincingly demonstrated how the local expression of slow waves might depend on the strength of synaptic weights and why it would progressively decrease across a night of sleep (Esser, Hill, & Tononi, 2007). According to this large-scale computer model, recruiting of a given neuron into an ongoing slow wave occurs the faster the stronger it is connected to other neurons, which should result in higher amplitudes and steeper slopes of slow waves after synaptic potentiation. Moreover, with increased network synchronization, single slow waves should less often express multiple peaks, indicating a stronger synchronization of local neuron populations. As synaptic weights are successively downscaled during the course of sleep, not only slow wave activity in general should decrease but

also their slopes should become less steep and multiple peaks more frequent (Esser et al., 2007). These model predictions could be supported by intracortical recordings in the rat (Vyazovskiy, Riedner, Cirelli, & Tononi, 2007) as well as human high-density EEG recordings (Riedner et al., 2007).

It has been argued that synaptic downscaling might be a direct function of the slow oscillations' alternation between highly synchronous firing and complete synaptic silence (Tononi & Cirelli, 2006). This is corroborated by the fact that the slow oscillation frequency is below 1 Hz which has also been found ideal for inducing depression both by electrical *in vivo* and *in vitro* stimulation paradigms in animals (Citri & Malenka, 2008; Dudek & Bear, 1992) and by transcranial magnetic stimulation paradigms in humans (Fitzgerald, Fountain, & Daskalakis, 2006). However, the exact cellular mechanisms mediating these effects, presumably due to changes in Ca^{2+} dynamics, are not yet fully understood, and direct evidence is still missing that the slow oscillation itself is responsible for synaptic downscaling. A drawback of the theory is that it assumes only LTP to occur during learning and to be downscaled during sleep. As LTD is known to be as importance in learning as LTP (Griffiths et al., 2008; Kemp & Manahan-Vaughan, 2007), there should also be *synaptic upscaling* during sleep. Homeostasis might not be a one-way street.

1.3.2 System Memory Consolidation

Beside basic homeostatic maintenance of brain plasticity (i.e. synaptic downscaling), sleep is also thought to actively support processes of system memory consolidation (Diekelmann & Born, 2010). In fact, behavioral evidence for the beneficial effects of sleep on declarative, emotional, perceptual as well as procedural memory consolidation which has largely accumulated within the last decade. Using a variety of tasks and controlling for circadian effects by wake control groups, nap and sleep deprivation studies, it could be shown that sleep counteracts forgetting of declarative material (word pairs, texts, picture-location associations, spatial maps etc.) and emotional items (pictures or texts), and that it mediates even offline improvements in procedural (finger tapping sequences, mirror drawing, etc.) or perceptual (e.g. visual discrimination) skills (for comprehensive reviews on these studies see Born et al., 2006; Diek-

elmann, Wilhelm, & Born, 2009; Ellenbogen, Payne, & Stickgold, 2006; Stickgold & Walker, 2005; Walker & Stickgold, 2006).

However, although sleep obviously supports memory consolidation, the exact mediating neuronal mechanisms are yet to be discovered. Building on the standard consolidation theory (Section 1.1.2.1), Born and coworkers have proposed a model for sleep-dependent consolidation in the declarative memory system which integrates the unique sleep-specific oscillatory brain activity during NREM sleep (Born et al., 2006; Diekelmann & Born, 2010; Gais & Born, 2004; Marshall & Born, 2007; Rasch & Born, 2007). According to this model the hippocampo-neocortical transfer of memory traces is organized by the cortical slow oscillation, synchronizing hippocampal sharp wave-ripple activity with thalamo-cortical spindles (Figure 1-17). Sharp wave-ripple activity in the CA1 region of the hippocampus is proposed to reflect the joint reactivation of previously acquired hippocampo-neocortical memory traces, while sleep spindles might be the mechanism by which plastic processes are triggered at cortical neurons to make up or at least strengthen cortico-cortical connections. Although the function of REM sleep has recently been re-integrated into a common model of *active system consolidation* (Diekelmann & Born, 2010), I will keep the focus of my thesis on the more elaborated neuronal mechanisms taking place during NREM sleep. In the next subsections I will review empirical evidences corroborating the proposed relevance of all three types of oscillations, i.e. ripples, spindles, and slow oscillations.

1.3.2.1 Hippocampal Sharp Wave-Ripples

The proposed role of hippocampal sharp wave-ripple complexes is the reactivation of hippocampo-neocortical traces, previously bound together during learning. Animal research in rats could in fact repeatedly demonstrate that those hippocampal neurons which code for the location of the animal in space (so called place cells, O'Keefe & Dostrovsky, 1971) during spatial learning are reactivated in the same - though accelerated (Lee & Wilson, 2002; Nadasdy, Hirase, Czurko, Csicsvari, & Buzsaki, 1999) - temporal sequence during ripple events in subsequent SWS (Ji & Wilson, 2007; Kudrimoti, Barnes, & McNaughton, 1999; Lee & Wilson, 2002; Sutherland & McNaughton, 2000; Wilson & McNaughton, 1994). Moreover, recordings in medial prefrontal neurons after a rule-learning task also indicate a replay of cortical patterns

time-locked to hippocampal ripples (Peyrache et al., 2009). Recent studies could add causality to this correlational link, demonstrating that suppression of hippocampal ripple events by means of time-locked electrical stimulation of the hippocampus in fact impairs spatial memory consolidation (Ego-Stengel & Wilson, 2009; Girardeau, Benchenane, Wiener, Buzsaki, & Zugaro, 2009). Although similar patterns of reactivation have also been observed during subsequent REM sleep (Louie & Wilson, 2001), thus questioning the state specificity of this reactivation phenomenon, the overall data supports the role of hippocampal sharp wave-ripple complexes in sleep dependent memory consolidation.

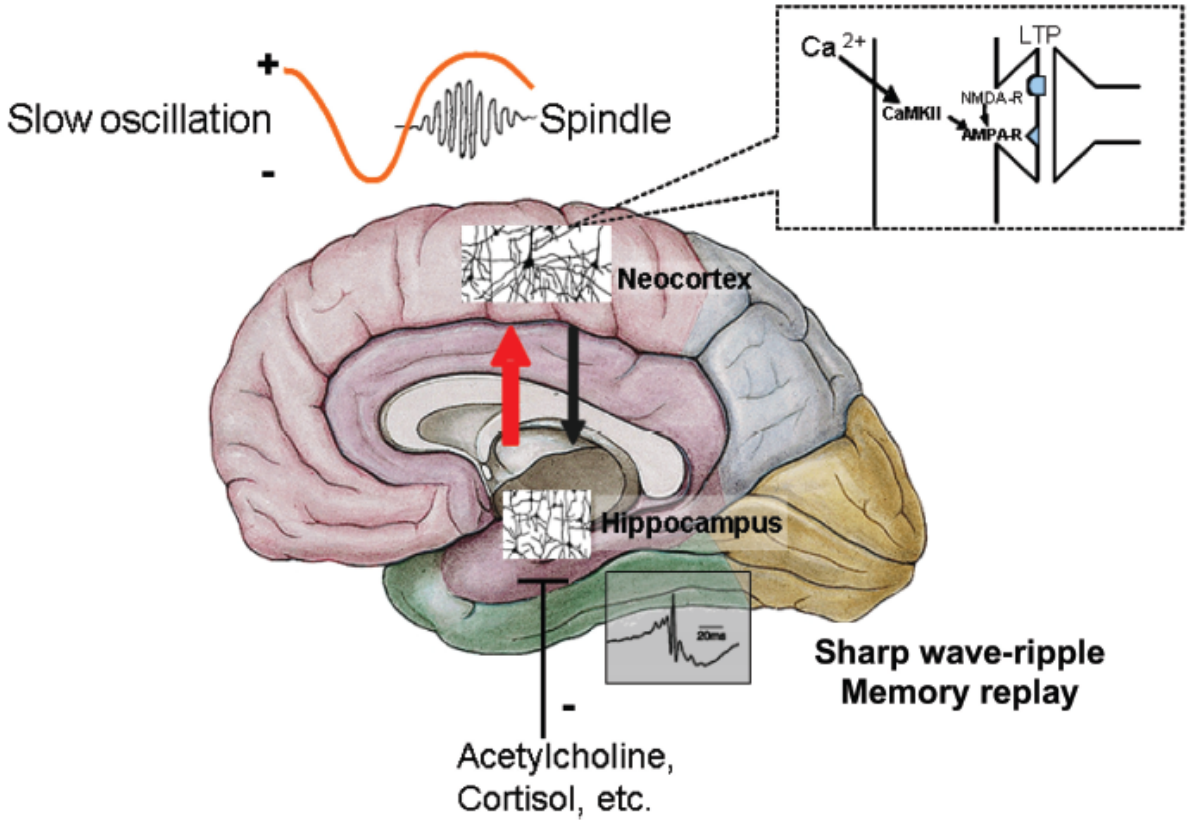

Figure 1-17: A model of hippocampo-neocortical memory transfer during sleep. The model assumes a well-orchestrated interaction between cortical slow oscillations, thalamo-cortical spindles, and hippocampal sharp wave-ripples driving the hippocampo-neocortical dialogue during SWS. The slow oscillation groups sharp wave-ripples and spindles in its depolarized up state by triggering their emergence in hippocampal CA1 and thalamo-cortical neurons, respectively. Hippocampal ripples reactivate those cortical representations (red arrow) which have been bound together during prior learning (black arrow), while the time-locked spindle input enables plastic processes at cortical synapses due to the associated massive Ca^{2+} influx. Furthermore, switching between information readout and uptake, in the hippocampus is modulated by decreased acetylcholine levels during SWS. (Taken from Born et al., 2006).

1.3.2.2 Thalamo-Cortical Sleep Spindles

Thalamo-cortical sleep spindles, occurring time-locked to hippocampal ripple events are thought to mediate plastic processes in the neocortex. The augmenting firing patterns of thalamo-cortical neurons cause massive bursts of Ca^{2+} influx into the apical dendrites of neocortical pyramidal neurons, thereby potentially inducing synaptic plasticity at these synapses (Destexhe et al., 2007). In fact, as in vivo recordings in the rat could show, spindle activity occurs preferentially at those synapses where LTP had previously been induced (Werk, Harbour, & Chapman, 2005). In turn, sleep spindle related spike-trains have been successfully used to trigger LTP at synapses in rat somatosensory cortex slices (Rosanova & Ulrich, 2005). However, also LTD can be induced in vivo in the rat somatosensory cortex (Werk, Klein, Nesbitt, & Chapman, 2006), presumably depending on whether or not spindle-like stimulation is accompanied by postsynaptic action potentials in a Hebbian way (Rosanova & Ulrich, 2005). As the postsynaptic excitability of cortical neurons during SWS largely depends on the prevailing phase (up vs. down) of the slow oscillation, the exact temporal location of a given spindle within the slow oscillation cycle might determine the actual direction of induced plasticity. In parallel, hippocampal ripple bursts have been found to be nested in individual spindle troughs (Siapas & Wilson, 1998), probably organizing hippocampo-neocortical information processing on a more fine-scaled level (Mölle & Born, 2009; Sirota, Csicsvari, Buhl, & Buzsaki, 2003).

Further evidence for the relevance of sleep spindles for declarative memory consolidation comes from human experiments, showing the dependency of sleep spindle density on prior learning experience. After learning of a word association task spindle density increased compared to a non-learning control task and was correlated to recall performance before and after sleep (Gais, Mölle, Helms, & Born, 2002). Subsequent studies even demonstrated some topographical specificity of this effect depending on the task material, that is stronger increases in left frontal regions for verbal (Clemens, Fabo, & Halasz, 2005), in posterior parietal regions for visuospatial memory (Clemens, Fabo, & Halasz, 2006), and in the contralateral motor cortex after finger motor-skill learning (Nishida & Walker, 2007). Moreover, it could be shown that the amount of sleep spindle activity is related to individual learning and general cognitive abilities in a trait-like manner (Schabus et al., 2006) which is independent of the acute learning related increase in spindle activity that is associated

with overnight task improvements (Schabus et al., 2008). The learning related increase in spindle activity further appears to have some temporal specificity, that is being grouped in slow oscillation up states (Mölle, Eschenko, Gais, Sara, & Born, 2009) and being strongest within the first 90 min of post-learning NREM sleep (Gais et al., 2002).

1.3.2.3 Cortical Slow Oscillations

In the context of sleep-dependent system consolidation, the role of the slow oscillation is mainly seen in the initiation and synchronization of the hippocampo-neocortical cross-talk. Its enormous relevance becomes clear in experiments either disrupting or boosting slow oscillatory activity during sleep after learning. Studies using sound stimuli to selectively suppress slow waves during NREM sleep without affecting total sleep time found a devastating effect on the otherwise clear overnight improvement in texture discrimination (Aeschbach, Cutler, & Ronda, 2008) or visuospatial tasks (Landsness et al., 2009).

Even stronger support comes from studies employing transcranial direct current stimulation (tDCS) during sleep after learning (Marshall, Helgadottir et al., 2006; Marshall, Mölle, & Born, 2006; Marshall, Mölle, Hallschmid, & Born, 2004). The initial rationale behind theses experiments was that SWS is usually accompanied by a pronounced endogenous negative DC potential shift in frontal regions (Marshall, Mölle, & Born, 2003) and anodal tDCS of the frontal cortex should thus amplify slow oscillatory activity and thereby also facilitate declarative memory consolidation. Indeed, exogenous application of constant (Marshall et al., 2004) as well as 0.75 Hz slow oscillation-like oscillatory anodal DC stimulation (Marshall, Helgadottir et al., 2006) increased endogenous slow oscillations outlasting the stimulation itself and improved consolidation of a declarative, hippocampus-dependent word pair learning task but not of a procedural, hippocampus-independent mirror drawing task. Notably, stimulation during wakefulness or REM sleep as well as oscillatory tDCS with theta-like 5 Hz during SWS had no positive effects. When using oscillatory 0.75 Hz tDCS, endogenous slow oscillations even appeared to remain in phase with the stimulation cycles for several seconds after its termination, suggesting actual entrainment of brain activity by the external current (Marshall, Helgadottir et al., 2006). Together these results

indicate an important function of the slow oscillation in driving processes of hippocampus-dependent memory consolidation during sleep.

1.3.2.4 Evidence from Functional Neuroimaging in Humans

As invasive electrophysiological recordings of hippocampal or cortical patterns cannot be done as easily in humans as in rats (but see Axmacher, Haupt, Fernandez, Elger, & Fell, 2008; Clemens et al., 2007), non-invasive functional neuroimaging techniques such as positron emission tomography (PET) or functional magnetic resonance imaging (fMRI) play an important role in the investigation of reactivation and system consolidation processes in humans. Principally, two different approaches have been applied. (i) The indirect consequences of sleep-dependent system consolidation have been accessed by measuring changes in task-specific brain activations across sleep and wake, respectively (referred to as *offline approach*). (ii) Reactivation processes have been tried to be directly accessed during sleep following learning and control conditions, respectively (referred to as *online approach*).

The *offline approach* asks whether sleep actually reorganizes memory traces, that is redistribute them across distant networks of the brain. fMRI studies using this approach have revealed interesting results for both procedural and declarative memory consolidation. One of the earlier studies demonstrated for example that sleep compared to sleep deprivation not only improves behavioral performance but also changes activity within and connectivity between task-related brain regions in a *pursuit rotor task* (Maquet, Schwartz, Passingham, & Frith, 2003). Similar studies on the *serial reaction time task* (SRTT) reported conflicting results, that is finding either a decrease (Fischer, Nitschke, Melchert, Erdmann, & Born, 2005) or increase (Walker, Stickgold, Alsop, Gaab, & Schlaug, 2005) in task-related motor regions to be associated with a night of sleep. However, lacking a comprehensive model for sleep-dependent system memory consolidation in the procedural domain these results are difficult to interpret and need further clarification.

Regarding the hippocampus-dependent declarative memory system, the predictions are much more clear. Over time (and sleep), the hippocampus should loose its implication in memory retrieval while the involvement of cortical regions should become even more pronounced. Yet, the results are far from consistent. For exam-

ple, brain activity associated with spatial navigation in a virtual town paradigm shifted towards striatal involvement across sleep, while the decrease in hippocampal involvement was influenced by time but not by sleep (Orban et al., 2006). In another study, however, a short nap was sufficient to reduce hippocampal activity associated with the recognition of previously encoded landscape photographs (Takashima et al., 2006). Additionally SWS duration correlated positively with memory performance and negatively with later hippocampal involvement. Conversely, a full night of sleep (compared to sleep deprivation) led to increased hippocampal activity in a word pair association task, accompanied with increased connectivity to medial prefrontal regions (Gais et al., 2007). Medial prefrontal cortex activity was still enhanced after six month in the sleep condition. However, increased hippocampal activity after sleep rather contradicts what is predicted by the model of sleep-dependent hippocampo-neocortical memory transfer. Other studies reporting a decrease of hippocampal activity over time did not control for the impact of sleep (Takashima et al., 2009). One possible reason for this inconsistency might be the unknown time scale on which the proposed system consolidation processes actually occur, as during its course there might be phases of both stronger and weaker hippocampal involvement.

The *online approach* comes with other, mostly methodological, problems. As fMRI measurements come with loud noise and marked movement restrictions, they provide a challenging environment for falling asleep. Thus, for the sake of feasibility, mainly PET imaging studies have been applied in the beginning, accepting the drawback of lower temporal and spatial resolution. The first studies still focused on REM sleep as the proposed state for memory replay, showing that brain areas involved in the acquisition of basic visuomotor skills (SRTT) are more active (in terms of regional cerebral blood flow, rCBF) during REM sleep after learning than after a control task (Maquet et al., 2000) and that this reactivation is related to the extraction of implicit rules hidden in the task (Peigneux et al., 2003). Later the same group demonstrated that the amount of hippocampal activity during SWS after a spatial navigation paradigm predicted subsequent behavioral performance (Peigneux et al., 2004).

Finally, elegant evidence for the causal role of hippocampal reactivation in sleep-dependent memory consolidation comes from a much noticed study which triggered hippocampal memory traces by odor cues during SWS (Rasch, Buchel, Gais, & Born, 2007). Subjects learned picture-location associations (i.e. the game “Con-

centration"; in Germany called "Memory") before going to sleep. During learning they either were or were not exposed to a specific odor which then either was or was not administered again during SWS (or REM sleep as a control). During subsequent retrieval the next day, subjects performed much better when they had been re-exposed to the learning-associated odor during SWS but not during REM sleep. An additional functional magnetic resonance (fMRI) experiment corroborated the interpretation that odor cues during sleep could directly trigger hippocampal memory traces (as the olfactory system bypasses the sensory gate of the thalamus) thereby facilitating the reactivation of odor-related picture-location associations.

1.3.3 Synaptic Homeostasis vs. Systemic Memory Consolidation

Are the concepts of synaptic homeostasis (Tononi & Cirelli, 2006) and sleep-dependent system memory consolidation (Born et al., 2006) mutually exclusive, independent, or just two sides of the same coin (Diekelmann & Born, 2010)? The data employed to corroborate either hypothesis are largely overlapping and frequently the same studies are cited as support for both of them. As both theories make pretty much the same predictions regarding a lot of different experimental designs and measures, no study has ever directly tested them against each other. Here are some examples for why the direct comparison of both models is highly problematic:

(i) While slow oscillations/slow waves should drive synaptic downscaling on the one hand, they are thought to orchestrate the hippocampo-neocortical dialogue on the other. However, both scenarios predict them to be enhanced after learning or LTP-induction. The same prediction holds also true for spindles as they are inevitably associated with slow oscillations, although no particular function of sleep spindles has been proposed for downscaling.

(ii) Synaptic downscaling is proposed to improve the signal-to-noise ratio of neuronal representations by global depotentiation and removal of unnecessary weak synapses, whereas memory consolidation by reactivation is believed to stabilize memory representations by increasing or at least maintaining synaptic strengths. Again, both models predict improved memory performance after sleep compared to wakefulness and would expect e.g. slow wave activity to be correlated with this improvement. It is however problematic that usually cortical excitability changes or sim-

ple procedural tasks are used to test the synaptic downscaling assumption while the core model of sleep dependent memory consolidation is mainly focused on declarative hippocampus-dependent memory.

(iii) Neuronal reactivations of learning related patterns during sleep, as measureable by electrophysiological recordings or functional neuroimaging, are often cited as evidence for ongoing memory consolidation but could just as well be the mere reverberation of a system in which some connections had been modified by learning and which is now activated unspecifically by the powerful, wide spread oscillations of the sleeping brain.

Thus up till now, all results are at least compatible with both theories, although some results may be more easily explained by either one of them. I therefore argue that both, synaptic downscaling to maintain homeostasis of synaptic weights and system memory consolidation by reactivation and redistribution of memory traces may take place during sleep, simultaneously and independently (Diekelmann & Born, 2010). However, they might share some basic neuronal mechanisms regarding how neuronal oscillations induce plastic processes. Uncovering these basic mechanisms of sleep-dependent plasticity is one of the most important enterprises in the field.

2 Methodological Considerations

2.1 A Multimodal Neuroscientific Approach

Neuroscientific research in humans compared to animal studies is always limited regarding the neuronal level of recordings (no measures of membrane potentials, firing rates, multi-unit activity, etc.) as well as the kind of possible experimental interventions (no well defined lesions, toxic agents, genetic knock out/in, etc.), as most invasive techniques are ineligible due to ethical concerns. Since all available non-invasive techniques for human systems neuroscience have their specific assets and drawbacks, it is of particular importance to combine different approaches in order to compensate for the respective limitations. However, the consecutive or simultaneous application of different imaging modalities or even the combination with transcranial stimulation techniques comes with a bunch of technically demanding challenges. In principal, all multimodal combinations can be applied consecutively or simultaneously with the latter usually being more informative but also much more problematic.

As this multimodal approach is an outstanding methodological feature of most studies included in this thesis, I will raise and briefly discuss some of the most important aspects in the following subsections. The recording methods I applied comprise electromyography (EMG), polysomnography (PSG), electroencephalography (EEG), and functional magnetic resonance imaging (fMRI). Additionally, I made use of the non-invasive brain stimulation techniques of transcranial magnetic stimulation (TMS) and transcranial direct current stimulation (tDCS). A basic introduction into these techniques or even a comprehensive discussion of the applied multimodal combinations (i.e. EEG-fMRI, TMS-tDCS, and TMS-EEG), however, is not in the scope of this thesis and beyond a few introductory sentences the reader will be kindly referred to the respective methodological review papers in each subsection. Specific methodological details relevant for my own work can further be found in the methods sections of the respective original research papers.

2.2 Combining fMRI and EEG

The most widely available non-invasive recording techniques are electroencephalography (EEG), measuring the summed potentials of postsynaptic activity in neuronal populations, and functional magnetic resonance imaging (fMRI), indirectly assessing

neuronal activity by means of associated local increases in blood oxygenation. While EEG has a fantastic temporal resolution (in the submillisecond range) and is therefore able to realistically depict neurons' ongoing electrical activity, its spatial resolution is relatively bad (in the order of centimeters) as even high-density recordings with up to 256 electrodes suffer from spatial smearing due to volume conduction of skull an skin. Moreover, surface EEG recordings are dominated by radially oriented neocortical neurons and are mostly blind towards subcortical structures, and source modeling approaches could not overcome the inverse problem (numerous different electrical source combinations can result in the same surface EEG pattern) so far. Conversely, fMRI has a comparably low temporal resolution (in the order of seconds) but can spatially resolve the whole brain on a millimeter scale, thus allowing access to deep brain structures such as hippocampus, thalamus and amygdala or ventromedially oriented cortical regions like the inferior temporal lobes. The simultaneous application of both imaging modalities can partly compensate for the respective limitations. Moreover, in the context of sleep research the EEG is not only of critical importance to distinguish sleep and its various substages from wakefulness but also provides important details about specific neuronal events such as slow oscillations and sleep spindles to inform the fMRI analyses. However, simultaneous EEG-fMRI recordings are highly challenging. Not only because the EEG equipment has to be fully MRI compatible in technical and safety terms but also as (i) the strong high-frequency magnetic gradients of the MRI scanner cause massive distortions in the EEG, and (ii) small electrode movements in the static magnetic field due to cardiac pulsation result in highly variable EEG artifacts. The same holds true for other electrophysiological recordings such as EMG or electrooculogram (EOG), used for PSG during sleep. Within the last years it has become possible to acquire high-quality EEG recordings during continuous fMRI sampling, providing new insights into oscillatory processes in the human brain. For recent and comprehensive reviews on the technique of EEG-fMRI please refer to (Debener, Ullsperger, Siegel, & Engel, 2006; Herrmann & Debener, 2008; Ritter & Villringer, 2006).

2.3 Combining TMS and tDCS

Currently, there are three different types of non-invasive, since transcranial, brain stimulation techniques available for human application: transcranial electric stimula-

tion (TES), transcranial direct current stimulation (tDCS), and transcranial magnetic stimulation (TMS).

In TES, a focal bipolar electrode arrangement is placed on the head and a short but rather strong constant electric pulse (< 100 µs, 200-400 V) is applied which is able to fully depolarize neurons in the underlying brain tissue and thus to evoke action potentials. However, as TES is very unpleasant (or even painful), this technique is only rarely used nowadays and will not be discussed here any further. Please see the following papers for details (Brandt, Brocke, & Irlbacher, 2007; Di Lazzaro et al., 2004). For tDCS, less focal large sponge electrodes are attached to distant parts of the head and a weak direct current (current density between 0.03 and 0.5 mA/cm^2) is applied for several minutes. This direct current is insufficient to evoke action potentials by itself but rather shifts the resting membrane potential of neurons to a more depolarized or more hyperpolarized level, thus facilitating or reducing spontaneous firing rates of these neurons, respectively, depending on current polarity. However, tDCS can not only induce acute but also long-lasting shifts in cortical excitability, which are presumably mediated by LTP-/LTD-like mechanisms. See (M. Nitsche et al., 2008; M. Nitsche & Paulus, 2007; M. A. Nitsche & Paulus, 2000) for details. Last but not least, TMS is the most widely used tool for non-invasively and painlessly stimulating the human brain. It has been invented about 25 years ago (Barker, Jalinous, & Freeston, 1985), was repeatedly refined, and has by now been used in more than thousand studies. Basically, an encased copper coil is connected to a stimulation device with large capacitors and held against the subjects head. When the capacitors discharge, a strong (up to 3 Tesla) but very brief (< 1 ms) electromagnetic field with a steep gradient is produced around the coil by electromagnetic induction which in turn, by means of magnetoelectric induction, elicits a current flow in the brain tissue, capable of evoking action potentials in cortical neurons. Thus, TMS eventually is an electrical stimulation, though unlike TES the magnetic pulse penetrates the skull painlessly rendering TMS a much more comfortable technique. TMS can be used for multiple purposes and principally on all neocortical regions close to enough to the surface (within a few centimeters) to be accessible by the magnetic field. Single-pulse TMS can evoke muscle twitches or phosphenes when stimulating the primary motor or visual cortex, respectively, allowing the quantitative assessment of cortical excitability by measuring motor evoked potentials (MEP) in the innervated

muscles or psychophysiologically determining perception thresholds. Moreover, repetitive TMS (rTMS) in low (<1 Hz) or high (> 5 Hz) frequencies can be used to induce LTP- and LTD-like excitability changes, respectively (Fitzgerald et al., 2006), lasting for minutes to hours, but also more complex paradigms have been invented in the last years (Huang, Edwards, Rounis, Bhatia, & Rothwell, 2005; Stefan, Kunesch, Cohen, Benecke, & Classen, 2000). Additionally, TMS can be applied in a so called *virtual lesion approach* to disrupt neuronal activity in a given cortical region prior to (*offline*) or during (*online*) the performance of a specific cognitive task. As disturbance of task-relevant neuron populations will result in altered behavior (errors or increased reaction time) the causal contribution of a cortical region can be accessed (H. R. Siebner, Hartwigsen, Kassuba, & Rothwell, 2009; Walsh & Cowey, 2000). For an introduction into the broad field of TMS (but also TES and tDCS) as well as further detailed readings regarding all topics addressed above I suggest the following books (H.R. Siebner & Ziemann, 2007; Wassermann et al., 2008).

TMS and tDCS can be combined consecutively to investigate the interaction of different plasticity inducing stimulation protocols in order to gain new insight into processes of homeostatic metaplasticity or gating (Ziemann & Siebner, 2008). However, they can also be combined simultaneously with single-pulse TMS as a means for measuring cortical excitability changes induced by ongoing tDCS. This is principally unproblematic, when taking care of some minor caveats such as proper positioning of electrode leads to avoid the induction of currents by magnetic stimulation and adjustment of TMS intensity to the increased coil-brain distance due to the large sponge electrodes. This online-measurements of cortical excitability during tDCS have become important since the recent development of tDCS protocols with oscillating current strength or even changing polarity (transcranial alternating current stimulation, tACS), as it is totally unclear how these time-varying exogenous currents acutely change cortical excitability.

2.4 Combining TMS and EEG

As mentioned above, the impact of TMS on the human cortex can be assessed by MEPs in the motor cortex and by phosphenes in visual areas but for all other brain regions behavioral measures have been for a long time the only accessible variable.

Due to recent technical and methodological developments, however, it is now possible to measure the direct cortical response to TMS with simultaneously acquired high-density (64-256 channel) EEG (Esser et al., 2006; Ilmoniemi & Kicic, 2009; Massimini et al., 2007; Massimini et al., 2005; Virtanen, Ruohonen, Naatanen, & Ilmoniemi, 1999).

Although this approach is also of essential relevance in the context of sleep and plasticity research, I will not go into methodological details here but kindly refer the reader to an up-to-date consensus paper I recently coauthored (H. R. Siebner, Bergmann et al., 2009):

PAPER I

Siebner, H. R., Bergmann, T. O., Bestmann, S., Massimini, M., Johansen-Berg, H., Mochizuki, H., Bohning, D. E., Boorman, E. D., Groppa, S., Miniussi, C., Pascual-Leone, A., Huber, R., Taylor, P. C., Ilmoniemi, R. J., De Gennaro, L., Strafella, A. P., Kähkönen, S., Klöppel, S., Frisoni, G. B., George, M. S., Hallett, M., Brandt, S. A., Rushworth, M. F., Ziemann, U., Rothwell, J. C., Ward, N., Cohen, L. G., Baudewig, J., Paus, T., Ugawa, Y., Rossini, P. M. (2009). Consensus paper: Combining transcranial stimulation with neuroimaging. *Brain Stimulation*, 2(2), 58-80.

This consensus paper comprehensively reviews the current state of the art as well as conceptual and methodological considerations regarding TMS-EEG and other combinations of TMS and neuroimaging methods such as structural and functional MRI, PET, magnetoencephalography (MEG), and near infrared spectroscopy (NIRS).

3 Empirical Studies

3.1 Research Agenda

Neuroscientific research of the last decades has considerably extended our knowledge of how sleep and brain plasticity might be connected. However, the specific neuronal mechanisms mediating this relationship are still uncovered and some key assumptions of the major theories on synaptic homeostasis during sleep (Tononi & Cirelli, 2006) and on sleep-dependent active system memory consolidation by reactivation (Born et al., 2006; Diekelmann & Born, 2010; Marshall & Born, 2007; Rasch & Born, 2007) have not been proven yet. Moreover, a promising new technique for modulating neuronal processing modes of memory acquisition during wakefulness (Kirov, Weiss, Siebner, Born, & Marshall, 2009) and consolidation during sleep (Marshall, Helgadottir et al., 2006; Marshall, Mölle et al., 2006) by transcranial application of oscillating currents has recently emerged. However, the mechanisms of action underlying this stimulation technique are still unknown and it is of vital importance to determine these before the technique might become a therapeutical tool in the future. The empirical research branch of this thesis can therefore be divided into three major parts:

The first part is concerned with the synaptic homeostasis hypothesis, testing its major assumptions (i) that extent and topography of SWA depend on the amount and direction of previously induced synaptic plasticity and (ii) that synaptic strength is actually downscaled during SWS (→ PAPER II).

The second part focuses on the neuronal mechanisms of sleep-dependent system consolidation of declarative memories. I will first report research on how slow and fast sleep spindles are differentially grouped in the slow oscillation cycle, presumably undertaking different functions in cortical plasticity (→ PAPER III). I will then provide first-time evidence from simultaneous EEG-fMRI recordings during sleep, demonstrating that spindles actually drive learning-specific hippocampo-neocortical reactivation in humans (→ PAPER IV).

The third part aims at elucidating the neurophysiological basis on which the exogenous application of oscillatory tDCS may interact with ongoing endogenous oscillations of the brain. I will report two studies on how slow oscillation-like tDCS can

affect both acute (→ PAPER V) and lasting (→ PAPER VI) changes in cortical excitability during wakefulness.

Each of the next subsections will start with outlining the specific research questions of the study followed by a concise summary of its experimental design and results and will be closed by a brief conclusion. For any methodological details, a full presentation of the results, and a more comprehensive discussion the reader is kindly referred to the respective original research paper provided in the appendix.

3.2 Part I: Synaptic homeostasis during Sleep

The synaptic homeostasis hypothesis (Tononi & Cirelli, 2003, 2006) proposes a process of synaptic downscaling during NREM sleep, downregulating previous synaptic potentiation to maintain a proper range of plasticity and the functionality of neuronal networks (see Section 1.3.1). This process is believed to be mediated by the cortical slow oscillation, which should therefore depend in its extend and localization on the amount and topography of previous potentiation.

3.2.1 How Plasticity Affects Subsequent Sleep

PAPER II

Bergmann, T. O., Mölle, M., Marshall, L., Kaya-Yildiz, L., Born, J., & Siebner, H. R. (2008). A local signature of LTP- and LTD-like plasticity in human NREM sleep. *European Journal of Neuroscience, 27*(9), 2241-2249.

The prediction that the local expression of slow wave activity (SWA) directly depends on bidirectional synaptic plasticity has gained empirical evidence from various sources, including human data (Huber et al., 2007; Huber et al., 2006; Huber et al., 2004). It has, however, remained unclear whether the observed bidirectional changes in local SWA actually depend on previous synaptic potentiation and depression or rather on the mere amount of neuronal activation in the respective neuron populations. Moreover, despite repeatedly reported changes in spindle activity associated with altered SWA and the widely proposed function of sleep spindles in cortical plasticity, the direct dependency of spindle expression on basic cortical plasticity para-

digms has never been tested. In addition, data on actual sleep-dependent changes in cortical excitability are rare, although the *synaptic homeostasis hypothesis* would predict a general reduction caused by downscaling during SWS.

Research Question 1: Is it bidirectional synaptic plasticity or mere usage of cortical neurons that modulates subsequent local SWA?

Research Question 2: Does the local cortical expression of sleep spindles directly depend on previously induced cortical plasticity?

Research Question 3: Is (motor-)cortical excitability globally reduced during sleep while enhancing differential effects (signal-to-noise ratio)?

To address these questions we employed a relatively new transcranial brain stimulation paradigm termed paired associative stimulation (PAS) to induce either LTP- or LTD-like plasticity in the hand area of the primary motor cortex ($M1_{HAND}$). PAS can induce bidirectional plasticity in the motor or somatosensory cortex just by varying the interstimulus interval (ISI) according to the rules of STDP (Section 1.1.1.3), nevertheless applying the same absolute amount of neuronal input (Stefan, Kunesch, Benecke, Cohen, & Classen, 2002; Stefan et al., 2000; Wolters et al., 2003). During motor PAS, single-pulse TMS over the left $M1_{HAND}$ is repeatedly paired with electrical stimulation of the contralateral median nerve at the wrist. If the peripheral volley (presumably via sensorimotor projections) arrives at the motor cortex shortly before the TMS pulse, excitability of corticospinal motor neurons will be facilitated (LTP-like). Conversely, if the TMS pulse shortly precedes the peripheral input into $M1_{HAND}$, lasting inhibition of motor cortical excitability is caused (LTD-like). These excitability changes are topographically specific to the proximal hand muscles innervated by the median nerve (i.e. the abductor pollicis brevis muscle, APB) and can be assessed by measuring changes in peak-to-peak amplitudes of motor evoked potentials (MEP) due to single-pulse TMS. The paradigm can be further individualized by adjusting the ISI to the subject-specific N20 latency of the somatosensory evoked potential (SEP) (Muller-Dahlhaus, Orekhov, Liu, & Ziemann, 2008; J. F. Müller, Orekhov, Liu, & Ziemann, 2007; Ziemann, Ilic, Pauli, Meintzschel, & Ruge, 2004).

We applied PAS_{LTP} (ISI = N20+2ms), PAS_{LTD} (ISI = N20-5ms), or $PAS_{control}$ (eight randomized and per se ineffective ISIs; to adjust for any unspecific stimulation or time effects) to the $M1_{HAND}$ of twelve subjects directly before they went to bed in

the evening. MEPs were acquired before and after PAS as well as the next morning after a full night of sleep, during which PSG and 27-channel EEG was continuously recorded. Changes in MEP amplitudes were used to determine successful induction of bidirectional plasticity and its modulation across sleep. EEG activity was analyzed to reveal plasticity-related changes in local SWA as well as power and density of slow (10-13 Hz) and fast (13-16 Hz) sleep spindles.

MEPs showed high inter-individual variations in the conditioning effects of PAS_{LTP} and PAS_{LTD} on cortical excitability and a marked general excitability decrease across the night. Nevertheless, $PAS_{control}$-adjusted data revealed a differential effect of both protocols which did not decay but, if anything, increased across a full night of sleep - though usually vanishing within about an hour (Figure 1, Bergmann et al., 2008). This was true for the targeted APB muscle only, but not for the control first dorsal interosseus (FDI) and abductor digiti minimi (ADM) muscles. EEG analyses revealed widespread and topographically rather unspecific effects of PAS on SWA as well as slow spindle power and density during the first hour of non-rapid eye movement (NREM) sleep (Figure 2, Bergmann et al., 2008). However, the individual efficacy of PAS_{LTP} and PAS_{LTD} to potentiate or suppress cortical excitability strongly ($r > 0.8$) correlated with the differential effect of both protocols on slow spindle power and density focally in the stimulated $M1_{HAND}$ and adjacent premotor cortex (Figure 3, Bergmann et al., 2008). However, no relation was found between overnight MEP changes and any of the EEG measures.

Conclusion 1: While SWA was indeed differentially affected by LTP- and LTD-like PAS (producing the same amount of neuronal activity), the effects were relatively widespread and even showed a reversed directionality, expressing stronger SWA after PAS_{LTD}. Notably, two other groups have published quite similar studies shortly afterwards, also using PAS to probe plasticity-related changes in subsequent sleep. While Huber and colleagues reported the proposed bidirectional and topographically specific changes in SWA (Huber et al., 2008), De Gennaro et al. also found inconsistent results lacking the proposed specificity (De Gennaro et al., 2008). Thus, changes in SWA actually depend on previously induced synaptic plasticity and not merely neuronal activity, however, the direction of these changes does not appear to be as straight forward as expected.

Conclusion 2: The comparably strong correlation ($r > 0.8$) between PAS effects and focal changes in spindle power and density indicates that the bidirectional induction of cortical plasticity shapes the local expression of slow sleep spindles during subsequent NREM sleep. As this effect was exclusive for slow spindles and was mainly driven by the PAS_{LTD} protocol, potentially different functions of slow and fast sleep spindles are extensively discussed in the original research paper.

Conclusion 3: While (motor-)cortical excitability fundamentally decreased over night, the differential effect between both plasticity protocols rather became stronger. These results could either be explained in terms of synaptic downscaling and increased signal-to-noise ratio (*synaptic homeostasis hypothesis*) or as sleep-dependent consolidation and strengthening of initially weak and labile memory traces. However, lacking a waking control group, other effects such as circadian rhythm, immobilization effects etc. cannot be ruled out and hamper a clear interpretation of the results. Future studies have to explicitly address these points.

3.3 Part II: System Memory Consolidation during Sleep

The temporally fine-tuned interplay of cortical slow oscillations, hippocampal sharp wave-ripples, and thalamo-cortical spindles during NREM sleep has been proposed to mediate the process of sleep-dependent active system memory consolidation by reactivation (Born et al., 2006; Diekelmann & Born, 2010; Marshall & Born, 2007; Rasch & Born, 2007) (Section 1.3.2). However, the exact rules according to which theses oscillations interact are still unknown and so is the potential functional difference between slow and fast sleep spindles. Moreover, although learning-related hippocampal activation has been shown by neuroimaging in humans during SWS (Peigneux et al., 2004) the reactivation has never been temporally related to specific EEG events. Yet, if the proposed model is correct, cortical representations which had been connected by the hippocampus during declarative learning should be reactivated by sleep spindles time-locked to the hippocampal sharp wave-ripples during subsequent NREM sleep.

3.3.1 Differential Grouping of Slow and Fast Sleep Spindles in the Slow Oscillation

PAPER III

Mölle, M., Bergmann, T. O., Marshall, L., & Born, J. (in prep). Slow and fast spindles grouped in opposite phase during slow sleep oscillations.

Sleep spindles group hippocampal ripples events (Siapas & Wilson, 1998) as they are themselves grouped by the cortical slow oscillation (Mölle et al., 2002). The thalamo-cortical sleep spindle is the proposed key mechanism for a sleep-dependent modulation of cortical plasticity by causing massive Ca^{2+}-influx into the apical dendrites of neocortical neurons (Destexhe et al., 2007; Marshall & Born, 2007), thereby potentially acting as an amplifier for the incoming hippocampal information. However, since probably relying on the principles of STDP, the exact timing of ripples, spindles, and slow oscillations is believed to be critical (Diekelmann & Born, 2010). Therefore variations in the temporal arrangement of these nested oscillations might provide the basis for bidirectional plasticity, i.e. LTP and LTD, a functional difference that has already been suggested to distinguish fast and slow sleep spindles (Paper II, Bergmann et al., 2008).

Research Question: Are slow and fast sleep spindles differently grouped in slow oscillations and may they thus have different functions in sleep dependent plasticity?

Polysomnography and 27-channel EEG were recorded during a full night of sleep in eleven healthy male subjects. EEG data were analyzed with respect to the exact grouping of slow and fast sleep spindles in the slow oscillation. Individual slow oscillations and sleep spindles were detected according to standard algorithms (Gais et al., 2002; Mölle et al., 2002) in those channels expressing the largest power in the respective frequency band, that is fronto-central for slow oscillations (0.5-1.1 Hz) and slow spindles (9-12 Hz), and centro-parietal for fast spindles (12-15 Hz) (see Figure 1 for power distribution and Figure 2 for averaged event plots, Mölle et al., in prep.).

Event correlation histograms of spindle activity were calculated to determine the temporal relationship between the three oscillators. These analyses revealed that fast centro-parietal spindles preceded slow frontal spindles by roughly 500 ms (Figure 3, Mölle et al., in prep.). Notably, while fast spindles were most pronounced

during the slow oscillation up state (cf. Mölle et al., 2002), slow spindles were predominantly located in the up-to-down state transition of the slow oscillation, peaking briefly before its negative peak (Figure 4, Mölle et al., in prep.). Analyses of slow oscillation sequences further revealed that fast spindles were largest when occurring in the first of a series of continuous slow oscillations, while the slow oscillation itself became largest when already preceded by another one, and the slow spindle size varied in parallel with the slow oscillation (Figure 7, Mölle et al., in prep.).

Conclusion: Slow and fast sleep spindles are in fact grouped in opposite phases of the cortical slow oscillation, therefore providing an ideal mechanism for bidirectional plasticity. Slow spindles arrive in the neocortex during phases of widespread hyperpolarization (down state), finding neocortical neurons in a relatively unresponsive state. Conversely, neocortical fast spindle input coincides with massive depolarization (up state) and is therefore likely followed by suprathreshold excitation of cortical neurons. According to the rules of STDP (Section 1.1.1.3), this temporal relationship might favor LTP and LTD, respectively. Moreover, the cortical depolarization by fast spindles seems to drive the development of further slow oscillations, while slow spindles do not appear to be much involved into slow oscillation initiation.

3.3.2 Sleep Spindles Drive Learning-specific Hippocampo-Neocortical Reactivation

PAPER IV

Bergmann, T. O., Mölle, M., Diedrichs, J., Born, J., & Siebner, H. R. (in prep). Sleep spindles drive learning-specific hippocampo-neocortical reactivation.

Reactivation of temporally specific neuronal patterns has been shown to take place time-locked to sharp-wave ripple activity during post learning NREM sleep in rodents' hippocampus (Ji & Wilson, 2007; Lee & Wilson, 2002; Sutherland & McNaughton, 2000; Wilson & McNaughton, 1994) and prefrontal cortex (Peyrache et al., 2009), whereas in humans there is only coarse evidence for stronger hippocampal activity during SWS after spatial learning coming from PET imaging work with low temporal and spatial resolution (Peigneux et al., 2004). However, we actually have quite precise predictions about when and where reactivation should occur. Hippocampo-

neocortical crosstalk should take place when the cortical slow oscillation synchronizes hippocampal sharp wave-ripples and thalamo-cortical spindles (Born et al., 2006). Moreover, the hippocampus should jointly reactivate those cortical representations, that have been bound together during previous learning (Frankland & Bontempi, 2005). We therefore chose learning material for which the cortical sites of processing are well known, i.e. faces (fusiform face area, FFA; occipital face area, OFA) and scenes (parahippocampal place area, PPA). Stimuli had to be linked during a paired associates learning task, thus requiring the hippocampus. During subsequent NREM sleep simultaneous EEG-fMRI was acquired, allowing to detect individual sleep spindles and to inform the fMRI model accordingly.

Research Question: Are previously acquired hippocampo-neocortical memory traces, linking hippocampus with FFA, OFA and PPA, specifically reactivated during sleep spindles in subsequent NREM sleep?

Subjects were preselected in an adaptation night depending on whether they managed to reach deep SWS during continuous EEG-fMRI scanning. From 24 subjects participating in the adaptation night only eleven could be included and only nine data sets could be analyzed due to data quality reasons. Prior to the adaptation night we also acquired the structural MR images (see experimental time line in Figure 1, Bergmann et al., in preparation). Then, in two separate experimental nights, subjects performed either a paired associates learning task, associating pictures of faces and scenes (LEARNING) or a basic visuomotor task, matched for basic visual stimulation and motor output but not requiring any learning or processing of faces and scenes (CONTROL) (for a detailed task description see Figure 1, Bergmann et al., in preparation). Then, subjects were equipped with MRI-compatible 32-channel EEG-caps and were allowed to sleep max. 2.5 h (i.e. the first sleep cycle) in the MRI scanner.

Sleep EEG was scored and sleep spindles and slow oscillations were automatically detected in all NREM epochs (Mölle et al., 2002). Sleep spindles where entered in the fMRI model as events with a parametric modulator accounting for individual spindle amplitudes. Additionally, slow oscillations and their amplitudes were also entered to reduce error variance in the model (Dang-Vu et al., 2008; Schabus et al., 2007). Moreover, cardiovascular and head movement related artifacts were modeled using ECG- parameters and realignment parameters, respectively.

Subjects performed well on the paired associates LEARNING Task (Figure 2, Bergmann et al., in preparation). When contrasted against the CONTROL TASK, face cues selectively activated bilateral fusiform face area (FFA), occipital face areas (OFA), and the Amygdala. Conversely, scene cues bilaterally activated the parahippocampal place area (PPA) as well as wide clusters in the parieto-occipital sulcus, the transverse occipital sulcus, and the intraparietal sulcus (Figure 4, Bergmann et al., in preparation).

During subsequent sleep, individual sleep spindles were associated with increased blood oxygenation level dependent (BOLD)-signal, mainly in the thalamus, bilateral hippocampi and adjacent parahippocampal gyri, clearly reflecting thalamic spindle generation and either direct spindle input into the hippocampus or time-locked hippocampal sharp wave-ripple activity (Figure 5, Bergmann et al., in preparation). In several regions including the bilateral hippocampus, insula, anterior cingulate cortex and supplementary motor area, spindle-related BOLD-responses even covaried with the respective size of individual spindle amplitudes, suggesting a direct relationship between surface EEG amplitude and BOLD-response. Contrasting sleep spindle amplitude regressors from LEARNING and CONTROL conditions revealed that spindles were more strongly associated with brain activity in the right hippocampus, left PPA, right FFA and bilateral OFA after LEARNING than after CONTROL (Figure 6, Bergmann et al., in preparation). Notably, this learning-dependent spindle-related neuronal activity was topographically highly specific and largely overlapped with face- and scene-specific neocortical regions involved in the LEARNING TASK during prior wakefulness (Figure 7, Bergmann et al., in preparation).

Conclusion: We could demonstrate for the first time that neocortical areas representing the learned material (i.e. FFA, OFA and PPA) are indeed jointly reactivated together with the hippocampus time-locked to sleep spindles in subsequent NREM sleep. This findings tie nicely in with the idea of a sleep-dependent active system consolidation of declarative memories by concerted reactivation of the involved neuronal assemblies (Born et al., 2006; Diekelmann & Born, 2010; Marshall & Born, 2007; Rasch & Born, 2007).

3.4 Part III: Neuromodulation by Slow Oscillatory Stimulation

Slow oscillatory transcranial direct current stimulation (so-tDCS) has been used to boost endogenous slow oscillations and associated spindles during NREM sleep, thereby also enhancing sleep-dependent consolidation of declarative memories (Marshall, Helgadottir et al., 2006) (see Section 1.3.2.3). However, a similar approach using constant tDCS (c-tDCS) had previously been successful in enhancing both endogenous slow oscillations and declarative memory consolidation (Marshall et al., 2004). As the idea of frequency-specific transcranial oscillatory stimulation has recently been adopted to modulate memory encoding (Kirov et al., 2009) or even visual perception and voluntary movements (Kanai, Chaieb, Antal, Walsh, & Paulus, 2008; Pogosyan, Gaynor, Eusebio, & Brown, 2009, these studies used alternating currents) during wakefulness, the questions arise (i) how so-tDCS actually affects acute ongoing activity in the stimulated cortex and (ii) whether or not so-tDCS also induces lasting after-effects in cortical excitability as it is known from c-tDCS. We therefore transferred the so-tDCS paradigm to fit into the well documented framework of primary motor cortex tDCS during wakefulness (M. Nitsche et al., 2008; M. A. Nitsche & Paulus, 2000).

3.4.1 Acute effects of Slow Oscillatory Stimulation

PAPER V

Bergmann, T. O., Groppa, S., Seeger, M., Mölle, M., Marshall, L., & Siebner, H. R. (2009). Acute changes in motor cortical excitability during slow oscillatory and constant anodal transcranial direct current stimulation.
***Journal of Neurophysiology*, 102(4): 2303-2311.**

Though boosting of endogenous slow oscillatory activity during NREM sleep is obviously possible with both so-tDCS and c-tDCS, entrainment of endogenous oscillations might only be possible using oscillatory tDCS in the currently preferred frequency range of the brain, that is ~ 0.75 Hz during NREM sleep. Alternatively, as tDCS is known to alter motor cortical excitability within a few seconds (M. A. Nitsche et al., 2007; M. A. Nitsche et al., 2003; M. A. Nitsche & Paulus, 2000), it might also be possible to actively impose an exogenous oscillation on the cortex irrespective of

the prevailing endogenous oscillations just by shifting the membrane potential of cortical neurons forth and back repeatedly. As it makes a huge difference to the development of oscillatory stimulation techniques whether mere entrainment of ongoing endogenous rhythms or even imposition of arbitrary frequencies is possible, this is an important question to address.

Research Question: Can so-tDCS interact with ongoing activity in the (motor) cortex in a way that cortical excitability actually couples to and thus covaries with the exogenous slow oscillation?

In ten healthy individuals we used online single-pulse TMS to detect systematic shifts in the excitability of corticospinal motor neurons of $M1_{HAND}$ during oscillatory anodal tDCS. In separate sessions, we repeatedly applied 30s trials (2 x 20 min blocks) of either sleep slow oscillation-like 0.8Hz sinusoidal (so-tDCS) or traditional constant anodal tDCS (c-tDCS) to the $M1_{HAND}$ during quiet wakefulness. Simultaneously and time-locked to different phase angles of the exogenous slow oscillation, MEPs were obtained as an index of corticospinal excitability in the contralateral hand muscles 10, 20, and 30 s after the onset of tDCS. MEPs were also measured offline before, between and after both stimulation blocks to detect any lasting excitability shifts (Figure 1, Bergmann et al., 2009).

Both tDCS modes increased MEP amplitudes during 30-s periods of stimulation with an attenuation of the facilitatory effect towards the end of a 30s tDCS trial (Figure 3,Bergmann et al., 2009). However, no phase-locking of corticospinal excitability to the exogenous oscillation was observed during so-tDCS. Offline TMS revealed that both types of tDCS resulted in a lasting increase in corticospinal excitability (Figure 4,Bergmann et al., 2009) with the individual magnitude of MEP facilitation during the first trials of tDCS predicting the lasting facilitation of MEP amplitudes found after tDCS (Figure 5, Bergmann et al., 2009).

Conclusion: At least during wakefulness, excitability of the motor cortex does not couple to the exogenously applied rhythm of so-tDCS, while so-tDCS is as effective as c-tDCS in producing general excitability shifts, even outlasting the stimulation itself. Therefore it seems unlikely that oscillatory tDCS can actively impose rhythms to the cortex which are not preferred by the current brain state. However, to clarify this point the experimental paradigm could be either transferred to NREM sleep, or

oscillatory tDCS in more wake-like frequencies could be applied to awake subjects. However, both alternatives come with major technical challenges.

3.4.2 After-effects of Slow Oscillatory Stimulation

PAPER VI

Groppa, S., Bergmann, T. O., Siems, C., Mölle, M., Marshall, L., & Siebner, H. R. (2010). Slow-oscillatory transcranial DC stimulation can induce bidirectional shifts in motor cortical excitability in awake humans.
***Neuroscience*, 166(4): 1219-1225.**

Paradigms of transcranial oscillatory stimulation are used more and more often as a means to interact with ongoing cognition, perception, and movements through modulation of ongoing oscillatory brain activity (Kanai et al., 2008; Kirov et al., 2009; Marshall, Helgadottir et al., 2006; Marshall, Mölle et al., 2006; Pogosyan et al., 2009). However, as in most of theses studies the stimulation targets on non-motor brain areas and the dependent measures focus on changes in behavior and EEG oscillatory activity, lasting cortical excitability changes have mostly been neglected (but see Antal et al., 2008; Bergmann et al., 2009). However, the capability of inducing long lasting (> 1 h) excitability shifts is the most well and consistently described feature of traditional constant tDCS applications (M. Nitsche et al., 2008). Changes in cortical excitability could therefore be an alternative explanation for some behavioral and EEG effects which so far have rather been ascribed to the exogenously applied oscillation itself. It is thus highly important to clarify if and by which means oscillatory tDCS may induce bidirectional LTP- and LTD-like plasticity, that is lasting cortical excitability changes as a “side effect”.

Research Question: Is so-tDCS capable of inducing bidirectional, polarity-dependent plasticity in the $M1_{HAND}$ and is it as effective as c-tDCS when matching for the total amount of injected current?

Experiment 1. In separate sessions, we applied 10 min of either anodal or cathodal c-tDCS or so-tDCS to the left $M1_{HAND}$ of ten healthy subjects (with a peak intensity of 0.75 mA, i.e. a maximal current density of 0.0625 mA/cm^2 in both protocols). MEPs were measured before as well as 0, 5, 10, and 20 min after the stimula-

tion to monitor changes in motor cortical excitability (Figure 1, Groppa et al., 2010). While anodal and cathodal c-tDCS induced significant excitability increases and decreases, respectively, lasting for at least 20 min, so-tDCS had no effects at this intensity (Figure 2, Groppa et al., 2010).

Experiment 2. In a separate group of ten subjects, peak current intensity of so-tDCS was doubled to 1.5 mA (maximal current density 0.125 mA/cm^2), matching the total amount of injected current to that of c-tDCS at 0.75 mA (Experiment 1), while leaving all other stimulation parameters constant. Now, anodal and cathodal so-tDCS also produced bidirectional changes in corticospinal excitability comparable to those of c-tDCS at 0.75 mA (Figure 2, Groppa et al., 2010).

Conclusion: Ten minutes of anodal and cathodal so-tDCS can induce lasting bidirectional changes in (motor-)cortical excitability. The effects are moreover comparable to those caused by c-tDCS when matched for total current charge, whereas the effectiveness of both tDCS modes might slightly differ regarding the duration of after-effects and the minimal effective current density. Moreover, the impact of other potentially contributing factors such as the frequency of stimulation, peak current density, stimulation duration, electrode size, etc. and the interaction between these factors have yet to be determined. However, it is at least obvious that tDCS with oscillating current strength can lastingly affect cortical excitability, rendering c-tDCS an important control condition for experimental designs. The effects on cortical excitability are less clear when using alternating currents (Antal et al., 2008) although the development of new protocols such as transcranial random noise stimulation (Terney, Chaieb, Moliadze, Antal, & Paulus, 2008) suggests that polarity does not have to be constant to induce lasting excitability changes.

4 Discussion

Sleep benefits plastic brain processes in general and processes of synaptic homeostasis and systemic memory consolidation in particular. With respect to the empirical evidence that has accumulated over the last decade this can nowadays be stated as a fact. However, the very neuronal mechanisms underlying these sleep-dependent processes are still largely unknown. The objective of my own theoretical considerations and empirical studies that are constituting this thesis is to further unravel these relationships. Focusing on the role of sleep-specific brain oscillations, that is particularly on sleep spindles and slow oscillations, I used a multimodal neuroscientific approach to investigate how the interaction of these oscillations might mediate brain plasticity during sleep.

While detailed interpretations of the empirical results can be found in the respective original research papers (see Appendix), in the following I will more generally embed my own findings in the context of the existing literature and discuss their implications for further research. Beyond that, I will outline some of the most important open questions in the field which need to be answered in the future. The studies will be discussed in the same order as introduced in Section 3.

4.1 Synaptic Homeostasis during Sleep

The *synaptic homeostasis hypothesis* (Tononi & Cirelli, 2003, 2006) has gained substantial support over the last years from both animal and human studies. In the latter, evidence has mainly come from high-density EEG recordings during NREM sleep after either LTP- or LTD-like plasticity had experimentally been induced (Huber et al., 2007; Huber et al., 2006; Huber et al., 2004). Changes in slow wave activity (neglecting the spindle frequency range) were interpreted as a direct consequence of changed synaptic weights. Above that, changes in SWA are in turn believed to reflect the amount of synaptic downscaling taking place in order to return to a homeostatic level of synaptic plasticity. As could be demonstrated by our own work (Paper II, Bergmann et al., 2008) as well as by other groups (De Gennaro et al., 2008; Huber et al., 2008), changes in sleep oscillatory activity are actually caused by plastic changes instead of merely depending on the amount of prior use. However, these changes are obviously not confined to slow waves but also extend to theta and alpha power

(De Gennaro et al., 2008) as well as sleep spindles (Bergmann et al., 2008). Other oscillations like sleep spindles might therefore interact with the slow oscillation to mediate plastic processes including synaptic downscaling. However, how exactly the slow oscillation, whether per se or by interactions with other oscillations, might cause synaptic changes is still unclear and for sure one of the major issues to address in the next years.

Beside that, the final proof is still missing that synaptic downscaling is actually taking place during sleep at all. Alternatively, changed oscillatory activity could just reflect prior synaptic changes during wakefulness without having an effect on its own. And if there is downscaling, as suggested by the observed decrease in cortical excitability across a night of sleep (Bergmann et al., 2008), it might not be mediated by the slow oscillation itself but due to mere depotentiation through motor immobilization and sensory deprivation. This would of course be most prominent during the state of sleep but not unique to it. In fact, preliminary evidence from our own lab (Nowak, 2009; von Borstel, 2009) suggests that the excitability of the motor cortex is equally reduced during a sensory restricted and immobilized period of quiet wakefulness. However, this possibility has to be carefully investigated in greater detail.

Another core prediction of the synaptic homeostasis hypothesis is that downscaling during sleep maintains synaptic plasticity in a functional range. Therefore LTP should be more easily induced after sleep. Unfortunately, a recent attempt to test this prediction explicitly by repeated premotor rTMS before and after sleep and wakefulness, respectively, failed due to lacking effectivity of the employed rTMS protocol (Nowak, 2009; von Borstel, 2009), and therefore the question still remains to be answered. Here, electrophysiological recordings in animals combined with invasive LTP-inducing electrical stimulation *in vivi*o would be even more instructive.

In the future, enormous informational gain will hopefully come from other animal studies applying the emerging technique of two-photon imaging (Holtmaat & Svoboda, 2009). With this method synaptic growth and shrinkage can be repeatedly observed in vivo in the intact mouse cortex which may bring final evidence for the synaptic homeostasis hypothesis.

4.2 System Memory Consolidation during Sleep

The mechanistic model of *active system consolidation* (Born et al., 2006; Diekelmann & Born, 2010; Marshall & Born, 2007) is highly promising but still in the early stages of development. Its core assumption is the orchestrated interaction of nested sleep-specific oscillations, that is cortical slow oscillations, thalamo-cortical sleep spindles, and hippocampal sharp wave-ripples, providing the processing mode for memory reorganization and redistribution by reactivation (Rasch & Born, 2007). While the principal involvement of these neuronal oscillations in learning and memory is corroborated by a huge body of evidence (see Section1.3.2), its fine temporospatial characteristic have yet to be determined in order to allow for a more detailed understanding of how information processing and storage is maintained by these brain rhythms.

Uncovering the different timing of slow and fast sleep spindles on the background of undulating cortical excitability in the slow oscillation cycle (Paper III, Mölle et al., in prep.) puts forward the idea of *oscillation-mediated* gating and STDP as key mechanisms for information processing and synaptic plasticity during sleep. The entrainment of faster rhythms by slower oscillations seems to be a fundamental mechanism for the organization of information flow in the brain (Jensen & Colgin, 2007). Nested oscillations cannot only be found during sleep (cortical slow oscillations grouping thalamo-cortical spindles in turn grouping hippocampal ripples) but also during wakefulness (hippocampal theta (Sirota et al., 2008) and thalamo-cortical alpha (Osipova, Hermes, & Jensen, 2008) grouping the cortical gamma rhythm). Therefore, future research should focus on further disentangling the fine-tuned relationships between brain rhythms in wakefulness and sleep. For example, it has to be investigated whether in analogy to theta during wakefulness, sleep spindles might also entrain cortical gamma oscillations representing the temporal units of cortical computation (Fries, 2009). It might be the synchronization of hippocampal ripples and cortical gamma which eventually provides the critical temporal resolution for information transfer by STDP in the hippocampo-neocortical dialogue.

While hippocampal and neocortical reactivations of learning-specific areas during post-learning sleep in humans have earlier been demonstrated on a rough temporospatial scale using PET imaging (Maquet et al., 2000; Peigneux et al., 2004; Peigneux et al., 2003), we could by simultaneous application of EEG and fMRI now

provide first-time evidence that the hippocampus and learning material-specific neocortical representations are conjointly reactivated time-locked to the thalamo-cortical sleep spindle (Paper IV, Bergmann, Mölle, Diedrichs, Born, & Siebner, in prep.). Detection power for the involved cortical representations was relatively low during sleep compared to their initial activation during wakefulness, presumably due to a higher noise level during memory replay (Diekelmann & Born, 2010). Nevertheless, the activation of material-specific cortical representations was closely coupled to the magnitude of individual sleep spindles and was topographically highly specific (involving almost none but the expected brain regions). These findings are in perfect accordance with the *active system consolidation hypothesis* (Born et al., 2006; Diekelmann & Born, 2010; Marshall & Born, 2007). However, it is still possible that this kind of reactivation is just a natural consequence of a local learning-dependent strengthening of neuronal connections which in turn causes a stronger passive activation by otherwise functionally meaningless spindle activity (Tononi, personal communication, October 23, 2009). This argument is of general relevance to all correlative approaches like functional neuroimaging and can only be overcome by adding causality through experimental manipulation of neuronal activity. In humans this has been done by application of learning-related odor (Rasch et al., 2007) or acoustic cues (Rudoy, Voss, Westerberg, & Paller, 2009) or by transcranial stimulation techniques (Marshall, Helgadottir et al., 2006; Marshall et al., 2004) during sleep. However, a temporally much more specific manipulation of sleep spindles, paralleling the electrical disturbance of hippocampal sharp-wave ripples in mice (Ego-Stengel & Wilson, 2009; Girardeau et al., 2009), has yet to come.

Future research also has to determine the very conditions under which synaptic weights can actually be modified during sleep. It is currently unclear whether LTP can be induced during SWS at all (Bramham & Srebro, 1989), since both the expression of LTP-related genes and the level of neuromodulators like acetylcholine and noradrenaline are low (Cirelli, 2009; Diekelmann & Born, 2010). It has therefore been suggested that the above described spindle-related mechanisms only tags cortical networks to be than potentiated during subsequent REM sleep when the prerequisites for LTP are more beneficial (Bramham & Srebro, 1989; Diekelmann & Born, 2010). Alternatively, it might be possible that LTP can be induced only during short windows of slow oscillation up states where neuronal activity is orchestrated in the

right way (see above) and paired with noradrenergic burst activity in the locus coeruleus (Eschenko & Sara, 2008). Electrophysiological data from human and animal experiments has to clarify how and when synaptic plasticity can be induced during sleep, as this affects the core of any theory on sleep-dependent memory processing.

Finally, the current theoretical knowledge has to be extended to the consolidation of non-declarative forms of memory. It is likely that for procedural memory the same or at least highly similar mechanisms are working on a slightly different neuronal substrate, that is involving other brain regions like the cerebellum, basal ganglia and cortical motor areas. I therefore suggest a stronger focus on the similarities at the neuronal than on the differences on the phenomenological level.

4.3 Neuromodulation by Slow Oscillatory Stimulation

Our current understanding of how concerted oscillatory brain activity gives rise to different state-dependent information processing modes is still in its infancy. Nevertheless, first pioneering attempts to manipulate ongoing neuronal computation by means of exogenously applied oscillatory currents have already been successful regarding memory processing (Kirov et al., 2009; Marshall, Helgadottir et al., 2006; Marshall, Mölle et al., 2006), perception (Kanai et al., 2008; but see Schwiedrzik, 2009), and motor performance (Pogosyan et al., 2009). However, to exploit the full potential of this emerging technique, we need to know much more about its very mechanisms and the precise conditions rendering a specific intervention effective. Various stimulation parameters such as current flow (DC vs. AC), current polarity (anodal vs. cathodal), current modulation (constant vs. oscillatory), current intensity (maximum or averaged strength, total charge, etc.), frequency, duration, and electrode positioning may interact in numerous ways with the present state of the brain, depending on its vigilance state (wake, drowsiness, sleep, anesthesia, etc.) and ongoing processing modes.

Currently, it is not even fully determined whether entrainment of endogenous oscillations by exogenous time-variant currents is possible at all. The key findings of slow oscillatory anodal DC stimulation during NREM sleep (Marshall, Helgadottir et al., 2006), i.e. increased slow oscillatory and associated spindle activity during subsequent stimulation-free periods and improved declarative memory consolidation,

have previously been shown by application of non-oscillatory constant anodal tDCS during NREM sleep (Marshall et al., 2004). Therefore, it might have been the mere average membrane potential shift induced by anodal charge over the prefrontal cortex that increased endogenous slow oscillations and thereby memory consolidation. Although endogenous oscillations after termination of slow oscillatory stimulation seemed to keep in phase for a few cycles, strong statistical evidence for actual phase-locking is still missing. Notably, 0.75 Hz stimulation during REM sleep as well as 5 Hz stimulation during NREM sleep remained ineffective. While the first fact could be fully attributed to a different role of REM sleep in memory consolidation, the latter strongly suggests an impact of the stimulation frequency. As constant tDCS (virtually the lower bound of the frequency range) is still effective, it might be possible that not frequency but total current charge are important and the neuronal membrane potential is just not affected any more when periods of high current strength become too short with increasing frequency.

This idea is corroborated by the two slow oscillatory tDCS studies included in this thesis (Paper V, Bergmann et al., 2009; Paper VI, Groppa et al., 2010). By transferring the idea of slow oscillatory DC stimulation to wakefulness, applying it to the well studied primary motor cortex, and using a standard electrode montage, we established comparability with the existent large body of empirical tDCS data, embedding our results in the present theoretical framework. Notably, we found slow oscillatory tDCS to be as effective as classical constant tDCS in facilitating acute motor cortical excitability, totally independent of the actual phase of the exogenous slow oscillation (Paper V, Bergmann et al., 2009). Not even time points of maximal and zero current strength within the continuous oscillatory stimulation differed regarding their impact on cortical excitability, while stimulation pauses of several seconds were sufficient for acute facilitation to decay again. Moreover, the well known polarity-dependent after-effects on cortical excitability were comparable for slow oscillatory and constant tDCS for both anodal (Paper V, Bergmann et al., 2009; Paper VI, Groppa et al., 2010) and cathodal (Paper VI, Groppa et al., 2010) polarity, when protocols were matched for total current charge, although minimal necessary current strength or stimulation duration might be lower for constant tDCS (which has to be explored in future studies).

Taken together, these results suggest that the effective mechanism of transcranial DC stimulation might be its unspecific depolarizing (anodal) or hyperpolarizing (cathodal) effect on the membrane potential of cortical neurons, with the stimulation frequency only determining the boundaries of effectivity due to the neurons' frequency-dependent responsiveness (Hutcheon & Yarom, 2000). However, our results might not be generalized to other vigilance states (i.e. sleep) as filter characteristics of stimulated neurons may shift depending on the neurochemical background of the prevailing brain state, thus becoming more or less responsive to specific stimulation frequencies. Unfortunately, recent slow oscillatory DC stimulation studies during wakefulness (e.g. Kirov et al., 2009) lack the control by constant stimulation and are therefore uninformative regarding the impact of the stimulation's oscillatory nature (as compared to a mere DC shift). The situation might be different for protocols using AC stimulation, as there is average DC capacity and only stimulation frequency (and may be current gradients) can be effective. However, recent results suggesting a strong brain state-dependency for the effective AC frequency (Kanai et al., 2008) have been questioned (Schwiedrzik, 2009).

To actually uncover how exogenous transcranial current stimulation interacts with ongoing endogenous oscillations, it will be essential to develop new techniques in order to cope with the comparably massive tDCS artifacts in simultaneous EEG recordings (EEG in µV vs. tDCS in mV). This feasibility is crucial for investigating the details of acute stimulation-induced changes in cortical activity.

On condition of a more thorough understanding of its mechanisms, transcranial oscillatory stimulation could be used as a therapeutical tool in the future to facilitate functional and inhibit pathological oscillatory activity in patients with neurological diseases or maybe even in the elderly when normal brain function deteriorates with time.

5 Conclusions

Sleep plays a fundamental role in brain plasticity both on the synaptic and on the system level. While processes of global synaptic downscaling take effect independently on individual neurons to maintain synaptic homeostasis, system consolidation involves not only the stabilization of newly acquired memory traces but also their reorganization and spatial redistribution within large-scale neuronal networks.

The loss of consciousness, passively protecting against interference with ongoing information processing, may provide the indispensable framework for these profound changes to occur. However, beyond that, an active function of sleep in terms of covert information (re-)processing, is more than likely. As during wakefulness, cross-talk within and between distant neuronal networks has to be organized in time to enable an effective information flow. This is achieved by a set of hierarchically coupled oscillators of different frequencies, establishing the exact timing that is necessary for the integration of distributed information and the modification of individual synapses, resembling the subunits of memory. In NREM sleep, the crucial set of oscillations mainly (though not exclusively) consists of the cortical slow oscillation (< 1 Hz), thalamo-cortical sleep spindles (~10-16 Hz), presumably cortical gamma (~40-100 Hz), and hippocampal sharp wave-ripples (~100-600 Hz).

The theoretical considerations and empirical research projects my thesis is based on aimed at a more thorough investigation of how these neuronal oscillations interact to serve brain plasticity and memory processing during sleep. Further, I intended to set the neurophysiological ground for a more well founded application of transcranial oscillatory techniques to actively modify these oscillatory processing modes. I therefore employed a multimodal neuroscientific approach at the systems level by combining the techniques of TMS, tDCS, fMRI, and EEG (Paper I, H. R. Siebner, Bergmann et al., 2009).

While verifying the idea that the activity of slow waves does in fact depend on the previous induction of bidirectional synaptic plasticity and not on mere usage, we found this effect to be not as specific as predicted regarding its direction and topography. Instead, the expression sleep spindles revealed a topographically highly specific marker for previously induced cortical plasticity (Paper II, Bergmann et al., 2008). Furthermore, our findings suggested a possible dissociation of the functions of

frontal slow spindles (~10-13 Hz) and centro-parietal fast spindles (~13-16 Hz) in brain plasticity, which might be mediated by a different timing with respect to the slow oscillation.

This idea is supported by the finding that fast and slow spindles are grouped in opposite phases of the slow oscillation, i.e. in its up and down states, respectively (Paper III, Mölle et al., in prep.). By this means, the two spindle types might feed information into the neocortex which either becomes facilitated (up state) or suppressed (down state), thus making up a potential mechanism for the bidirectional modification of synaptic strength. However, this is highly speculative and has to be systematically investigated in the future.

Eventually, we could demonstrate for the first time in humans that learning material-specific neocortical representations are in fact conjointly reactivated together with the hippocampus driven by sleep spindles during post-learning NREM sleep (Paper IV, Bergmann et al., in prep.). It, however, remains unclear whether this reactivation is a mere echo of previously strengthened synaptic connections or actually represents a functionally meaningful reactivation in terms of memory redistribution. This is an important question for future research.

Finally, basic physiological investigations on the effects of slow oscillatory tDCS on the excitability of the awake primary motor cortex shed new light on the potential mechanisms of oscillatory tDCS. While principally as effective as conventional constant tDCS regarding the induction of excitability changes during (Paper V, Bergmann et al., 2009) and outlasting (Paper VI, Groppa et al., 2010) the stimulation, cortical excitability was not entrained by the exogenous slow oscillation. Whether this lack of entrainment must be attributed to the current brain state and would have been possible during NREM sleep or whether the effective component of oscillatory tDCS is actually restricted to its average current charge has yet to be determined. While first steps are done, a sensible application of this technique has to rely on further, more thorough investigations.

Taken together, our understanding of sleep-dependent plasticity has significantly increased, but we are still at the very beginning of our endeavor to fully characterize the mechanisms of its underlying oscillatory processing modes.

6 References

Abbott, L. F., & Nelson, S. B. (2000). Synaptic plasticity: taming the beast. *Nat. Neurosci., 3 Suppl*, 1178-1183.

Abraham, W. C. (2008). Metaplasticity: tuning synapses and networks for plasticity. *Nat.Rev.Neurosci., 9*(5), 387.

Abraham, W. C., & Bear, M. F. (1996). Metaplasticity: the plasticity of synaptic plasticity. *Trends Neurosci., 19*(4), 126-130.

Abraham, W. C., & Tate, W. P. (1997). Metaplasticity: a new vista across the field of synaptic plasticity. *Prog. Neurobiol., 52*(4), 303-323.

Achermann, P., & Borbely, A. A. (1997). Low-frequency (< 1 Hz) oscillations in the human sleep electroencephalogram. *Neuroscience, 81*(1), 213-222.

Aeschbach, D., Cutler, A. J., & Ronda, J. M. (2008). A role for non-rapid-eye-movement sleep homeostasis in perceptual learning. *J. Neurosci., 28*(11), 2766-2772.

Albouy, G., Sterpenich, V., Balteau, E., Vandewalle, G., Desseilles, M., Dang-Vu, T., et al. (2008). Both the hippocampus and striatum are involved in consolidation of motor sequence memory. *Neuron, 58*(2), 261-272.

Amzica, F., & Steriade, M. (1997). The K-complex: its slow (<1-Hz) rhythmicity and relation to delta waves. *Neurology, 49*(4), 952-959.

Antal, A., Boros, K., Poreisz, C., Chaieb, L., Terney, D., & Paulus, W. (2008). Comparatively weak after-effects of transcranial alternating current stimulation (tACS) on cortical excitability in humans. *Brain Stimulation, 1*(2), 97-105.

Axmacher, N., Haupt, S., Fernandez, G., Elger, C. E., & Fell, J. (2008). The role of sleep in declarative memory consolidation--direct evidence by intracranial EEG. *Cereb. Cortex, 18*(3), 500-507.

Barker, A. T., Jalinous, R., & Freeston, I. L. (1985). Non-invasive magnetic stimulation of human motor cortex. *Lancet, 1*(8437), 1106-1107.

Barrionuevo, G., Schottler, F., & Lynch, G. (1980). The effects of repetitive low frequency stimulation on control and "potentiated" synaptic responses in the hippocampus. *Life Sci., 27*(24), 2385-2391.

Benington, J. H., & Heller, H. C. (1995). Restoration of brain energy metabolism as the function of sleep. *Prog. Neurobiol., 45*(4), 347-360.

Bergmann, T. O., Groppa, S., Seeger, M., Molle, M., Marshall, L., & Siebner, H. R. (2009). Acute changes in motor cortical excitability during slow oscillatory and constant anodal transcranial direct current stimulation. *J. Neurophysiol., 102*(4), 2303-2311.

Bergmann, T. O., Mölle, M., Diedrichs, J., Born, J., & Siebner, H. R. (in prep.). Sleep spindles drive learning-specific hippocampo-neocortical reactivation.

Bergmann, T. O., Mölle, M., Diedrichs, J., Born, J., & Siebner, H. R. (in preparation). Sleep spindles drive learning-specific hippocampo-neocortical reactivation.

Bergmann, T. O., Molle, M., Marshall, L., Kaya-Yildiz, L., Born, J., & Siebner, H. R. (2008). A local signature of LTP- and LTD-like plasticity in human NREM sleep. *Eur. J. Neurosci., 27*(9), 2241-2249.

Bienenstock, E. L., Cooper, L. N., & Munro, P. W. (1982). Theory for the development of neuron selectivity: orientation specificity and binocular interaction in visual cortex. *J. Neurosci., 2*(1), 32-48.

Bliss, T. V., & Lømo, T. (1973). Long-lasting potentiation of synaptic transmission in the dentate area of the anaesthetized rabbit following stimulation of the perforant path. *J Physiol, 232*(2), 331-356.

Borbely, A. A. (2009). Refining sleep homeostasis in the two-process model. *J. Sleep Res., 18*(1), 1-2.

Borbély, A. A. (1980). Sleep: Circadian rhythm versus recovery process
In M. Koukkou, D. Lehmann & J. Angst (Eds.), *Functional States of the Brain: Their Determinants* (pp. 151- 161). Amsterdam: Elsevier.

Borbely, A. A., & Achermann, P. (1999). Sleep homeostasis and models of sleep regulation. *J. Biol. Rhythms, 14*(6), 557-568.

Born, J., Rasch, B., & Gais, S. (2006). Sleep to remember. *Neuroscientist, 12*(5), 410-424.

Bosshardt, S., Degonda, N., Schmidt, C. F., Boesiger, P., Nitsch, R. M., Hock, C., et al. (2005). One month of human memory consolidation enhances retrieval-related hippocampal activity. *Hippocampus, 15*(8), 1026-1040.

Bosshardt, S., Schmidt, C. F., Jaermann, T., Degonda, N., Boesiger, P., Nitsch, R. M., et al. (2005). Effects of memory consolidation on human hippocampal activity during retrieval. *Cortex, 41*(4), 486-498.

Bramham, C. R., & Srebro, B. (1989). Synaptic plasticity in the hippocampus is modulated by behavioral state. *Brain Res., 493*(1), 74-86.

Brandt, S. A., Brocke, J., & Irlbacher, K. (2007). Transkranielle elektrische Stimulation. In H. R. Siebner & U. Ziemann (Eds.), *Das TMS–Buch. Handbuch der transkraniellen Magnetstimulation* (pp. 211-217). Heidelberg: Springer Medizin Verlag.

Burgess, N. (2008). Spatial cognition and the brain. *Ann. N. Y. Acad. Sci., 1124*, 77-97.

Buzsaki, G. (1989). Two-stage model of memory trace formation: a role for "noisy" brain states. *Neuroscience, 31*(3), 551-570.

Buzsaki, G. (2006). *Rhythms of the Brain*. New York: Oxford University Press.

Caporale, N., & Dan, Y. (2008). Spike timing-dependent plasticity: a hebbian learning rule. *Annu. Rev. Neurosci., 31*, 25-46.

Cash, S. S., Halgren, E., Dehghani, N., Rossetti, A. O., Thesen, T., Wang, C., et al. (2009). The human K-complex represents an isolated cortical down-state. *Science, 324*(5930), 1084-1087.

Cavanna, A. E., & Trimble, M. R. (2006). The precuneus: a review of its functional anatomy and behavioural correlates. *Brain*.

Cirelli, C. (2009). The genetic and molecular regulation of sleep: from fruit flies to humans. *Nat. Rev. Neurosci., 10*(8), 549-560.

Cirelli, C., Gutierrez, C. M., & Tononi, G. (2004). Extensive and divergent effects of sleep and wakefulness on brain gene expression. *Neuron, 41*(1), 35-43.

Cirelli, C., & Tononi, G. (2008). Is sleep essential? *PLoS Biol., 6*(8), e216.

Citri, A., & Malenka, R. C. (2008). Synaptic plasticity: multiple forms, functions, and mechanisms. *Neuropsychopharmacology, 33*(1), 18-41.

Clemens, Z., Fabo, D., & Halasz, P. (2005). Overnight verbal memory retention correlates with the number of sleep spindles. *Neuroscience, 132*(2), 529-535.

Clemens, Z., Fabo, D., & Halasz, P. (2006). Twenty-four hours retention of visuospatial memory correlates with the number of parietal sleep spindles. *Neurosci. Lett., 403*(1-2), 52-56.

Clemens, Z., Mölle, M., Eross, L., Barsi, P., Halasz, P., & Born, J. (2007). Temporal coupling of parahippocampal ripples, sleep spindles and slow oscillations in humans. *Brain, 130*(Pt 11), 2868-2878.

Colrain, I. M. (2005). The K-complex: a 7-decade history. *Sleep, 28*(2), 255-273.

Crunelli, V., & Hughes, S. W. (2009). The slow (<1 Hz) rhythm of non-REM sleep: a dialogue between three cardinal oscillators. *Nat. Neurosci.*

Dang-Vu, T. T., Schabus, M., Desseilles, M., Albouy, G., Boly, M., Darsaud, A., et al. (2008). Spontaneous neural activity during human slow wave sleep. *Proc. Natl. Acad. Sci. U. S. A., 105*(39), 15160-15165.

Dash, M. B., Douglas, C. L., Vyazovskiy, V. V., Cirelli, C., & Tononi, G. (2009). Long-term homeostasis of extracellular glutamate in the rat cerebral cortex across sleep and waking states. *J. Neurosci., 29*(3), 620-629.

De Gennaro, L., & Ferrara, M. (2003). Sleep spindles: an overview. *Sleep Med Rev, 7*(5), 423-440.

De Gennaro, L., Fratello, F., Marzano, C., Moroni, F., Curcio, G., Tempesta, D., et al. (2008). Cortical plasticity induced by transcranial magnetic stimulation during wakefulness affects electroencephalogram activity during sleep. *PLoS ONE, 3*(6), e2483.

Debener, S., Ullsperger, M., Siegel, M., & Engel, A. K. (2006). Single-trial EEG-fMRI reveals the dynamics of cognitive function. *Trends Cogn Sci, 10*(12), 558-563.

Destexhe, A., Contreras, D., & Steriade, M. (1999). Cortically-induced coherence of a thalamic-generated oscillation. *Neuroscience, 92*(2), 427-443.

Destexhe, A., Hughes, S. W., Rudolph, M., & Crunelli, V. (2007). Are corticothalamic 'up' states fragments of wakefulness? *Trends Neurosci., 30*(7), 334-342.

Di Lazzaro, V., Oliviero, A., Pilato, F., Saturno, E., Dileone, M., Mazzone, P., et al. (2004). The physiological basis of transcranial motor cortex stimulation in conscious humans. *Clin. Neurophysiol., 115*(2), 255-266.

Diekelmann, S., & Born, J. (2010). The memory function of sleep. *Nat. Rev. Neurosci.*

Diekelmann, S., Wilhelm, I., & Born, J. (2009). The whats and whens of sleep-dependent memory consolidation. *Sleep Med Rev*.

Doyon, J., & Benali, H. (2005). Reorganization and plasticity in the adult brain during learning of motor skills. *Curr. Opin. Neurobiol., 15*(2), 161-167.

Doyon, J., & Ungerleider, L. G. (2002). Functional anatomy of motor skill learning. In L. R. Squire & D. L. Schacter (Eds.), *Neuropsychology of memory* (3rd ed., pp. 225-238). New York: The Guilford Press.

Dudai, Y. (2004). The neurobiology of consolidations, or, how stable is the engram? *Annu. Rev. Psychol., 55*, 51-86.

Dudek, S. M., & Bear, M. F. (1992). Homosynaptic long-term depression in area CA1 of hippocampus and effects of N-methyl-D-aspartate receptor blockade. *Proc. Natl. Acad. Sci. U. S. A., 89*(10), 4363-4367.

Ego-Stengel, V., & Wilson, M. A. (2009). Disruption of ripple-associated hippocampal activity during rest impairs spatial learning in the rat. *Hippocampus*.

Eichenbaum, H. (2000). A cortical-hippocampal system for declarative memory. *Nat. Rev. Neurosci., 1*(1), 41-50.

Ellenbogen, J. M., Payne, J. D., & Stickgold, R. (2006). The role of sleep in declarative memory consolidation: passive, permissive, active or none? *Curr. Opin. Neurobiol.*

Eschenko, O., & Sara, S. J. (2008). Learning-Dependent, Transient Increase of Activity in Noradrenergic Neurons of Locus Coeruleus during Slow Wave Sleep in the Rat: Brain Stem-Cortex Interplay for Memory Consolidation? *Cereb. Cortex*.

Esser, S. K., Hill, S. L., & Tononi, G. (2007). Sleep homeostasis and cortical synchronization: I. Modeling the effects of synaptic strength on sleep slow waves. *Sleep, 30*(12), 1617-1630.

Esser, S. K., Huber, R., Massimini, M., Peterson, M. J., Ferrarelli, F., & Tononi, G. (2006). A direct demonstration of cortical LTP in humans: A combined TMS/EEG study. *Brain Res. Bull., 69*(1), 86-94.

Faraguna, U., Vyazovskiy, V. V., Nelson, A. B., Tononi, G., & Cirelli, C. (2008). A causal role for brain-derived neurotrophic factor in the homeostatic regulation of sleep. *J. Neurosci., 28*(15), 4088-4095.

Fischer, S., Nitschke, M. F., Melchert, U. H., Erdmann, C., & Born, J. (2005). Motor memory consolidation in sleep shapes more effective neuronal representations. *J. Neurosci., 25*(49), 11248-11255.

Fitzgerald, P. B., Fountain, S., & Daskalakis, Z. J. (2006). A comprehensive review of the effects of rTMS on motor cortical excitability and inhibition. *Clin. Neurophysiol., 117*(12), 2584-2596.

Fletcher, P. C., & Henson, R. N. (2001). Frontal lobes and human memory: insights from functional neuroimaging. *Brain, 124*(Pt 5), 849-881.

Franken, P., & Dijk, D. J. (2009). Circadian clock genes and sleep homeostasis. *Eur. J. Neurosci., 29*(9), 1820-1829.

Frankland, P. W., & Bontempi, B. (2005). The organization of recent and remote memories. *Nat. Rev. Neurosci., 6*(2), 119-130.

Frankland, P. W., & Bontempi, B. (2006). Fast track to the medial prefrontal cortex. *Proc. Natl. Acad. Sci. U. S. A., 103*(3), 509-510.

Fries, P. (2009). Neuronal gamma-band synchronization as a fundamental process in cortical computation. *Annu. Rev. Neurosci., 32*, 209-224.

Fuller, P. M., Saper, C. B., & Lu, J. (2007). The pontine REM switch: past and present. *J Physiol, 584*(Pt 3), 735-741.

Gais, S., Albouy, G., Boly, M., Dang-Vu, T. T., Darsaud, A., Desseilles, M., et al. (2007). Sleep transforms the cerebral trace of declarative memories. *Proc. Natl. Acad. Sci. U. S. A.*

Gais, S., & Born, J. (2004). Declarative memory consolidation: mechanisms acting during human sleep. *Learn. Mem., 11*(6), 679-685.

Gais, S., Mölle, M., Helms, K., & Born, J. (2002). Learning-dependent increases in sleep spindle density. *J. Neurosci., 22*(15), 6830-6834.

Girardeau, G., Benchenane, K., Wiener, S. I., Buzsaki, G., & Zugaro, M. B. (2009). Selective suppression of hippocampal ripples impairs spatial memory. *Nat. Neurosci., 12*(10), 1222-1223.

Gold, J. I., & Bear, M. F. (1994). A model of dendritic spine Ca2+ concentration exploring possible bases for a sliding synaptic modification threshold. *Proc. Natl. Acad. Sci. U. S. A., 91*(9), 3941-3945.

Greenberg, D. L., & Rubin, D. C. (2003). The neuropsychology of autobiographical memory. *Cortex, 39*(4-5), 687-728.

Griffiths, S., Scott, H., Glover, C., Bienemann, A., Ghorbel, M. T., Uney, J., et al. (2008). Expression of long-term depression underlies visual recognition memory. *Neuron, 58*(2), 186-194.

Groppa, S., Bergmann, T. O., Siems, C., Molle, M., Marshall, L., & Siebner, H. R. (2010). Slow-oscillatory transcranial DC stimulation can induce bidirectional shifts in motor cortical excitability in awake humans. *Neuroscience, 166*(4), 1219-1225.

Hebb, D. O. (1949). *The organization of behavior*. New York: Wiley.

Herrmann, C. S., & Debener, S. (2008). Simultaneous recording of EEG and BOLD responses: a historical perspective. *Int. J. Psychophysiol., 67*(3), 161-168.

Hill, S., & Tononi, G. (2005). Modeling sleep and wakefulness in the thalamocortical system. *J. Neurophysiol., 93*(3), 1671-1698.

Hobson, J. A., & Pace-Schott, E. F. (2002). The cognitive neuroscience of sleep: neuronal systems, consciousness and learning. *Nat. Rev. Neurosci., 3*(9), 679-693.

Holtmaat, A., & Svoboda, K. (2009). Experience-dependent structural synaptic plasticity in the mammalian brain. *Nat. Rev. Neurosci., 10*(9), 647-658.

Huang, Y. Z., Edwards, M. J., Rounis, E., Bhatia, K. P., & Rothwell, J. C. (2005). Theta burst stimulation of the human motor cortex. *Neuron, 45*(2), 201-206.

Huber, R., Esser, S. K., Ferrarelli, F., Massimini, M., Peterson, M. J., & Tononi, G. (2007). TMS-induced cortical potentiation during wakefulness locally increases slow wave activity during sleep. *PLoS ONE, 2*, e276.

Huber, R., Ghilardi, M. F., Massimini, M., Ferrarelli, F., Riedner, B. A., Peterson, M. J., et al. (2006). Arm immobilization causes cortical plastic changes and locally decreases sleep slow wave activity. *Nat. Neurosci., 9*(9), 1169-1176.

Huber, R., Ghilardi, M. F., Massimini, M., & Tononi, G. (2004). Local sleep and learning. *Nature, 430*(6995), 78-81.

Huber, R., Maatta, S., Esser, S. K., Sarasso, S., Ferrarelli, F., Watson, A., et al. (2008). Measures of cortical plasticity after transcranial paired associative stimulation predict changes in electroencephalogram slow-wave activity during subsequent sleep. *J. Neurosci., 28*(31), 7911-7918.

Hutcheon, B., & Yarom, Y. (2000). Resonance, oscillation and the intrinsic frequency preferences of neurons. *Trends Neurosci., 23*(5), 216-222.

Ilmoniemi, R. J., & Kicic, D. (2009). Methodology for Combined TMS and EEG. *Brain Topogr.*

Jensen, O., & Colgin, L. L. (2007). Cross-frequency coupling between neuronal oscillations. *Trends Cogn Sci, 11*(7), 267-269.

Ji, D., & Wilson, M. A. (2007). Coordinated memory replay in the visual cortex and hippocampus during sleep. *Nat. Neurosci., 10*(1), 100-107.

Kalia, M. (2006). Neurobiology of sleep. *Metabolism., 55*(10 Suppl 2), S2-6.

Kanai, R., Chaieb, L., Antal, A., Walsh, V., & Paulus, W. (2008). Frequency-Dependent Electrical Stimulation of the Visual Cortex. *Curr. Biol.*

Kandel, E. R. (2001). The molecular biology of memory storage: a dialogue between genes and synapses. *Science, 294*(5544), 1030-1038.

Kemp, A., & Manahan-Vaughan, D. (2007). Hippocampal long-term depression: master or minion in declarative memory processes? *Trends Neurosci., 30*(3), 111-118.

Kim, S. J., & Linden, D. J. (2007). Ubiquitous plasticity and memory storage. *Neuron, 56*(4), 582-592.

Kirov, R., Weiss, C., Siebner, H. R., Born, J., & Marshall, L. (2009). Slow oscillation electrical brain stimulation during waking promotes EEG theta activity and memory encoding. *Proc. Natl. Acad. Sci. U. S. A.*

Kopelman, M. D., & Kapur, N. (2001). The loss of episodic memories in retrograde amnesia: single-case and group studies. *Philos. Trans. R. Soc. Lond. B. Biol. Sci., 356*(1413), 1409-1421.

Krakauer, J. W., & Shadmehr, R. (2006). Consolidation of motor memory. *Trends Neurosci., 29*(1), 58-64.

Kudrimoti, H. S., Barnes, C. A., & McNaughton, B. L. (1999). Reactivation of hippocampal cell assemblies: effects of behavioral state, experience, and EEG dynamics. *J. Neurosci., 19*(10), 4090-4101.

Lamprecht, R., & LeDoux, J. (2004). Structural plasticity and memory. *Nat. Rev. Neurosci., 5*(1), 45-54.

Landsness, E. C., Crupi, D., Hulse, B. K., Peterson, M. J., Huber, R., Ansari, H., et al. (2009). Sleep-dependent improvement in visuomotor learning: a causal role for slow waves. *Sleep, 32*(10), 1273-1284.

Lechner, H. A., Squire, L. R., & Byrne, J. H. (1999). 100 years of consolidation--remembering Muller and Pilzecker. *Learn. Mem., 6*(2), 77-87.

Lee, A. K., & Wilson, M. A. (2002). Memory of sequential experience in the hippocampus during slow wave sleep. *Neuron, 36*(6), 1183-1194.

Levy, W. B., & Steward, O. (1983). Temporal contiguity requirements for long-term associative potentiation/depression in the hippocampus. *Neuroscience, 8*(4), 791-797.

Louie, K., & Wilson, M. A. (2001). Temporally structured replay of awake hippocampal ensemble activity during rapid eye movement sleep. *Neuron, 29*(1), 145-156.

Lynch, M. A. (2004). Long-term potentiation and memory. *Physiol. Rev., 84*(1), 87-136.

Maddock, R. J. (1999). The retrosplenial cortex and emotion: new insights from functional neuroimaging of the human brain. *Trends Neurosci., 22*(7), 310-316.

Malenka, R. C., & Bear, M. F. (2004). LTP and LTD: an embarrassment of riches. *Neuron, 44*(1), 5-21.

Maquet, P. (2001). The role of sleep in learning and memory. *Science, 294*(5544), 1048-1052.

Maquet, P., Laureys, S., Peigneux, P., Fuchs, S., Petiau, C., Phillips, C., et al. (2000). Experience-dependent changes in cerebral activation during human REM sleep. *Nat. Neurosci., 3*(8), 831-836.

Maquet, P., Schwartz, S., Passingham, R., & Frith, C. (2003). Sleep-related consolidation of a visuomotor skill: brain mechanisms as assessed by functional magnetic resonance imaging. *J. Neurosci., 23*(4), 1432-1440.

Marshall, L., & Born, J. (2002). Brain-immune interactions in sleep. *Int. Rev. Neurobiol., 52*, 93-131.

Marshall, L., & Born, J. (2007). The contribution of sleep to hippocampus-dependent memory consolidation. *Trends Cogn Sci, 11*(10), 442-450.

Marshall, L., Helgadottir, H., Mölle, M., & Born, J. (2006). Boosting slow oscillations during sleep potentiates memory. *Nature, 444*(7119), 610-613.

Marshall, L., Mölle, M., & Born, J. (2003). Spindle and slow wave rhythms at slow wave sleep transitions are linked to strong shifts in the cortical direct current potential. *Neuroscience, 121*(4), 1047-1053.

Marshall, L., Mölle, M., & Born, J. (2006, 2006). Oscillating current stimulation-slow oscillation stimulation during sleep. *Nat. Protoc.*, from http://www.natureprotocols.com/2006/11/09/oscillating_current_stimulatio.php

Marshall, L., Mölle, M., Hallschmid, M., & Born, J. (2004). Transcranial direct current stimulation during sleep improves declarative memory. *J. Neurosci., 24*(44), 9985-9992.

Massimini, M., Ferrarelli, F., Esser, S. K., Riedner, B. A., Huber, R., Murphy, M., et al. (2007). Triggering sleep slow waves by transcranial magnetic stimulation. *Proc. Natl. Acad. Sci. U. S. A., 104*(20), 8496-8501.

Massimini, M., Ferrarelli, F., Huber, R., Esser, S. K., Singh, H., & Tononi, G. (2005). Breakdown of cortical effective connectivity during sleep. *Science, 309*(5744), 2228-2232.

Massimini, M., Huber, R., Ferrarelli, F., Hill, S., & Tononi, G. (2004). The sleep slow oscillation as a traveling wave. *J. Neurosci., 24*(31), 6862-6870.

Massimini, M., Tononi, G., & Huber, R. (2009). Slow waves, synaptic plasticity and information processing: insights from transcranial magnetic stimulation and high-density EEG experiments. *Eur. J. Neurosci., 29*(9), 1761-1770.

McClelland, J. L., McNaughton, B. L., & O'Reilly, R. C. (1995). Why there are complementary learning systems in the hippocampus and neocortex: insights from the successes and failures of connectionist models of learning and memory. *Psychol. Rev., 102*(3), 419-457.

McGaugh, J. L. (2000). Memory--a century of consolidation. *Science, 287*(5451), 248-251.

Mölle, M., Bergmann, T. O., Marshall, L., & Born, J. (in prep.). Slow and fast spindles grouped in opposite phase during slow sleep oscillations.

Mölle, M., & Born, J. (2009). Hippocampus whispering in deep sleep to prefrontal cortex--for good memories? *Neuron, 61*(4), 496-498.

Mölle, M., Eschenko, O., Gais, S., Sara, S. J., & Born, J. (2009). The influence of learning on sleep slow oscillations and associated spindles and ripples in humans and rats. *Eur. J. Neurosci., 29*(5), 1071-1081.

Mölle, M., Marshall, L., Gais, S., & Born, J. (2002). Grouping of spindle activity during slow oscillations in human non-rapid eye movement sleep. *J. Neurosci., 22*(24), 10941-10947.

Mölle, M., Yeshenko, O., Marshall, L., Sara, S. J., & Born, J. (2006). Hippocampal sharp wave-ripples linked to slow oscillations in rat slow-wave sleep. *J. Neurophysiol., 96*(1), 62-70.

Muller-Dahlhaus, J. F., Orekhov, Y., Liu, Y., & Ziemann, U. (2008). Interindividual variability and age-dependency of motor cortical plasticity induced by paired associative stimulation. *Exp. Brain Res.*

Müller, G. E., & Pilzecker, A. (1900). Experimentelle Beiträge zur Lehre vom Gedächtnis. *Z Psychol, Ergänzungsband 1*, 1–300.

Müller, J. F., Orekhov, Y., Liu, Y., & Ziemann, U. (2007). Homeostatic plasticity in human motor cortex demonstrated by two consecutive sessions of paired associative stimulation. *Eur. J. Neurosci., 25*(11), 3461-3468.

Murphy, M., Riedner, B. A., Huber, R., Massimini, M., Ferrarelli, F., & Tononi, G. (2009). Source modeling sleep slow waves. *Proc. Natl. Acad. Sci. U. S. A., 106*(5), 1608-1613.

Nadasdy, Z., Hirase, H., Czurko, A., Csicsvari, J., & Buzsaki, G. (1999). Replay and time compression of recurring spike sequences in the hippocampus. *J. Neurosci., 19*(21), 9497-9507.

Nadel, L., & Moscovitch, M. (1997). Memory consolidation, retrograde amnesia and the hippocampal complex. *Curr. Opin. Neurobiol., 7*(2), 217-227.

Nishida, M., & Walker, M. P. (2007). Daytime naps, motor memory consolidation and regionally specific sleep spindles. *PLoS ONE, 2*, e341.

Nitsche, M., Cohen, L. G., Wassermann, E. M., Priori, A., Lang, N., Antal, A., et al. (2008). Transcranial direct current stimulation: State of the art 2008. *Brain Stimulation, 1*(3), 206-223.

Nitsche, M., & Paulus, W. (2007). Transkranielle Gleichstromstimulation. In H. R. Siebner & U. Ziemann (Eds.), *Das TMS–Buch. Handbuch der transkraniellen Magnetstimulation* (pp. 533-542). Heidelberg: Springer Medizin Verlag.

Nitsche, M. A., Doemkes, S., Karakoese, T., Antal, A., Liebetanz, D., Lang, N., et al. (2007). Shaping the effects of transcranial direct current stimulation of the human motor cortex. *J. Neurophysiol.*

Nitsche, M. A., Fricke, K., Henschke, U., Schlitterlau, A., Liebetanz, D., Lang, N., et al. (2003). Pharmacological modulation of cortical excitability shifts induced by transcranial direct current stimulation in humans. *J Physiol, 553*(Pt 1), 293-301.

Nitsche, M. A., & Paulus, W. (2000). Excitability changes induced in the human motor cortex by weak transcranial direct current stimulation. *J Physiol, 527 Pt 3*, 633-639.

Nowak, A. (2009). *Die Funktion des Tiefschlafs in der Homöostase neuronaler Erregbarkeit. Eine kombinierte TMS/EEG-Studie am motorischen Kortex.*, Christian-Albrechts-Universität, Kiel.

O'Keefe, J., & Dostrovsky, J. (1971). The hippocampus as a spatial map. Preliminary evidence from unit activity in the freely-moving rat. *Brain Res., 34*(1), 171-175.

Orban, P., Rauchs, G., Balteau, E., Degueldre, C., Luxen, A., Maquet, P., et al. (2006). Sleep after spatial learning promotes covert reorganization of brain activity. *Proc. Natl. Acad. Sci. U. S. A.*

Osipova, D., Hermes, D., & Jensen, O. (2008). Gamma power is phase-locked to posterior alpha activity. *PLoS ONE, 3*(12), e3990.

Pace-Schott, E. F., & Hobson, J. A. (2002). The neurobiology of sleep: genetics, cellular physiology and subcortical networks. *Nat. Rev. Neurosci., 3*(8), 591-605.

Peigneux, P., Laureys, S., Fuchs, S., Collette, F., Perrin, F., Reggers, J., et al. (2004). Are spatial memories strengthened in the human hippocampus during slow wave sleep? *Neuron, 44*(3), 535-545.

Peigneux, P., Laureys, S., Fuchs, S., Destrebecqz, A., Collette, F., Delbeuck, X., et al. (2003). Learned material content and acquisition level modulate cerebral reactivation during posttraining rapid-eye-movements sleep. *Neuroimage, 20*(1), 125-134.

Peyrache, A., Khamassi, M., Benchenane, K., Wiener, S. I., & Battaglia, F. P. (2009). Replay of rule-learning related neural patterns in the prefrontal cortex during sleep. *Nat. Neurosci.*

Pogosyan, A., Gaynor, L. D., Eusebio, A., & Brown, P. (2009). Boosting cortical activity at Beta-band frequencies slows movement in humans. *Curr. Biol., 19*(19), 1637-1641.

Rasch, B., & Born, J. (2007). Maintaining memories by reactivation. *Curr. Opin. Neurobiol., 17*(6), 698-703.

Rasch, B., Buchel, C., Gais, S., & Born, J. (2007). Odor cues during slow-wave sleep prompt declarative memory consolidation. *Science, 315*(5817), 1426-1429.

Rechtschaffen, A., & Kales, A. (1968). *A manual of standardized terminology, techniques and scoring system for sleep stages of human subjects*. Washington, DC: United States Government Printing Office.

Reimund, E. (1994). The free radical flux theory of sleep. *Med. Hypotheses, 43*(4), 231-233.

Rempel-Clower, N. L., Zola, S. M., Squire, L. R., & Amaral, D. G. (1996). Three cases of enduring memory impairment after bilateral damage limited to the hippocampal formation. *J. Neurosci., 16*(16), 5233-5255.

Ribeiro, S., Gervasoni, D., Soares, E. S., Zhou, Y., Lin, S. C., Pantoja, J., et al. (2004). Long-lasting novelty-induced neuronal reverberation during slow-wave sleep in multiple forebrain areas. *PLoS Biol., 2*(1), E24.

Ribot, T. (1882). *Diseases of Memory*. New York: Appleton-Century-Crofts.

Riedner, B. A., Vyazovskiy, V. V., Huber, R., Massimini, M., Esser, S., Murphy, M., et al. (2007). Sleep homeostasis and cortical synchronization: III. A high-density EEG study of sleep slow waves in humans. *Sleep, 30*(12), 1643-1657.

Ritter, P., & Villringer, A. (2006). Simultaneous EEG-fMRI. *Neurosci. Biobehav. Rev., 30*(6), 823-838.

Rosanova, M., & Ulrich, D. (2005). Pattern-specific associative long-term potentiation induced by a sleep spindle-related spike train. *J. Neurosci., 25*(41), 9398-9405.

Rudoy, J. D., Voss, J. L., Westerberg, C. E., & Paller, K. A. (2009). Strengthening individual memories by reactivating them during sleep. *Science, 326*(5956), 1079.

Sanchez-Vives, M. V., & McCormick, D. A. (2000). Cellular and network mechanisms of rhythmic recurrent activity in neocortex. *Nat. Neurosci., 3*(10), 1027-1034.

Schabus, M., Dang-Vu, T. T., Albouy, G., Balteau, E., Boly, M., Carrier, J., et al. (2007). Hemodynamic cerebral correlates of sleep spindles during human non-rapid eye movement sleep. *Proc. Natl. Acad. Sci. U. S. A., 104*(32), 13164-13169.

Schabus, M., Hodlmoser, K., Gruber, G., Sauter, C., Anderer, P., Klosch, G., et al. (2006). Sleep spindle-related activity in the human EEG and its relation to general cognitive and learning abilities. *Eur. J. Neurosci., 23*(7), 1738-1746.

Schabus, M., Hoedlmoser, K., Pecherstorfer, T., Anderer, P., Gruber, G., Parapatics, S., et al. (2008). Interindividual sleep spindle differences and their relation to learning-related enhancements. *Brain Res., 1191*, 127-135.

Schwiedrzik, C. M. (2009). Retina or visual cortex? The site of phosphene induction by transcranial alternating current stimulation
Front Integr Neurosci
doi:10.3389/neuro.07.006.2009

Sejnowski, T. J., & Destexhe, A. (2000). Why do we sleep? *Brain Res., 886*(1-2), 208-223.

Siapas, A. G., & Wilson, M. A. (1998). Coordinated interactions between hippocampal ripples and cortical spindles during slow-wave sleep. *Neuron, 21*(5), 1123-1128.

Siebner, H. R., Bergmann, T. O., Bestmann, S., Massimini, M., Johansen-Berg, H., Mochizuki, H., et al. (2009). Consensus paper: Combining transcranial stimulation with neuroimaging *Brain Stimulation, 2*(2), 58-80.

Siebner, H. R., Hartwigsen, G., Kassuba, T., & Rothwell, J. C. (2009). How does transcranial magnetic stimulation modify neuronal activity in the brain? Implications for studies of cognition. *Cortex, 45*(9), 1035-1042.

Siebner, H. R., & Ziemann, U. (2007). *Das TMS-Buch. Handbuch der transkraniellen Magnetstimulation.* Heidelberg: Springer Medizin Verlag.

Siegel, J. M. (2001). The REM sleep-memory consolidation hypothesis. *Science, 294*(5544), 1058-1063.

Siegel, J. M. (2004). The neurotransmitters of sleep. *J. Clin. Psychiatry, 65 Suppl 16*, 4-7.

Siegel, J. M. (2008). Do all animals sleep? *Trends Neurosci., 31*(4), 208-213.

Siegel, J. M. (2009). Sleep viewed as a state of adaptive inactivity. *Nat. Rev. Neurosci.*

Simons, J. S., & Spiers, H. J. (2003). Prefrontal and medial temporal lobe interactions in long-term memory. *Nat. Rev. Neurosci., 4*(8), 637-648.

Sirota, A., Csicsvari, J., Buhl, D., & Buzsaki, G. (2003). Communication between neocortex and hippocampus during sleep in rodents. *Proc. Natl. Acad. Sci. U. S. A., 100*(4), 2065-2069.

Sirota, A., Montgomery, S., Fujisawa, S., Isomura, Y., Zugaro, M., & Buzsaki, G. (2008). Entrainment of neocortical neurons and gamma oscillations by the hippocampal theta rhythm. *Neuron, 60*(4), 683-697.

Song, S., Miller, K. D., & Abbott, L. F. (2000). Competitive Hebbian learning through spike-timing-dependent synaptic plasticity. *Nat. Neurosci., 3*(9), 919-926.

Squire, L. R., & Alvarez, P. (1995). Retrograde amnesia and memory consolidation: a neurobiological perspective. *Curr. Opin. Neurobiol., 5*(2), 169-177.

Squire, L. R., Stark, C. E., & Clark, R. E. (2004). The medial temporal lobe. *Annu. Rev. Neurosci., 27*, 279-306.

Squire, L. R., & Zola-Morgan, S. (1991). The medial temporal lobe memory system. *Science, 253*(5026), 1380-1386.

Squire, L. R., & Zola, S. M. (1996). Structure and function of declarative and nondeclarative memory systems. *Proc. Natl. Acad. Sci. U. S. A., 93*(24), 13515-13522.

Stefan, K., Kunesch, E., Benecke, R., Cohen, L. G., & Classen, J. (2002). Mechanisms of enhancement of human motor cortex excitability induced by interventional paired associative stimulation. *J Physiol, 543*(Pt 2), 699-708.

Stefan, K., Kunesch, E., Cohen, L. G., Benecke, R., & Classen, J. (2000). Induction of plasticity in the human motor cortex by paired associative stimulation. *Brain, 123 Pt 3*, 572-584.

Steriade, M. (2000). Corticothalamic resonance, states of vigilance and mentation. *Neuroscience, 101*(2), 243-276.

Steriade, M. (2003). The corticothalamic system in sleep. *Front. Biosci., 8*, d878-899.

Steriade, M. (2006). Grouping of brain rhythms in corticothalamic systems. *Neuroscience, 137*(4), 1087-1106.

Steriade, M., Contreras, D., Curro Dossi, R., & Nunez, A. (1993). The slow (< 1 Hz) oscillation in reticular thalamic and thalamocortical neurons: scenario of sleep rhythm generation in interacting thalamic and neocortical networks. *J. Neurosci., 13*(8), 3284-3299.

Steriade, M., Nunez, A., & Amzica, F. (1993a). Intracellular analysis of relations between the slow (< 1 Hz) neocortical oscillation and other sleep rhythms of the electroencephalogram. *J. Neurosci., 13*(8), 3266-3283.

Steriade, M., Nunez, A., & Amzica, F. (1993b). A novel slow (< 1 Hz) oscillation of neocortical neurons in vivo: depolarizing and hyperpolarizing components. *J. Neurosci., 13*(8), 3252-3265.

Steriade, M., & Timofeev, I. (2003). Neuronal plasticity in thalamocortical networks during sleep and waking oscillations. *Neuron, 37*(4), 563-576.

Steriade, M., Timofeev, I., & Grenier, F. (2001). Natural waking and sleep states: a view from inside neocortical neurons. *J. Neurophysiol., 85*(5), 1969-1985.

Stickgold, R. (2005). Sleep-dependent memory consolidation. *Nature, 437*(7063), 1272-1278.

Stickgold, R., & Walker, M. P. (2005). Memory consolidation and reconsolidation: what is the role of sleep? *Trends Neurosci., 28*(8), 408-415.

Sutherland, G. R., & McNaughton, B. (2000). Memory trace reactivation in hippocampal and neocortical neuronal ensembles. *Curr. Opin. Neurobiol., 10*(2), 180-186.

Sweatt, J. D. (1999). Toward a molecular explanation for long-term potentiation. *Learn. Mem., 6*(5), 399-416.

Takashima, A., Nieuwenhuis, I. L., Jensen, O., Talamini, L. M., Rijpkema, M., & Fernandez, G. (2009). Shift from hippocampal to neocortical centered retrieval network with consolidation. *J. Neurosci., 29*(32), 10087-10093.

Takashima, A., Petersson, K. M., Rutters, F., Tendolkar, I., Jensen, O., Zwarts, M. J., et al. (2006). Declarative memory consolidation in humans: A prospective functional magnetic resonance imaging study. *Proc. Natl. Acad. Sci. U. S. A., 103*(3), 756-761.

Terney, D., Chaieb, L., Moliadze, V., Antal, A., & Paulus, W. (2008). Increasing human brain excitability by transcranial high-frequency random noise stimulation. *J. Neurosci., 28*(52), 14147-14155.

Teyler, T. J., & DiScenna, P. (1986). The hippocampal memory indexing theory. *Behav. Neurosci., 100*(2), 147-154.

Timofeev, I., Grenier, F., Bazhenov, M., Sejnowski, T. J., & Steriade, M. (2000). Origin of slow cortical oscillations in deafferented cortical slabs. *Cereb. Cortex, 10*(12), 1185-1199.

Tononi, G., & Cirelli, C. (2003). Sleep and synaptic homeostasis: a hypothesis. *Brain Res. Bull., 62*(2), 143-150.

Tononi, G., & Cirelli, C. (2006). Sleep function and synaptic homeostasis. *Sleep Med Rev, 10*(1), 49-62.

Tulving, E. (1972). Episodic and semantic memory. In E. Tulving & W. Donaldson (Eds.), *Organization of Memory* (pp. 381–403). New York: Academic.

Tulving, E. (2002). Episodic memory: from mind to brain. *Annu. Rev. Psychol., 53*, 1-25.

Vertes, R. P. (2004). Memory consolidation in sleep; dream or reality. *Neuron, 44*(1), 135-148.

Virtanen, J., Ruohonen, J., Naatanen, R., & Ilmoniemi, R. J. (1999). Instrumentation for the measurement of electric brain responses to transcranial magnetic stimulation. *Med. Biol. Eng. Comput., 37*(3), 322-326.

von Borstel, J. (2009). *Hat Tiefschlaf einen Einfluss auf die Regulation kortikaler Plastizität? Eine TMS-EEG Studie am motorischen Kortex.*, Christian-Albrechts-Universität, Kiel.

Vyazovskiy, V. V., Cirelli, C., Pfister-Genskow, M., Faraguna, U., & Tononi, G. (2008). Molecular and electrophysiological evidence for net synaptic potentiation in wake and depression in sleep. *Nat. Neurosci., 11*(2), 200-208.

Vyazovskiy, V. V., Faraguna, U., Cirelli, C., & Tononi, G. (2009). Triggering slow waves during NREM sleep in the rat by intracortical electrical stimulation: effects of sleep/wake history and background activity. *J. Neurophysiol.*

Vyazovskiy, V. V., Olcese, U., Lazimy, Y. M., Faraguna, U., Esser, S. K., Williams, J. C., et al. (2009). Cortical firing and sleep homeostasis. *Neuron, 63*(6), 865-878.

Vyazovskiy, V. V., Riedner, B. A., Cirelli, C., & Tononi, G. (2007). Sleep homeostasis and cortical synchronization: II. A local field potential study of sleep slow waves in the rat. *Sleep, 30*(12), 1631-1642.

Wagner, A. D., Shannon, B. J., Kahn, I., & Buckner, R. L. (2005). Parietal lobe contributions to episodic memory retrieval. *Trends Cogn Sci, 9*(9), 445-453.

Walker, M. P., & Stickgold, R. (2006). Sleep, memory, and plasticity. *Annu. Rev. Psychol., 57*, 139-166.

Walker, M. P., Stickgold, R., Alsop, D., Gaab, N., & Schlaug, G. (2005). Sleep-dependent motor memory plasticity in the human brain. *Neuroscience, 133*(4), 911-917.

Walsh, V., & Cowey, A. (2000). Transcranial magnetic stimulation and cognitive neuroscience. *Nat. Rev. Neurosci., 1*(1), 73-79.

Wassermann, E. M., Epstein, C. M., Ziemann, U., Walsh, V., Paus, T., & Lisanby, S. (2008). *The Oxford Handbook of Transcranial Stimulation*. Oxford: Oxford University Press.

Werk, C. M., Harbour, V. L., & Chapman, C. A. (2005). Induction of long-term potentiation leads to increased reliability of evoked neocortical spindles in vivo. *Neuroscience, 131*(4), 793-800.

Werk, C. M., Klein, H. S., Nesbitt, C. E., & Chapman, C. A. (2006). Long-term depression in the sensorimotor cortex induced by repeated delivery of 10 Hz trains in vivo. *Neuroscience, 140*(1), 13-20.

Wilson, M. A., & McNaughton, B. L. (1994). Reactivation of hippocampal ensemble memories during sleep. *Science, 265*(5172), 676-679.

Wolters, A., Sandbrink, F., Schlottmann, A., Kunesch, E., Stefan, K., Cohen, L. G., et al. (2003). A temporally asymmetric Hebbian rule governing plasticity in the human motor cortex. *J. Neurophysiol., 89*(5), 2339-2345.

Ziemann, U., Ilic, T. V., Pauli, C., Meintzschel, F., & Ruge, D. (2004). Learning modifies subsequent induction of long-term potentiation-like and long-term depression-like plasticity in human motor cortex. *J. Neurosci., 24*(7), 1666-1672.

Ziemann, U., & Siebner, H. R. (2008). Modifying motor learning through gating and homeostatic metaplasticity. *Brain Stimulation, 1*(1), 60-66.

7 Summary in German / Deutsche Zusammenfassung

Warum schlafen wir? Diese scheinbar simple Frage beschreibt tatsächlich eines der interessantesten Rätsel aktueller neurowissenschaftlicher Forschung. Die Tatsache, dass Schlaf sich evolutionär durchgesetzt hat, obwohl wir dabei das Bewusstsein verlieren und somit ein hohes Risiko eingehen, spricht für seine fundamentale Notwendigkeit (Cirelli & Tononi, 2008; aber vergleiche Siegel, 2008). Neben einer Vielzahl restorativer Funktionen auf metabolischer Ebene (die auch im entspannten Wachzustand möglich wären) wird die Kernfunktion des Schlafs heute in der Regulation und Reorganisation *neuronaler Plastizität* gesehen (Born et al., 2006; Diekelmann & Born, 2010; Hobson & Pace-Schott, 2002; Maquet, 2001; Sejnowski & Destexhe, 2000; Steriade & Timofeev, 2003; Stickgold, 2005; Tononi & Cirelli, 2006).

Neuronale Plastizität bezeichnet die Fähigkeit des Gehirns sich beständig an eine veränderte Umwelt anzupassen indem es gleichsam die Funktion und Struktur seiner synaptischen Verknüpfungen verändert. Diese Modifikationsmöglichkeit der Übertragungsstärke einzelner Synapsen stellt den Grundbaustein jeglichen Lernens dar. Sie ermöglicht die flexible Zusammenstellung ganzer neuronaler Netzwerke, welche schließlich auch die Komplexität menschliche Erinnerungen repräsentieren können.

Zwei der wichtigsten derzeit propagierten Funktionen schlafbedingter neuronaler Plastizität sind (i) auf synaptischer Ebene die homöostatische Regulation synaptischer Gewichte (Tononi & Cirelli, 2006) und (ii) auf systemischer Ebene die Konsolidierung frisch angelegter Gedächtnisspuren sowie deren Reorganisation und Integration in bestehende Erinnerungen (Born et al., 2006; Diekelmann & Born, 2010). Während die förderlichen Effekte des Schlafs auf die neuronale Plastizität und Gedächtniskonsolidierung auf breiter empirischer Grundlage stehen, sind die vermittelnden neuronalen Mechanismen noch weitgehend ungeklärt. Inzwischen existieren allerdings vielversprechende Modelle, welche insbesondere die Bedeutung schlafspezifischer *neuronaler Oszillationen* in den Vordergrund stellen (Born et al., 2006; Diekelmann & Born, 2010; Marshall & Born, 2007; Rasch & Born, 2007; Tononi & Cirelli, 2006). *Neuronale Oszillationen* bezeichnen die rhythmisch wiederkehrende neuronale Aktivität einer bestimmten Frequenz, die oft durch das Zusammenspiel großer Neuronenpopulationen zustande kommen. Eine ganze Hierarchie dieser Oszillationen, die sich hinsichtlich ihrer Entstehung, Ausbreitung und Frequenz unterscheiden,

organisiert die zeitliche Taktung der Informationsverarbeitung im Gehirn (für eine exzellente Ausarbeitung dieses Themas siehe Buzsaki, 2006).

Obwohl die exakten neuronalen Mechanismen, die diesen Modellen zugrunde liegen, noch weiter ausgearbeitet werden müssen, lieferten sie bereits die Grundlage für erste Ansätze um mittels oszillierender transkranieller Gleichstromstimulation auf die oszillatorische neuronale Informationsverarbeitung während des Schlafs einzuwirken (Marshall, Helgadottir et al., 2006). Um diese Methoden zukünftig effektiv einsetzen zu können, müssen jedoch ihre neurophysiologischen Wirkmechanismen genauer erforscht werden.

Ziel dieser Arbeit ist es daher, die Interaktion schlafspezifischer neuronaler Oszillationen, ihre Bedeutung für die homöostatische Regulation neuronaler Plastizität und die systemische Gedächtniskonsolidierung, sowie schließlich die Modifikationsmöglichkeiten mittels non-invasiver Stimulationstechniken genauer zu erforschen.

Der Prozess der Stabilisierung einer frischen, zunächst labilen Gedächtnisspur wird seit Müller und Pilzecker als *Konsolidierung* bezeichnet (G. E. Müller & Pilzecker, 1900). Diese findet sowohl auf synaptischer Ebene (synaptische Veränderungen an einzelnen Neuronen innerhalb von Minuten bis Stunden) wie auch systemischer Ebene (Reorganisation komplexer neuronalen Netzwerke innerhalb von Stunden bis Jahren) statt (Kapitel 1.1).

Auf synaptische Ebene basiert die Verstärkung/Abschwächung der synaptischen Gewichte zunächst auf einer vorübergehend funktionell erhöhten/erniedrigten Neurotransmitterausschüttung und -aufnahme (Kapitel 1.1.1). Der Prozess der Konsolidierung bezieht sich hier auf den Übergang in eine längerfristige strukturelle Vergrößerung/Verkleinerung und sogar den Aufbau/Abbau synaptischer Verbindungen. Diese Zu- bzw. Abnahme synaptischer Effektivität wird als Langzeitpotenzierung (LTP; Kapitel 1.1.1.1) und Langzeitdepression (LTD; Kapitel 1.1.1.2) bezeichnet und stellt die Grundlage allen Lernens und Erinnerns dar. Ob eine Synapse verstärkt oder abgeschwächt wird hängt von unter anderem vom exakten zeitlichen Zusammenspiel prä- und postsynaptischer Aktivität ab, eine Abhängigkeit die als *spike timing-dependent plasticity* (STDP) bezeichnet wird (Kapitel 1.1.1.3.). Zudem existiert eine übergeordnete Form der Plastizität, die dafür sorgt, dass Synapsen weder übermäßig verstärkt noch abgeschwächt werden um so ein ausgeglichenes Funktionsniveau zu bewahren: die *Homöostatische Metaplastizität* (Kapitel 1.1.1.4.).

Auf systemischer Ebene bezieht sich der Begriff der Konsolidierung auf die Reorganisation und räumliche Umverteilung von komplexeren neuronalen Repräsentationen innerhalb von Gedächtnissystemen (1.1.2). Man unterscheidet hier unter anderem das *deklarative* (Erinnerung an Erlebnisse und Fakten; Kapitel 1.1.2.1) und das *prozedurale* (Erlernen von Fertigkeiten; Kapitel 1.1.2.2) Gedächtnissystem. Für das deklarative Gedächtnis bestehen besserer theoretische Modelle einer systemischen Konsolidierung, weshalb es auch im Fokus dieser Arbeit steht. So wird angenommen, dass der Hippokampus, eine Struktur in der Tiefe der Schläfenlappen die über Zwischenstationen Eingänge von allen Bereichen des Gehirns erhält, seine Synapsengewichte sehr leicht ändern und somit schnell lernen kann, während der Neokortex seine Verschaltungen nur langsam adaptiert und deshalb ein langsamer Lerner ist (McClelland et al., 1995). Aufgabe des Hippokampus ist es nun den Neokortex gleichsam zu trainieren indem er die hippokampo-neokortikalen Verknüpfungen (die Gedächtnisspuren) wiederholt gemeinsam reaktiviert und so direkte kortiko-kortikale Repräsentationen als Langzeitgedächtnis generiert (Frankland & Bontempi, 2005). Auf lange Sicht werden die Erinnerungen dadurch unabhängig von der Integrität des Hippokampus. Eben diese hippokampo-neokortikale Reaktivierung findet vermutlich aktiv im Schlaf statt.

Schlafphasen (ihrerseits einem zirkadianen Rhythmus folgend) grenzen sich durch eine einzigartige oszillatorische Hirnaktivität deutlich vom Wachzustand ab (Kapitel 1.2). Schlaf ist jedoch kein einheitliches Phänomen, sondern setzt sich aus einer Reihe alternierender Schlafstadien zusammen, die ihrerseits durch bestimmte Oszillationsfrequenzen und Ereignisse im Elektroenzephalogramm (EEG) sowie im Elektromyogramm (EMG) und Elektrookkulogramm (EOG) gekennzeichnet sind (Kapitel 1.2.1). Die Wesentliche Unterteilung besteht in der Abgrenzung von *rapid eye movement* (REM)-Schlaf und non-REM (NREM)-Schlaf, wobei letzterer noch je nach Schlaftiefe in bis zu vier Unterstadien untergliedert ist (Rechtschaffen & Kales, 1968).

Entsprechend der wichtigsten Modelle schlafabhängiger Plastizität soll hier der Fokus allein auf dem NREM Schlaf liegen. Während die kortikale Aktivität im Wachzustand wesentlich durch den sensorischen Input mitbestimmt wird, ist das Gehirn im Schlaf durch eine Blockade im Thalamus von der Außenwelt abgeschnitten und spricht im Wesentlichen mit sich selbst. Hieraus ergeben sich eine Reihe hierarchisch organisierter und ineinander gruppierter Oszillationen (Kapitel 1.2.2.). Dabei

sind insbesondere die thalamo-kortikalen Schlafspindeln (Kapitel 1.2.2.1) und die kortikalen langsamen Oszillationen (Kapitel 1.2.2.3) zu nennen. Schlafspindeln sind kurzzeitig (0,5 – 3 s) zu- und wieder abnehmende Oszillationen im Bereich von 10-13 (langsame frontale Spindeln) bzw. 13-16 Hz (schnelle zentro-parietale Spindeln), die unter kortikalem Einfluss im Thalamus generiert und zurück in den Kortex projiziert werden (De Gennaro & Ferrara, 2003; Steriade, 2003). Langsame Oszillationen (< 1 Hz) werden im Wesentlichen lokal kortikal generiert und breiten sich vom Entstehungsort über den gesamten Kortex sowie in subkortikal gelegene Strukturen aus. Sie bestehen aus alternierenden Phasen der Hyperpolarisation (*down state*) und der Depolarisation (*up state*) in denen fast alle kortikalen Neurone gemeinsam schweigen bzw. feuern (Steriade, Nunez et al., 1993b). Die langsame Oszillation stellt die wichtigste ordnende Komponente im NREM Schlaf dar indem sie alle anderen schnelleren Oszillationen während der *down states* unterdrückt und während der *up states* synchronisiert verstärkt (Mölle et al., 2002; Steriade, 2006).

Diese eben beschriebenen schlaf-spezifischen Oszillationen bilden auch das Kerngerüst zwei der gegenwärtig einflussreichsten Theorien schafbedingter neuronaler Plastizität (Kapitel 1.3): (i) der *synaptic homeostasis hypothesis* und (ii) der *active system consolidation hypothesis*.

Die „Hypothese der synaptischen Homöostase“ *(Tononi & Cirelli, 2003, 2006)* nimmt an, dass die zunehmende Potenzierung synaptischer Gewichte während des Lernens im anschließenden Schlaf wieder kompensiert werden muss, um sie auf einem effektiven Ausgangsniveau zu halten und übermäßigen Energie- und Platzbedarf zu reduzieren (Kapitel 1.3.1). Dies soll durch sogenanntes *synaptic downscaling* geschehen, ein globales - jedoch für alle Synapsen eines Neurons proportionales - Herunterskalieren der Synapsengewichte, welches als zudem ein verbessertes Signal-Rausch-Verhältnis der repräsentierten Informationen zur Folge hat. Dieses Herunterskalieren soll durch die langsamen Oszillationen vermittelt werden, deren Ausprägung ihrerseits auch ein wichtiger Marker zuvor induzierter Plastizität darstellt.

Die Hypothese „aktiver systemischer Konsolidierung“ (Born et al., 2006; Diekelmann & Born, 2010; Marshall & Born, 2007; Rasch & Born, 2007) basierend auf der Idee des hippokampo-neokortikalen Gedächtnistransfers (Kapitel 1.3.2). Sie nimmt an, dass die Reaktivierung und Umverteilung deklarativer Gedächtnisinhalte während bestimmter Zeitfenster des NREM Schlafs stattfindet. Namentlich sind dies

die *up states* langsamer Oszillationen, in welchen neben den thalamo-kortikalen Schlafspindeln auch die hippokampalen *sharp wave-ripples*, ultraschnelle (~100-600 Hz) Salven hippokampaler Neurone, gruppiert sind. Im Rahmen dieser konzertierten oszillatorischen Aktivität sollen Information aus dem Hippokampus in den Neokortex geschrieben werden. Zahlreiche Hinweise auf die Gültigkeit dieser Hypothese kommen aus der Kombination von Verhaltensstudien und elektrophysiologischen Untersuchungen von *sharp wave-ripples* (Kapitel 1.3.2.1), Spindeln (Kapitel 1.3.2.2) und langsamen Oszillationen (Kapitel 1.3.2.3), sowie dem Einsatz funktioneller Bildgebung (Kapitel 1.3.2.4). Dennoch sind die exakten neuronalen Mechanismen dieser schlafbedingten systemischen Konsolidierung noch weitestgehend ungeklärt.

Synaptische Homöostase und systemische Gedächtniskonsolidierung sind aller Wahrscheinlichkeit nach keine konkurrierenden Theorien sondern erklären vielmehr gleichzeitig stattfindende Phänomene auf unterschiedlichen Ebenen (Kapitel 1.3.3).

Um die oszillatorischen Prozesse zu untersuchen, welche synaptischer Homöostase und systemischer Gedächtniskonsolidierung zugrunde liegen, sowie die Möglichkeiten und Mechanismen der transkranieller Modulation dieser Oszillationen auszuloten, habe ich mich unterschiedlicher neurowissenschaftlicher Verfahren bedient (Kapitel 2). Durch die Nutzung von bildgebenden Verfahren wie der Elektroenzephalographie (EEG) und der funktionellen Magnetresonanztomographie (fMRT) wie auch non-invasiven Stimulationsverfahren wie der transkraniellen Magnetstimulation (TMS) und der transkraniellen Gleichstromstimulation (tDCS), sowie insbesondere durch deren kombinierten Einsatz (Kapitel 2.1) - EEG-fMRT (Kapitel 2.2), TMS-tDCS (Kapitel 2.3), TMS-EEG (Kapitel 2.4) - konnten Nachteile einzelner Methoden (z.B. hinsichtlich räumlicher und zeitlicher Auflösung) kompensiert werden. Die Kombination von TMS mit bildgebenden Verfahren ist ausführlich im angehängten Konsens-Manuskript beschrieben, zu welchem ich als Zweitautor beigetragen habe (Paper I, H. R. Siebner, Bergmann et al., 2009).

Die empirischen Arbeiten (Kapitel 3) auf denen diese Dissertationsschrift beruht lassen sich in drei inhaltliche Teilbereiche untergliedern (Kapitel 3.1). Sie untersuchen die oszillatorischen Mechanismen (i) der synaptischen Homöostase (Paper II, Bergmann et al., 2008), (ii) der schlafbedingten systemischen Gedächtniskonsolidie-

rung (Paper IV, Bergmann et al., in prep.; Paper III, Mölle et al., in prep.) und (iii) der langsam oszillierenden tDCS als Interventionsverfahren (Paper V, Bergmann et al., 2009; Paper VI, Groppa et al., 2010). Die Inhalte der einzelnen Arbeiten werden im Folgenden kurz abgerissen, eine ausführliche Darstellung findet sich in den entsprechenden Kapiteln sowie den Manuskripten im Anhang.

Paper II (Bergmann et al., 2008): Diese Arbeit konnte mittels TMS am motorischen Kortex zeigen, dass die Ausprägung langsamer oszillatorischer EEG Aktivität von der Richtung zuvor induzierter neuronaler Plastizität abhängt und nicht lediglich vom Ausmaß der neuronalen Aktivität während des Wachzustandes. Wir, wie auch andere (De Gennaro et al., 2008), fanden jedoch nicht die vorhergesagte topographische Spezifität und Richtung (Tononi & Cirelli, 2006). Hingegen zeigte sich eine höchst fokale Abhängigkeit der langsamen Schlafspindeln im stimulierten motorischen Kortex, sowie eine Konsolidierung der induzierten bidirektionalen kortikalen Erregbarkeitsveränderungen über den Schlaf hinweg (Kapitel 3.2.1).

Paper III (Mölle et al., in prep.): Ausführliche EEG-Analysen konnten zeigen, dass schnelle und langsame Schlafspindeln in gegensätzlichen Phasen der langsamen Oszillationen gruppiert werden, was auch eine unterschiedliche Funktion der beiden nahelegt. So ist denkbar, dass der thalamo-kortikale Input schneller Spindeln in den *up states* langsamer Oszillationen verstärkt, der Input langsamer Spindeln in den *down states* hingegen unterdrückt wird. Dies könnte entsprechend der Regeln der STDP eine Potenzierung bzw. Depression kortikaler Synapsen zur Folge haben, was einen bidirektionalen Mechanismus oszillationsbedingter Plastizität im Schlaf darstellen würde (Kapitel 3.3.1).

Paper IV (Bergmann et al., in prep.): Mittels simultaner EEG und fMRT Aufnahmen während des Schlafs konnte erstmalig am Menschen gezeigt werden, dass Schlafspindeln tatsächlich mit der Reaktivierung hippokampo-neokortikaler Gedächtnisspuren assoziiert sind. Nach dem Lernen von Gesichter-Landschafts-Assoziationen war die neuronale Aktivität sowohl im Hippokampus als auch in Gesichts- und Landschafts-spezifischen neokortikalen Regionen stärker von den Amplituden thalamo-kortikaler Spindeln abhängig als nach dem Ausführen einer vergleichbaren visuo-motorischen Kontrollaufgabe. Dies stimmt mit der propagierten Bedeutung von Schlafspindeln in der aktiven systemischen Gedächtniskonsolidierung überein (Born et al., 2006; Diekelmann & Born, 2010; Marshall & Born, 2007; Rasch & Born, 2007). Es besteht allerdings die Möglichkeit, dass Reaktivierungen dieser Art

lediglich einen bedeutungslosen Nachhall vergangener Aktivität bzw. verstärkter neuronaler Verknüpfungen darstellen und keine direkte Funktonalität besitzen. Dies muss in weiteren Untersuchungen ausgeschlossen werden (Kapitel 3.3.2).

Paper V (Bergmann et al., 2009): Erregbarkeitsmessungen am wachen motorischen Kortex mittels TMS während der gleichzeitigen Applikation langsam (0.8 Hz) oszillierender vs. konstanter anodaler tDCS zeigten, dass zwar beide Verfahren eine ähnliche akute Fazilitierung der kortikalen Erregbarkeit verursachen können, diese jedoch nicht gemeinsam mit der transkraniell angelegten Stromstärke variieren. Dies deutet darauf hin, dass - zumindest während des Wachzustandes - keine Ankopplung der neuronalen Membranpotenziale an die transkranielle Potenzialverschiebungen im Bereich schlafähnlicher langsamer Oszillationen möglich ist. Dieser Befund macht die Möglichkeit einer direkten Beeinflussung endogener Oszillationen durch oszillierende tDCS weniger wahrscheinlich. Allerdings könnte der negative Befund auch allein auf die während des Wachzustandes nicht präferierte langsame Frequenz zurückzuführen sein (vergleiche Marshall, Helgadottir et al., 2006) (Kapitel 3.4.1).

Paper VI (Groppa et al., 2010): Messungen der anhaltenden Fazilitierung bzw. Inhibition motorkortikaler Erregbarkeit mittels TMS infolge anodaler bzw. kathodaler tDCS konnten zeigen, dass langsam oszillatorische und konstante tDCS gleich wirksam sein können, wenn die Gesamtladung (und nicht die maximale Stromstärke) übereinstimmen. Es ist also zu bedenken, dass der Einsatz oszillierender tDCS je nach Polarität immer auch eine anhaltende LTP-artige Potenzierung bzw. LTD-artige Depression im stimulierten Gewebe bewirkt, was wiederum frequenzunabhängige Veränderungen der endogenen oszillatorischen Aktivität zur Folge haben kann. Möglicherweise ist also der Einsatz von tACS (mit wechselnder Polarität) vielversprechender wenn es darum geht nur indirekt über die Modifikation endogener Oszillationen auf plastische Prozesse einzuwirken (Kapitel 3.4.2).

Zusammenfassend weisen die theoretischen Überlegungen und empirischen Befunde in dieser Dissertationsschrift auf die maßgebliche Rolle hin, die interagierende neuronale Oszillationen – insbesondere langsame Oszillationen und Schlafspindeln – bei der Regulation synaptischer Plastizität sowie der systemischen Gedächtniskonsolidierung spielen. Wir haben jedoch gerade erst begonnen, die zugrundeliegenden Mechanismen dieser Prozesse zu verstehen.

8 Curriculum Vitae

English version

	Personal data
Name	Til Ole Bergmann
Date of birth	13.04.1980
Place of birth	Kiel, Germany
Family status	Unmarried
Nationality	German

	Education
07/1986-06/1990	Primary school: *Grund- und Hauptschule Heikendorf*
07/1990-06/1999	Secondary School: *Hans-Geiger-Gymnasium*, Kiel
06/1999	*Abitur* (Grade 2.0)
09/1999-07/2000	Civilian Service: hospice *Haus Porsefeld*, Rendsburg
10/2000-09/2005	Study of psychology: *Christian-Albrechts-University of Kiel*
09/2005	Diploma (Grade 1.3) Thesis: "*What is real in real memories? The influence of valence and arousal of real vs. fictitious autobiographical memories on neuronal activity: an fMRI study.*"
since 2005	PhD study at the *Institute of Psychology, Christian-Albrechts-University of Kiel*

	Work experience
03/2001-09/2005	Undergraduate research fellow at the *Section of Social Psychology, Institute of Psychology, Christian-Albrechts-University of Kiel*
06/2004-03/2005	Project assistant (neuropsychological assessment and autobiographical interviews with schizophrenia patients) at the *Zentrum für Integrative Psychiatrie (ZiP)*, Kiel
since 2005	Graduate research fellow at the *Department of Neurology*, *Christian-Albrechts-University of Kiel*

Deutsche Fassung

	Persönliche Daten
Name	Til Ole Bergmann
Geburtsdatum	13.04.1980
Geburtsort	Kiel, Deutschland
Familienstand	Ledig
Staatsangehörigkeit	Deutsch

	Ausbildung
07/1986-06/1990	Grundschule: *Grund- und Hauptschule Heikendorf*
07/1990-06/1999	Gymnasium: *Hans-Geiger-Gymnasium*, Kiel
06/1999	*Abitur* (Gesamtnote 2,0)
09/1999-07/2000	Zivildienst: Hospiz *Haus Porsefeld*, Rendsburg
10/2000-09/2005	Studium der Psychologie: *Christian-Albrechts-Universität zu Kiel*
09/2005	Diplom (Gesamtnote 1,3) Diplomarbeit: "*Was ist das Echte an echten Erinnerungen? Der Einfluss von Valenz und Arousal realer versus fiktiver autobiographischer Erinnerungen auf die neuronale Aktivität: eine fMRT Studie."*
seit 2005	Promotionsstudium am *Institut für Psychologie, Christian-Albrechts-Universität zu Kiel*

	Arbeitserfahrung
03/2001-09/2005	Studentische Hilfskraft am *Lehrstuhl für Sozialpsychologie, Institut für Psychologie, Christian-Albrechts-Universität zu Kiel*
06/2004-03/2005	Projektmitarbeiter (Neuropsychologische Diagnostik und autobiographische Interviews bei Schizophreniepatienten) am *Zentrum für Integrative Psychiatrie (ZiP)*, Kiel
seit 2005	Wissenschaftlicher Mitarbeiter in der *Klinik für Neurologie*, *Christian-Albrechts-Universität zu Kiel*

List of Publications / Publikationsliste

JOURNAL ARTICLES / ARTIKEL IN FACHZEITSCHRIFTEN

Groppa S, **Bergmann TO**, Siems C, Mölle M, Marshall L, Siebner HR (2010) Slow-oscillatory transcranial DC stimulation can induce bidirectional shifts in motor cortical excitability in awake humans. *Neuroscience*, 166(4): 1219-1225.

Bergmann TO, Groppa S, Seeger S, Mölle M, Marshall L, Siebner HR (2009) Acute changes in motor cortical excitability during slow oscillatory and constant anodal transcranial direct current stimulation. *Journal of Neurophysiology*, 102(4):2303-2311.

Prehn-Kristensen A, Wiesner C, **Bergmann TO**, Wolff S, Jansen O, Mehdorn HM, Ferstl R, Pause BM (2009) Induction of empathy by the smell of anxiety. *PLoS One*, 4(6), e5987.

Siebner HR, **Bergmann TO**, Bestmann S, Massimini M, Johansen-Berg H, Mochizuki H, Bohning DE, Boorman ED, Groppa S, Miniussi C, Pascual-Leone A, Huber R, Taylor PC, Ilmoniemi RJ, De Gennaro L, Strafella AP, Kähkönen S, Klöppel S, Frisoni GB, George MS, Hallett M, Brandt SA, Rushworth MF, Ziemann U, Rothwell JC, Ward N, Cohen LG, Baudewig J, Paus T, Ugawa Y, Rossini PM (2009) Consensus paper: Combining transcranial stimulation with neuroimaging. *Brain Stimulation* 2(2): 58-80.

Bergmann TO, Mölle M, Marshall L, Kaya-Yildiz L, Born J, Siebner HR (2008) A local signature of LTP- and LTD-like plasticity in human NREM sleep. *European Journal of Neuroscience* 27:2241-2249.

BOOK CHAPTERS / BUCHKAPITEL

Bergmann TO & Siebner HR (2007) Visuelle Verarbeitung. In Siebner HR & Ziemann U (Eds.), *Das TMS–Buch. Handbuch der transkraniellen Magnetstimulation*, Springer Medizin Verlag, Heidelberg: 449-457.

Bergmann TO (2007) False Memories - Können wir unserem Gedächtnis trauen? In Dresler M & Klein TG (Eds.) *Wissenschaft an den Grenzen des Verstandes. Beiträge aus den Natur- und Lebenswissenschaften*. Hirzel, Stuttgart: 137-44.

PUBLISHED ABSTRACTS / PUBLIZIERTE KONFERENZBEITRÄGE

Bergmann TO, Groppa S, Seeger M, Mölle M, Marshall L, Siebner HR (2009). Cortical excitability changes during oscillatory transcranial direct current stimulation in humans. Abstract Viewer and Itinerary Planner, Online. *Society for Neuroscience Meeting 2009*, Chicago, IL, Program No. 375.9.

Bergmann TO, Mölle M, Marshall L, Kaya-Yildiz L, Born J, Siebner HR (2008) Paired associative stimulation modulates slow sleep spindles in human motor cortex during subsequent non-rapid eye movement (NREM) sleep. *FENS* Abstr. vol 4, A095.2.

Bergmann TO, Mölle M, Marshall L, Kaya-Yildiz L, Born J, Siebner HR (2007). Paired associative stimulation of the motor cortex affects local NREM sleep in humans: a TMS-EEG study. Abstract Viewer and Itinerary Planner, Online. *Society for Neuroscience Meeting 2007*, San Diego, CA, Program No. 22.7.

Bergmann TO, Goebel S, Siebner HR, Ferstl R, Wiesner CD (2006). How to identify true memories: retrieval of real and fictitious autobiographical memories under control of their emotional content. *Neuroimage* 31 (Suppl. 1): p164.

Bergmann TO, Wiesner CD, Goebel S, Siebner H, Wolff S, Ferstl R, Mehdorn HM & Jansen O (2005). Was ist das Echte an echten Erinnerungen? Der Einfluss von Valenz und Arousal realer versus fiktiver autobiographischer Erinnerungen auf die neuronale Aktivität: Eine fMRT-Studie. GNP-Jahrestagung 2005 in Bremen. *Zeitschrift für Neuropsychologie*, 16 (Supplementum), S7-6, p14.

INVITED TALKS / EINGELADENE VORTRÄGE

Bergmann TO (2010) TMS und EEG. Fortbildung Richard-Jung-Kolleg, 54. Wissenschaftliche Jahrestagung der Deutschen Gesellschaft für Klinische Neurophysiologie und Funktionelle Bildgebung, Halle, 18th-20th of March 2010

Bergmann TO (2009) Combining EEG and fMRI. PhD Course: Advances in magnetic resonance imaging of human brain structure and function, Hvidovre Hospital Copenhagen, 6th-9th of October 2009

Bergmann TO (2009) The role of sleep in plasticity and memory consolidation. XXIII Sandbjerg Symposium on Neuroplasticity and Neurorehabilitation, Danish Society for Neuroscience, Sandbjerg, 3rd-5th of May 2009

Bergmann TO (2008) Oszillatorische Hirnaktivität im Schlaf und Gedächtnisbildung. 81. Kongress der Deutschen Gesellschaft für Neurologie. Hamburg, 10th-13th of September 2008

Bergmann TO (2007) Funktionelle Bildgebung schlafbedingter Gedächtniskonsolidierung. 10. Jahrestagung der Sektion Sportmotorik der Deutschen Vereinigung für Sportwissenschaft. Giessen, 25th-27th of January 2007

Bergmann TO (2006) False Memories - Können wir unserem Gedächtnis trauen?. 6. MIND AKADEMIE "Jenseits des Verstandes" des MinD Hochschul Netzwerkes. Marburg, 6th-8th of Oktober 2006

9 Statement of Originality

English version

I hereby declare that this thesis is my own work and information derived from the literature or unpublished work of others has been acknowledged in the text and a list of references provided. This thesis has not been submitted in any form for another degree at any university.

Deutsche Fassung

Hiermit erkläre ich, dass ich die vorliegende Dissertation selbständig angefertigt habe und keine anderen als die angegebenen Quellen und Hilfsmittel von mir eingesetzt worden sind. Des weiteren versichere ich, dass die vorliegende Dissertation weder ganz noch zum Teil bei einer anderen Stelle im Rahmen eines Prüfungsverfahrens vorgelegen hat.

Kiel, den 04.02.2010

_____

Til Ole Bergmann

10 Appendix

The appendix entails the following research papers (*used with permission*):

I. Siebner, H. R., **Bergmann, T. O.**, Bestmann, S., Massimini, M., Johansen-Berg, H., Mochizuki, H., Bohning, D. E., Boorman, E. D., Groppa, S., Miniussi, C., Pascual-Leone, A., Huber, R., Taylor, P. C., Ilmoniemi, R. J., De Gennaro, L., Strafella, A. P., Kähkönen, S., Klöppel, S., Frisoni, G. B., George, M. S., Hallett, M., Brandt, S. A., Rushworth, M. F., Ziemann, U., Rothwell, J. C., Ward, N., Cohen, L. G., Baudewig, J., Paus, T., Ugawa, Y., Rossini, P. M. (2009). Consensus paper: Combining transcranial stimulation with neuroimaging. *Brain Stimulation*, 2(2), 58-80. http://www.sciencedirect.com/science/journal/1935861X

II. **Bergmann, T. O.,** Molle, M., Marshall, L., Kaya-Yildiz, L., Born, J., & Siebner, H. R. (2008). A local signature of LTP- and LTD-like plasticity in human NREM sleep. *European Journal of Neuroscience, 27*(9), 2241-2249. www.interscience.wiley.com

III. Mölle, M., **Bergmann, T. O.**, Marshall, L., & Born, J. (in prep). Slow and fast spindles grouped in opposite phase during slow sleep oscillations.

IV. **Bergmann, T. O.**, Mölle, M., Diedrichs, J., Born, J., & Siebner, H. R. (in prep). Sleep spindles drive learning-specific hippocampo-neocortical reactivation.

V. **Bergmann, T. O.**, Groppa, S., Seeger, M., Mölle, M., Marshall, L., & Siebner, H. R. (2009). Acute changes in motor cortical excitability during slow oscillatory and constant anodal transcranial direct current stimulation. *Journal of Neurophysiology*, 102(4): 2303-2311. http://jn.physiology.org/

VI. Groppa, S., **Bergmann, T. O.**, Siems, C., Mölle, M., Marshall, L., & Siebner, H. R. (2010). Slow-oscillatory transcranial DC stimulation can induce bidirectional shifts in motor cortical excitability in awake humans. *Neuroscience*, 166(4): 1219-1225. http://www.sciencedirect.com/science/journal/03064522

Paper I

Brain Stimulation (2009) 2, 182

ELSEVIER

BRAIN
STIMULATION

www.brainstimjrnl.com

Erratum

Erratum to 'Consensus paper: Combining trascranial stimulation with neuroimaging' [Brain Stimulation 2(2):58-80]

Hartwig R. Siebner Til O. Bergmann, Sven Bestmann, Marcello Massimini, Heidi Johansen-Berg, Hitoshi Mochizuki, Daryl E. Bohning, Erie D. Boorman, Sergiu Groppa, Carlo Miniussi, Alvaro Pascual-Leone, Reto Huber, Paul C.J. Taylor, Risto J. Ilmoniemi, Luigi De Gennaro, Antonio P. Strafella, Seppo Kähkönen, Stefan Klöppel, Giovanni B. Frisoni, Mark S. George, Mark Hallett, Stephan A. Brandt, Matthew F. Rushworth, Ulf Ziemann, John C. Rothwell, Nick Ward, Leonardo G. Cohen, Jürgen Baudewig, Tomáš Paus, Yoshikazu Ugawa, Paolo M. Rossini

The publisher regrets that some of the authors' degrees were listed incorrectly in the above mentioned paper. Please see corrected list below:

Hartwig R. Siebner, MD, Til O. Bergmann, MSc, Sven Bestmann, PhD, Marcello Massimini, MD, PhD, Heidi Johansen-Berg, PhD, Hitoshi Mochizuki, MD, PhD, Daryl E. Bohning, PhD, Erie D. Boorman, MSc, Sergiu Groppa, MD, Carlo Miniussi, PhD, Alvaro Pascual-Leone, MD, PhD, Reto Huber, PhD, Paul C.J. Taylor, PhD, Risto J. Ilmoniemi, PhD, Luigi De Gennaro, PhD, Antonio P. Strafella, MD, PhD, Seppo Kähkönen, MD, PhD, Stefan Klöppel, MD, Giovanni B. Frisoni, MD, Mark S. George, MD, Mark Hallett, MD, Stephan A. Brandt, MD, PhD, Matthew F. Rushworth, PhD, Ulf Ziemann, MD, John C. Rothwell, PhD, Nick Ward, MD, PhD, Leonardo G. Cohen, MD, Jürgen Baudewig, PhD, Tomáš Paus, MD, PhD, Yoshikazu Ugawa, MD, Paolo M. Rossini, MD

1935-861X/09/$ -see front matter
doi:10.1016/j.brs.2009.06.003

Brain Stimulation (2009) 2, 58–80

ELSEVIER

BRAIN
STIMULATION

www.brainstimjrnl.com

ORIGINAL RESEARCH

Consensus paper: Combining transcranial stimulation with neuroimaging

Hartwig R. Siebner, MD[a,b], Til O. Bergmann, MD[b], Sven Bestmann, MD[c,d], Marcello Massimini, MD[e], Heidi Johansen-Berg, MD[f,g], Hitoshi Mochizuki, MD[h], Daryl E. Bohning, MD[i,j], Erie D. Boorman, MD[f], Sergiu Groppa, MD[b], Carlo Miniussi, MD[k,l], Alvaro Pascual-Leone, MD[m], Reto Huber, MD[n], Paul C. J. Taylor, MD[o], Risto J. Ilmoniemi, MD[p,q], Luigi De Gennaro, MD[k,r], Antonio P. Strafella, MD[s], Seppo Kähkönen, MD[p,t], Stefan Klöppel, MD[u], Giovanni B. Frisoni, MD[v], Mark S. George, MD[i,w], Mark Hallett, MD[x], Stephan A. Brandt, MD[y], Matthew F. Rushworth, MD[z], Ulf Ziemann, MD[aa], John C. Rothwell, MD[c], Nick Ward, MD[c,d], Leonardo G. Cohen, MD[bb], Jürgen Baudewig, MD[cc], Tomáš Paus, MD[dd,ee], Yoshikazu Ugawa, MD[h], Paolo M. Rossini, MD[ff,gg,hh]

[a]*Danish Research Center for Magnetic Resonance, Copenhagen University Hospital-Hvidovre, Denmark*
[b]*Department of Neurology, Christian-Albrechts-University, Kiel, Germany*
[c]*Sobell Department of Motor Neuroscience and Movement Disorders, Institute of Neurology, Queen Square, London, UK*
[d]*Wellcome Trust Center for Neuroimaging, Institute of Neurology, University College, London, UK*
[e]*Department of Clinical Science, Faculty of Medicine, University of Milan, Italy*
[f]*Centre for Functional Magnetic Resonance Imaging of the Brain, University of Oxford, Oxford, UK*
[g]*Department of Clinical Neurology, University of Oxford, Oxford, UK*
[h]*Department of Neurology, School of Medicine, Fukushima Medical University, Fukushima, Japan*
[i]*Center for Advanced Imaging Research, Medical University of South Carolina, Charleston, South Carolina*
[j]*Department of Radiology, Medical University of South Carolina, Charleston, South Carolina*
[k]*IRCCS S. Giovanni di Dio Fatebenefratelli, Brescia, Italy*
[l]*Department of Biomedical Sciences and Biotechnology, National Institute of Neuroscience, University of Brescia, Brescia, Italy*
[m]*Department of Neurology, Berenson-Allen Center for Noninvasive Brain Stimulation, Beth Israel Deaconess Medical Center and Harvard Medical School, Boston, Massachusetts*
[n]*University Children's Hospital, Zurich, Switzerland*
[o]*The Henry Wellcome Building, School of Psychology, Birkbeck College, Torrington Square, London, UK*

Correspondence: Dr. Hartwig R. Siebner, Danish Research Center for Magnetic Resonance, Copenhagen University Hospital-Hvidovre, Kettegaards Alle 30, 2650 Hvidovre, Denmark.
E-mail address: hartwig.siebner@drcmr.dk
Submitted October 21, 2008. Accepted for publication November 30, 2008.

1935-861X/09/$ -see front matter
doi:10.1016/j.brs.2008.11.002

[p]BioMag Laboratory, Helsinki University Central Hospital, Helsinki, Finland
[q]Department of Biomedical Engineering and Computational Science, Helsinki University of Technology, Helsinki, Finland
[r]Department of Psychology, University of Rome ''La Sapienza,'' Rome, Italy
[s]Movement Disorders Center, Toronto Western Hospital, Division of Neurology, University of Toronto, Ontario, Canada
[t]Pain Clinic, Helsinki University Central Hospital, Helsinki, Finland
[u]Department of Psychiatry and Psychotherapy, Freiburg Brain Imaging, University Clinic Freiburg, Freiburg, Germany
[v]The National Centre for Alzheimer's and Mental Diseases, Brescia, Italy
[w]Brain Stimulation Laboratory, Medical University of South Carolina, Charleston, South Carolina
[x]Human Motor Control Section, NINDS, NIH, Bethesda, Maryland
[y]Department of Neurology, Berlin NeuroImaging Center, Charité, Berlin, Germany
[z]Department of Experimental Psychology, University of Oxford, Oxford, UK
[aa]Department of Neurology, Goethe-University Frankfurt, Germany
[bb]Human Cortical Physiology and Stroke Neurorehabilitation Section, National Institute of Health, National Institute of Neurological Disorders and Stroke, Bethesda, Maryland
[cc]MR-Research in Neurology and Psychiatry, Medical Faculty, Georg-August University, Goettingen, Germany
[dd]Brain and Body Centre, University of Nottingham, Nottingham, UK
[ee]Montreal Neurological Institute, McGill University, Montreal, Quebec, Canada
[ff]Casa di Cura S. Raffaele Cassino and IRCCS S. Raffaele Pisana, Roma, Italy
[gg]AFaR, Department of Neuroscience, Hosp. Fatebenefratelli, Isola Tiberina, Rome, Italy
[hh]Neurology Clinic, University Campus Biomedico, Rome, Italy

In the last decade, combined transcranial magnetic stimulation (TMS)-neuroimaging studies have greatly stimulated research in the field of TMS and neuroimaging. Here, we review how TMS can be combined with various neuroimaging techniques to investigate human brain function. When applied during neuroimaging (online approach), TMS can be used to test how focal cortex stimulation acutely modifies the activity and connectivity in the stimulated neuronal circuits. TMS and neuroimaging can also be separated in time (offline approach). A conditioning session of repetitive TMS (rTMS) may be used to induce rapid reorganization in functional brain networks. The temporospatial patterns of TMS-induced reorganization can be subsequently mapped by using neuroimaging methods. Alternatively, neuroimaging may be performed first to localize brain areas that are involved in a given task. The temporospatial information obtained by neuroimaging can be used to define the optimal site and time point of stimulation in a subsequent experiment in which TMS is used to probe the functional contribution of the stimulated area to a specific task. In this review, we first address some general methodologic issues that need to be taken into account when using TMS in the context of neuroimaging. We then discuss the use of specific brain mapping techniques in conjunction with TMS. We emphasize that the various neuroimaging techniques offer complementary information and have different methodologic strengths and weaknesses.

Keywords transcranial magnetic stimulation; TMS; neuroimaging; multimodal brain mapping; EEG; fMRI; MRI; PET; NIRS; MEG

Transcranial magnetic stimulation (TMS) is an important method for noninvasive stimulation of the human cortex through the intact skull without producing significant discomfort.[1] TMS uses a rapidly changing magnetic field to induce brief electric current pulses in the brain that can trigger action potentials in cortical neurons, especially in superficial parts of the cerebral cortex. In a clinical setting, TMS is mainly used to examine the functional integrity of the corticospinal motor projections.

Since its introduction in 1985,[1] the scientific applications of TMS have rapidly expanded. TMS has become a valuable tool to probe the excitability of intracortical circuits in the motor and visual cortex.[2] TMS produces a synchronized activation of cortical neurons, followed by a long-lasting inhibition. This explains why single pulses or short bursts of TMS can effectively perturb ongoing neuronal processing in the stimulated cortex. This transient disruptive effect of TMS, often referred to as "virtual lesion,"[3] has been extensively used by cognitive neuroscientists to examine the functional relevance of the stimulated area for behavior.[3-5] It should be noted, however, that the disruptive effect of TMS may not always adversely affect task performance. Under certain circumstances, the neurodisruptive effect of TMS may even result in a paradoxical improvement of behavior because of complex interactions at a systems level (eg, interhemispheric or intrahemispheric interactions).[6,7]

Dual-site TMS can induce coordinated stimulation of two interconnected cortical areas. Using a conditioning-test approach, dual-site TMS has been applied to assess cortico-cortical connectivity of pathways projecting onto the primary motor hand area.[8] When long continuous trains or short intermittent bursts are repeatedly applied to a cortical area, repetitive TMS (rTMS) can induce changes in neuronal excitability that persist beyond the time of stimulation.[9,10] These neuromodulatory effects of TMS have been exploited in many in vivo studies on cortical plasticity[11,12] and may be of some use in patients with neurologic and psychiatric diseases to maintain or restore brain function.[13]

Brain mapping benefits from transcranial stimulation

In the last 2 decades, advances in functional mapping techniques have revolutionized human brain research, providing a sensitive means of identifying brain regions where neuronal activity correlates with behavior. Although brain mapping can readily identify the spatial extent and the temporal profile of brain activation during an experimental task, the "correlative nature" of these techniques precludes conclusions about the causal importance of an activated brain area to task performance. In contrast to neuroimaging techniques, TMS is an interventional method that can be used to transiently and reversibly interfere with ongoing neuronal activity in the stimulated neuronal circuitries of the brain.[14] The "interventional nature" of TMS has added a new dimension to human brain mapping, opening up unique possibilities to probe causality at the systems level of sensory, cognitive, and motor brain networks.[8] For instance, when TMS is applied during an experimental task, its perturbative effects can be used to make causal inferences regarding the functional contribution of the stimulated cortex to a specific brain function.[4] In addition, the high temporal resolution of single-pulse TMS can be exploited to identify critical periods during which the stimulated area and its connections to other brain regions make a critical contribution to the experimental task (often referred to as chronometry).[3] Hence, the combined TMS-neuroimaging approach is capable of tracing the temporospatial dynamics of causal interactions within functional brain networks.

TMS can also be used to activate and study mechanisms of acute cortical reorganization in the healthy human brain. This is achieved by applying periods of rTMS over a target area to produce effects on cortical circuits that outlast the duration of the rTMS session. The functional after effects that can be elicited with rTMS depend on the variables of stimulation such as intensity, frequency, and total number of stimuli and the functional state of the cortex targeted by rTMS. These neuromodulatory effects have great potential for studies on adaptive neuroplasticity in the human brain.[12] Critically, the conditioning effects of rTMS are not limited to the stimulated cortex, but focal rTMS gives rise to functional changes in interconnected cortical areas as well.[12] Functional brain mapping techniques offer a wide range of methods to map the temporospatial patterns of local and distal reorganizational changes in brain function. As such, neuroimaging offers a valuable means of exploring how rTMS impacts on the human brain, providing new insights into the changeability of functional brain networks.[15-17]

Transcranial stimulation benefits from brain mapping

It is worth bearing in mind that TMS represents a nonphysiologic means of producing neuronal activity in the human brain. A key question is how this nonphysiologic mode of brain stimulation interacts with the intrinsic neuronal activity in the human brain. Motor evoked potentials (MEPs) or TMS-induced percepts (eg, phosphenes) have been used to explore how TMS excites the human cortex. Most of the knowledge about the physiologic mechanisms of actions has been gathered with TMS of the primary motor hand area (M1-HAND) in studies that recorded MEPs elicited by single or paired transcranial stimuli in a contralateral hand muscle. Other studies examined the behavioral consequences of TMS in well-defined experimental tasks. Although these studies can highlight the functional involvement of cortical areas in perception, cognition, and motor control, they provide no clues regarding the physiologic mechanisms that cause or prevent a TMS-evoked change in behavior. The limited insights into the mechanisms of action revealed by MEP recordings or behavioral testing motivated the use of neuroimaging techniques to map the acute and conditioning effects of TMS on brain function.

General considerations

The timing of TMS relative to neuroimaging

The timing of TMS in relation to neuroimaging defines which questions can be tackled using a combined TMS-neuroimaging approach (Figure 1). In principle, TMS can be applied while neuroimaging is being performed (referred to as "online" TMS-neuroimaging approach). Online neuroimaging experiments are technically demanding because TMS may adversely affect data acquisition during neuroimaging. This requires methodologic refinements to effectively avoid or control for TMS induced artifacts, especially when combining TMS with electroencephalography (EEG) or functional magnetic resonance imaging (fMRI).

Alternatively, TMS may be applied "offline" before or after neuroimaging. This "offline" TMS-neuroimaging approach is technically easier to establish because rTMS and neuroimaging are separated in time. TMS and

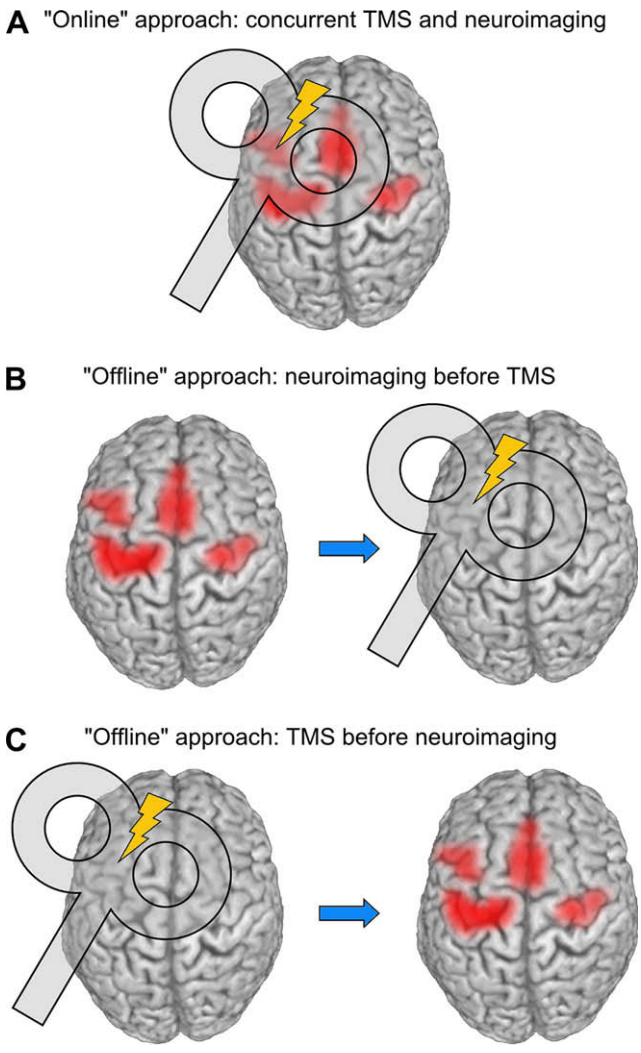

Figure 1 The "online" TMS-neuroimaging approach applies TMS while brain mapping is being performed **(A).** The "offline" TMS-neuroimaging approach separates TMS from neuroimaging in (space and) time: neuroimaging may be performed before TMS is applied **(B)** or neuroimaging is performed after the brain has been conditioned with TMS **(C).** TMS = transcranial magnetic stimulation.

neuroimaging can also be separated in space. For instance, TMS can be applied outside the MRI suite when conducting an offline rTMS-fMRI study. In practice, no specific methodologic precautions are necessary when offline TMS is combined with any of the available neuroimaging techniques. (Refer to Table 1 for terminology and definition of the various TMS-neuroimaging approaches to which we refer in this consensus paper.)

Online approach: Neuroimaging during TMS

TMS may be performed during neuroimaging (ie, online TMS). In this case, neuroimaging provides a temporospatial assay of the immediate effects of TMS on neuronal activity ("perturb-and-measure" approach; Table 1). If the experiment systematically varies the functional state of the brain at the time of stimulation, concurrent TMS-neuroimaging can probe how the "neuronal context" at the time of stimulation determines the induced activity changes locally as well as in connected brain areas (also shown by transcranial electric stimulation[18,19]).

The interpretation of online neuroimaging studies is complicated by the fact that TMS results in multimodal sensory stimulation. In addition to the "direct" cortical effects induced by the time-varying magnetic field, TMS has multiple "indirect" effects on brain activity.[20] TMS elicits auditory and somatosensory sensations (eg, activation of the cochlea, trigeminal activation). The TMS-associated sensory stimulation may produce a startle response or be perceived as unpleasant. All of these effects largely depend on the site and intensity of the stimulation being delivered. These indirect effects related to the multisensory nature of TMS need to be considered and controlled for. Furthermore, experiments and subsequent analysis must be carefully designed and executed, taking into account these potential confounds.[20] This includes

Table 1 Terminology and definition of TMS-neuroimaging approaches

Online TMS-neuroimaging	Concurrent application of TMS and neuroimaging
"perturb-and-measure"	Neuroimaging during application of single-pulse or burst-rTMS to measure the immediate and transient neuronal responses caused by TMS perturbation.*
Offline TMS-neuroimaging	Consecutive application of TMS and neuroimaging
"map-and-perturb"	Neuroimaging before TMS to map the brain regions/networks involved in a given task to identify target sites for subsequent (1) conditioning with rTMS to alter* neuronal processing in a subsequent behavioural task or (2) single-pulse or burst-rTMS applied during a behavioural task to transiently perturb* neuronal processing (so-called "virtual lesion") within specific time windows
"condition-and-map"	Neuroimaging after conditioning with rTMS to map brain areas/networks that show persistently altered* activity during subsequent (1) resting-state (eg, due to metabolic changes) or (2) task performance (eg, due to rapid reorganisation)

TMS = transcranial magnetic stimulation; rTMS = repetitive TMS.
*Principally, despite the acute perturbation of neuronal processing, rTMS as well as single-pulse or burst-rTMS can both inhibit and facilitate task performance on a behavioral level, critically depending on target area, timing of stimulation and the nature of the task.

possible interactions among brain areas activated by the direct effects of TMS on brain activity and indirect (cross-modal) effects on brain activity associated with the multisensory nature of TMS.

Offline approach: Neuroimaging before TMS

Neuroimaging may be performed before a TMS experiment to reveal the temporal (eg, with EEG) or spatial (eg, with fMRI) brain activation pattern during the performance of an experimental task. The temporospatial information of regional task-related activity can then be used to define the optimal time window during which TMS should be applied during a task and to guide the placement of the coil over the cortical target side. This a priori knowledge is of particular value when designing experiments in which TMS is used to interfere with task performance.

This "map-and-perturb" approach (Table 1) can be used to make causal interferences about the contribution of a cortical area or its interconnected network to a distinct brain function. Although functional brain mapping techniques can reliably identify networks that are activated during an experimental task, the correlational nature of neuroimaging precludes any inference about the causal importance of a regional brain activation for behavior. This question can be addressed using TMS. TMS can be applied over the area of interest to disrupt regular neuronal processing while participants perform the same experimental task. If TMS modulates task performance, it can be concluded that the stimulated cortical area or its closely interconnected areas make a relevant contribution to the task.

An early demonstration of this approach was given by Cohen et al[21] in a TMS study on blind subjects. Previous neuroimaging studies had shown that Braille reading consistently activated visual cortical areas in blind subjects but not in those with sight. To investigate the significance of task-related activation in the occipital cortex, short trains of 10-Hz rTMS were applied over several brain regions time-locked to Braille reading. Occipital rTMS induced errors and distorted the tactile perceptions of congenitally blind subjects but had no effects on tactile performance in the normal sighted. This finding proved that the occipital visual cortex makes a relevant contribution to the processing of tactile input in blind subjects.

In addition, neuroimaging is of great value to localize functionally the optimal site for TMS in individual subjects. One possibility is to let subjects perform the experimental task during fMRI and use the regional peak activation to define the target for subsequent TMS.[22] Individual peak activations can then be superimposed on the structural image of the subject's brain and inform frameless stereotaxy where to position the coil over the cortical region that is to be targeted with TMS. An alternative strategy is to base the coil placement on the group result revealed by a functional neuroimaging study that had used the same or a similar experimental task. The stereotactic coordinates of task-related peak activation in the area of interest defines the site of stimulation. This voxel is marked in the normalized structural MRI of each subject who participates in the TMS experiment. The individual site of stimulation can then be derived from the normalized MRIs by reversing the normalization procedure.

Offline approach: Neuroimaging after TMS

Neuroimaging techniques have a great potential to map temporospatial patterns of functional reorganization that are induced in the human brain by rTMS.[12] This scenario requires that neuroimaging needs to be performed after a conditioning session of rTMS. This "condition-and-map" approach (Table 1) probes the changeability of functional brain networks. Among other possibilities, neuroimaging after rTMS conditioning can map the lasting functional impact of rTMS on task-related neuronal activity at a systems level.[16,17] Neuroimaging should start as quickly as possible after rTMS to ensure that short-lasting after-effects of rTMS are captured. The task specificity of functional reorganization can be shown by having participants perform an additional control task during the same fMRI session.

One way of detecting the conditioning effects of rTMS on regional neuronal activity is to compare task-related activation before and after rTMS. However, any change in activation may simply be a time effect caused by the fact that the experimental task has been repeatedly performed in the MRI scanner. To dissociate temporal order effects from "real" effects that are causally related to rTMS, the experimental design should include a control session in which subjects perform the same experimental task but without effective rTMS. The order of the "real rTMS" session and control session should be counterbalanced across subjects, or within the same subjects on different days. In the control session, sham rTMS might be applied to the cortical target area. Ideally, sham rTMS should be matched to real rTMS in terms of auditory and somatosensory stimulation but without effective transcranial stimulation of the cortex. A specific change in the pattern of task-related activation after real but not after sham rTMS would indicate a true reorganisation in response to rTMS conditioning.

Temporal and spatial resolution

The temporal and spatial resolution of neuroimaging techniques represents important selection criteria when planning a combined TMS-neuroimaging study (Figure 2). If temporal aspects of neuronal processing are the main focus, the use of a neuroimaging method with a high temporal resolution such as EEG will be preferable. Conversely, a neuroimaging method with good spatial resolution and whole brain coverage such as fMRI will be appropriate if the goal of the experiment is to test the spatial pattern of TMS-induced changes in brain activity.

It is also worthwhile to consider the temporal and spatial resolution of TMS in the context of neuroimaging. The spatial resolution and penetration depth of TMS are limited. When using a figure-8 shaped coil, the maximum electric field induced in the brain lies in the junction region with the area of effective stimulation being several square centimeters. The volume of tissue stimulated by any TMS coil depends on many factors, including the geometry of the coil, stimulus configuration, stimulus intensity, and the electrical properties of the stimulated cortex. Another important feature of TMS is that the induced electric field decreases very rapidly with distance from the TMS coil. Hence, TMS induces stronger electric currents in superficial regions than in deeper structures. This explains why superficial cortical areas are relatively easy to stimulate, whereas those cortical areas that are located far from the scalp surface are much harder to stimulate. The attenuation of the induced electric field with the distance from the coil also explains why deep brain structures such as the thalamus and basal ganglia cannot be directly stimulated with conventional TMS coils. However, it is important to emphasize that TMS can effectively activate neuronal outputs that project from the stimulated site to other distant areas of the brain. This means that TMS can modify

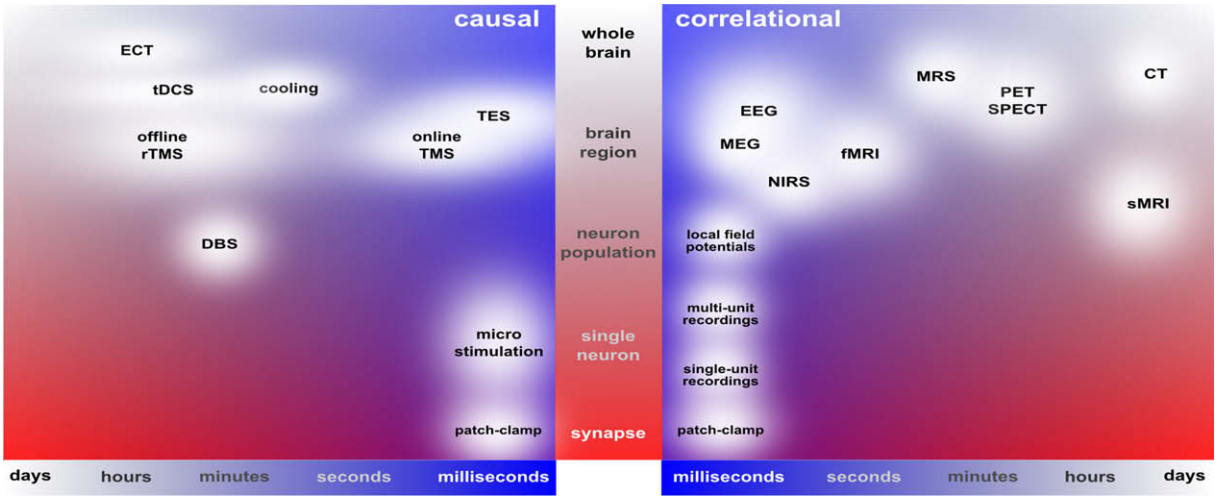

Figure 2 Different temporal and spatial scales: Neurostimulation and neuroimaging techniques are arranged according to their temporal and spatial resolution.

ongoing neuronal activity within complex neuronal circuits, and not just those at the site of stimulation.

The temporal resolution of TMS depends on how TMS is applied (Figure 2). A single TMS stimulus will induce an electric current in the brain lasting less than 1 millisecond. The electric current in the brain tissue causes a synchronized high frequency burst of discharge in a relatively large population of neurones that is terminated by a long-lasting GABA-ergic inhibition. This TMS-induced change in neuronal activity can last for several hundred milliseconds depending on the intensity of TMS. If short bursts of high-frequency ($\geq$ 5 Hz) TMS are applied, the influence of TMS on neuronal activity can be prolonged, lowering the temporal resolution of TMS. Finally, TMS protocols that apply prolonged trains of TMS can induce changes in neuronal excitability that may last for more than 1 hour after the end of TMS.[9,12] These persisting offline effects on brain activity that can be observed after rTMS conditioning are likely to differ substantially from the acute neuronal excitation that is directly induced by the time-varying magnetic field. The bottom line is that the spatial and temporal resolution of both the neuroimaging method and the TMS protocol, have a substantial impact on the scientific questions that can be tackled with the combined TMS-neuroimaging approach.

Electroencephalography and magnetoencephalography

Basic methodology

EEG is the most commonly used noninvasive recording technique of electric brain activity in humans. By using surface electrodes, the EEG measures voltage changes on the scalp that reflect ion flow caused by excitatory and inhibitory postsynaptic potentials. The scalp EEG is most sensitive to postsynaptic currents of neuronal populations whose dendrites are oriented radially to the scalp (located in the gyri), whereas currents tangential to the scalp (located in the sulci) do produce weaker EEG signals.

Nonradial (tangential or tilted) electric currents, however, are the main source for the magnetic fields that are picked up by magnetoencephalography (MEG), rendering MEG and EEG complementary techniques with otherwise similar temporal characteristics. By using multiple small detector coils, the MEG principally measures the magnetic fields produced by the synchronous postsynaptic currents of neuronal populations. The excellent temporal resolution of both methods lies on the millisecond scale. Spatial resolution, however, essentially depends on the number of recording sites. Although high-density EEG (hd-EEG) or MEG can achieve spatial accuracy close to a few millimeters, the spatial resolution of standard EEG recordings is in the range of several centimeters depending on the number of electrodes. As the small signals (microvolt and femtotesla for EEG and MEG, respectively) rapidly decay over distance, activity in deep brain structures may be difficult to locate with either method. In the case of EEG, there is additional spatial smoothing caused by the tissue compartments between the electrodes and the cortex (skin, muscles, skull, meninges).

EEG can be recorded using a variety of different electrode configurations, ranging from a few electrodes (readiness potentials, somatosensory-evoked potentials) to hd-EEG using 64 or up to 256 channels, depending on the purpose of the study. EEG recordings can reveal temporal and spatial information about externally triggered event-related (event-related potentials, ERPs) or spontaneous brain activity. The measurement of ERPs requires averaging of many short EEG sweeps that are time locked to an experimentally defined event to subtract "neural noise" from the evoked cortical response. Event-related cortical activity can be quantified by measuring latencies and amplitudes of distinct ERP components. Spontaneous EEG is usually recorded over long periods to assess states of vigilance or consciousness like wakefulness and sleep. It can demonstrate transient spontaneous activity like epileptic seizures or sleep spindles. EEG analysis of oscillatory activity is often restricted to distinct frequency bands that are linked to specific neuronal processes.

Technical and safety aspects

When the application of TMS and EEG/MEG acquisition are separated in time (offline approach), the combination of TMS and EEG/MEG is methodologically relatively unproblematic. In offline TMS-MEG studies, TMS should be given outside the MEG room. For combined TMS-EEG studies, the only point to consider is whether TMS should be applied with electrodes being attached to the scalp. The decision might depend on the experimental design as well as number and montage of electrodes. Standard electrodes increase the distance between the TMS coil and the cortex. Therefore, TMS with electrodes in place will require a higher intensity of stimulation to induce a stimulation effect that matches the effect induced by TMS without electrodes. However, extremely flat electrodes have become available to minimize this problem.

The simultaneous use of TMS and EEG/MEG is more problematic relative to the offline approach. Simultaneous use of TMS and MEG is impossible with present techniques because of the huge (15 orders of magnitude) difference between the magnetic field strengths relevant in MEG and TMS. MEG measures the weak time-varying magnetic fields generated by nonradial electric currents in the brain, whereas TMS induces a very strong time-varying electric field to produce a suprathreshold electric current in the cortex. In contrast, online TMS-EEG was first performed in 1997.[23] The main problem that one has to face when applying TMS during EEG is the powerful electric field that is induced by the discharge of the TMS coils in the electrode leads. Considering a typical pulse intensity of 1

Tesla and a rise time of 0.1 millisecond, the voltage induced in the electrodes underlying the stimulator can reach an amplitude of 10 volts. This voltage, being several orders of magnitude larger than the signal produced by the brain, can cause large artifacts in the recordings and may put an ordinary EEG amplifier out of the operating range for a few seconds. In fact, high-quality EEG recording during TMS can only be obtained with specifically designed amplifiers. Up to now, a few different technical solutions have been implemented. Virtanen et al[24] developed a 60-channel TMS-compatible EEG system that includes gain-control and sample-and-hold circuits to block the artifact induced by TMS in the leads. This system pins the acquired signal to a constant level for a couple of milliseconds around the pulse and records TMS-evoked EEG potentials (TEPs) that are completely free from artifacts. An alternative way to deal with the TMS artifact has been implemented by Thut et al.[25] They use a slew-limited amplifier that prevents the electronics from saturating during the TMS pulse resulting in a short-lasting artifact that decays within 30 milliseconds. Finally, Bonato et al[26] have recently used an MRI-compatible DC amplifier with a wide dynamic range to successfully record TEPs preceded by a short artifact (10-20 milliseconds). With this method, recordings have to be obtained without any filtering, as these might interact with the TMS artifact, producing ripples for up to a second. However, filtering can be applied after removing artifacts from the data.[27]

Beside the artifact induced by discharging the transducing coil, additional high-amplitude artifacts lasting several tens of milliseconds are caused by recharging the capacitors of the stimulating device immediately after the stimulation. A possible workaround is to introduce a delay between discharge and the onset of recharging.

Even with an optimal amplifier, TEPs of sufficient quality can only be recorded at the stimulated site if additional measures are taken. During the application of the TMS pulse, some current can pass through the electrode-electrolyte interface, thereby causing a polarization and, possibly, an EEG baseline shift that can last for hundreds of milliseconds.[24] In addition, especially when large traditional electrodes are used, the induced currents can interact with the magnetic field, causing a force and thus movement of the electrodes. Finally, overheating of the EEG electrodes may occur, particularly when long trains of pulses are delivered.[28] All these problems can be effectively addressed using special electrodes, such as ring electrodes with a slit,[2] small Ag/AgCl pellet electrodes, or plastic sensors covered by silver epoxy.[29] In addition, these problems of drift, motion, and heating are only evident at electrode sites immediately underneath the stimulating coil.[24] In all cases, it is strongly recommended to work carefully on the electrode-to-scalp contact to minimize impedances as much as possible. Gently scraping the skin with an abrasive paste before applying the conductive gel normally results in a suitable impedance level (< 5 kOhm). Recently, minipuncturing of the epithelium under the electrode contacts has been suggested to reduce skin resistance and thereby TMS artifact size even further.[30] Electrode leads should be kept relatively fixed and free of loops. Avoidance of physical contact between TMS coil and electrodes (eg, by foam) can reduce some mechanical artifacts induced by coil vibrations.[27] However, this will increase the coil-to-cortex distance and thus, adversely affect the efficacy of TMS.[27]

If the TMS coil is positioned over scalp and facial nerves or muscles, these may be activated, resulting in a large biologic muscle artifact lasting for tens of milliseconds. Unless new strategies, such as optimal pulse shapes or shielding devices, are developed to minimize scalp muscle activation, this kind of artifact can not be eliminated. For now, the problem can be avoided only by moving the coil to a more favorable location (more central scalp regions), or orientation, and/or by reducing the strength of stimulation. The coil's discharge is associated with a loud click (up to 130 dB), which might trigger a blink reflex and thereby eye movement artifacts in the EEG. More importantly, this noise obviously evokes an undesired auditory response that overlaps with TEPs.[31] This major confound can be effectively eliminated by using earplugs and additionally masking the coil's click with white noise, or with a sound that has an optimal spectral content.[32] By stimulating sensory nerve fibers of the cranial nerves, TMS may also trigger somatosensory evoked potentials. However, their contribution to the overall activation appears to be negligible.[26,33] As for behavioral TMS studies, the stimulation of control sites or the use of a proper sham stimulation can be helpful to disentangle the contribution of the different sources.[27]

Although coil placement by means of MRI-guided frameless stereotactical neuronavigation has already become state of the art, it is of superior importance in combined TMS-EEG studies. Small shifts in coil orientation can cause marked changes in TEPs. Here neuronavigation is able to provide a high degree of reproducibility, even across separate sessions.[34] Some commercially available navigation systems even provide an estimation of location and strength of the maximum electric field induced in the cortex based on realistic head models.[35] Future navigation system might also incorporate information about the orientation of axons in the stimulated area.[36]

Neuroscientific and clinical applications

As pointed out above, the simultaneous use (online) is only possible when TMS is combined with EEG (but not with MEG), whereas TMS-MEG as well as TMS-EEG both can be combined consecutively (offline). Furthermore, the majority of published articles in the field have combined TMS with EEG rather than with MEG. Therefore, we will mainly focus on the combination of TMS and EEG in this review.

The offline TMS-EEG approach can be applied in both directions. When using EEG (or MEG) before TMS, the spatial distribution of cortical activity (eg, ERPs) in multichannel EEG can inform the experimenter where to place the TMS coil. More importantly, the excellent temporal resolution of EEG (and MEG) offers the possibility to optimize the timing of TMS based on the temporal signature of task-related EEG activity of each subject. This may help to determine the optimal time window for the induction of disruptive TMS effects in a subsequent behavioral TMS experiment.

Likewise, recordings of ERPs or spontaneous EEG can be used to study the lasting impact of rTMS on cortical processing. For instance, multichannel EEG recordings during sleep demonstrated changes in sleep associated oscillatory activity patterns (ie, slow oscillations and sleep spindles) in response to 5Hz rTMS of the dorsal premotor cortex[37] or paired associative stimulation of the M1-HAND.[38-40] Moreover, using a correlative approach, altered EEG theta power after 40 hours of prolonged wakefulness could be related to changed motor cortical excitability as determined by paired-pulse TMS measurements.[41]

The online TMS-EEG approach offers several additional possibilities. First, the EEG activity just before a TMS stimulus is applied contains information about the functional state of the stimulated cortex at the time of TMS. This information may be used to study the state dependency of the brain's responsiveness to TMS. The regional expression of spontaneous oscillatory activity directly preceding a TMS pulse may be predictive of the brain response to TMS. This has been shown for the expression of occipital alpha activity and the capability to evoke phosphenes with occipital TMS.[42] Second, online EEG recordings have revealed TMS induced changes in the frequency domain. For instance, a single TMS pulse can transiently synchronize activity in the beta range.[43] Furthermore, trains of 1-Hz and 5-Hz rTMS are associated with concurrent changes in cortical alpha and beta activity.[44,45] Third, functional connectivity between cortical areas in a given task can be investigated by probing the effect of TMS over one cortical site on the ERPs evoked in another area. This approach has been used to study the role of the frontal eye fields in controlling visual processing in posterior visual brain areas during the orienting of spatial attention[46] and the influence of the dorsal medial frontal cortex on lateralized action potentials in primary motor cortices during conflict resolution in an action selection task.[47] Application of TMS to the posterior parietal cortex during a visual search task also modulated the occipital N2pc component that is evoked by target detection.[48]

Finally, recording the TEPs provide a means of directly studying the excitability and response characteristics of practically any cortical area that is accessible to TMS. Beforehand, this was possible only by using indirect measures such as MEPs in the primary motor cortex or phosphenes in visual areas. A single TMS-pulse evokes a cortical potential waveform in the EEG, which strongly differs in polarity and amplitude of its peak components depending on several factors such as position and orientation of the TMS coil, stimulation intensity, electrode position, and reference. However, suprathreshold stimulation (biphasic pulse configuration) of the motor hand area with a coil orientation eliciting a posterolateral-to-anteriomedial current in the brain reliably evokes a response at the vertex (referenced to linked mastoids) with the following components: N10, P14, N15/18, P30*, N40/45*, P55/60, N100*, P180/190, and N280 (* indicates the most reliable ones).[26,43,49] As an alternative to peak analysis, especially for hd-EEG recordings, the calculation of *global mean field power* (GMFP)[50] has been introduced as a reference-free measure of local EEG variability. As the number of neurons recruited by a single TMS-pulse is directly related to their excitability, GMFP amplitude change has been proposed as a measure of cortical excitability, which is sensitive to TMS-induced changes in cortical plasticity.[37,38,51] Moreover, in combination with source localization, the temporospatial propagation of TMS-evoked cortical activity can be traced[32,52,53] to gain insight into the temporospatial dynamics of the corticocortical connectivity patterns that are activated by TMS. The online TMS-EEG approach can directly probe regional cortical excitability and corticocortical connectivity in humans. During a typical TMS-EEG session it is possible to (1) measure the strength of its immediate response in the cortical target area of interest,[54] (2) detect the temporospatial dynamics of the ensuing spread of activation,[23,32] (3) calculate corticocortical conduction times,[33] and (4) quantify complex dynamics such as phase locking or power modulation of EEG rhythms.[43-45,55]

Excitability and connectivity are essential properties of the nervous system and are abnormal in many neurologic and psychiatric disorders. They also can be altered by agents affecting brain function such as alcohol.[56,57] As TMS-EEG stimulates and records from the cerebral cortex, by-passing sensory pathways, subcortical structures, and motor pathways, the measurement does not depend on the integrity and status of sensory and motor systems and can be applied to any subject (deafferentiated, paralyzed, unconscious). Future clinical applications of TMS-EEG may therefore include: (1) measuring the excitability and the connectivity of frontal circuits in schizophrenia[58] and depressed patients, (2) measuring corticocortical conduction times in multiple sclerosis and neurodegenerative disorders, (3) monitoring the excitability of the lesioned and the contralateral homologous cortex after stroke, and (4) assessing the state of thalamocortical circuits in patients with impaired consciousness that are unable to communicate. More generally, TMS-EEG can be used to prospectively track and monitor the excitability and connectivity changes occurring in any cortical region during rehabilitation, pharmacologic therapy, TMS treatment, or spontaneous recovery.

Conclusion/Summary

The main advantage of EEG, compared with other TMS-imaging approaches, is its millisecond-scale temporal resolution, which allows one to measure the immediate cortical response to TMS. TMS triggers a combination of fast excitatory and inhibitory events in the stimulated area[59] that may cancel each other if averaged over time. Indeed, although TEPs invariably detect a strong activation in the stimulated area, positron emission tomography (PET) and fMRI often fail to do so.[60,61] In addition, TMS-EEG conveys precise information about the temporal order of activations of distant cortical areas. Likewise, the technique can also reveal, in real-time, TMS-induced oscillations with obvious safety implications and possible practical applications.[52] Its high-temporal resolution renders the EEG method a perfect complement to the transient perturbations caused by TMS in the brain's oscillatory processing modes.

Other advantages of TEPs are their high signal-to-noise ratio and the fact that they can be easily collected at the patient bedside at a relatively low cost. The main disadvantage of TEPs is their low spatial resolution, which can partly be compensated for by increasing electrode density and by performing advanced source modeling, yet the combined TMS-EEG approach is of limited use to map TMS induced activations in deep brain structures. Another limit is its susceptibility to artifacts, such as muscle interference and eye blinks, currently preventing the collection of clean TEPs when temporal and orbitofrontal cortices are stimulated.

The combined TMS-EEG technique is still in its early age and much methodologic work is needed to fully unfold its potential. For example, the contribution of different artificial and noncortical biologic sources to the TEP has yet to be disentangled to allow a fully comprehensive interpretation. Especially the very immediate cortical response to TMS within the first 10 or 20 milliseconds after TMS is still not fully accessible. Further research has to characterize the reproducibility of TEPs and gain normative data as well as knowledge about their changes in health and disease.

Functional MRI

Basic methodology

Among the neuroimaging techniques, the elegance of fMRI lies in its ability to measure the metabolic consequences of neural activity through changes in endogenous oxy- and deoxyhemoglobin concentration. Deoxyhemoglobin is paramagnetic and causes local magnetic field inhomogeneities that reduce the measured MR signal. Consequently, increased deoxyhemoglobin leads to a decreased MRI signal intensity and therefore acts as an endogenous contrast agent. Because this so-called blood-oxygenation-level-dependent (BOLD) contrast is tightly coupled to cerebral blood flow, neuronal activity, and energy use, regional changes in brain activity can be inferred throughout the human brain, including subcortical structures (for a comprehensive overview, ref. [62]). Functional MRI can measure such activity changes with a spatial resolution of a few millimeters. Its temporal resolution is on the order of seconds because changes in blood flow are delayed and more prolonged with respect to the underlying neural responses. Yet the hemodynamic lag is highly constant. Therefore, by using the appropriate design, one can "decorrelate" events and differentiate neural population activity-changes to events only a few hundred milliseconds apart.[63,64] Standard fMRI experiments acquire a large series of brain volumes (images) while the subject performs a task. The ensuing MR signal time series in each volume element (voxel) is then correlated with the experimental manipulation. Consequently, over the past 2 decades, fMRI has been uniquely successful in investigating the functional neuroanatomy in health and disease.

Technical and safety aspects

The high magnetic field strength of modern MRI scanners (between 1.5-7 T) imposes several limitations and challenges for its simultaneous combination with TMS, which was first performed by Bohning et al.[60,65] One can distinguish two principle problems for combined TMS-fMRI: static and dynamic artifacts. The former arise through the mere presence of the TMS setup itself, whereas the latter are due to operating the TMS setup, such as applying TMS pulses during fMRI.

Static artifacts

For safety reasons, all ferromagnetic material must be removed from any equipment (eg, TMS coils) entering the MRI scanner.[60,66] At the same time, MRI-compatible TMS coils need to withstand the increased mechanical stress during MRI. However, the presence of the MRI-compatible TMS coil may still lead to geometric image distortions.[67,68] These can be reduced by a shorter read-out time of echo-planar imaging (EPI) sequences, using stronger imaging gradients and/or parallel imaging. Oversampling of EPI images in phase-encoding direction can shift so-called "ghosting" artifacts outside the central field of view without compromising image resolution and compromising temporal resolution only minimally. Other parts of the stimulator unit must be safely placed outside the scanner room or in a radiofrequency-shielded cabinet inside the scanner room, at sufficient distance from the magnetic fringe field of the MRI scanner. This requires an increase in TMS coil cable length that may bring about unwanted increases in serial inductance, diminished effective TMS coil output,

and increased power requirements. TMS coil movement can be minimized with MR-compatible TMS coil holders that allow safe and accurate placement of the coil inside the scanner. MR-compatible automatic and computer-operated TMS-coil holder and positioning systems provide additional accuracy and reproducible positioning,[69] but are technically more challenging to implement.

Dynamic artifacts

Radiofrequency (RF) noise can additionally affect the signal-to-noise ratio of MRIs, but this may vary widely between different TMS and scanner setups. TMS stimulators may directly generate RF noise (eg, around 64 MHz at 1.5 T), and the antenna-like properties of the TMS coil cable can additionally guide RF noise into the scanner. Customized RF filtering can suppress this noise. Additional image distortions and artifactual signal changes may occur through leakage currents that originate through the high-voltage capacitors of the TMS stimulator. These leakage currents can change with different charge levels (output level) of the TMS machine, and can potentially lead to signal changes that are in the same order as physiologic BOLD signal changes. Remote-controlled high-voltage relay-diode systems can reduce leakage currents flowing between the stimulator and the TMS coil by several orders of magnitude, thus permitting BOLD-sensitive imaging in the direct vicinity of the coil.[70,71] The strong magnetic pulses induced by TMS can furthermore distort MRIs. The size of such distortions depends on several factors, such as TMS coil orientation, TMS pulse intensity, and MRI magnetic field strength.[66,68] The problem can be alleviated by applying sufficient temporal gaps between TMS pulses and subsequent MRI acquisition.[72] Increasing distance between the imaged brain slice and the TMS coil[67,68] further alleviates the problem. Direct TMS pulse–EPI excitation pulse interference should be avoided, and images being perturbed by TMS pulses must be replaced. This can be achieved through interpolation between preceding and subsequent (unperturbed) MRIs.[70,72,73]

While interleaving TMS with fMRI is technically challenging, offline studies in which TMS is given before or after an fMRI session are easy to perform because TMS can be given outside the room where fMRI is performed.

Neuroscientific and clinical applications

Concurrent TMS-fMRI holds great promise to supplement our understanding about the immediate and rapid changes TMS can evoke in cortical networks.[74] One way is to use TMS-fMRI in a "perturb-and-measure" approach[75] that can inform about the activity changes evoked by TMS at a systems level, by characterizing TMS-evoked BOLD-signal changes throughout the brain at rest.[60,76-80] Here, TMS serves as a causal input into the operation of a cortical region, whereas fMRI measures distributed activity changes evoked by this input. This is of interest as one can in principle now reveal the spatial topography of TMS effects at high-spatial resolution, including retinotopic early visual cortex[81] and subcortical structures.[78,80] In the motor[60,76-80] and visual systems,[73,81] this has revealed that even short TMS pulse series (500 milliseconds-10 seconds) can activate putatively interconnected cortical and subcortical brain regions ipsilaterally and contralaterally to the stimulation site.

Furthermore, TMS-fMRI can disclose how such remote TMS-induced activity changes interact with psychologic factors such as task-state.[70] Increasing evidence suggests that the effects of TMS are dependent on the state of activation at the time of stimulation. Recently, Bestmann et al[70] could show that the effects of short trains of TMS (11 Hz, 5 pulses) applied to left dorsal premotor cortex (PMd) reversed during performance of a weak left-hand power grip, compared to rest (Figure 3). During rest, TMS applied at a suprathreshold intensity decreased contralateral primary motor cortex and PMd activity, compared with a low-subthreshold intensity. By contrast, stimulation at the suprathreshold intensity increased task-related activity in these regions during power grip, compared with low-intensity stimulation. This finding illustrates how concurrent TMS-fMRI can map out causal interactions among brain regions and their dependence on activation state.

Online fMRI has also been successfully established in conjunction with TES, in which a strong rapidly varying electric current rather than a time varying magnetic field is applied to stimulate cortical neurons.[18,19] Single suprathreshold electrical stimuli induced a positive BOLD response both in the ipsilateral as well as in the homotopic contralateral M1-HAND, with the latter presumably resulting from transcallosal connections. Accordingly, when a contralateral conditioning stimulus preceded the test stimulus by 10 milliseconds (interhemispheric inhibition), the subsequent ipsilateral BOLD signal was significantly reduced.[19] Thus, cortical inhibitory processes are accompanied by attenuation of the local neurovascular signal. TES during fMRI has the advantage that there are no spatial constraints when placing the stimulating electrodes. In contrast, placing a bulky TMS coil between the head and the MRI head coil is often problematic because of space limitations. A major drawback of combining TES with fMRI is that TES is more painful relative to TMS.

Concurrent TMS-fMRI has also been successfully applied to measure the distribution of activity changes during behavioral studies,[82] causal top-down influences between brain regions in the visual system,[73,81] sensory processing,[83] as well as the cortical signatures of an TMS-evoked sense of movement after upper limb amputation.[84] These findings suggest that attributing the behavioral consequences of TMS to the stimulation site often neglects remote activity changes induced by TMS and their contribution to possible behavioral consequences. Concurrent TMS-fMRI can reveal how these behavioral consequences

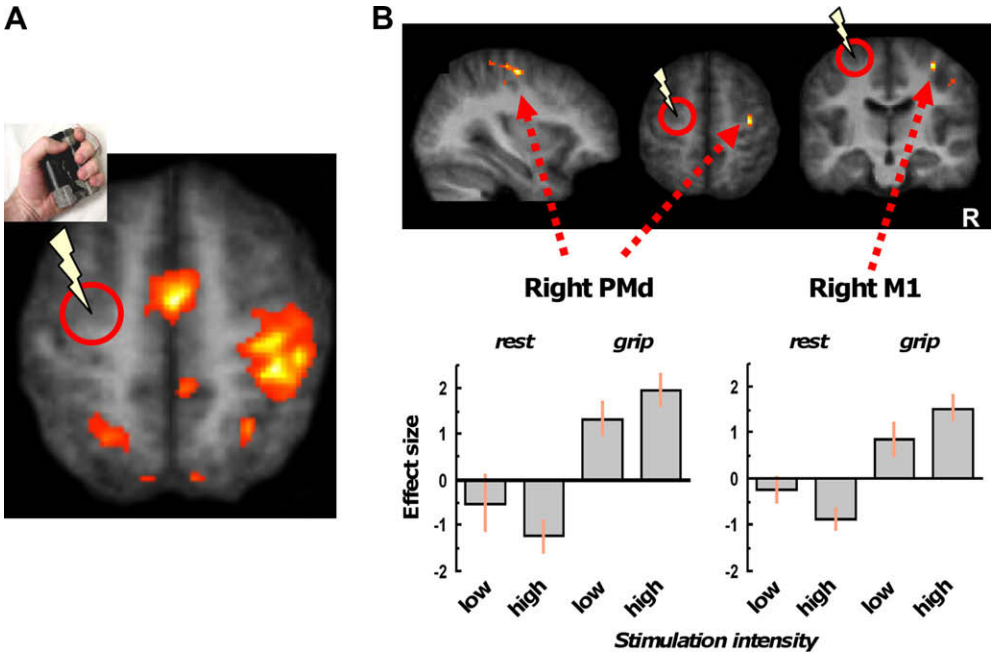

Figure 3 State-dependent interregional interactions evoked by transcranial magnetic stimulation (TMS) **(A)** Main effect of left hand grip, irrespective of TMS stimulation intensity. This illustrates how one can obtain blood-oxygenation-level-dependent (BOLD) activation maps during concurrent application of TMS pulses (5 pulses, 11 Hz) inside an magnetic resonance image (MRI) scanner. **(B)** Task-state dependent effects of TMS on causal interactions in the human motor system. At rest, TMS applied to the left dorsal premotor cortex (PMd) increased activity in contralateral PMd and primary motor cortex (M1) at high stimulation intensity (110% of resting motor threshold), compared with stimulation at a lower control intensity (70% active motor threshold). By contrast, this effect was reversed during a simple motor task that activated right PMd and M1. Now high-intensity stimulation increased task-related activity, compared with lower intensity stimulation. The results show how TMS can causally affect activity in contralateral regions, and that these influences are dependent on the activation state of these regions (adapted from Bestmann et al[70,72]).

emerge through concerted causal interplay among interconnected brain regions; alternatively, concurrent TMS-fMRI can show rapid compensatory activity changes that may prevent behavioral perturbation. Therefore, another exciting prospect of concurrent TMS-fMRI is to study the capacity of the brain to rapidly react to perturbations (caused by TMS), owing to the degeneracy in cognitive anatomy.[85]

In general, these approaches provide unique insight into the physiologic underpinnings of TMS, and the interregional layout of causal interactions. For clinical applications of TMS, this may be of critical importance because their effectiveness is commonly inferred indirectly through an improvement of clinical symptoms. It is often unknown, however, whether TMS actually targets and affects the brain regions implied in a specific clinical symptom. Li et al[86] have used concurrent TMS-fMRI in chronically depressed patients to investigate the brain regions affected by stimulation of left dorsolateral prefrontal cortex (DLPFC), a region often linked to major depression. Not only was 1-Hz TMS associated with increased activity at the site of stimulation, but also affected putatively interconnected regions including the bilateral middle PFC, right orbital frontal cortex, and insula. This study demonstrates that TMS to DLPFC can indeed affect entire brain networks associated with depression. Concurrent TMS-fMRI therefore holds promise to identify the brain regions targeted by clinical TMS applications, and thereby to increase their safety and effectiveness as well as point out novel strategies for TMS therapy. Li et al[86] have also shown how the interleaved TMS technique can be used to assess the modulatory effects of medications. Healthy subjects were scanned with interleaved TMS-fMRI over motor cortex while they were on or off lamotrigine, an anticonvulsant. Predictably, there was less TMS-induced motor cortex activation when subjects were on medication. Paradoxically, the exact opposite pattern occurred when these same subjects were stimulated over the PFC. There, the lamotrigine caused an increase in TMS-induced prefrontal activation.[87]

There is also a substantial potential for offline TMS-fMRI studies. First, fMRI can be used to guide the coil placement in a subsequent behavioral TMS experiment (fMRI-guided TMS).[22] Second, fMRI can map the functional consequences of a conditioning rTMS session on neuronal activity across the whole brain.[88,89] For instance, offline fMRI has been successfully applied to examine short-term reorganization in the right PMd after 1-Hz rTMS to the left PMd.[17] Although rTMS had no effect on behavior, fMRI revealed increased activity in the right

PMd and connected medial premotor areas during action selection but not simple action execution. Because subsequent online TMS of the reorganized right PMd impaired action selection, it was concluded that the functional reorganization as revealed by fMRI played a causal role in maintaining behavior after an rTMS induced interference with neuronal processing in the left PMd.

Conclusion/Summary

The future of TMS critically relies on identifying its mechanisms of action across the brain in more detail. One promising approach is the combination of TMS and BOLD fMRI. In measuring causal interactions throughout the brain in healthy humans, TMS-fMRI can therefore address questions that otherwise would be difficult to approach. In addition to BOLD sensitive MRI, several groups have started to combine TMS with other MR techniques such as MR spectroscopy[90,91] or arterial spin labeling,[92] which will reveal further valuable insights into the impact of TMS on brain function.

Structural MRI

Basic methodology

There are various MRI sequences that provide different insights into brain structure. Conventional structural imaging protocols include T1-weighted, T2-weighted, diffusion-weighted, and proton-density scans. These different protocols result in different tissue contrast, allowing particular anatomic or pathologic features to be visualized more easily. In the clinical setting, for example, T2-weighted images are particularly sensitive to inflammation, such as acute multiple sclerosis lesions; diffusion-weighted scans are most sensitive to very early pathologic changes following stroke; whereas T1-weighted images provide optimal contrast between grey and white matter and are therefore commonly used to provide fine anatomic detail. In a research setting, novel protocols have been developed to provide even richer anatomic information. For example, quantitative mapping of the relaxation contrasts, T1 and T2, can now be achieved over the whole brain at reasonable resolution in a feasible time. Such parameters are sensitive to pathologic factors and to anatomic microstructure. Extensions to conventional diffusion-weighted imaging (DWI) include acquisition of greater numbers of diffusion directions, which allows measurement of the directional dependence, or fractional anisotropy (FA), of the diffusion signal. This is a useful property to measure as FA reflects white matter integrity, and is therefore sensitive to changes in development, ageing, and disease. In addition, in white matter fiber bundles, the principal diffusion direction corresponds to the principal fiber direction and therefore, by following these directional estimates through white matter, it is possible to reconstruct the path of fiber bundles, to perform "diffusion tractography."

Technical and safety aspects

Given that structural imaging techniques, on the whole, provide static information, there is no particular reason for acquiring simultaneous TMS and structural MRI data (in contrast to the situation with fMRI, for example). Yet, as an MRI scanner can actually image the magnetic field created by a TMS coil, Bohning et al[93] demonstrated that one could acquire a phase map of the magnetic field distortions caused by running a constant current through a TMS coil. This TMS phase map, with appropriate scaling, can then directly image the magnetic field of the TMS coil over the subject's anatomy. However, in general, researchers have tended to relate TMS effects to structural data acquired separately. Therefore, there are no major technical challenges raised by combining these techniques.

Generic methodologic issues arise over acquisition, analysis, and interpretation of structural MRI data. Typical approaches to processing T1-weighted structural data include voxel-based and tensor-based morphometry (VBM[94] and TBM,[95] respectively) analyses. The VBM/TBM data processing includes segmentation of images into different tissue types (grey matter, white matter, cerebrospinal fluid), smoothing of resulting partial volume estimates, coregistration of images into standard space, and statistical comparison of voxel density values (VBM) or voxel displacement vectors (TBM) across subjects. Each step of this process raises issues. For example, the size of the smoothing kernel will greatly influence sensitivity to effects of different sizes. A number of groups are now also running VBM-style analyses of diffusion parameters, most commonly FA, which can be correlated with, for example, behavioral measures or the size of TMS effects.[96-99] Interpretation of FA correlates should vary depending on whether effects are seen in white matter or grey matter, and whether this localization is consistent across subjects after normalization. It is therefore important that regions of FA correlation are carefully localized in individual subjects, or that alternatives to VBM, such as tract-based spatial statistics,[100] or tractography-based definition of regions of interest, are used.

DWI can also be combined with TMS by using the anisotropic conductivity information to inform models of the current spread induced by a TMS pulse.[36]

Neuroscientific and clinical applications

The relationship between neuroanatomy and neurophysiology is a fundamental issue in neuroscience and is of clinical relevance. Caused in part by recent technologic advances in MRI, the neurosciences have seen an explosion of studies relating brain structure to function, where function is often assessed via behavior. Behavioral measures of function, however, reflect the aggregate operation of multiple brain regions. By contrast, TMS enables researchers to probe the physiology of a specific brain region, or functional

interactions between regions, both during resting and particular cognitive states. Such physiologic indices may provide more sensitive and informative measures with which to compare structural measures.

TMS-EMG measures of primary motor cortical excitability have been shown to correlate with gross conventional MRI volumetric measures, such as white matter hyperintensity volume and ventricular volume.[101] The majority of studies relating TMS to structural measures, however, have used measures derived from DWI. Recent work indicates that individual differences in cortical excitability and functional connectivity are associated with normal variation in white matter integrity in healthy adults. Primary motor cortical excitability, for example, was shown to correlate positively with FA in white matter underlying primary motor and premotor cortex, as well as parts of the corona radiata, internal capsule, cerebral peduncles, and corpus callosum (Figure 4A),[99] suggesting a substantial corticocortical contribution to motor threshold variation in healthy adults. Paired-pulse TMS, giving a measure of physiologic connectivity between stimulated cortical regions, has been recently used to interrogate the microstructural correlates of functional connectivity in healthy adults.[96-97] In one study, resting-state physiologic connectivity between hand regions of the left and right primary motor cortex was correlated positively with FA in hand callosal motor fibers identified with combined fMRI and diffusion tractography, but not adjacent foot fibers (Figure 4B), demonstrating an impressive degree of selectivity even within subregions of the same fiber bundle.[97] In the only study to date testing the importance of cognitive context to these relationships, functional connectivity from PMd to contralateral primary motor cortex, specifically during an action selection task, was positively correlated with FA in white matter underlying the premotor and primary motor cortex, the corpus callosum, and the superior longitudinal fascicles (Figure 4C).[96] Moreover, diffusion tractography from these regions of correlation reproduced the specific parietal-dorsal premotor-contralateral premotor-motor networks predicted to mediate the physiologic effects by previous fMRI findings.

The potential power of this approach is also evident in a clinical setting, where longer central motor conduction time to both the hands and legs has been associated with reduced FA in motor, premotor, and corticospinal tract white matter in patients with amyotrophic lateral sclerosis (ALS) with and without clinical symptoms of upper motor neuron disease.[102] Moreover, the presence of MEPs and the degree of corticospinal tract FA asymmetry predict the extent of functional recovery in chronic stroke.[98] These findings highlight the potential complementary value of combining TMS with DWI in both clinical diagnosis and prognosis.

Conclusion/Summary

Combination of TMS and structural MRI provides powerful approaches for testing the relationship between structure and function in the human brain. This approach enables us to address questions relating to development, ageing, and individual differences, as well as providing measures that could have important clinical application.

PET

Basic methodology

PET maps the regional binding and metabolism of compounds that have been tagged with short-lived positron-emitting isotopes such as carbon-11, oxygen-15, or fluorine-18. The emitted positrons, when they annihilate with electrons, produce pairs of gamma rays that are detected by the PET scanner. The resulting PET images provide three-dimensional (3D) maps of the tracer distribution in tissue. PET offers a range of possibilities to study human brain function.[103] Using different radioactive tracers (radioligands), PET can quantify changes in regional cerebral blood flow (rCBF) or regional cerebral metabolic rate of glucose (rCMRglc).[104] Because rCBF and rCMRglc are tightly coupled with synaptic activity, PET imaging of regional blood flow or glucose metabolism provides an index of regional synaptic activity at rest and during specific tasks. Other radioligands can be used to examine specific neurotransmitter and receptor systems, or to map amino-acid uptake or microglial activation.[104,105] The radioisotope-based imaging technique with the highest resolution and greatest sensitivity to differentiate between normal and abnormal functional states is 3D PET. The most available technique, however, is single-photon emission computed tomography (SPECT). SPECT uses radioisotopes with a long half-life and does not require an on-site cyclotron. SPECT and PET are discussed together because the general issues regarding the combined use of SPECT and TMS are identical to those encountered when combining TMS with PET.

Technical and safety aspects

The most important drawback of PET and SPECT is the exposure to radiation. This limits the number of measurements that can be performed in human subjects. It also adversely affects the general acceptance of the method. Because radiation exposure is far less problematic in animals, serial PET measurements in animals are very useful to assess long-term effects of TMS on brain activity. In anesthetized monkeys, Hayashi et al[106] performed four ^{18}FDG-PET measurements before, during, as well as 8 and 16 days after 2000 stimuli of 5-Hz rTMS were applied over the right precentral gyrus. They found that the rTMS decreased rCMRglc in motor/premotor cortices, whereas rCMRglc in the anterior/posterior cingulate and orbitofrontal cortices was enhanced. Critically, these changes in regional

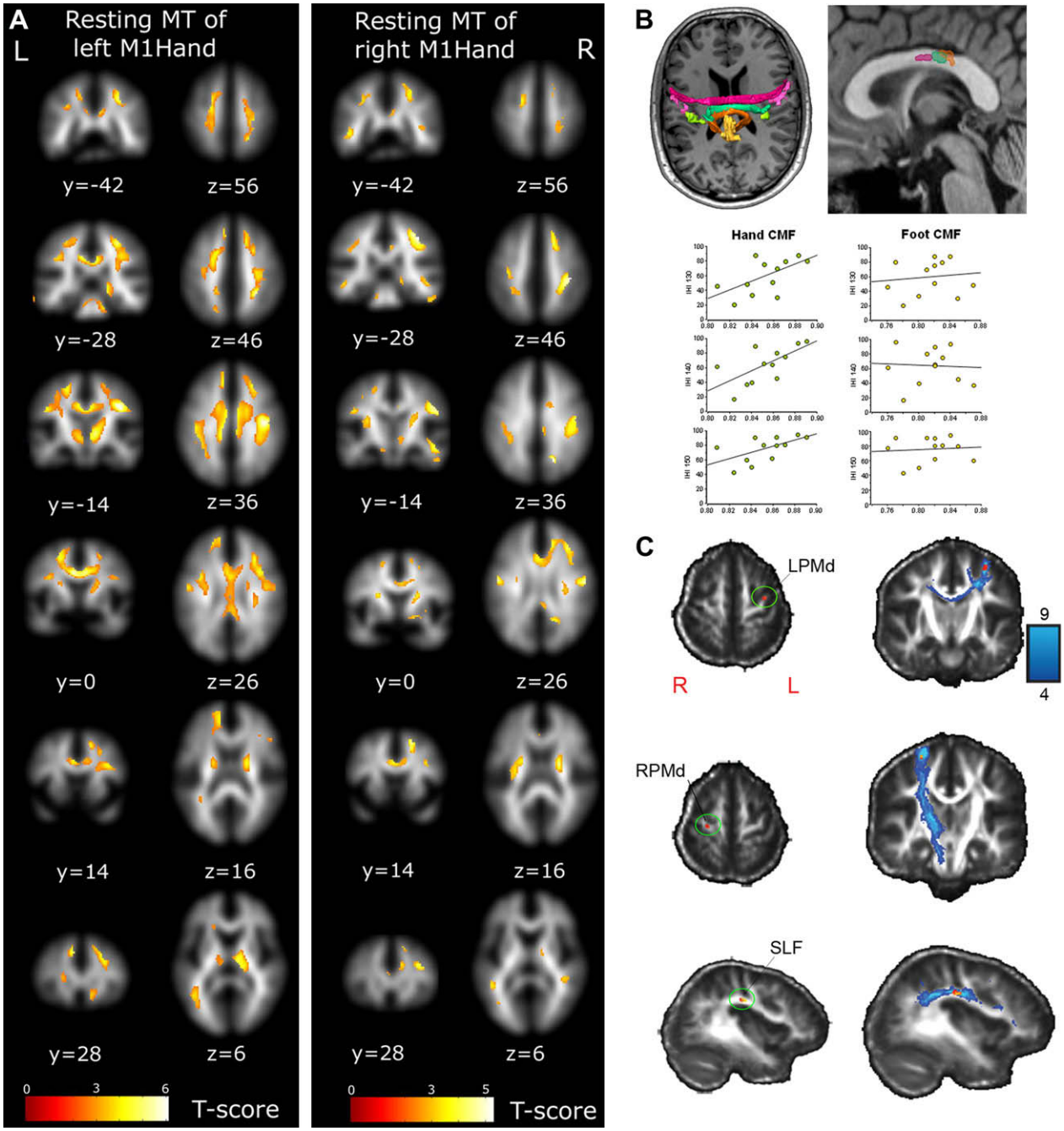

Figure 4 **(A)** Correlations between fractional anisotropy (FA) and primary motor cortical excitability (as measured by resting motor threshold) for left (left) and right (right) M1 (after Kloeppel et al[99]). **(B)** fMRI-defined M1 representations (lip: light red; hand: light green; foot: yellow) and tracked CMFs (lip: dark red; hand: dark green; foot: orange) visualized as three-dimensional objects in one subject (top). Hand but not foot FA measured from the midbody of CMFs correlated significantly with the degree of interhemispheric inhibition between the hand areas of M1 (bottom) (after Wahl et al[97]). **(C)** Local regions of correlation between functional connectivity from left dorsal premotor cortex (LPMd) to right M1 during action selection and FA in white matter underlying LPMd, RPMd, and the superior longitudinal fascilculus (SLF) (left column). Probabilistic diffusion tractography from the clusters of correlation demonstrating the white matter tracts in which local correlations were found and their gray matter targets (right column) (after Boorman et al[96]).

metabolism persisted for at least 8 days.[106] Such a longitudinal study would be impossible to perform in humans because of the excessive exposure to radiation.

No specific methodologic precautions are required if TMS is given outside the scanner before or after PET measurements (ie, offline TMS). TMS during PET (ie, online TMS) is also easy to establish. After initial concerns,[107] there is now consensus that the phasic magnetic field produced by each TMS pulse does not affect the function of the PET detectors.[108] The TMS coil on the

subject's head, however, attenuates the radiation that is picked up by the PET detectors. Therefore, it is necessary to acquire a transmission scan with the TMS coil in situ to correct for coil-induced signal attenuation during preprocessing. If two cortical areas are sequentially targeted during the same PET experiment, one needs to have separate transmission scans for each of the coil positions.

An advantage of the combined PET-TMS approach is that all currently available rTMS protocols can be given in the PET scanner since PET does not impose any temporal constraints on TMS. The PET environment imposes less spatial constraints to position the coil than MRI, rendering it possible to use frameless stereotaxy to place and monitor the coil position during online imaging.[109,110] Alternatively, correct coil position can be identified with frameless stereotaxy outside the scanner and marked on the subject's head. The coil can then be centered on the marked area after the subject has been positioned in the scanner. Correct placement of the coil can be verified on the transmission scan where the coil is clearly visible. The anatomic location of the coil can be determined by coregistering the transmission scan on the individual structural MRI scan.[110] In addition, a vitamin E capsule can be taped on the scalp under the center of the coil, and the correct placement of the coil can be confirmed with standard T1-weighted structural MRI after the end of PET measurements.

For target areas close to the central sulcus, the TMS-induced motor response can alternatively be used to localize the primary motor cortex, which can be used as a reference area to locate somatosensory or premotor areas.[15] Some groups have also used the international 10-20 system for placement of EEG electrodes to localize the site of TMS. A drawback of this approach is that the 10-20 system does not take into account interindividual differences in cortical anatomy. In addition to correct coil placement, it is essential to ensure a constant coil position during consecutive PET measurements. A mechanical or robotic fixation unit should be integrated in the bore of the PET scanner for positioning and fixating the coil over the cortical target area. In addition, coil position should be checked between consecutive PET measurements.

Neuroscientific and clinical applications

Most studies combined TMS with PET techniques that measure regional synaptic activity over several tens of seconds ($H_2{}^{15}O$-PET of rCBF) or minutes (^{18}FDG-PET of $rCMR_{glc}$). Because of its low temporal resolution, continuous train or intermittent bursts of rTMS need to be given to induce a detectable change in regional neuronal activity. A single PET scan always represents the cumulative effects of individual stimuli on regional synaptic activity during the period of measurement. This feature defines the strength and weakness of the combined TMS-PET approach: On the one hand, the combined TMS-PET approach is not suited to examine the effects of a single pulse or a short train of TMS on regional neuronal activity. On the other hand, combined TMS-PET measurements can readily probe cumulative changes in regional neuronal activity in the stimulated cortex and connected brain regions during rTMS because the neuronal effects of each stimulus can sum up during a single PET scan.

TMS can be applied during concurrent PET measurement of regional neural activity to visualize immediate effects of TMS on regional synaptic activity in the stimulated cortical area and connected brain regions. PET of rCBF or rCMRglc during the administration of TMS can map immediate TMS-induced changes in regional activity and connectivity independent of behavior. This "online" approach has been successfully used to assess how TMS-induced changes in neuronal activity depend on the intensity, frequency, or site of TMS.[109-114] Most studies examined the acute effects of TMS on rCBF or rCMRglc while participants were at rest, but online TMS-PET imaging can also be used to examine how focal TMS interacts with the regional activation pattern during a specific task.[115,116]

Although early TMS-PET studies focused on acute effects on rCBF or rCMRglc produced during TMS, more recent studies examined how rTMS shapes regional neuronal activity in the human brain beyond the time of TMS. Serial PET measurements of rCBF can track the time-course of functional after effects induced by rTMS both at rest and during a task.[16,117] A $H_2{}^{15}O$-PET study showed that 1-Hz rTMS given at an intensity of 90% resting motor threshold to left primary motor cortex (M1) caused bilateral increases in regional neuronal activity in primary motor and premotor cortices and cerebellum relative to sham rTMS.[16] The same 1-Hz rTMS protocol applied to left PMd yielded bilateral decreases in activity (compared with sham rTMS) in primary motor, premotor, prefrontal, and subcortical areas.[15] Changes in rCBF persisted for at least 1 hour after the end of rTMS, showing that rTMS can produce lasting effects on regional neuronal activity in the stimulated cortex and connected brain regions.

From measurements of the MEP, it is known that 1-Hz rTMS to M1 or PMd can reduce the amplitude of MEPs elicited in the conditioned M1. Despite of similar suppressive effects on corticospinal excitability, the PET measurements revealed marked differences in the effects of 1-Hz rTMS over M1 or PMd on regional neuronal activity. Two PET studies examined changes both in cortical excitability (by measuring MEPs) and in regional neuronal activity (by measuring rCBF) in response to focal rTMS.[118,119] Chouinard et al[118] correlated changes in MEP amplitude after 1-Hz rTMS to M1 or PMd with changes in rCBF before and after rTMS. They identified a number of brain regions in which decreases in MEP amplitude were associated with increased rCBF after rTMS. The regional patterns of correlations differed according to whether rTMS had been given to PMd or M1. Taken together, these results provide

converging evidence that the after effects of rTMS critically depend on the site of rTMS. They also highlight that it is problematic to draw simple parallels between changes in overall regional neuronal activity (as indexed by rCBF) and electrophysiologic tests of neural excitability (as indexed by the amplitude of the MEP).

Another line of research used rTMS to induce acute reorganization in functional brain networks. Several PET studies have shown that rTMS has lasting effects on task-related regional activity and interregional coupling during a given task.[16,120] Lee et al[16] reported marked changes in functional brain activity after 1-Hz rTMS of left M1 in the absence of any overt behavioral change. Movement-related activity increased in the right PMd and the inferomedial portion of the left M1 along with increased coupling between the inferomedial M1 and premotor areas during movement. These changes indicate rapid compensatory reorganization within the motor system that may help to maintain functional integrity. It was proposed that these acute reorganization patterns may be analogous to plastic changes associated with natural recovery of function after brain injury.[16] Lasting changes in interregional connectivity can also be tested by applying focal rTMS to a cortical area and subsequently probing the responsiveness of the stimulated network with online PET during focal TMS. A conditioning session of 10-Hz rTMS applied to the mid-DLPFC modulated the acute response of the frontocingulate circuit to TMS.[121]

Only a relatively small number of studies have used the combined TMS-PET approach in patients, mainly to examine the therapeutic effects of repeated sessions of prefrontal rTMS on rCBF and rCMRglc as a treatment for depression,[122-125] as introduced by George et al.[126] These studies show that serial metabolic PET or SPECT studies provide important insights into the mechanism of action of rTMS in patients and may help to predict antidepressant efficacy of different stimulation paradigms. The combined TMS-PET approach can also shed new light on the pathophysiology of neurologic and psychiatric disorders. For instance, patients with focal hand dystonia showed a greater suppression of regional synaptic activity in lateral and medial premotor areas, putamen, and thalamus after 1-Hz rTMS of left PMd, indicating enhanced plasticity of the corticobasal gangliathalamic loop in focal hand dystonia.[15]

Finally, PET provides the unique opportunity to investigate the effects of TMS on specific neurotransmitter systems (eg, the dopaminergic system) or cell populations (eg, the microglia). In healthy volunteers, ^{11}C-raclopride PET was used to measure changes in extracellular dopamine concentration after high-frequency rTMS of the left DLPFC[127] or the M1.[128] Focal rTMS to the DLPFC and M1-HAND led to spatially restricted decreases of ^{11}C-raclopride binding in ipsilateral corticostriatal projection zones of the stimulated cortical area. This regionally specific decrease in ^{11}C-raclopride binding potential indicates that focal rTMS can induce a lasting increase in endogenous dopamine release in the corresponding striatal projection zone, presumably through repetitive stimulation of corticostriatal connections during rTMS.

The rTMS/^{11}C-raclopride PET methodology offers the opportunity to investigate corticostriatal functional interactions in neurologic and psychiatric diseases. In fact, abnormalities in corticostriatal interactions are believed to play an important role in the pathophysiology of Parkinson's disease (PD).[129] The evidence of a spatially enlarged area of dopamine release in the symptomatic hemisphere after M1-TMS/^{11}C-raclopride PET may represent a possible in vivo expression of a loss of functional segregation of cortical information to the striatum and an indirect evidence of abnormal corticostriatal transmission in early PD.[129] Investigations of corticostriatal transmission have also been described in psychiatric conditions such as primary depression using SPECT[130,131] as well as in different animal models.[132-135] Ever since the adoption of rTMS as a research tool, there has been great interest regarding its potential clinical role. To date, studies addressing the contribution of placebo during TMS are limited. The placebo effect has been shown to be associated either with release of dopamine in the striatum.[136] Recently, Strafella et al[137] showed in patients with PD that expectation of therapeutic benefit from sham rTMS (placebo-rTMS) induced a diffuse, bilateral reduction in [^{11}C] raclopride BP (ie, release of dopamine) in dorsal and ventral striatum.[137] These observations confirm earlier evidence that expectation of clinical benefit (either from drugs or medical devices) induces significant dopaminergic placebo effects suggesting the importance of placebo-controlled studies for clinical trials involving brain stimulation techniques.

Conclusion/Summary

The combined use of TMS and PET has considerably expanded the applications of TMS in basic neuroscience and clinical research. The existing data convincingly show that online PET during TMS provides a behavior-independent assay of cortical excitability and connectivity. Offline PET after a conditioning session of rTMS provides a valuable means to investigate how rTMS shapes regional neuronal activity in the intact human brain. In recent years, several new protocols of rTMS have been introduced which consist of repeated bursts or paired stimuli.[9] Here, offline PET will be of great value to compare the topographic and temporal profiles of changes in regional activity produced by various rTMS protocols. As such, offline PET imaging can make an important contribution to the understanding of the mechanisms of action of rTMS. A unique strength of the combined TMS-PET is to map the effects of rTMS on regional neurotransmission. Although PET has only been used to map TMS-induced changes in dopaminergic neurotransmission, it would be very helpful to extend this approach to other neurotransmitter systems, including the serotoninergic and cholinergic system. Other

interesting extensions of the TMS-PET approach include the use of PET ligands that label activated microglia or amyloid deposits.

Near infrared spectroscopy

Basic methodology

Near infrared spectroscopy (NIRS) is a spectroscopic method measuring the wavelength and intensity of the absorption of near-infrared light by the tissue. NIRS can be used to probe brain function through the intact skull by detecting changes in blood hemoglobin concentrations associated with neural activity. Devices designed to estimate blood gas levels in the brain commonly use the light within the lower near infrared spectrum rather than visible light because of its greater penetration through the scalp. NIRS measures tissue absorbance and scattering of light at two or more wavelengths in the spectral region from 700-1000 nm, thus enabling the determination of concentration changes of oxygenated hemoglobin (oxy-Hb), deoxygenated hemoglobin (deoxy-Hb), and blood volume (total-Hb; oxy-Hb + deoxy-Hb) using mathematical models based on the modified Lambert-Beer law.[138]

Technical and safety aspects

Instrumentation for NIRS consists of a source (transmitter) that emits infrared light into the tissue, a detector (receiver) and a dispersive element (eg, a prism or a diffraction grating) to allow the intensity at different wavelengths to be recorded. A distance of each pair is adjusted to about 3 cm, which is suitable for detecting the Hb concentration at the cerebral cortex and reducing the influence of skin Hb changes.[139] Conventional NIRS has been limited to measurements from a few specific sites. Recent technologic advances enable to perform NIRS simultaneously from multiple sites and to display the results of multisite NIRS as cortical maps.

NIRS can be used to visualize the effects of TMS on cortical activity.[140] The NIRS method has several advantages over other neuroimaging techniques. It has a high signal-to-noise ratio. NIRS can be performed while TMS is being applied because the time-varying electromagnetic field induced by the TMS pulse does not interfere with NIRS. NIRS can be used in newborns and infants because of the lack of any side effects. NIRS devices are portable, enabling investigations in freely moving subjects.[141] Furthermore, NIRS has a temporal resolution that is comparable to fMRI.

There are also several limitations: The technique has a relatively poor spatial resolution when compared with fMRI. Because of the limited depth penetration of the infrared light, NIRS can only probe activity in superficial cortical regions. Because NIRS is highly sensitive to fluctuations in the light intensity of the environment, recordings need to be performed in a slightly darkened room and repeated at least 10 times. Trials need to be averaged to obtain stable results.

Although TMS has been successfully combined with NIRS, several issues remain to be solved. The placement of the probe interferes with the placement of the coil, increasing the distance between the TMS coil and the cortical target region. There is still some debate which wavelengths should be preferentially used and how strong lights should be used in combined TMS-NIRS studies. Another problem is that NIRS is difficult to perform in individuals with black hair. It is possible to record good responses in these subjects by increasing the intensity of the light that is emitted in the tissue. However, the safety guidelines for light exposure may limit the possibility to increase the intensity of the emitted infrared light, especially when studying children or infants. Finally, head movements induced by the vibration of the stimulating coil may sometimes disturb a good recording because of the movements of the NIRS probes in simultaneous NIRS-TMS studies.

Neuroscience and clinical applications

During physiologic brain activation (eg, in response to a sensory stimulus), NIRS typically shows a large oxy-Hb increase along with a small deoxy-Hb decrease.[138] If a region is deactivated, this is reflected by NIRS as an decrease in oxy-Hb and an increase in deoxy-Hb.[142] Only a few studies combined NIRS recordings with TMS. Interestingly, Hb concentration changes evoked during or after TMS appear to be different from the normal physiologic response profile. The first study that combined TMS and optical imaging reported a right-hemisphere response when the left motor cortex was stimulated.[143] The first study with two wavelengths reported local changes in Hb concentration just beneath the coil.[144] A significant increase in oxy-Hb was observed after single-pulse TMS (90% or 110% active motor threshold) when the subjects voluntarily contracted a target hand muscle. This spectroscopic response was similar to the physiologic activation pattern. On the other hand, single-pulse TMS (120% or 140% active motor threshold) induced large deoxy-Hb decreases and no significant oxy-Hb changes when the contralateral target muscle was relaxed.[145] This atypical response pattern may be explained by TMS-induced changes in the intrinsic firing rate of cortical and corticospinal neurons because of the lasting inhibition provoked by high-intensity TMS.

NIRS has also been used to measure regional changes in Hb concentration in the right PFC, PMd, M1-HAND, and primary sensory hand area (S1-HAND) during and after intermittent theta burst rTMS over the left PMd, M1 and S1, or sham stimulation. Intermittent theta burst rTMS over premotor or sensorimotor cortices induced large oxy-Hb

decrease and small deoxy-Hb increase (deactivation pattern) in the premotor or sensorimotor cortices contralaterally to the site of rTMS.[146] In another study,[147] NIRS recording was performed over the left M1-HAND during right-hand finger tapping before and after 1-Hz rTMS of the right M1-HAND. The 1-Hz rTMS of the right M1-HAND increased the level of oxy-Hb in the nonstimulated cortex for 40 minutes after the end of rTMS. Deoxy-Hb was found to be slightly decreased during the first 15 minutes after rTMS. These results confirm that 1-Hz rTMS of one hemisphere can produce persisting changes in cortical function in homologous regions of the nonstimulated hemisphere.

Conclusion/Summary

NIRS is a highly interesting method to assess the acute effects of TMS on cortical function because the spectroscopic measurements are not perturbed by concurrent TMS. Yet, there are still several problems to be solved before it will be possible to fully exploit the potential of NIRS for online TMS studies.

General conclusion and perspectives

The combined use of TMS with other brain mapping techniques has greatly expanded the scientific potential of TMS in basic neuroscience and clinical research. The offline and online TMS-neuroimaging approaches offer complementary applications. Online neuroimaging during the administration of TMS provides a behavior-independent assay of the functional brain response of the stimulated cortex as well as connected cortical and subcortical brain regions. Major progress has been made in solving technical problems caused by the interfering effects of TMS on data acquisition in concurrent TMS-fMRI and TMS-EEG studies. It remains a challenge, however, to optimize experimental approaches in a way that it is possible to disentangle the direct effects in the brain caused by TMS from nonspecific neuronal effects in response to associated auditory and somatosensory stimulation. A very promising avenue of research that can be pursued in online TMS-neuroimaging experiments is to systematically modulate the functional state of the stimulated cortex and connected brain regions at the time of stimulation (eg, by changing the behavioural context) and assess how distinct changes in functional state of the brain at the time of TMS impacts on the brain response to TMS. This offers new possibilities to probe effective connectivity in vivo. The online TMS-neuroimaging approach also allows us to explore how focal TMS interferes with task-related activity when given to different cortical regions or at different time points during a behavioral task. We anticipate that this approach will yield important insight into the mechanisms that mediate the disruptive effect of TMS on neuronal processing.

While online TMS-neuroimaging is technically demanding and requires specific safety precautions, the offline TMS-neuroimaging approach can be easily performed because TMS and neuroimaging are separated in time and possibly in space. Neuroimaging studies can be exploited to guide the timing and placement of TMS in studies that use TMS during experimental tasks to modify behavior. In addition, offline TMS-neuroimaging offers a powerful tool for investigating the neuromodulatory effects of rTMS. It provides unique opportunities to explore dynamic aspects of functional brain networks on spontaneous and task-related activity in space and time and how these functional interactions are affected by disease. As such the offline TMS-neuroimaging approach bears great potential for studying the brain's capability to undergo short-term reorganization in health and disease.

There is no general answer to the question which functional neuroimaging modality is best to use in conjunction with TMS. The previous sections show that each neuroimaging technique offers complementary information and is associated with different methodologic strengths and weaknesses. The selection of the neuroimaging technique should be tailored to the scientific question, taking into account which aspects of neuronal function are captured by a given neuroimaging technique along with its spatial and temporal resolution.

Combining TMS with structural neuroimaging is yet another promising avenue of research. One way to exploit structural neuroimaging is to correlate electrophysiologic measures of cortical excitability or corticocortical connectivity (as obtained with TMS) with measures of regional brain structure. Correlational analysis may alternatively test for relations between TMS-induced behavioural effects and neuroimaging measures of regional brain structure. Another application includes the morphometric assessment of changes in brain structure following the repeated application of rTMS over multiple sessions.[148]

Future extensions include the use of new imaging modalities such as resting-state fMRI, MR spectroscopy, or molecular PET imaging that use markers of activated microglia or amyloid deposits. Neuroimaging will also be key to better characterize and compare the impact of newly developed conditioning protocols on brain function and structure, including theta burst stimulation,[149] corticocortical paired associative stimulation,[150] or transcranial direct current stimulation.[151] Finally, combined TMS-neuroimaging studies in patients will be instrumental in clarifying the therapeutic effects of rTMS and will provide substantial new insights in the pathophysiology of neurologic or psychiatric diseases.

References

1. Barker AT, Jalinous R, Freeston IL. Non-invasive magnetic stimulation of human motor cortex. Lancet 1985;1(8437):1106-1107.

2. Kobayashi M, Pascual-Leone A. Transcranial magnetic stimulation in neurology. Lancet Neurol 2003;2(3):145-156.
3. Pascual-Leone A, Walsh V, Rothwell J. Transcranial magnetic stimulation in cognitive neuroscience–virtual lesion, chronometry, and functional connectivity. Curr Opin Neurobiol 2000;10(2):232-237.
4. Walsh V, Cowey A. Transcranial magnetic stimulation and cognitive neuroscience. Nature Rev 2000;1(1):73-79.
5. Jahanshahi M, Dirnberger G. The left dorsolateral prefrontal cortex and random generation of responses: studies with transcranial magnetic stimulation. Neuropsychologia 1999;37(2):181-190.
6. Grosbras MH, Paus T. Transcranial magnetic stimulation of the human frontal eye field facilitates visual awareness. Eur J Neurosci 2003;18(11):3121-3126.
7. Walsh V, Ellison A, Battelli L, Cowey A. Task-specific impairments and enhancements induced by magnetic stimulation of human visual area V5. Proc Biol Sci 1998;265(1395):537-543.
8. O'Shea J, Taylor PC, Rushworth MF. Imaging causal interactions during sensorimotor processing. Cortex 2008;44(5):598-608.
9. Thickbroom GW. Transcranial magnetic stimulation and synaptic plasticity: experimental framework and human models. Exp Brain Res 2007;180(4):583-593.
10. Ziemann U, Paulus W, Nitsche MA, et al. Consensus: motor cortex plasticity protocols. Brain Stimulation 2008;1(3):164-182.
11. Siebner HR, Lang N, Rizzo V, et al. Preconditioning of low-frequency repetitive transcranial magnetic stimulation with transcranial direct current stimulation: evidence for homeostatic plasticity in the human motor cortex. J Neurosci 2004;24(13): 3379-3385.
12. Siebner HR, Rothwell J. Transcranial magnetic stimulation: new insights into representational cortical plasticity. Exp Brain Res 2003;148(1):1-16.
13. Ridding MC, Rothwell JC. Is there a future for therapeutic use of transcranial magnetic stimulation? Nature Rev 2007;8(7):559-567.
14. Siebner HR, Hartwigsen G, Kassuba T, Rothwell JC. How does transcranial magnetic stimulation modify neuronal activity in the brain?—implications for studies of cognition. Cortex [in press].
15. Siebner HR, Filipovic SR, Rowe JB, et al. Patients with focal arm dystonia have increased sensitivity to slow-frequency repetitive TMS of the dorsal premotor cortex. Brain 2003;126(Pt 12):2710-2725.
16. Lee L, Siebner HR, Rowe JB, et al. Acute remapping within the motor system induced by low-frequency repetitive transcranial magnetic stimulation. J Neurosci 2003;23(12):5308-5318.
17. O'Shea J, Johansen-Berg H, Trief D, Gobel S, Rushworth MF. Functionally specific reorganization in human premotor cortex. Neuron 2007;54(3):479-490.
18. Brandt SA, Brocke J, Roricht S, Ploner CJ, Villringer A, Meyer BU. In vivo assessment of human visual system connectivity with transcranial electrical stimulation during functional magnetic resonance imaging. Neuroimage 2001;14(2):366-375.
19. Brocke J, Schmidt S, Irlbacher K, Cichy RM, Brandt SA. Transcranial cortex stimulation and fMRI: electrophysiological correlates of dual-pulse BOLD signal modulation. Neuroimage 2008;40(2): 631-643.
20. Siebner HR, Peller M, Willoch F, et al. Imaging functional activation of the auditory cortex during focal repetitive transcranial magnetic stimulation of the primary motor cortex in normal subjects. Neurosci Lett 1999;270(1):37-40.
21. Cohen LG, Celnik P, Pascual-Leone A, et al. Functional relevance of cross-modal plasticity in blind humans. Nature 1997;389(6647): 180-183.
22. Neggers SF, Huijbers W, Vrijlandt CM, Vlaskamp BN, Schutter DJ, Kenemans JL. TMS pulses on the frontal eye fields break coupling between visuospatial attention and eye movements. J Neurophysiol 2007;98(5):2765-2778.
23. Ilmoniemi RJ, Virtanen J, Ruohonen J, et al. Neuronal responses to magnetic stimulation reveal cortical reactivity and connectivity. Neuroreport 1997;8(16):3537-3540.
24. Virtanen J, Ruohonen J, Naatanen R, Ilmoniemi RJ. Instrumentation for the measurement of electric brain responses to transcranial magnetic stimulation. Med Biol Eng Comput 1999;37(3):322-326.
25. Thut G, Ives JR, Kampmann F, Pastor MA, Pascual-Leone A. A new device and protocol for combining TMS and online recordings of EEG and evoked potentials. J Neurosci Methods 2005;141(2): 207-217.
26. Bonato C, Miniussi C, Rossini PM. Transcranial magnetic stimulation and cortical evoked potentials: a TMS/EEG co-registration study. Clin Neurophysiol 2006;117(8):1699-1707.
27. Taylor PC, Walsh V, Eimer M. Combining TMS and EEG to study cognitive function and cortico-cortico interactions. Behav Brain Res 2008;191(2):141-147.
28. Roth BJ, Pascual-Leone A, Cohen LG, Hallett M. The heating of metal electrodes during rapid-rate magnetic stimulation: a possible safety hazard. Electroencephalogr Clin Neurophysiol 1992;85(2):116-123.
29. Ives JR, Rotenberg A, Poma R, Thut G, Pascual-Leone A. Electroencephalographic recording during transcranial magnetic stimulation in humans and animals. Clin Neurophysiol 2006;117(8):1870-1875.
30. Julkunen P, Paakkonen A, Hukkanen T, et al. Efficient reduction of stimulus artefact in TMS-EEG by epithelial short-circuiting by mini-punctures. Clin Neurophysiol 2008;119(2):475-481.
31. Nikouline V, Ruohonen J, Ilmoniemi RJ. The role of the coil click in TMS assessed with simultaneous EEG. Clin Neurophysiol 1999; 110(8):1325-1328.
32. Massimini M, Ferrarelli F, Huber R, Esser SK, Singh H, Tononi G. Breakdown of cortical effective connectivity during sleep. Science 2005;309(5744):2228-2232.
33. Komssi S, Aronen HJ, Huttunen J, et al. Ipsi- and contralateral EEG reactions to transcranial magnetic stimulation. Clin Neurophysiol 2002;113(2):175-184.
34. Lioumis P, Kicic D, Savolainen P, Makela JP, Kahkonen S. Reproducibility of TMS-Evoked EEG responses. Hum Brain Mapp 2008 Jun 6. [Published online ahead of print].
35. Ruohonen J, Ilmoniemi RJ. Modeling of the stimulating field generation in TMS. Electroencephalogr Clin Neurophysiol 1999;51:30-40.
36. De Lucia M, Parker GJ, Embleton K, Newton JM, Walsh V. Diffusion tensor MRI-based estimation of the influence of brain tissue anisotropy on the effects of transcranial magnetic stimulation. NeuroImage 2007;36(4):1159-1170.
37. Huber R, Esser SK, Ferrarelli F, Massimini M, Peterson MJ, Tononi G. TMS-induced cortical potentiation during wakefulness locally increases slow wave activity during sleep. PLoS ONE 2007;2:e276.
38. Huber R, Maatta S, Esser SK, et al. Measures of cortical plasticity after transcranial paired associative stimulation predict changes in electroencephalogram slow-wave activity during subsequent sleep. J Neurosci 2008;28(31):7911-7918.
39. Bergmann TO, Mölle M, Marshall L, Kaya-Yildiz L, Born J, Siebner HR. A local signature of LTP- and LTD-like plasticity in human NREM sleep. Eur J Neurosci 2008;27(9):2241-2249.
40. De Gennaro L, Fratello F, Marzano C, et al. Cortical plasticity induced by transcranial magnetic stimulation during wakefulness affects electroencephalogram activity during sleep. PLoS ONE 2008;3(6):e2483.
41. De Gennaro L, Marzano C, Veniero D, et al. Neurophysiological correlates of sleepiness: a combined TMS and EEG study. Neuroimage 2007;36(4):1277-1287.
42. Romei V, Brodbeck V, Michel C, Amedi A, Pascual-Leone A, Thut G. Spontaneous fluctuations in posterior alpha-band EEG activity reflect variability in excitability of human visual areas. Cereb Cortex 2008;18(9):2010-2018.
43. Paus T, Sipila PK, Strafella AP. Synchronization of neuronal activity in the human primary motor cortex by transcranial magnetic stimulation: an EEG study. J Neurophysiol 2001;86(4):1983-1990.
44. Brignani D, Manganotti P, Rossini PM, Miniussi C. Modulation of cortical oscillatory activity during transcranial magnetic stimulation. Hum Brain Mapp 2008;29(5):603-612.

45. Fuggetta G, Pavone EF, Fiaschi A, Manganotti P. Acute modulation of cortical oscillatory activities during short trains of high-frequency repetitive transcranial magnetic stimulation of the human motor cortex: a combined EEG and TMS study. Hum Brain Mapp 2008; 29(1):1-13.
46. Taylor PC, Nobre AC, Rushworth MF. FEF TMS affects visual cortical activity. Cereb Cortex 2007;17(2):391-399.
47. Taylor PC, Nobre AC, Rushworth MF. Subsecond changes in top down control exerted by human medial frontal cortex during conflict and action selection: a combined transcranial magnetic stimulation electroencephalography study. J Neurosci 2007;27(42):11343-11353.
48. Fuggetta G, Pavone EF, Walsh V, Kiss M, Eimer M. Cortico-cortical interactions in spatial attention: a combined ERP/TMS study. J Neurophysiol 2006;95(5):3277-3280.
49. Komssi S, Kahkonen S. The novelty value of the combined use of electroencephalography and transcranial magnetic stimulation for neuroscience research. Brain Res Rev 2006;52(1):183-192.
50. Lehmann D, Skrandies W. Reference-free identification of components of checkerboard-evoked multichannel potential fields. Electroencephalogr Clin Neurophysiol 1980;48(6):609-621.
51. Esser SK, Huber R, Massimini M, Peterson MJ, Ferrarelli F, Tononi G. A direct demonstration of cortical LTP in humans: a combined TMS/EEG study. Brain Res Bull 2006;69(1):86-94.
52. Massimini M, Ferrarelli F, Esser SK, et al. Triggering sleep slow waves by transcranial magnetic stimulation. Proc Natl Acad Sci U S A 2007;104(20):8496-8501.
53. Litvak V, Komssi S, Scherg M, et al. Artifact correction and source analysis of early electroencephalographic responses evoked by transcranial magnetic stimulation over primary motor cortex. Neuroimage 2007;37(1):56-70.
54. Komssi S, Savolainen P, Heiskala J, Kahkonen S. Excitation threshold of the motor cortex estimated with transcranial magnetic stimulation electroencephalography. Neuroreport 2007;18(1):13-16.
55. Fuggetta G, Fiaschi A, Manganotti P. Modulation of cortical oscillatory activities induced by varying single-pulse transcranial magnetic stimulation intensity over the left primary motor area: a combined EEG and TMS study. Neuroimage 2005;27(4):896-908.
56. Kahkonen S, Kesaniemi M, Nikouline VV, et al. Ethanol modulates cortical activity: direct evidence with combined TMS and EEG. Neuroimage 2001;14(2):322-328.
57. Kahkonen S, Wilenius J, Nikulin VV, Ollikainen M, Ilmoniemi RJ. Alcohol reduces prefrontal cortical excitability in humans: a combined TMS and EEG study. Neuropsychopharmacol 2003; 28(4):747-754.
58. Ferrarelli F, Massimini M, Peterson MJ, et al. Reduced evoked gamma oscillations in the frontal cortex in schizophrenia patients: a TMS/EEG study. Am J Psychiatry 2008;165:996-1005.
59. Esser SK, Hill SL, Tononi G. Modeling the effects of transcranial magnetic stimulation on cortical circuits. J Neurophysiol 2005; 94(1):622-639.
60. Bohning DE, Shastri A, Nahas Z, et al. Echoplanar BOLD fMRI of brain activation induced by concurrent transcranial magnetic stimulation. Invest Radiol 1998;33(6):336-340.
61. Ferrarelli F, Haraldsson HM, Barnhart TE, et al. A [17F]-fluoromethane PET/TMS study of effective connectivity. Brain Res Bull 2004;64(2):103-113.
62. Logothetis NK. The neural basis of the blood-oxygen-level-dependent functional magnetic resonance imaging signal. Philos Trans R Soc Lond B Biol Sci 2002;357(1424):1003-1037.
63. Formisano E, Goebel R. Tracking cognitive processes with functional MRI mental chronometry. Curr Opin Neurobio 2003;13(2):174-181.
64. Josephs O, Henson RN. Event-related functional magnetic resonance imaging: modelling, inference and optimization. Philos Trans R Soc Lond B Biol Sci 1999;354(1387):1215-1228.
65. Bohning DE, Shastri A, McConnell KA, et al. A combined TMS/fMRI study of intensity-dependent TMS over motor cortex. Biol Psychiatry 1999;45(4):385-394.
66. Shastri A, George MS, Bohning DE. Performance of a system for interleaving transcranial magnetic stimulation with steady-state magnetic resonance imaging. Electroencephalogr Clin Neurophysiol Suppl 1999;51:55-64.
67. Baudewig J, Paulus W, Frahm J. Artifacts caused by transcranial magnetic stimulation coils and EEG electrodes in T(2)*-weighted echo-planar imaging. Magn Reson Imaging 2000;18(4):479-484.
68. Bestmann S, Baudewig J, Frahm J. On the synchronization of transcranial magnetic stimulation and functional echo-planar imaging. J Magn Reson Imaging 2003;17(3):309-316.
69. Denslow S, Bohning DE, Bohning PA, Lomarev MP, George MS. An increased precision comparison of TMS-induced motor cortex BOLD fMRI response for image-guided versus function-guided coil placement. Cogn Behav Neurol 2005;18(2):119-126.
70. Bestmann S, Swayne O, Blankenburg F, et al. Dorsal premotor cortex exerts state-dependent causal influences on activity in contralateral primary motor and dorsal premotor cortex. Cereb Cortex 2008; 18(6):1281-1291.
71. Weiskopf N, Josephs O, Ruff CC. et al. Image artifacts in concurrent transcranial magnetic stimulation (TMS) and fMRI caused by leakage currents: Modeling and compensation. J Magn Reson Imaging [in press].
72. Bestmann S, Ruff CC, Driver J, Blankenburg F. Concurrent TMS and functional magnetic resonance imaging: methods and current advances. In: Wassermann EM, Epstein CM, Ziemann U, Walsh V, Paus T, Lisanby S, editors. The Oxford Handbook of Transcranial Stimulation. Oxford: Oxford University Press; 2008. p. 569-592.
73. Ruff CC, Bestmann S, Blankenburg F, et al. Distinct causal influences of parietal versus frontal areas on human visual cortex: evidence from concurrent TMS-fMRI. Cereb Cortex 2008;18(4): 817-827.
74. Bestmann S, Ruff CC, Blankenburg F, Weiskopf W, Driver J, Rothwell JC. Mapping causal interregional influences with concurrent TMS-fMRI. Exp Brain Res 2008;191:383-402.
75. Paus T. Inferring causality in brain images: a perturbation approach. Philos Trans R Soc Lond B Biol Sci 2005;360(1457):1109-1114.
76. Bohning DE, Shastri A, Wassermann EM, et al. BOLD-f MRI response to single-pulse transcranial magnetic stimulation (TMS). J Magn Reson Imaging 2000;11(6):569-574.
77. Bestmann S, Baudewig J, Siebner HR, Rothwell JC, Frahm J. BOLD MRI responses to repetitive TMS over human dorsal premotor cortex. Neuroimage 2005;28(1):22-29.
78. Denslow S, Lomarev M, George MS, Bohning DE. Cortical and subcortical brain effects of transcranial magnetic stimulation (TMS)-induced movement: an interleaved TMS/functional magnetic resonance imaging study. Biol Psychiatry 2005;57(7):752-760.
79. Bestmann S, Baudewig J, Siebner HR, Rothwell JC, Frahm J. Subthreshold high-frequency TMS of human primary motor cortex modulates interconnected frontal motor areas as detected by interleaved fMRI-TMS. Neuroimage 2003;20(3):1685-1696.
80. Bestmann S, Baudewig J, Siebner HR, Rothwell JC, Frahm J. Functional MRI of the immediate impact of transcranial magnetic stimulation on cortical and subcortical motor circuits. Eur J Neurosci 2004;19(7):1950-1962.
81. Ruff CC, Blankenburg F, Bjoertomt O, et al. Concurrent TMS-fMRI and psychophysics reveal frontal influences on human retinotopic visual cortex. Curr Biol 2006;16(15):1479-1488.
82. Sack AT, Kohler A, Bestmann S, et al. Imaging the brain activity changes underlying impaired visuospatial judgments: simultaneous FMRI, TMS, and behavioral studies. Cereb Cortex 2007;17(12): 2841-2852.
83. Blankenburg F, Ruff CC, Bestmann S, et al. Interhemispheric effect of parietal TMS on somatosensory response confirmed directly with concurrent TMS-fMRI. J Neurosci 2008;28(49):13202-13208.
84. Bestmann S, Oliviero A, Voss M, et al. Cortical correlates of TMS-induced phantom hand movements revealed with concurrent TMS-fMRI. Neuropsychologia 2006;44(14):2959-2971.

85. Friston KJ, Price CJ. Degeneracy and redundancy in cognitive anatomy. Trends Cogn Sci 2003;7(4):151-152.
86. Li X, Nahas Z, Kozel FA, Anderson B, Bohning DE, George MS. Acute left prefrontal transcranial magnetic stimulation in depressed patients is associated with immediately increased activity in prefrontal cortical as well as subcortical regions. Biol Psychiatry 2004;55(9):882-890.
87. Li X, Teneback CC, Nahas Z, et al. Interleaved transcranial magnetic stimulation/functional MRI confirms that lamotrigine inhibits cortical excitability in healthy young men. Neuropsychopharmacol 2004;29(7):1395-1407.
88. Tegenthoff M, Ragert P, Pleger B, et al. Improvement of tactile discrimination performance and enlargement of cortical somatosensory maps after 5 Hz rTMS. PLoS Biol 2005;3(11):e362.
89. Pleger B, Blankenburg F, Bestmann S, et al. Repetitive transcranial magnetic stimulation-induced changes in sensorimotor coupling parallel improvements of somatosensation in humans. J Neurosci 2006;26(7):1945-1952.
90. Rango M, Cogiamanian F, Marceglia S, et al. Myoinositol content in the human brain is modified by transcranial direct current stimulation in a matter of minutes: a 1H-MRS study. Magn Reson Med 2008; 60(4):782-789.
91. Stagg CJ, Best J, Stephenson M, et al. Imaging the functional and neurochemical effects of transcranial direct current stimulation: a rationale for rehabilitation (Abstract). Special issue: Proceedings from the Third International Conference on TMS and tDCS. October 1-4, Göttingen, Germany. Brain Stimulation 2008;1(3): 260-261.
92. Moisa M, Pohmann R, Uludag K, Thielscher A. Interleaved TMS/CASL: a motor cortex study (Abstract). Special Issue: Proceedings from the Third International Conference on TMS and tDCS. October 1-4, Göttingen, Germany. Brain Stimulation 2008;1(3): 290-291.
93. Bohning DE, Pecheny AP, Epstein CM, et al. Mapping transcranial magnetic stimulation (TMS) fields in vivo with MRI. Neuroreport 1997;8(11):2535-2538.
94. Ashburner J, Friston KJ. Voxel-based morphometry–the methods. Neuroimage 2000;11(6 Pt 1):805.
95. Ashburner J, Csernansky JG, Davatzikos C, Fox NC, Frisoni GB, Thompson PM. Computer-assisted imaging to assess brain structure in healthy and diseased brains. Lancet Neurol 2003;2(2):79-88.
96. Boorman ED, O'Shea J, Sebastian C, Rushworth MF, Johansen-Berg H. Individual differences in white-matter microstructure reflect variation in functional connectivity during choice. Curr Biol 2007;17(16):1426-1431.
97. Wahl M, Lauterbach-Soon B, Hattingen E, et al. Human motor corpus callosum: topography, somatotopy, and link between microstructure and function. J Neurosci 2007;27(45):12132-12138.
98. Stinear CM, Barber PA, Smale PR, Coxon JP, Fleming MK, Byblow WD. Functional potential in chronic stroke patients depends on corticospinal tract integrity. Brain 2007;130(Pt 1):170-180.
99. Kloppel S, Baumer T, Kroeger J, et al. The cortical motor threshold reflects microstructural properties of cerebral white matter. Neuroimage 2008;40(4):1782-1791.
100. Smith SM, Jenkinson M, Johansen-Berg H, et al. Tract-based spatial statistics: voxelwise analysis of multi-subject diffusion data. Neuroimage 2006;31(4):1487-1505.
101. Silbert LC, Nelson C, Holman S, et al. Cortical excitability and age-related volumetric MRI changes. Clin Neurophysiol 2006; 117(5):1029-1036.
102. Sach M, Winkler G, Glauche V, et al. Diffusion tensor MRI of early upper motor neuron involvement in amyotrophic lateral sclerosis. Brain 2004;127(Pt 2):340-350.
103. Piccini P, Whone A. Functional brain imaging in the differential diagnosis of Parkinson's disease. Lancet Neuro 2004;3(5):284-290.
104. Herholz K, Heiss WD. Positron emission tomography in clinical neurology. Mol Imaging Biol 2004;6(4):239-269.
105. Cagnin A, Gerhard A, Banati RB. In vivo imaging of neuroinflammation. Eur Neuropsychopharmacol 2002;12(6):581-586.
106. Hayashi T, Ohnishi T, Okabe S, et al. Long-term effect of motor cortical repetitive transcranial magnetic stimulation [correction]. Ann Neurol 2004;56(1):77-85.
107. Thompson CJ, Paus T, Clancy R. Magnetic schielding requirements for PET detectors during transcranial magnetic stimulation. IEEE Trans Nuclear Sci 1998;20:1923-1927.
108. Siebner HR, Peller M, Lee L. TMS and positron emission tomography: methods and current advances. In: Wassermann EM, Epstein CM, Ziemann U, Walsh V, Paus T, Lisanby S, editors. The Oxford Handbook of Transcranial Stimulation. Oxford: Oxford University Press; 2008. p. 549-567.
109. Paus T, Jech R, Thompson CJ, Comeau R, Peters T, Evans AC. Transcranial magnetic stimulation during positron emission tomography: a new method for studying connectivity of the human cerebral cortex. J Neurosci 1997;17(9):3178-3184.
110. Paus T, Wolforth M. Transcranial magnetic stimulation during PET: reaching and verifying the target site. Hum Brain Mapp 1998;6(5-6): 399-402.
111. Siebner H, Peller M, Bartenstein P, et al. Activation of frontal premotor areas during suprathreshold transcranial magnetic stimulation of the left primary sensorimotor cortex: a glucose metabolic PET study. Hum Brain Mapp 2001;12(3):157-167.
112. Speer AM, Willis MW, Herscovitch P, et al. Intensity-dependent regional cerebral blood flow during 1-Hz repetitive transcranial magnetic stimulation (rTMS) in healthy volunteers studied with H215O positron emission tomography: II, effects of prefrontal cortex rTMS. Biol Psychiatry 2003;54(8):826-832.
113. Speer AM, Willis MW, Herscovitch P, et al. Intensity-dependent regional cerebral blood flow during 1-Hz repetitive transcranial magnetic stimulation (rTMS) in healthy volunteers studied with H215O positron emission tomography: I, effects of primary motor cortex rTMS. Biol Psychiatry 2003;54(8):818-825.
114. Siebner HR, Takano B, Peinemann A, Schwaiger M, Conrad B, Drzezga A. Continuous transcranial magnetic stimulation during positron emission tomography: a suitable tool for imaging regional excitability of the human cortex. Neuroimage 2001; 14(4):883-890.
115. Mottaghy FM, Krause BJ, Kemna LJ, et al. Modulation of the neuronal circuitry subserving working memory in healthy human subjects by repetitive transcranial magnetic stimulation. Neurosci Lett 2000;280(3):167-170.
116. Mottaghy FM, Pascual-Leone A, Kemna LJ, et al. Modulation of a brain-behavior relationship in verbal working memory by rTMS. Brain Res Cogn Brain Res 2003;15(3):241-249.
117. Siebner HR, Peller M, Lee L. Applications of combined TMS-PET studies in clinical and basic research. Suppl Clin Neurophysiol 2003;56:63-72.
118. Chouinard PA, Van Der Werf YD, Leonard G, Paus T. Modulating neural networks with transcranial magnetic stimulation applied over the dorsal premotor and primary motor cortices. J Neurophysiol 2003;90(2):1071-1083.
119. Takano B, Drzezga A, Peller M, et al. Short-term modulation of regional excitability and blood flow in human motor cortex following rapid-rate transcranial magnetic stimulation. Neuroimage 2004; 23(3):849-859.
120. Rounis E, Lee L, Siebner HR, et al. Frequency specific changes in regional cerebral blood flow and motor system connectivity following rTMS to the primary motor cortex. Neuroimage 2005; 26(1):164-176.
121. Paus T, Castro-Alamancos MA, Petrides M. Cortico-cortical connectivity of the human mid-dorsolateral frontal cortex and its modulation by repetitive transcranial magnetic stimulation. Eur J Neurosci 2001; 14(8):1405-1411.
122. Catafau AM, Perez V, Gironell A, et al. SPECT mapping of cerebral activity changes induced by repetitive transcranial magnetic

stimulation in depressed patients: a pilot study. Psychiatry Res 2001; 106(3):151-160.
123. Nadeau SE, McCoy KJ, Crucian GP, et al. Cerebral blood flow changes in depressed patients after treatment with repetitive transcranial magnetic stimulation: evidence of individual variability. Neuropsychiatry Neuropsychol Behav Neurol 2002;15(3):159-175.
124. Shajahan PM, Glabus MF, Steele JD, et al. Left dorso-lateral repetitive transcranial magnetic stimulation affects cortical excitability and functional connectivity, but does not impair cognition in major depression. Prog Neuropsychopharmacol Biol Psychiatry 2002; 26(5):945-954.
125. Speer AM, Kimbrell TA, Wassermann EM, et al. Opposite effects of high and low frequency rTMS on regional brain activity in depressed patients. Biol Psychiatry 2000;48(12):1133-1141.
126. George MS, Wassermann EM, Williams WA, et al. Daily repetitive transcranial magnetic stimulation (rTMS) improves mood in depression. Neuroreport 1995;6(14):1853-1856.
127. Strafella AP, Paus T, Barrett J, Dagher A. Repetitive transcranial magnetic stimulation of the human prefrontal cortex induces dopamine release in the caudate nucleus. J Neurosci 2001;21(15):RC157.
128. Strafella AP, Paus T, Fraraccio M, Dagher A. Striatal dopamine release induced by repetitive transcranial magnetic stimulation of the human motor cortex. Brain 2003;126(Pt 12):2609-2615.
129. Strafella AP, Ko JH, Grant J, Fraraccio M, Monchi O. Corticostriatal functional interactions in Parkinson's disease: a rTMS/[11C]raclopride PET study. Eur J Neurosci 2005;22(11):2946-2952.
130. Pogarell O, Koch W, Popperl G, et al. Acute prefrontal rTMS increases striatal dopamine to a similar degree as D-amphetamine. Psychiatry Res 2007;156(3):251-255.
131. Pogarell O, Koch W, Popperl G, et al. Striatal dopamine release after prefrontal repetitive transcranial magnetic stimulation in major depression: preliminary results of a dynamic [123I] IBZM SPECT study. J Psychiatr Res 2006;40(4):307-314.
132. Keck ME, Welt T, Muller MB, et al. Repetitive transcranial magnetic stimulation increases the release of dopamine in the mesolimbic and mesostriatal system. Neuropharmacology 2002;43(1):101-109.
133. Erhardt A, Sillaber I, Welt T, Muller MB, Singewald N, Keck ME. Repetitive transcranial magnetic stimulation increases the release of dopamine in the nucleus accumbens shell of morphine-sensitized rats during abstinence. Neuropsychopharmacology 2004;29(11): 2074-2080.
134. Kanno M, Matsumoto M, Togashi H, Yoshioka M, Mano Y. Effects of acute repetitive transcranial magnetic stimulation on dopamine release in the rat dorsolateral striatum. J Neurol Sci 2004;217(1):73-81.
135. Ohnishi T, Hayashi T, Okabe S, et al. Endogenous dopamine release induced by repetitive transcranial magnetic stimulation over the primary motor cortex: an [11C]raclopride positron emission tomography study in anesthetized macaque monkeys. Biol Psychiatry 2004;55(5):484-489.
136. de la Fuente-Fernandez R, Ruth TJ, Sossi V, Schulzer M, Calne DB, Stoessl AJ. Expectation and dopamine release: mechanism of the placebo effect in Parkinson's disease. Science 2001;293(5532): 1164-1166.
137. Strafella AP, Ko JH, Monchi O. Therapeutic application of transcranial magnetic stimulation in Parkinson's disease: the contribution of expectation. Neuroimage 2006;31(4):1666-1672.
138. Villringer A, Chance B. Non-invasive optical spectroscopy and imaging of human brain function. Trends Neurosci 1997;20(10): 435-442.
139. Germon TJ, Evans PD, Barnett NJ, Wall P, Manara AR, Nelson RJ. Cerebral near infrared spectroscopy: emitter-detector separation must be increased. Br J Anaesth 1999;82(6):831-837.
140. Oliviero A, Di Lazzaro V, Piazza O, et al. Cerebral blood flow and metabolic changes produced by repetitive magnetic brain stimulation. J Neurol 1999;246(12):1164-1168.
141. Miyai I, Tanabe HC, Sase I, et al. Cortical mapping of gait in humans: a near-infrared spectroscopic topography study. Neuroimage 2001;14(5):1186-1192.
142. Wenzel R, Wobst P, Heekeren HH, et al. Saccadic suppression induces focal hypooxygenation in the occipital cortex. J Cereb Blood Flow Metab 2000;20(7):1103-1110.
143. Nissilä I, Kotilahti K, Komssi S, et al. Optical measurement of hemodynamic changes in the contralateral motor cortex induced by transcranial magnetic stimulation. In: Nowak H, Haueisen J, Gießler F, Huonker R, edis, editors. Proceedings of the 13th International Conference on Biomagnetism (BIOMAG 2002). Berlin: VDE Verlag; 2002. p. 851-854.
144. Noguchi Y, Watanabe E, Sakai KL. An event-related optical topography study of cortical activation induced by single-pulse transcranial magnetic stimulation. Neuroimage 2003;19(1):156-162.
145. Mochizuki H, Ugawa Y, Terao Y, Sakai KL. Cortical hemoglobinoncentration changes under the coil induced by single-pulse TMS in humans: a simultaneous recording with near-infrared spectroscopy. Exp Brain Res 200;169(3):302–310.
146. Mochizuki H, Furubayashi T, Hanajima R, et al. Hemoglobin concentration changes in the contralateral hemisphere during and after theta burst stimulation of the human sensorimotor cortices. Exp Brain Res 2007;180(4):667-675.
147. Chiang TC, Vaithianathan T, Leung T, Lavidor M, Walsh V, Delpy DT. Elevated haemoglobin levels in the motor cortex following 1 Hz transcranial magnetic stimulation: a preliminary study. Exp Brain Res 2007;181(4):555-560.
148. May A, Hajak G, Ganssbauer S, et al. Structural brain alterations following 5 days of intervention: dynamic aspects of neuroplasticity. Cereb Cortex 2007;17(1):205-210.
149. Huang YZ, Edwards MJ, Rounis E, Bhatia KP, Rothwell JC. Theta burst stimulation of the human motor cortex. Neuron 2005;45(2): 201-206.
150. Rizzo V, Siebner HS, Morgante F, Mastroeni C, Girlanda P, Quartarone A. Paired associative stimulation of left and right human motor cortex shapes interhemispheric motor inhibition based on a Hebbian mechanism. Cereb Cortex 2008 Sep 12. [Published online ahead of print.].
151. Lang N, Siebner HR, Ward NS, et al. How does transcranial DC stimulation of the primary motor cortex alter regional neuronal activity in the human brain? Eur J Neurosci 2005;22(2):495-504.

Paper II

European Journal of Neuroscience, Vol. 27, pp. 2241–2249, 2008 doi:10.1111/j.1460-9568.2008.06178.x

A local signature of LTP- and LTD-like plasticity in human NREM sleep

Til Ole Bergmann,[1] Matthias Mölle,[2] Lisa Marshall,[2] Leval Kaya-Yildiz,[1] Jan Born[2] and Hartwig Roman Siebner[1]
[1]Department of Neurology, Christian-Albrechts University Kiel, Schittenhelmstrasse 10, D-24105 Kiel, Germany
[2]Department of Neuroendocrinology, University Lübeck, Germany

Keywords: paired associative stimulation, primary motor cortex, sleep spindles, slow wave activity, transcranial magnetic stimulation

Abstract

Paired associative stimulation (PAS) repeatedly pairs electrical nerve stimulation with transcranial magnetic stimulation of the contralateral motor hand area ($M1_{HAND}$). Depending on the interstimulus interval, PAS can induce a long-term potentiation (LTP)-like facilitation or long-term depression (LTD)-like suppression of cortical excitability. In three experimental sessions, 12 awake men received PAS of the right median nerve and left $M1_{HAND}$ in the evening before sleep. To optimize the timing of paired stimulation in $M1_{HAND}$, the interstimulus interval of PAS was adjusted to the individual N20-latency of the somatosensory evoked potential to induce LTP-like effects ($PAS_{N20+2ms}$), LTD-like effects ($PAS_{N20-5ms}$), or no timing-dependent after-effects ($PAS_{control}$). Motor-evoked potentials (MEPs) showed high interindividual variations in the conditioning effects of $PAS_{N20+2ms}$ and $PAS_{N20-5ms}$ on cortical excitability. However, $PAS_{control}$ allowed us to adjust for any unspecific stimulation effects and the MEP increase after $PAS_{N20+2ms}$ differed significantly from the MEP decrease after $PAS_{N20-5ms}$. $PAS_{N20+2ms}$ and $PAS_{N20-5ms}$ also had a differential effect on regional expression of slow waves and slow spindle activity during the first hour of subsequent non-rapid eye movement (NREM) sleep. At the electrode sites overlying the conditioned $M1_{HAND}$ and the adjacent premotor cortex, local expression of slow spindle activity was significantly correlated with interindividual differences in the efficacy of $PAS_{N20+2ms}$ and $PAS_{N20-5ms}$ to potentiate or suppress cortical excitability. This correlation indicates that PAS shapes the local regulation of slow sleep spindles during subsequent NREM sleep.

Introduction

Sleep consolidates newly acquired memory traces (Stickgold, 2005; Born *et al*., 2006; Marshall & Born, 2007). Recent research suggests that oscillatory neuronal activity during non-rapid eye movement (NREM) sleep is involved in sleep-dependent memory consolidation (Marshall *et al*., 2006). Learning before sleep modulates the regional expression of slow wave activity (SWA) (Huber *et al*., 2004, 2006, 2007) and spindle density (Gais *et al*., 2002) during subsequent NREM sleep, particularly in those cortical areas that were initially involved in learning. Interestingly, the regional expression of SWA (Huber *et al*., 2004) and spindle density (Schabus *et al*., 2004; Fogel & Smith, 2006; Nishida & Walker, 2007; Schabus *et al*., 2008) also correlates with overnight improvements in memory performance.

Two recent studies 'artificially' induced regional cortical plasticity during wakefulness in humans. In one study, 5-Hz repetitive transcranial magnetic stimulation (rTMS) was given over the left M1 to induce long-term potentiation (LTP)-like plasticity (Huber *et al*., 2007). In the other study, the left arm was immobilized for 12 h to induce a long-term depression (LTD)-like effect in the contralateral sensorimotor cortex (Huber *et al*., 2006). The interventions had opposite effects on local SWA (0.5–4.5 Hz). Whereas rTMS led to an increase in SWA and fast sleep spindle power (13–16 Hz) in the left premotor cortex, arm immobilization attenuated SWA and fast spindle power in the contralateral sensorimotor cortex. These results are compatible with the hypothesis that the induction of either LTP- or LTD-like plasticity has opposite effects on local SWA (Tononi & Cirelli, 2006). However, the induction of cortical plasticity by 5-Hz rTMS and immobilization was confounded by the mere amount of evoked neuronal activity during both interventions (relative to the control conditions), which might have accounted for the effects on local NREM sleep as well.

To avoid this ambiguity, LTP- and LTD-inducing protocols should be matched in terms of their acute effects on cortical activity during wakefulness. Paired associative stimulation (PAS) meets these requirements. PAS repeatedly pairs electrical stimulation of a peripheral nerve with TMS of the contralateral sensory or motor cortex at a constant interstimulus interval (ISI) (Stefan *et al*., 2000; Wolters *et al*., 2003; Wolters *et al*., 2005). Paralleling spike-time-dependent plasticity (STDP) in slice preparations, the direction of PAS-induced cortical plasticity critically depends upon the ISI. If sensory input from median nerve stimulation reaches the $M1_{HAND}$ shortly prior to TMS, PAS potentiates regional cortical excitability. Conversely, if TMS precedes the arrival of sensory input to the cortex, PAS causes a suppression of cortical excitability. These excitability changes are timing-dependent, long-lasting, effector-specific (Stefan *et al*., 2000), and can be blocked by *N*-methyl-D-aspartate (NMDA) receptor antagonists (Stefan *et al*., 2002), and are thus thought to reflect LTP-like and LTD-like plasticity.

In three sessions, we applied PAS of the right median nerve and left $M1_{HAND}$ before sleep to induce either LTP-like ($PAS_{N20+2ms}$), LTD-like ($PAS_{N20-5ms}$), or no after-effects ($PAS_{control}$) on excitability in the conditioned $M1_{HAND}$. We expected $PAS_{N20+2ms}$ and $PAS_{N20-5ms}$ to produce opposite effects on local oscillatory activity in sensorimotor

Correspondence: T. O. Bergmann, as above.
E-mail: t.bergmann@neurologie.uni-kiel.de

Received 3 December 2007, revised 29 January 2008, accepted 26 February 2008

areas during subsequent NREM sleep. Specifically, we hypothesized that interindividual differences in the efficacy of $PAS_{N20+2ms}$ and $PAS_{N20-5ms}$ to alter regional cortical excitability should be reflected in the local expression of SWA and sleep spindles in the conditioned $M1_{HAND}$. Preliminary results have been presented at the Society for Neuroscience Meeting 2007 (Bergmann *et al.*, 2007).

Materials and methods

Participants

Twelve healthy right-handed male volunteers (mean age 25.9 years, range 19–33 years) participated in the experiments after they had given written informed consent. All participants were non-smokers, free of medication, and had no history of neurological or psychiatric disease. They slept 7–9 h per night and reported no major disruptions of the sleep–wake cycle during the 4 weeks before experimentation. Participants were not allowed to ingest alcohol or engage in excessive manual activities involving physical exertion (e.g. sport) or skilled movements (e.g. piano playing) during the day before experimental nights. They reported to have slept about 7 h 39 min (± 1 h 21 min SD) during the preceding night and a repeated-measures ANOVA revealed no differences between PAS protocols. An adaptation night, approximately 1 week prior to the first experimental night, accustomed participants to sleeping under laboratory conditions. Participants were not preselected due to their responsiveness to PAS and had never been exposed to transcranial stimulation prior to the study. While cortical excitability changes could be analysed for the entire group ($n = 12$), EEG data of two participants had to be excluded from analyses ($n = 10$) because they showed early REM sleep onset and no slow wave sleep during the first sleep cycle. Experimental procedures conformed to the Declaration of Helsinki and were approved by the Ethics Committee of the University of Kiel.

Experimental procedure

Each participant took part in three experimental sessions performed at least 1 week apart (Fig. 1A). In each session, participants received $PAS_{N20+2ms}$, $PAS_{N20-5ms}$ or $PAS_{control}$ of the right median nerve and the left $M1_{HAND}$ before they went to sleep. The order of PAS interventions was counterbalanced across participants, who were blind regarding the purpose of the study and the type of PAS that was applied in a given session. Participants arrived at the laboratory around 20:00 h and PAS sessions started around 22:00 h after placement of recording electrodes. During PAS, participants were seated in a bed in a comfortable semi-upright position. The head and right arm were stabilized with cushions. The conditioning effects of PAS on excitability of the left $M1_{HAND}$ were probed at rest using single-pulse TMS. We recorded 60 motor-evoked potentials (MEPs) from three relaxed hand muscles before and 10 min after the end of PAS conditioning. The room was then darkened and subjects were allowed to sleep from 23:00 to 07:00 h. Polysomnography and 27-channel EEG were continuously recorded during sleep. Finally, we recorded 60 additional MEPs in the next morning, approximately 20 min after participants had woken up.

Paired associative stimulation

PAS consisted of 200 pairs of stimuli which were given every 6 s (varied from 5.1 to 6.9 s), resulting in a total stimulation time of 20 min. Each stimulus pair consisted of a peripheral stimulus given to the right median nerve at the wrist followed by a transcranial magnetic stimulus applied to the left $M1_{HAND}$ after a certain ISI. According to the approach of Ziemann and colleagues (Ziemann *et al.*, 2004; McDonnell *et al.*, 2007; Müller *et al.*, 2007) we individually adjusted the ISI to the shortest neuronal travel time of afferent input from wrist to cortex, which is reflected in the latency of the N20 component of the somatosensory evoked potential, to optimize the pairing of stimulation in $M1_{HAND}$. Somatosensory evoked potentials (200 trials; C3′-Fz electrode montage; stimulation parameters equivalent to PAS, see below) were obtained from each participant at the evening of the adaptation night (mean N20 latency = 20.07 ms, SD = 0.83 ms, min. = 19.0 ms, max. = 21.4 ms). For each participant, we chose an ISI that was 2 ms longer than the N20 latency (ensuring that the

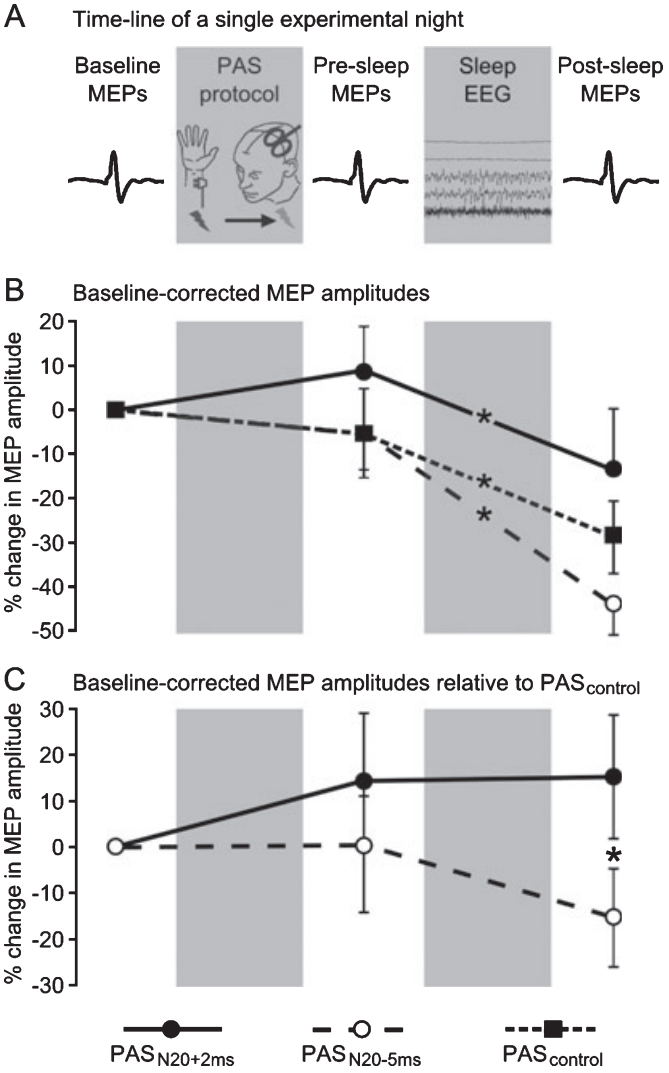

FIG. 1. (A) Schematic illustration of the time-line of a single experimental night. MEPs were measured directly before (baseline MEPs) application of PAS protocols ($PAS_{N20+2ms}$, $PAS_{N20-5ms}$ or $PAS_{control}$), 10 min afterwards (pre-sleep MEPs) and the next morning 20 min after awakening (post-sleep MEPs). Sleep was recorded polysomnographically during the night. Means and standard errors of the means (SEM) of 60 MEPs in the APB muscle are displayed for each time of measurement and PAS condition ($PAS_{N20+2ms}$ = solid line, filled circles; $PAS_{N20-5ms}$ = dashed line, empty circles; $PAS_{control}$ = dotted line, filled squares). Asterisks indicate significant paired *t*-tests at $P < 0.05$. (B) MEP amplitude depicted as percentage change from individual baseline. (C) MEP amplitude depicted as percentage change from individual baseline followed by subtraction of the corresponding $PAS_{control}$ values.

sensory input reaches $M1_{HAND}$ shortly before TMS) to potentiate the excitability of corticospinal output neurons in the left $M1_{HAND}$ ($PAS_{N20+2ms}$). Conversely, we selected an ISI that was 5 ms shorter than the N20 latency (ensuring that the sensory input reaches $M1_{HAND}$ shortly after TMS) to cause a lasting suppression of excitability ($PAS_{N20-5ms}$). As a control ($PAS_{control}$), we applied PAS with variable ISIs (290, 250, 210, 170, −60, −100, −140 and −180 ms randomized across trials) (cf. Müller *et al*., 2007). As $PAS_{control}$ lacked a consistent temporal pairing between the peripheral and transcranial stimulus, it is thought to be ineffective in producing a lasting change in motor cortical excitability due to STDP-dependent plasticity. Additionally, we extended the approach of Müller and colleagues by only using ISIs lying outside the time window in which PAS was shown to induce STDP-like plasticity effectively (Wolters *et al*., 2003). The individual N20 latencies were determined during the evening before the adaptation night.

The right median nerve, innervating the abductor pollicis brevis (APB) muscle, was stimulated at the wrist using standard bar electrodes, with the cathode positioned proximally. A Digitimer DS7A constant-current stimulator (Digitimer, Welwyn Garden City, Herts., UK) generated square-wave stimuli with a duration of 1 ms. Stimulus intensity was 4.5 mA, corresponding to approximately 450% of the averaged perceptual threshold (individual range 281–750%) and evoking slight thumb twitches. TMS over the left $M1_{HAND}$ was performed using a figure-of-eight shaped magnetic coil with an outer diameter of 70 mm connected to a High Power Magstim 200 stimulator (Magstim, Whitland, Dyfed, UK). The magnetic stimulus had a nearly monophasic pulse configuration with a rise time of about 100 μs, decaying back to zero over about 800 μs. The coil was held tangentially to the skull with the handle pointing backwards and laterally at an angle of 45° to the sagittal plane. At this position, the monophasic electromagnetic pulse induced an electrical current in the brain tissue with a posterior-lateral to anterior-medial direction approximately perpendicular to the central sulcus. This current orientation is known to be optimal for evoking a motor response in the contralateral hand (Mills *et al*., 1992). The site at which stimuli at slightly suprathreshold intensity consistently yielded maximal MEPs in the contralateral APB muscle was marked with a pen on the EEG cap as the 'motor hot spot' and used for TMS of the $M1_{HAND}$. For PAS and MEP measurements, TMS intensity was adjusted at the beginning of each experimental session ($PAS_{N20+2ms}$, $PAS_{N20-5ms}$, $PAS_{control}$) to elicit a mean peak-to-peak MEP amplitude of approximately 1 mV in the relaxed contralateral APB muscle (mean ± SD: 66.5 ± 13% maximal stimulator output). During the TMS measurements, the experimenter who held the coil received no on-line feedback of the evoked MEP amplitudes to avoid any bias towards the expected effects.

Measurements of motor cortex excitability

Single-pulse TMS was used to assess corticospinal excitability before (baseline MEP measurement), 10 min after the end of PAS (pre-sleep MEP measurement) and the next morning 20 min after participants had woken up (post-sleep MEP measurement). The coil position and orientation as well as stimulus configuration were the same as during PAS and stimulation intensity remained constant during baseline, pre- and post-sleep measurements of each experimental session. This ensured that we probed excitability in the same set of neurons that were conditioned by PAS. Cortical excitability was assessed in two consecutive blocks of 30 trials with an ISI of 7 s, varying from 4.9 to 9.1 s. Surface electromyographic (EMG) activity was recorded from the right APB muscle (targeted by PAS) as well as first dorsal interosseus (FDI) muscle and abductor digiti minimi (ADM) muscle (both not targeted by PAS) with Ag-AgCl surface electrodes using a bipolar belly tendon montage. During sleep, the right hand was bandaged to ensure a constant position of the EMG electrodes.

The raw EMG signals were amplified ×1000 (EEG-4421G, Nihon-Koden, Tokyo, Japan), filtered between 2 and 2000 Hz (plus 50-Hz notch) and digitized at 5000 Hz per channel (CED 1401 Plus, 12-bit-ADC; Cambridge Electronics, Cambridge, UK). The administration of TMS pulses as well as EMG data recording, storage and analyses was performed with Signal software (Cambridge Electronics). Peak-to-peak amplitudes of each MEP (mV) were measured off-line and mean MEP amplitudes were calculated for each time of measurement (i.e. baseline, pre-sleep and post-sleep). Sensitive for unspecific effects of stimulation and time, mean MEP amplitudes were initially expressed as percentage change from the individual baseline measurement. To control additionally for any unspecific effects depending on time, sleep or circadian rhythm, MEP amplitudes were thereafter adjusted by subtracting the corresponding $PAS_{control}$ values.

Polysomnographic and EEG recordings

EEG recordings were obtained from 27 channels (F3, F1, Fz, F2, F4, FC5, FC3, FC1, FC2, FC4, FC6, C5, C3, C1, Cz, C2, C4, C6, CP5, CP3, CP1, CP2, CP4, CP6, P3, Pz, P4; cap with Ag-AgCl ring electrodes; impedance < 5 kΩ) and both mastoids (A1, A2) referenced to Cz (later re-referenced to averaged A1 and A2). Additionally, we recorded surface EMG of the chin muscles and vertical and horizontal electro-oculograms with Ag-AgCl cup electrodes. The raw EEG signals were amplified ×10 000, filtered between 0.05 and 100 Hz (plus 50-Hz notch), and digitized at 500 Hz per channel (SynAmps, 16-bit-ADC; Neuroscan, El Paso, TX, USA). Data were recorded and stored with Acquire software version 4.2 (Neuroscan) and analysed using BrainVision Analyser software version 1.05.0004 (Brainproducts, Gilching, Germany).

Sleep stages were visually scored per 30-s epoch according to standard criteria (Rechtschaffen & Kales, 1968). Scoring was based on recordings from Fz (rather than C3 or C4) because PAS was given approximately over C3, and we wished to score sleep stages over a non-motor area that was not conditioned by PAS. Therefore, the overall proportion of SWS might have been slightly overestimated, although equally, for all experimental conditions. Only 30-s epochs of NREM sleep stages 2, 3 and 4 free of movement artefacts were included.

Previous studies reported distinct effects of plasticity-inducing protocols on local EEG activity during the first hour of NREM sleep (Huber *et al*., 2004, 2006, 2007). We thus performed EEG power analyses (FFT, 0.031 Hz per bin, 50% Hanning window) separately for all electrodes and PAS conditions, dividing the first NREM episode into three consecutive 20-min segments. Individual mean power values were calculated for the frequency bands of SWA (0.5–4 Hz), slow spindle activity (10–13 Hz) and fast spindle activity (13–16 Hz) for the entire time spend in NREM sleep. Values were normalized as percentage change from the $PAS_{control}$ condition to adjust for interindividual variance in EEG power and unspecific stimulation effects. Densities of slow and fast sleep spindles (as amount of discrete spindles per 30-s epoch) were separately calculated for all channels, 20-min epochs of NREM sleep and PAS conditions using an automatic spindle detection algorithm (Mölle *et al*., 2002; Clemens *et al*., 2005; Schmidt *et al*., 2006).

Data were band-pass filtered at 10–13 Hz (slow spindles) or 13–16 Hz (fast spindles) using a Butterworth zero phase distortion filter (48 dB per octave). To allow a clear dissociation between slow and fast spindles, additional band-rejection filters (4th order) were used to suppress the remaining power of adjacent frequency bands at 7–10 Hz and 13–16 Hz (slow spindles) or at 10–13 Hz and 16–20 Hz (fast spindles). A root mean square of the filtered signal was calculated using a moving average of 0.25 s width. Spindles were detected by the algorithm when the root mean square signal exceeded the threshold of three standard deviations (calculated over all channels, segments and PAS protocols for each subject individually to adjust for interindividual variance) for at least 0.5 s but less than 3 s (ignoring very short signal drops under threshold for less than 100 ms). Comparisons between $PAS_{N20+2ms}$ and $PAS_{N20-5ms}$ were conducted after adjusting for unspecific stimulation effects by subtracting corresponding values of the $PAS_{control}$ condition.

Statistical analyses

Statistical analyses of MEP amplitudes relied on repeated-measures ANOVA as well as *post hoc* paired *t*-tests. To test for any unspecific effects depending on time, sleep or circadian rhythm, ANOVA was based on the factors PAS protocol ($PAS_{N20+2ms}$, $PAS_{N20-5ms}$, $PAS_{control}$) and time of measurement (pre-sleep, post-sleep) with the baseline-adjusted MEP amplitudes as dependent variable. To reveal PAS-specific differences, ANOVA was based on the factors PAS protocol ($PAS_{N20+2ms}$, $PAS_{N20-5ms}$) and time of measurement (pre-sleep, post-sleep) using the additionally $PAS_{control}$-adjusted MEP amplitudes as dependent measure. For statistical analyses of EEG power and spindle density we applied non-parametric permutation testing (Nichols & Holmes, 2002; Huber *et al*., 2004, 2006, 2007) corrected for multiple comparisons (27 electrodes; $P_{corr} < 0.05$) to test for topographically specific differences in SWA as well as slow and fast spindle power and density between PAS conditions (see Supplementary material, Appendix S1 for details). We also used non-parametric permutation testing (see supplementary Appendix S1 for details) to test for correlations between the 'individual PAS efficacy' (separately calculated for pre- and post-sleep measurements) and the differential effect of PAS protocols on EEG power and spindle density. 'Individual PAS efficacy' was defined as the combined efficacy of $PAS_{N20+2ms}$ to potentiate and $PAS_{N20-5ms}$ to suppress motor cortical excitability relative to the individual baseline (percentage change in mean MEP amplitude after $PAS_{N20+2ms}$ minus percentage change in mean MEP amplitude after $PAS_{N20-5ms}$) (see supplementary Fig. S1).

Results

Motor evoked potentials

MEP amplitudes in the APB muscle showed a substantial decrease relative to individual baseline across a night of sleep ($F_{1,11} = 31.18$, $P < 0.001$), which was evident in all experimental sessions ($PAS_{N20+2ms}$: $T_{11} = 3.00$, $P = 0.012$; $PAS_{N20-5ms}$: $T_{11} = 4.63$, $P < 0.001$; $PAS_{control}$: $T_{11} = 2.95$, $P = 0.013$; Fig. 1B; see raw MEP data in supplementary Table S1). This decrease in MEP size might reflect a general synaptic downscaling mechanism in the framework of a hypothesized homeostatic function of sleep (Tononi & Cirelli, 2006). Focusing on the differences between PAS protocols, we found a differential effect of PAS on post-interventional MEPs. The increase of $PAS_{control}$-adjusted MEP amplitudes after $PAS_{N20+2ms}$ differed significantly from the decrease after $PAS_{N20-5ms}$ ($F_{1,11} = 6.82$, $P = 0.024$). This difference had previously been masked by the global overnight attenuation of MEP amplitudes (Fig. 1C). Consequently, after adjustment there was no effect of time of measurement ($P = 0.417$). Of note, we found no interaction between the type of PAS protocol and the time of measurement ($P = 0.169$), showing that the differential effect of $PAS_{N20+2ms}$ and $PAS_{N20-5ms}$ on MEP amplitudes did not decay during a night of sleep. Previous experiments examined the after-effects of PAS on MEP amplitude only during wakefulness, showing that PAS-induced MEP changes had tapered off 90 min after the end of PAS (Stefan *et al*., 2000; Wolters *et al*., 2003). Therefore, we were interested to know whether $PAS_{N20+2ms}$ and $PAS_{N20-5ms}$ still resulted in a significant difference in MEP amplitude after a night of sleep. To this end, we used paired *t*-tests as a more descriptive approach to explore the difference between $PAS_{N20+2ms}$ and $PAS_{N20-5ms}$ separately for pre-sleep and post-sleep measurements although *post-hoc* testing was not motivated by a significant interaction in the ANOVA. Notably, we found a consistent difference in the after-effect on MEP amplitude between the two PAS protocols after a full night of sleep ($T_{11} = 2.59$, $P = 0.025$), while this difference was less pronounced in the evening shortly after PAS ($T_{11} = 1.66$, $P = 0.124$). Thus, if anything, PAS after-effects became strengthened over night.

In addition, FDI and ADM muscles, which were not targeted by PAS, also showed an unspecific overnight decrease in MEP amplitudes but no differential after-effects of PAS conditioning for the $PAS_{control}$-adjusted values (see supplementary Tables S2 and S3 for details).

Sleep EEG power and spindle density

No differences in global sleep architecture were present among PAS protocols for any of the 20-min segments or for the 60 min in total, as revealed by separate one-way repeated-measures ANOVA for every sleep parameter listed in Table 1. As a consequence, the following comparisons of regional EEG power and spindle density were not biased by global differences in sleep architecture after $PAS_{N20+2ms}$, $PAS_{N20-5ms}$ and $PAS_{control}$.

SWA showed the well-known topographic distribution (Huber *et al*., 2004, 2006, 2007; Massimini *et al*., 2004) with a medial frontal maximum and a gradual attenuation towards posterior-lateral electrodes (supplementary Fig. S2). Regional SWA differed between $PAS_{N20+2ms}$ and $PAS_{N20-5ms}$ in the right parietal cortex (CP2, CP4, CP6) (Fig. 2A and B). At these electrodes, the regional expression of SWA was reduced after $PAS_{N20+2ms}$ relative to $PAS_{N20-5ms}$ during the first 20 min of NREM sleep.

Power and density of slow spindles peaked at frontal electrodes while fast spindles were most strongly expressed over centro-parietal

TABLE 1. Sleep architecture for the analysed 60-min sleep period

	$PAS_{N20+2ms}$	$PAS_{N20-5ms}$	$PAS_{control}$
Sleep latency (min)	13.85 ± 4.12	7.50 ± 1.43	7.20 ± 1.88
Waking (%)	1.66 ± 1.14	0.08 ± 0.50	0.50 ± 0.41
Stage 1 (%)	0.83 ± 0.50	0.08 ± 0.08	0.08 ± 0.08
Stage 2 (%)	36.75 ± 4.32	39.50 ± 7.36	35.25 ± 5.82
Slow wave sleep (%)	59.25 ± 5.47	58.25 ± 7.86	60.58 ± 7.93
NREM sleep (%)	96.83 ± 1.38	97.83 ± 1.08	95.92 ± 2.65
REM sleep (%)	1.50 ± 0.89	2.08 ± 1.10	3.42 ± 2.62

Mean values ± SEM are shown for the analysed 60 min of sleep beginning with first epoch of sleep stage 2 ($n = 10$). One-way repeated-measures ANOVAs revealed no significant differences between PAS conditions.

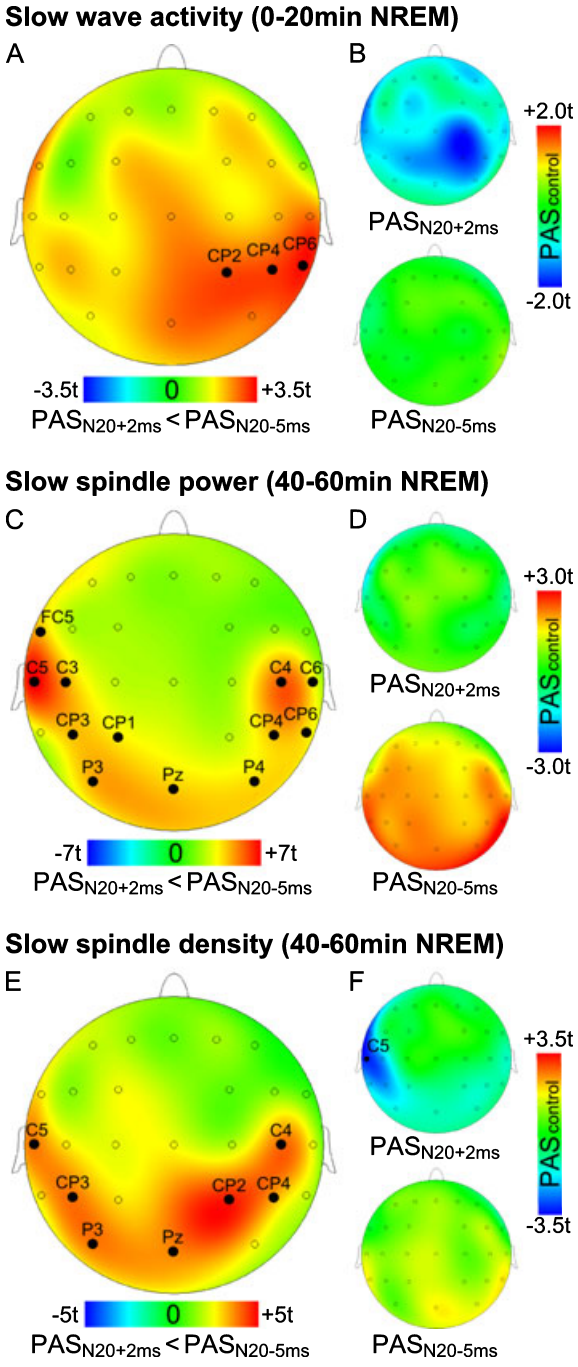

FIG. 2. Topographic distribution of *t*-values representing differences in SWA (A, B), slow spindle power (C, D) and slow spindle density (E, F). Note that the *t*-values of each map are scaled differently to highlight the regional differences. The left panels (A,C,E) give the *t*-maps of regional differences in SWA (A), slow spindle power (C) and slow spindle density (E) between $PAS_{N20+2ms}$ and $PAS_{N20-5ms}$. These maps are based on percentage changes in power values and absolute change of spindle density. Filled circles indicate electrode sites where $PAS_{N20-5ms}$ significantly exceeds $PAS_{N20+2ms}$ as revealed by non-parametric permutation testing ($P_{corr} \leq 0.05$, corrected for multiple comparisons). The right panels (B,D,F) provide *t*-maps of deviations in SWA (B), slow spindle power (D) and slow spindle density (F) after $PAS_{N20+2ms}$ and $PAS_{N20-5ms}$ relative to $PAS_{control}$. The *t*-maps are based on percentage changes in power values and absolute change of spindle density. Changes in SWA refer to the first 20-min NREM segment, while changes in slow spindle power and density refer to the third 20-min NREM segment.

regions (supplementary Figs S2 and S3), which is in good agreement with previous work (De Gennaro & Ferrara, 2003; Schabus *et al.*, 2006, 2008; Schmidt *et al.*, 2006). $PAS_{N20-5ms}$ and $PAS_{N20+2ms}$ resulted in regional differences in power and density of slow but not fast sleep spindles, reaching significance in the third 20-min segment of NREM sleep. We found slow spindle power after $PAS_{N20-5ms}$ to be enhanced compared with $PAS_{N20+2ms}$ at electrodes overlying left fronto-central cortex (FC5) and the lateral part of the right and left centro-parietal cortex (C5, C3, C4, C6, CP3, CP1, CP4, CP6, P3, Pz, P4; Fig. 2C and D). Likewise, slow spindle density after $PAS_{N20-5ms}$ exceeded that after $PAS_{N20+2ms}$ measured bilaterally over centro-parietal areas (C5, C4, CP3, CP2, CP4, P3, Pz; Fig. 2E and F).

Correlational analyses of PAS efficacy and sleep EEG

To take into account the substantial interindividual variation in the efficacy of $PAS_{N20+2ms}$ to potentiate and of $PAS_{N20-5ms}$ to suppress pre-sleep MEP amplitudes (see supplementary Fig. S1), we additionally performed correlational analyses.

Individual pre-sleep PAS efficacy on MEP amplitude correlated with differences in the expression of slow sleep spindles at those electrode sites approximately overlying the conditioned $M1_{HAND}$ and the adjacent premotor cortex. In parallel with comparisons of mean EEG values, this correlation was only found during the third 20 min of NREM sleep. At C3, pre-sleep PAS efficacy was strongly correlated with the differential effect of $PAS_{N20-5ms}$ and $PAS_{N20+2ms}$ on slow spindle density (i.e. mean spindle density after $PAS_{N20-5ms}$ minus mean spindle density after $PAS_{N20+2ms}$) ($r = 0.82$, $P_{corr} = 0.033$; Fig. 3A and D). The more $PAS_{N20-5ms}$ suppressed mean MEP amplitude relative to the increase by $PAS_{N20+2ms}$, the stronger the regional density of slow spindles at C3 after $PAS_{N20-5ms}$ relative to $PAS_{N20+2ms}$. Practically the same correlation was present for slow spindle power at the neighbouring recording site FC3 ($r = 0.81$, $P_{corr} = 0.035$; Fig. 3B and E).

In turn, the differential effect on slow spindle density in the third 20-min NREM segment at the adjacent recording site FC5 was significantly correlated with individual post-sleep PAS efficacy ($r = 0.82$, $P_{corr} = 0.049$; Fig. 3C and F). That is, the more the density of slow sleep spindles increased after $PAS_{N20-5ms}$ and decreased after $PAS_{N20+2ms}$, the stronger the individual PAS-efficacy the next morning.

In contrast, neither SWA nor fast spindle power or density correlated with PAS-efficacy (pre- or post-sleep) at any recording site during the analysed 60-min period of NREM sleep. Also, none of the analysed frequency bands or spindle densities significantly predicted the overnight change in cortical excitability.

Discussion

Using PAS as a non-invasive means to induce regional plasticity in the human cortex (Stefan *et al.*, 2000, 2002, 2004; Wolters *et al.*, 2003; Classen *et al.*, 2004), we show that the induction of regional LTP- and LTD-like plasticity in the human $M1_{HAND}$ during wakefulness is followed by changes in the regional expression of slow spindles and SWA within the first hour of NREM sleep. Interestingly, the efficacy of $PAS_{N20+2ms}$ and $PAS_{N20-5ms}$ to produce LTP- or LTD-like after-effects on motor cortical excitability prior to sleep predicted the individual changes in slow spindle power and density in the conditioned $M1_{HAND}$. Given that slow spindles, in contrast to fast spindles, seemed to be affected by the induction of LTD-like plasticity through $PAS_{N20-5ms}$, we further discuss their potential functional significance.

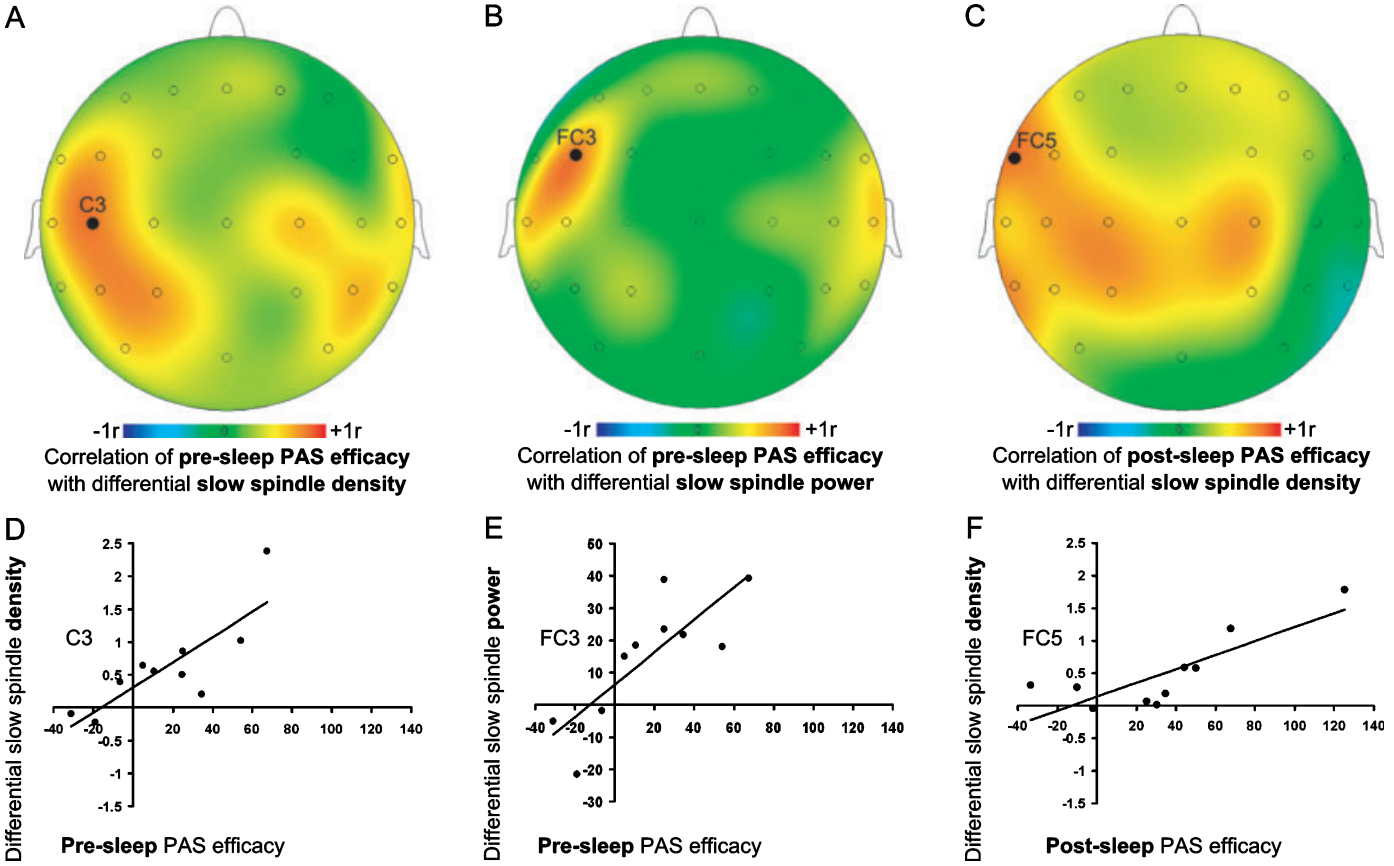

FIG. 3. Topographic distribution of correlation coefficients (*r*-values) between individual PAS efficacy ($PAS_{N20+2ms}$ minus $PAS_{N20-5ms}$) and the differential effect of the two PAS protocols on EEG values ($PAS_{N20-5ms}$ minus $PAS_{N20+2ms}$): (A) pre-sleep PAS efficacy and slow spindle density, (B) pre-sleep PAS efficacy and slow spindle power, (C) post-sleep PAS efficacy and slow spindle density. All data refer to the third 20-min NREM segment. Filled circles indicate electrodes with significant correlations ($P_{corr} < 0.05$, corrected for multiple comparisons). Thus, the more $PAS_{N20+2ms}$ potentiated and $PAS_{N20-5ms}$ suppressed motor cortical excitability, the stronger were the decrease and increase, respectively, of slow spindle density and power at the site of TMS (over left $M1_{HAND}$) and adjacent premotor cortex. Scatter plots with regression lines depicting individual data for (D) pre-sleep PAS efficacy and slow spindle density at C3 ($r = 0.82$, $P_{corr} = 0.033$), (E) pre-sleep PAS efficacy and slow spindle power at FC3 ($r = 0.81$, $P_{corr} = 0.035$) and (F) post-sleep PAS efficacy and slow spindle density at FC5 ($r = 0.82$, $P_{corr} = 0.049$).

PAS was chosen for two reasons. First, its efficacy depends critically on the consistent temporal pairing of the peripheral and cortical stimulus (Müller *et al.*, 2007). Thus, it was possible to include a control condition (i.e. $PAS_{control}$) which produced the same amount of neuronal stimulation as $PAS_{N20+2ms}$ and $PAS_{N20-5ms}$ without inducing plastic changes in the stimulated cortex. Second, the appropriate ISI between the peripheral and cortical stimulus defines the direction of PAS-induced plasticity (Wolters *et al.*, 2003). This enabled us to induce LTP- and LTD-like plasticity by means of stimulation protocols which differed only in the ISI (i.e. $PAS_{N20+2ms}$ and $PAS_{N20-5ms}$) but were identical with respect to number of stimuli applied, stimulus intensity and overall duration of intervention. This excludes the possibility that differences in the effects of $PAS_{N20+2ms}$ and $PAS_{N20-5ms}$ were caused by general differences in brain stimulation.

PAS effects on motor cortical excitability

Although we found a consistent differential effect of $PAS_{N20+2ms}$ and $PAS_{N20-5ms}$ on cortical excitability at the group level, individual PAS efficacy showed considerable interindividual variability (see supplementary Fig. S1). This finding ties in with previous studies showing a considerable inter- as well as intra-individual variability in both strength and direction of PAS-induced plasticity (Fratello *et al.*, 2006; Meunier *et al.*, 2007; Sale *et al.*, 2007). Using a facilitatory PAS_{25ms} protocol, Meunier *et al.* (2007) demonstrated that about one-third of the participants did respond with a decrease in MEP amplitude size. As we did not preselect participants for the present study, both responsive as well as non-responsive participants were included. Furthermore, Sale *et al.* (2007) showed that a daytime difference in the application of PAS_{25ms} of only 4 h (~10:00 vs. ~14:00 h) markedly altered the robustness of PAS effects. It is thus conceivable that the late application of PAS in the present study (~22:00 h) along with the diverging individual responsiveness to PAS accounted for the large inter-individual variations in PAS efficacy.

Apparently, PAS-induced excitability changes are determined by several factors such as individual characteristics of motoneuron excitability (Meunier *et al.*, 2007), previous learning experience (Ziemann *et al.*, 2004; Müller *et al.*, 2007), neuronal background activity (Nitsche *et al.*, 2007), attentional state (Stefan *et al.*, 2004) and circadian rhythm (Sale *et al.*, 2007). Therefore, a combination of these factors might have contributed to the variable responses to PAS conditioning in the present study.

Despite the high inter-individual variability in PAS efficacy, the mean differential effect of $PAS_{N20+2ms}$ and $PAS_{N20-5ms}$ on the excitability of

$M1_{HAND}$ did persist after a full night of sleep. Concurrently, overnight sleep was associated with a general MEP attenuation evident across all PAS protocols and muscles. While FDI and ADM muscles (innervated by the ulnar nerve) were also affected by the global overnight attenuation of MEP amplitudes, only the APB muscle (innervated by the median nerve and thus targeted by PAS) showed a relative LTP- and LTD-like after-effect. The somatotopic specificity of the PAS effect is in accordance with previous studies (Stefan *et al*., 2000; Quartarone *et al*., 2003; Wolters *et al*., 2005; Weise *et al*., 2006), and corroborates the interpretation that the bidirectional changes in cortical excitability were indeed caused by $PAS_{N20+2ms}$ and $PAS_{N20-5ms}$.

The maintenance of PAS-induced changes in cortical excitability across a night of sleep is consistent with the notion that sleep supports the consolidation of newly acquired memories (Stickgold, 2005; Born *et al*., 2006). Within this framework, the initially labile and weak PAS-induced memory trace in the $M1_{HAND}$ is strengthened during subsequent sleep via repeated reactivation of the involved neuronal circuits (Born *et al*., 2006; Marshall & Born, 2007). The PAS-induced changes in cortical excitability are also in accord with the concept of synaptic downscaling, i.e. a process linked to SWA that prevents neuronal networks from becoming overactive due to cumulated induction of LTP during wakefulness (Tononi & Cirelli, 2006). Synaptic downscaling globally reduces excitability of neurons while maintaining the proportion of its synaptic weights and thereby improves the signal-to-noise ratio of neuronal representations. In line with this concept, motor cortical excitability was consistently reduced in all PAS conditions and muscles after a night of sleep, while the bidirectional effector-specific effect of $PAS_{N20+2ms}$ and $PAS_{N20-5ms}$ persisted at least until the next morning.

Because we did not study the after-effects of PAS on cortical excitability in the absence of sleep, we cannot prove that the apparent overnight maintenance of PAS-induced LTP- and LTD-like plasticity was actually caused by sleep, as merely time or circadian rhythm could be alternative explanations. However, this seems unlikely because after-effects of PAS during wakefulness usually attenuate over time and last for only 30–90 min (Stefan *et al*., 2000; Wolters *et al*., 2003), whereas in the present study PAS-induced changes in cortical excitability did not taper off during a night of sleep. Additional work needs to be done to clarify how sleep shapes the excitability changes that are induced by transcranial stimulation techniques during wakefulness.

PAS effects on oscillatory cortical activity during NREM sleep

PAS of the right median nerve and left $M1_{HAND}$ during wakefulness modified the regional expression of SWA and slow spindles within the first hour of subsequent NREM sleep while leaving global sleep architecture unaffected. In agreement with previous studies (Huber *et al*., 2004, 2006, 2007), effects on cortical oscillatory activity were restricted to limited time windows within the first hour of NREM sleep. More precisely, changes in SWA were observed during the first 20 min only, whereas slow spindle power and density were affected exclusively during the third 20 min, suggesting that differences might become evident only when the power of the respective frequency band is at its relative minimum within all three analysed 20-min NREM segments (as can be seen in supplementary Figs S2 and S3).

Regional SWA was reduced in right parietal somatosensory areas after $PAS_{N20+2ms}$ compared with $PAS_{N20-5ms}$ (Fig. 2A and B). No change in regional SWA occurred in the stimulated $M1_{HAND}$. At first sight, these findings seem to be at variance with a recent TMS-EEG study (Huber *et al*., 2007), which might have predicted an increase in regional SWA of the stimulated $M1_{HAND}$ after $PAS_{N20+2ms}$. It is possible that the presumed facilitatory effect of $PAS_{N20+2ms}$ on local SWA was simply not strong enough to be detected by the limited number of EEG channels (i.e. 27) as Huber found significant changes in only three to six out of 60–256 channels (Huber *et al*., 2004, 2006, 2007). Alternatively, in those previous studies the mere amount of evoked neuronal activity during the intervention might actually have had substantial impact on the local expression of SWA. In the present study, however, for the first time the amount of evoked neuronal activity was held constant across experimental manipulations. This methodological difference may also contribute to the lack of a significant change in SWA in $M1_{HAND}$.

However, in accordance with our findings, Huber *et al*. (2007) also failed to find SWA changes in the stimulated $M1_{HAND}$ after inducing LTP-like plasticity with 5-Hz rTMS, but found changes in SWA in remote cortical areas. In that study, pre-sleep 5-Hz rTMS led to an marked regional increase in SWA and fast spindle power in the left premotor cortex. Additionally, there was a non-significant decrease of SWA covering most of the contralateral right parietal cortex (cf. Huber *et al*., 2007; Fig. 2A). The ability of PAS to modify neuronal activity in distant brain areas was also demonstrated in a recent TMS-EEG study (Murakami *et al*., 2008), which found a consistent change in somatosensory evoked potentials and high-frequency oscillations in the somatosensory cortex after ipsilateral PAS of the $M1_{HAND}$. Likewise, we found regional changes in the expression of slow sleep spindles not to be restricted to the conditioned $M1_{HAND}$ as PAS had relatively widespread effects on slow spindle activity in remote sensorimotor regions and parietal association areas (Fig. 2C–F). The fact that differences in slow spindles were predominantly observed at centro-parietal sites is not in contrast to their well-known frontal maximum, given the assumption that changes in cortical oscillatory activity during sleep are topographically related to the location of previously induced changes in cortical plasticity and not to the general distribution of the frequency band.

How can these widespread effects of PAS be explained? It is known that TMS-evoked neuronal activity spreads via long-range trans-synaptic connections to associated brain regions (Massimini *et al*., 2005, 2007; Huber *et al*., 2007), where it can induce effects on cortical plasticity via inhibitory pathways (Gilio *et al*., 2003). In the case of PAS, peripheral nerve stimulation excites multiple sensorimotor cortical areas, and the transcranial stimulus produces a trans-synaptic spread of neuronal excitation from the stimulated $M1_{HAND}$ to other cortical regions via cortico-cortical connections. Thus, PAS might induce excitability changes paralleling STDP not only in the $M1_{HAND}$ but also in other sensorimotor areas that receive sensory input and are connected with the $M1_{HAND}$. The actual temporal order of inputs may therefore determine the particular direction of PAS-induced after-effects on cortical excitability in these remote cortical areas, which may differ from those induced in the $M1_{HAND}$.

However, correlational analyses, accounting for the substantial variability of the PAS effect, disclosed a strikingly focal signature of PAS efficacy in the expression of slow sleep spindles (Fig. 3). The more $PAS_{N20+2ms}$ had potentiated and $PAS_{N20-5ms}$ had suppressed excitability of $M1_{HAND}$ in the evening, the stronger was the augmentation of slow sleep spindles during NREM sleep after $PAS_{N20-5ms}$ relative to $PAS_{N20+2ms}$. This correlation was closely restricted to the conditioned $M1_{HAND}$ and the adjacent premotor cortex (as a more precise anatomical localization is not possible by means of 27-channel EEG recordings). Moreover, this differential expression of slow spindles still correlated with the individual PAS efficacy the next morning (about 8–9 h later), though we did not find a direct relationship between the expression of sleep spindles and the overnight change in motor cortical excitability. The remarkable size of correlations ($r > 0.8$), however,

indicates that regional expression of slow sleep spindles strongly depends on whether predominant LTD- or LTP-like plasticity has been induced in respective circuitry.

These $PAS_{N20-5ms}$ effects on slow spindle power and density may appear counterintuitive at first sight. One might expect that the more learning in the evening, the more LTP will be induced, and the stronger the local up-regulation of sleep spindles. However, this idea might be oversimplified for two reasons. First, learning does not equal LTP, but is rather a tuning of synaptic weights in neuronal networks that is based on both LTP and LTD. Second, sleep spindles are not a uniform phenomenon, as there is increasing evidence that slow and fast spindles do not only differ in their topography (Anderer *et al*., 2001) but are also functionally segregated. It is known that both spindle types are functionally dissociated regarding age and maturation, homeostatic and circadian factors, menstrual cycle phase, pregnancy, and pharmacological agents (for a review see De Gennaro & Ferrara, 2003) as well as their haemodynamic correlates (Schabus *et al*., 2007). It has also been suggested that slow spindles, which have a greater topographical variability including also parietal areas, predominantly reflect cortico-cortical coupling, while fast spindles are more closely associated with thalamo-cortical coupling (Doran, 2003).

This study provides further evidence that both slow (≤ 13 Hz) and fast (≥ 13 Hz) sleep spindles are differently influenced by recent changes in neuronal plasticity and might play a different role for plasticity during sleep. Unfortunately, most behavioural learning studies neither differentiated between slow and fast spindles nor used a consistent frequency range when relating the expression of sleep spindles to the sleep-dependent consolidation of declarative (Gais *et al*., 2002: 12–15 Hz; Schabus *et al*., 2004: 11.5–16 Hz; Clemens *et al*., 2005, 2006: 11–16 Hz; Schmidt *et al*., 2006: 11.25–13.75 Hz) or procedural memories (Fogel & Smith, 2006: 12–16 Hz; Fogel *et al*., 2007: 12–14 Hz; Nishida & Walker, 2007: 12–16Hz). While some studies involving declarative memory consolidation reported enhanced slow spindle activity, in part associated with enhanced SWA (Mölle *et al*., 2004; Marshall *et al*., 2006), Huber and colleagues (Huber *et al*., 2004, 2006, 2007) found changes in fast but not slow spindle power mirroring those in SWA at selected electrode sites after different interventional protocols. However, power values in the spindle range were not consistently reported in these studies for electrode sites lacking changes in SWA. While topographical specificity of fast spindle power has been demonstrated in one study (Huber *et al*., 2006), it remains open whether changes also occurred in slow spindle power at the remaining electrode sites. On a mere descriptive level, effects on slow spindle power even appeared to be inverted relative to those on fast spindle power (cf. Huber *et al*., 2004: fig. 3a; Huber *et al*., 2006: fig. 6a).

As spindles are thought to be associated with considerable dendritic Ca^{2+} influx, they have been commonly related to the induction of LTP rather than LTD (Werk *et al*., 2005). However, recent studies have revealed that *in vitro* as well as *in vivo* stimulation in the slow spindle frequency range of ~10 Hz can induce both LTP as well as LTD in the somatosensory cortex of the rat (Rosanova & Ulrich, 2005; Werk *et al*., 2006) depending on whether or not the stimulation is accompanied by postsynaptic action potentials in a Hebbian way (Rosanova & Ulrich, 2005). The synchronization with cortical slow oscillations (Mölle *et al*., 2002) as a gating mechanism might therefore be defining for the direction of plastic changes associated with the different spindle types. Potentially, slow and fast spindles are differentially grouped by slow oscillations, which might cause their suggested differential relation to LTP and LTD. However, future studies need specifically to test the hypothesis that fast spindles are more closely related to LTP-like plasticity and slow spindles are preferably associated with LTD-like plasticity.

Using PAS, we show that local expression of slow sleep spindles depends on the amount of previously induced cortical plasticity, as PAS-induced changes in spindle activity cannot be attributed to differences in the mere amount of induced neuronal activity during stimulation. Future research is necessary to elucidate further the neuronal mechanisms controlling the effects of cortical plasticity on oscillatory activity during sleep.

Supplementary material

The following supplementary material may be found on
http://www.blackwell-synergy.com

Appendix S1. Supplementary methods: non-parametric permutation testing.

Fig. S1. Individual MEP data of 10 subjects, for PASN20+2ms and PASN20-5ms, and related 'individual PAS efficacy'.

Fig. S2. The topographic distribution of slow wave activity, and slow and fast spindle power during the first 60 min of NREM sleep.

Fig. S3. The topographic distribution of slow and fast spindle density during the first 60 minutes of NREM sleep, averaged across all PAS protocols.

Table S1. Raw values for MEP amplitude size at the APM muscle.

Table S2. Statistical results as derived from ANOVA and *post-hoc* paired *t*-tests for baseline-corrected MEPs of the APM, FDI, and ADM muscles.

Table S3. Statistical results as derived from ANOVA for baseline-corrected MEPs adjusted to PAS control values of the APM, FDI, and ADM muscles.

Please note: Blackwell Publishing are not responsible for the content or functionality of any supplementary materials supplied by the authors. Any queries (other than missing material) should be directed to the correspondence author for the article.

Acknowledgements

This work was funded by the Deutsche Forschungsgemeinschaft (Project A6, SFB 654 'Plasticity and Sleep'). H.R.S. was supported by a structural grant from the Bundesministerium für Bildung und Forschung (01GO0511) to NeuroImageNord. We would like to thank Björn Rasch and Oliver Granert for computational assistance on the sleep spindle detection algorithm and the permutation tests.

Abbreviations

ADM, abductor digiti minimi; APB, abductor pollicis brevis; EEG, electroencephalogram; EMG, electromyogram; FDI, first dorsal interosseus; ISI, interstimulus interval; LTP, long-term potentiation; LTD, long-term depression; $M1_{HAND}$, hand area of the primary motor cortex; MEP, motor-evoked potential; NREM, non-rapid eye movement; PAS, paired associative stimulation; REM, rapid eye movement; rTMS, repetitive transcranial magnetic stimulation; STDP, spike-time-dependent plasticity; SWA, slow wave activity; TMS, transcranial magnetic stimulation.

References

Anderer, P., Klosch, G., Gruber, G., Trenker, E., Pascual-Marqui, R.D., Zeitlhofer, J., Barbanoj, M.J., Rappelsberger, P. & Saletu, B. (2001) Low-resolution brain electromagnetic tomography revealed simultaneously active frontal and parietal sleep spindle sources in the human cortex. *Neuroscience*, **103**, 581–592.

Bergmann, T.O., Mölle, M., Marshall, L., Kaya-Yildiz, L., Born, J. & Siebner, H.R. (2007) Paired associative stimulation of the motor cortex

affects local NREM sleep in humans: a TMS-EEG study. *Soc. Neurosci. Abstr.*, 22.7.
Born, J., Rasch, B. & Gais, S. (2006) Sleep to remember. *Neuroscientist*, **12**, 410–424.
Classen, J., Wolters, A., Stefan, K., Wycislo, M., Sandbrink, F., Schmidt, A. & Kunesch, E. (2004) Paired associative stimulation. *Suppl. Clin. Neurophysiol.*, **57**, 563–569.
Clemens, Z., Fabo, D. & Halasz, P. (2005) Overnight verbal memory retention correlates with the number of sleep spindles. *Neuroscience*, **132**, 529–535.
Clemens, Z., Fabo, D. & Halasz, P. (2006) Twenty-four hours retention of visuospatial memory correlates with the number of parietal sleep spindles. *Neurosci. Lett.*, **403**, 52–56.
De Gennaro, L. & Ferrara, M. (2003) Sleep spindles: an overview. *Sleep Med. Rev.*, **7**, 423–440.
Doran, S.M. (2003) The dynamic topography of individual sleep spindles. *Sleep Res. Online*, **5**, 133–139.
Fogel, S.M. & Smith, C.T. (2006) Learning-dependent changes in sleep spindles and Stage 2 sleep. *J. Sleep Res.*, **15**, 250–255.
Fogel, S.M., Smith, C.T. & Cote, K.A. (2007) Dissociable learning-dependent changes in REM and non-REM sleep in declarative and procedural memory systems. *Behav. Brain Res.*, **180**, 48–61.
Fratello, F., Veniero, D., Curcio, G., Ferrara, M., Marzano, C., Moroni, F., Pellicciari, M.C., Bertini, M., Rossini, P.M. & De Gennaro, L. (2006) Modulation of corticospinal excitability by paired associative stimulation: reproducibility of effects and intraindividual reliability. *Clin. Neurophysiol.*, **117**, 2667–2674.
Gais, S., Molle, M., Helms, K. & Born, J. (2002) Learning-dependent increases in sleep spindle density. *J. Neurosci.*, **22**, 6830–6834.
Gilio, F., Rizzo, V., Siebner, H.R. & Rothwell, J.C. (2003) Effects on the right motor hand-area excitability produced by low-frequency rTMS over human contralateral homologous cortex. *J. Physiol.*, **551**, 563–573.
Huber, R., Esser, S.K., Ferrarelli, F., Massimini, M., Peterson, M.J. & Tononi, G. (2007) TMS-induced cortical potentiation during wakefulness locally increases slow wave activity during sleep. *PLoS ONE*, **2**, e276.
Huber, R., Ghilardi, M.F., Massimini, M., Ferrarelli, F., Riedner, B.A., Peterson, M.J. & Tononi, G. (2006) Arm immobilization causes cortical plastic changes and locally decreases sleep slow wave activity. *Nature Neurosci.*, **9**, 1169–1176.
Huber, R., Ghilardi, M.F., Massimini, M. & Tononi, G. (2004) Local sleep and learning. *Nature*, **430**, 78–81.
Marshall, L. & Born, J. (2007) The contribution of sleep to hippocampus-dependent memory consolidation. *Trends Cogn. Sci.*, **11**, 442–450.
Marshall, L., Helgadottir, H., Molle, M. & Born, J. (2006) Boosting slow oscillations during sleep potentiates memory. *Nature*, **444**, 610–613.
Massimini, M., Ferrarelli, F., Esser, S.K., Riedner, B.A., Huber, R., Murphy, M., Peterson, M.J. & Tononi, G. (2007) Triggering sleep slow waves by transcranial magnetic stimulation. *Proc. Natl Acad. Sci. USA*, **104**, 8496–8501.
Massimini, M., Ferrarelli, F., Huber, R., Esser, S.K., Singh, H. & Tononi, G. (2005) Breakdown of cortical effective connectivity during sleep. *Science*, **309**, 2228–2232.
Massimini, M., Huber, R., Ferrarelli, F., Hill, S. & Tononi, G. (2004) The sleep slow oscillation as a traveling wave. *J. Neurosci.*, **24**, 6862–6870.
McDonnell, M.N., Orekhov, Y. & Ziemann, U. (2007) Suppression of LTP-like plasticity in human motor cortex by the GABA (B) receptor agonist baclofen. *Exp. Brain Res.*, **180**, 181–186.
Meunier, S., Russmann, H., Dambrosia, J. & Hallett, M. (2007) Susceptibility to develop PAS-induced plasticity depends on motoneurone excitability. *Soc. Neurosci. Abstr.*, 191.15.
Mills, K.R., Boniface, S.J. & Schubert, M. (1992) Magnetic brain stimulation with a double coil: the importance of coil orientation. *Electroencephalogr. Clin. Neurophysiol.*, **85**, 17–21.
Mölle, M., Marshall, L., Gais, S. & Born, J. (2002) Grouping of spindle activity during slow oscillations in human non-rapid eye movement sleep. *J. Neurosci.*, **22**, 10941–10947.
Mölle, M., Marshall, L., Gais, S. & Born, J. (2004) Learning increases human electroencephalographic coherence during subsequent slow sleep oscillations. *Proc. Natl Acad. Sci. USA*, **101**, 13963–13968.
Müller, J.F., Orekhov, Y., Liu, Y. & Ziemann, U. (2007) Homeostatic plasticity in human motor cortex demonstrated by two consecutive sessions of paired associative stimulation. *Eur. J. Neurosci.*, **25**, 3461–3468.
Murakami, T., Sakuma, K., Nomura, T., Uemura, Y., Hashimoto, I. & Nakashima, K. (2008) Changes in somatosensory-evoked potentials and high-frequency oscillations after paired-associative stimulation. *Exp. Brain Res.*, **184**, 339–347.
Nichols, T.E. & Holmes, A.P. (2002) Nonparametric permutation tests for functional neuroimaging: a primer with examples. *Hum. Brain Mapp.*, **15**, 1–25.
Nishida, M. & Walker, M.P. (2007) Daytime naps, motor memory consolidation and regionally specific sleep spindles. *PLoS ONE*, **2**, e341.
Nitsche, M.A., Roth, A., Kuo, M.F., Fischer, A.K., Liebetanz, D., Lang, N., Tergau, F. & Paulus, W. (2007) Timing-dependent modulation of associative plasticity by general network excitability in the human motor cortex. *J. Neurosci.*, **27**, 3807–3812.
Quartarone, A., Bagnato, S., Rizzo, V., Siebner, H.R., Dattola, V., Scalfari, A., Morgante, F., Battaglia, F., Romano, M. & Girlanda, P. (2003) Abnormal associative plasticity of the human motor cortex in writer's cramp. *Brain*, **126**, 2586–2596.
Rechtschaffen, A. & Kales, A. (1968) *A Manual of Standardized Terminology, Techniques and Scoring System for Sleep Stages of Human Subjects.* United States Government Printing Office, Washington, DC.
Rosanova, M. & Ulrich, D. (2005) Pattern-specific associative long-term potentiation induced by a sleep spindle-related spike train. *J. Neurosci.*, **25**, 9398–9405.
Sale, M.V., Ridding, M.C. & Nordstrom, M.A. (2007) Factors influencing the magnitude and reproducibility of corticomotor excitability changes induced by paired associative stimulation. *Exp. Brain Res.*, **181**, 615–626.
Schabus, M., Dang-Vu, T.T., Albouy, G., Balteau, E., Boly, M., Carrier, J., Darsaud, A., Degueldre, C., Desseilles, M., Gais, S., Phillips, C., Rauchs, G., Schnakers, C., Sterpenich, V., Vandewalle, G., Luxen, A. & Maquet, P. (2007) Hemodynamic cerebral correlates of sleep spindles during human non-rapid eye movement sleep. *Proc. Natl Acad. Sci. USA*, **104**, 13164–13169.
Schabus, M., Gruber, G., Parapatics, S., Sauter, C., Klosch, G., Anderer, P., Klimesch, W., Saletu, B. & Zeitlhofer, J. (2004) Sleep spindles and their significance for declarative memory consolidation. *Sleep*, **27**, 1479–1485.
Schabus, M., Hodlmoser, K., Gruber, G., Sauter, C., Anderer, P., Klosch, G., Parapatics, S., Saletu, B., Klimesch, W. & Zeitlhofer, J. (2006) Sleep spindle-related activity in the human EEG and its relation to general cognitive and learning abilities. *Eur. J. Neurosci.*, **23**, 1738–1746.
Schabus, M., Hoedlmoser, K., Pecherstorfer, T., Anderer, P., Gruber, G., Parapatics, S., Sauter, C., Kloesch, G., Klimesch, W., Saletu, B. & Zeitlhofer, J. (2008) Interindividual sleep spindle differences and their relation to learning-related enhancements. *Brain Res.*, **1191**, 127–135.
Schmidt, C., Peigneux, P., Muto, V., Schenkel, M., Knoblauch, V., Munch, M., de Quervain, D.J., Wirz-Justice, A. & Cajochen, C. (2006) Encoding difficulty promotes postlearning changes in sleep spindle activity during napping. *J. Neurosci.*, **26**, 8976–8982.
Stefan, K., Kunesch, E., Benecke, R., Cohen, L.G. & Classen, J. (2002) Mechanisms of enhancement of human motor cortex excitability induced by interventional paired associative stimulation. *J. Physiol.*, **543**, 699–708.
Stefan, K., Kunesch, E., Cohen, L.G., Benecke, R. & Classen, J. (2000) Induction of plasticity in the human motor cortex by paired associative stimulation. *Brain*, **123**, 572–584.
Stefan, K., Wycislo, M. & Classen, J. (2004) Modulation of associative human motor cortical plasticity by attention. *J. Neurophysiol.*, **92**, 66–72.
Stickgold, R. (2005) Sleep-dependent memory consolidation. *Nature*, **437**, 1272–1278.
Tononi, G. & Cirelli, C. (2006) Sleep function and synaptic homeostasis. *Sleep Med. Rev.*, **10**, 49–62.
Weise, D., Schramm, A., Stefan, K., Wolters, A., Reiners, K., Naumann, M. & Classen, J. (2006) The two sides of associative plasticity in writer's cramp. *Brain*, **129**, 2709–2721.
Werk, C.M., Harbour, V.L. & Chapman, C.A. (2005) Induction of long-term potentiation leads to increased reliability of evoked neocortical spindles in vivo. *Neuroscience*, **131**, 793–800.
Werk, C.M., Klein, H.S., Nesbitt, C.E. & Chapman, C.A. (2006) Long-term depression in the sensorimotor cortex induced by repeated delivery of 10 HZ. trains in vivo. *Neuroscience*, **140**, 13–20.
Wolters, A., Sandbrink, F., Schlottmann, A., Kunesch, E., Stefan, K., Cohen, L.G., Benecke, R. & Classen, J. (2003) A temporally asymmetric Hebbian rule governing plasticity in the human motor cortex. *J. Neurophysiol.*, **89**, 2339–2345.
Wolters, A., Schmidt, A., Schramm, A., Zeller, D., Naumann, M., Kunesch, E., Benecke, R., Reiners, K. & Classen, J. (2005) Timing-dependent plasticity in human primary somatosensory cortex. *J. Physiol.*, **565**, 1039–1052.
Ziemann, U., Ilic, T.V., Pauli, C., Meintzschel, F. & Ruge, D. (2004) Learning modifies subsequent induction of long-term potentiation-like and long-term depression-like plasticity in human motor cortex. *J. Neurosci.*, **24**, 1666–1672.

Supplemental methods to:

A local signature of LTP- and LTD-like plasticity in human NREM sleep

Til Ole Bergmann[1,*], Matthias Mölle[2], Lisa Marshall[2], Leval Kaya-Yildiz[1], Jan Born[2], Hartwig Roman Siebner[1]

[1]*Department of Neurology, Christian-Albrechts-University Kiel, Germany*

[2]*Department of Neuroendocrinology, University Lübeck, Germany*

Supplemental methods: nonparametric permutation testing

Comparing means

Briefly, t-values for all possible permutations of how PAS protocols could theoretically be allocated to the empirical differences between experimental conditions were calculated for each electrode, thereby generating the empirical t-distribution under the assumption of no effect (null-hypothesis). Correction for multiple comparisons was realized for each analysis by thresholding with the 95th percentile of the maximum t-statistic over all electrodes. T-values exceeding this threshold were taken as significant ($p_{corr} < 0.05$) (Nichols and Holmes, 2002; Huber et al., 2004; Huber et al., 2006; Huber et al., 2007).

Correlational analyses

Significance testing for correlational analyses between MEP and EEG data was done analogously by calculating r-values for 100,000 samples randomly drawn out of all possible permutations of data pairs (10! = 3628800 possibilities for n = 10). Maximum values for all electrodes in each permutation thereby constitute the maximum r-statistic with the 95th percentile forming the threshold corrected for multiple comparisons ($p_{corr} < 0.05$).

Supplemental Table 1: Raw values for MEP amplitude size at the APM muscle .

	$PAS_{N20+2ms}$		$PAS_{N20-5ms}$		$PAS_{control}$	
(n = 12)	Mean	SEM	Mean	SEM	Mean	SEM
baseline MEP (mV)	1.23	0.07	1.28	0.09	1.19	0.11
pre-sleep MEP (mV)	1.34	0.16	1.22	0.15	1.13	0.16
post-sleep MEP (mV)	1.06	0.18	0.70	0.10	0.84	0.13

Table gives mean values and standard errors of the mean (SEM) for raw (i.e. not adjusted) MEP amplitude size in mV measured at the APM muscle.

Supplemental Table 2: Statistical results as derived from ANOVA and post-hoc paired t-tests for baseline-corrected MEPs of the APM, FDI, and ADM muscle.

	APB		FDI		ADM	
ANOVA	**$F_{(2,22)}$**	**p**	**$F_{(2,22)}$**	**P**	**$F_{(2,22)}$**	**p**
ME *PAS protocol*	2.03	0.156	1.00	0.385	0.50	0.613
ME *time of measurement*	31.18	**<0.001***	7.19	**0.021***	4.04	0.070
IA *PAS protocol x time*	1.52	0.242	1.20	0.321	0.29	0.750
Paired t-tests	**$T_{(11)}$**	**p**	**$T_{(11)}$**	**P**	**$T_{(11)}$**	**p**
post-sleep – pre-sleep (PAS_{N20+2})	3.00	**0.012***	-3.00	**0.012***	-1.88	0.086
post-sleep – pre-sleep (PAS_{N20-5})	4.63	**<0.001***	-2.78	**0.018***	-1.15	0.275
post-sleep – pre-sleep ($PAS_{control}$)	2.95	**<0.013***	-1.24	0.243	-1.41	0.187

The upper part of the table gives the F- and p-values for two-way repeated measures ANOVA (ME = main effect, IA = interaction) for baseline-corrected MEPs with the within-subject factors *PAS protocol* ($PAS_{N20+2ms}$, $PAS_{N20-5ms}$, $PAS_{control}$) and *time of measurement* (pre-sleep, post-sleep). The lower part of the table gives the T- and p-values for post-hoc paired t-tests. Significant results ($p < 0.05$) are written in bold letters and indicated by asterisks.

Supplemental Table 3: Statistical results as derived from ANOVA for baseline-corrected MEPs adjusted to $PAS_{control}$ values of the APM, FDI, and ADM muscle.

	APB		FDI		ADM	
ANOVA	**$F_{(1,11)}$**	**p**	**$F_{(1,11)}$**	**p**	**$F_{(1,11)}$**	**p**
ME *PAS protocol*	6.82	**0.024***	1.72	0.217	0.17	0.687
ME *time of measurement*	0.71	0.417	1.80	0.206	0.60	0.454
IA *PAS protocol x time*	2.17	0.169	0.01	0.928	0.12	0.732

Paired t-tests	**$T_{(11)}$**	**p**	**$T_{(11)}$**	**P**	**$T_{(11)}$**	**p**
PAS_{N20+2} - PAS_{N20-5} (pre-sleep)	1.66	0.124	0.96	0.356	-0.08	0.94
PAS_{N20+2} - PAS_{N20-5} (post-sleep)	2.59	**0.025***	1.76	0.10	-0.90	0.38

The upper part of the table gives the F- and p-values for two-way repeated measures ANOVA (ME = main effect, IA = interaction) with the within-subject factors *PAS protocol* ($PAS_{N20+2ms}$, $PAS_{N20-5ms}$, $PAS_{control}$) and *time of measurement* (pre-sleep, post-sleep). The baseline-corrected MEPs adjusted to individual $PAS_{control}$ values were used as dependent variable. The lower part of the table gives the T- and p-values for post-hoc paired t-tests. Significant results ($p < 0.05$) are written in bold letters and indicated by asterisks.

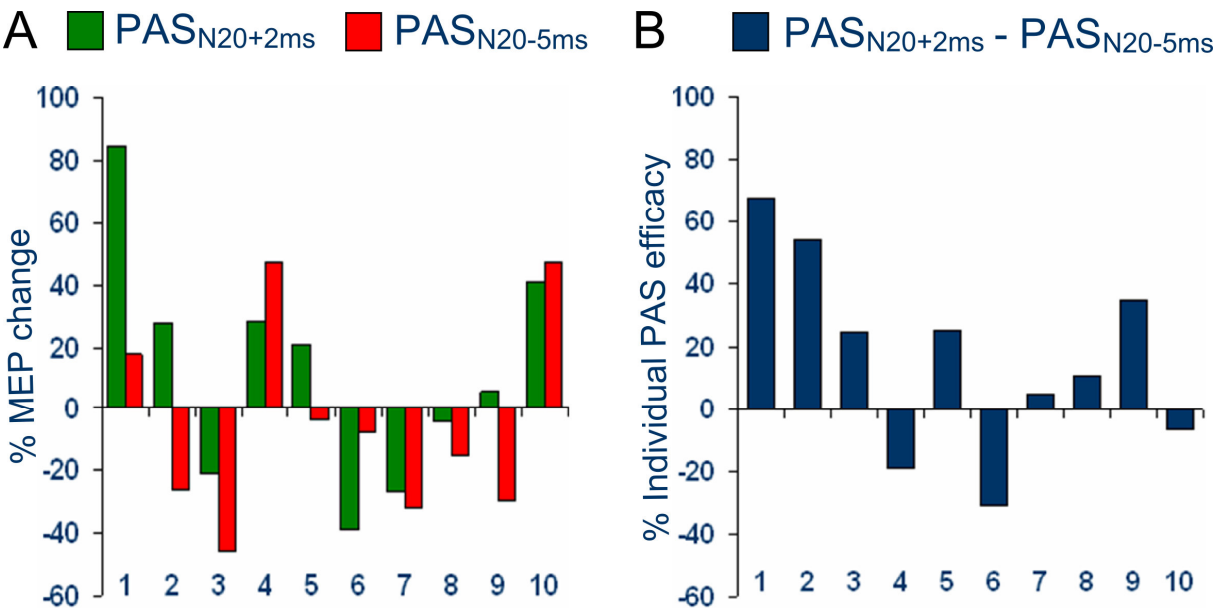

Supplemental Figure 1: (A) Diagram depicts individual MEP data of 10 subjects (as percent change from baseline, $PAS_{control}$-adjusted) for $PAS_{N20+2ms}$ (green) and $PAS_{N20-5ms}$ (red). **(B)** Diagram depicts values for "individual PAS efficacy" (blue), calculated as the difference between $PAS_{N20+2ms}$ and $PAS_{N20-5ms}$.

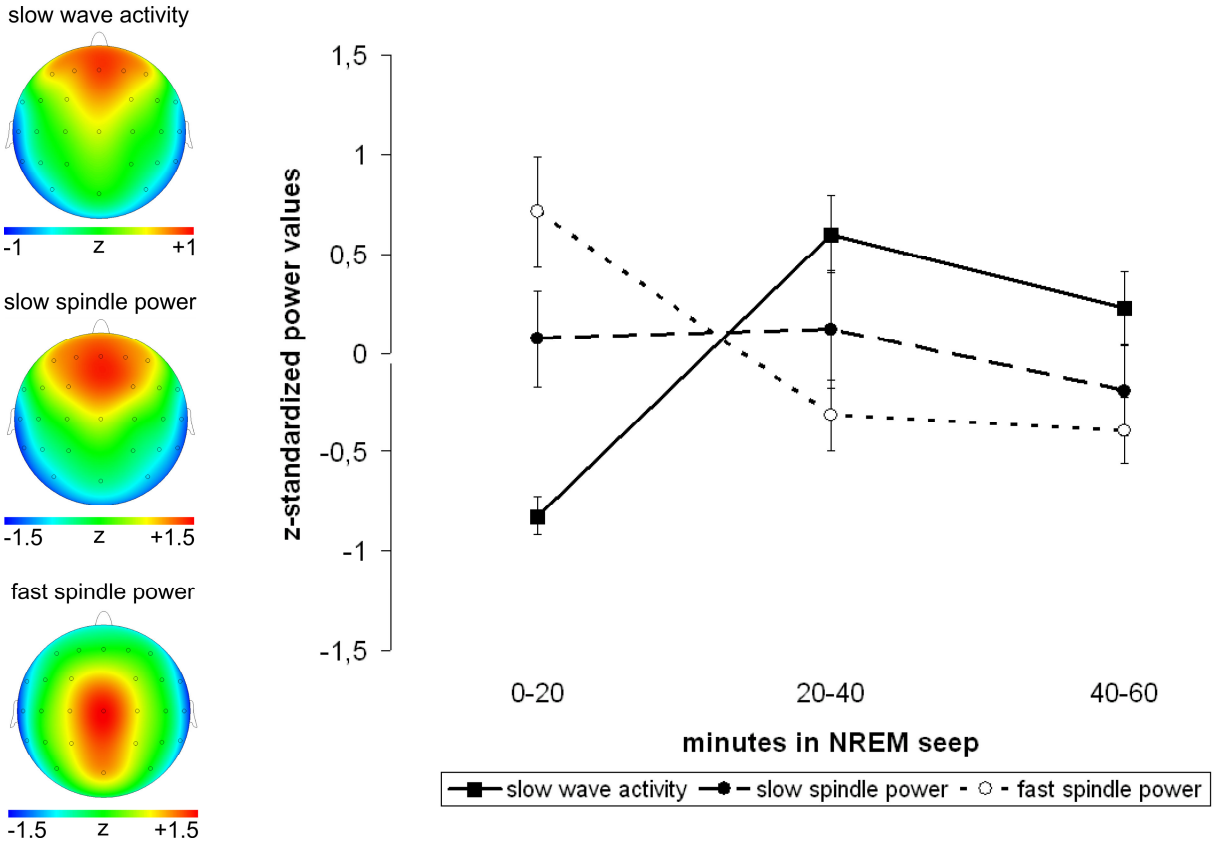

Supplemental Figure 2: Maps showing the topographic distribution of slow wave activity (0.5-4 Hz), slow spindle (10-13 Hz) and fast spindle power (13-16 Hz)) during the first 60 minutes of NREM sleep. The diagram plots the time course of z-standardized power values across the three analyzed 20-min NREM segments (error bars equal SEM). Data were averaged across all PAS protocols and z-standardized relative to the grand mean of the respective frequency band to allow depiction on a common scale.

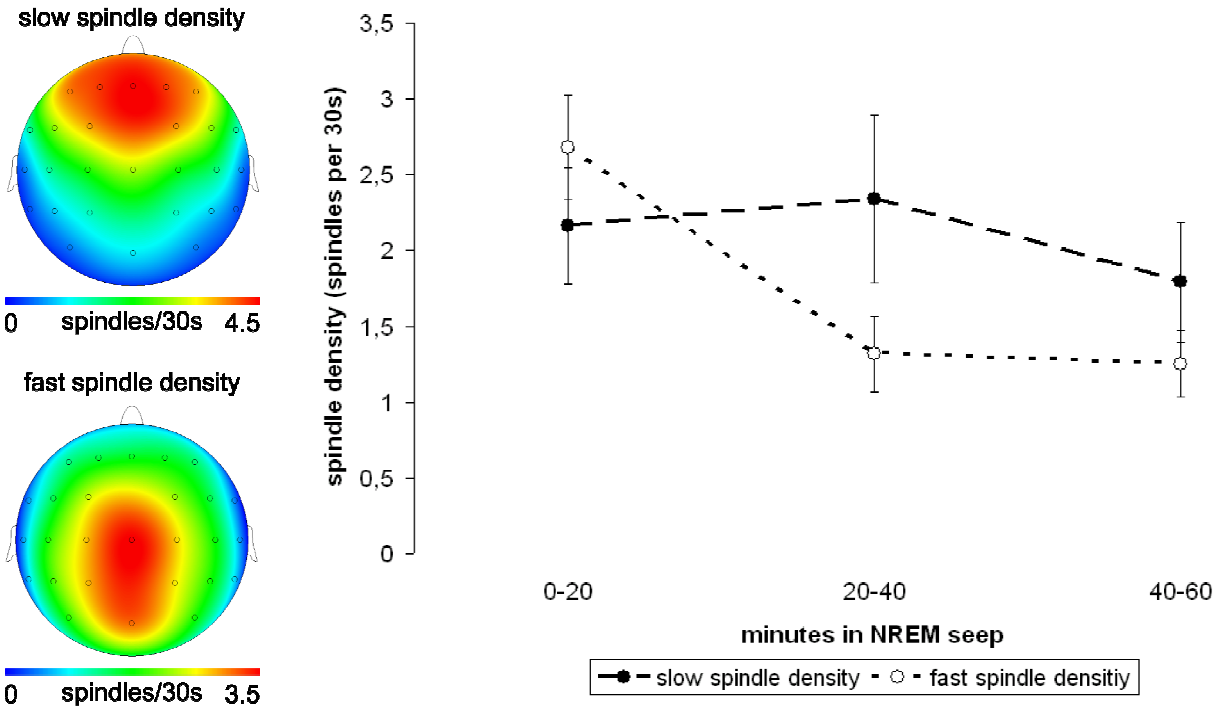

Supplemental Figure 3: Maps illustrate the topographic distribution of slow (10-13 Hz) and fast spindle (13-16 Hz) density (number of spindles per 30 s epoch) during the first 60 minutes of NREM sleep averaged across all PAS protocols. The diagram gives the mean course of spindle densities (error bars equal SEM) for these frequency bands over the analyzed 20 min segments.

References

Huber R, Ghilardi MF, Massimini M, Tononi G (2004) Local sleep and learning. Nature 430:78-81.

Huber R, Esser SK, Ferrarelli F, Massimini M, Peterson MJ, Tononi G (2007) TMS-Induced Cortical Potentiation during Wakefulness Locally Increases Slow Wave Activity during Sleep. PLoS ONE 2:e276.

Huber R, Ghilardi MF, Massimini M, Ferrarelli F, Riedner BA, Peterson MJ, Tononi G (2006) Arm immobilization causes cortical plastic changes and locally decreases sleep slow wave activity. Nat Neurosci 9:1169-1176.

Nichols TE, Holmes AP (2002) Nonparametric permutation tests for functional neuroimaging: a primer with examples. Hum Brain Mapp 15:1-25.

Paper III

Slow and fast spindles grouped in opposite phase during slow sleep oscillations

Matthias Mölle[1], Til O. Bergmann[2], Lisa Marshall[1] and Jan Born[1*]

[1]Department of Neuroendocrinology, University of Lübeck, Ratzeburger Allee 160, Haus 23a, 23538 Lübeck, Germany

[2]Department of Neurology, Schleswig-Holstein University Hospital, Kiel Campus Arnold-Heller-Str. 3, Haus 41, 24105 Kiel, Germany

*corresponding author

Summary

Neocortical slow (<1 Hz) oscillations (SOs) and spindles represent EEG hallmarks of slow-wave sleep. The thalamic generation of spindles is widely thought to be driven by the depolarizing SO up-state, a mechanism also supporting memory consolidation. Here, we examined in humans interactions between SOs and spindles, taking into account hints for the presence of two kinds of spindles, i.e., slow (10-12 Hz) frontocortical spindles and fast (12-15 Hz) centro-parietal spindles. We show: (i) Fast centro-parietal spindles precede by ~500 ms slow frontal spindles. (ii) Only centro-parietal spindles are synchronized to the SO up-state, whereas frontal spindles occur during the hyperpolarizing down-state. (iii) In SO sequences, centro-parietal spindles are largest for 'initial' SOs, not preceded by another SO, whereas SO amplitude is largest for 'middle' SOs. Thus, centro-parietal spindles are not only driven by the SO up-state but themselves feed back to enhance the succeeding SO, and the likelihood of frontal spindles. Our findings point to disparate generating mechanisms and plastic functions for the two spindle types.

Introduction

Electrical oscillations of brain activity coordinate information transfer and spike time dependent plasticity between different brain circuits and regions (Buzsáki and Draguhn, 2004). Slow wave sleep (SWS) is characterized by the occurrence of two distinct oscillatory phenomena, i.e., the EEG slow oscillation (SO) and spindle activity, which both have been implicated in memory consolidation and the induction of synaptic plastic processes during sleep (Gais et al., 2002; Rosanova and Ulrich, 2005; Eschenko et al., 2006; Marshall et al., 2006; Tononi and Cirelli, 2006; Czarnecki et al., 2007; Marshall and Born, 2007). The SO occurs in humans at a peak frequency of ~0.75 Hz and is generated within neocortical networks (Mölle et al., 2002; Massimini et al., 2004; Steriade, 2006). It synchronizes neuronal activity into generalized down-states (hyperpolarization) of global neuronal silence and subsequent up-states (depolarization) of increased wake-like neuronal firing, not only in neocortex but also via efferent pathways in other brain regions, including the thalamus as the source of spindle activity. There is compelling evidence that the depolarizing up-state of the SO via cortico-thalamic volleys drives the generation of spindle activity spreading back to the neocortex (Contreras and Steriade, 1995; Steriade et al., 1996; Destexhe et al., 1999; Steriade, 2006). Accordingly, spindle activity becomes temporally grouped by the SO occurring preferentially during the depolarizing up-phase of the SO, and also learning-dependent increases in spindle activity are restricted to the depolarizing up-state (Mölle et al., 2002, 2006, 2009). Spindles occurring during SO up-states are considered a key mechanism underlying the long-term storage of memories in neocortical networks because via massive Ca^{2+} influx into pyramidal cells they are able to promote lasting plastic synaptic changes (Sejnowski and Destexhe, 2000; Rosanova and Ulrich, 2005; Werk et al., 2005; Marshall and Born, 2007).

There is growing evidence for the existence of two types of spindles during SWS which differ in frequency and topography, i.e., the “slow” spindles (<12 Hz) that dominate

over the frontal cortical sites and the “fast” spindles (>12 Hz) that show a more widespread distribution over parietal and central sites (Terrier and Gottesmann, 1978; Anderer et al., 2001; De Gennaro and Ferrara, 2003). In accord, low-resolution brain electromagnetic tomography has revealed two separate cortical spindle sources, one for slow spindles in a mesial frontal region and another for fast spindles in the precuneus (Anderer et al., 2001). Functional magnetic resonance imaging indicated distinct patterns of brain activation associated with the two types of spindles (Schabus et al., 2007). Beyond common activity in the thalamus and superior temporal gyri slow spindles were associated with increased activity in the superior frontal gyrus whereas fast spindles recruited a set of cortical regions involved in sensory motor processing, as well as the mesial frontal cortex and hippocampus. A functional differentiation has been suggested whereby slow frontal spindle activity reflects predominant coupling among cortical networks, whereas the faster parietal spindle activity is more closely associated with thalamo-cortical coupling (Doran, 2003).

Considering the temporal grouping of spindles by the SO a key mechanism underlying sleep-dependent memory consolidation, here we asked whether this effect pertains in the same way both to the slow frontal and fast centro-parietal spindles. Specifically, we aimed at characterizing the temporal relationships between SO down and up-states and fast and slow sleep spindles during human SWS. Here, we find that only the fast centro-parietal spindles show the expected synchronization to the depolarizing up-state of the SO. In contrast, slow frontal spindles are associated with the transition into the hyperpolarizing SO down-state. With further analysis of trains of SOs we show that fast centro-parietal spindles appear to be not only driven by the depolarizing SO up-state but themselves feed back to enhance the succeeding SO, as well as the likelihood of frontal spindles during the corresponding hyperpolarizing phase.

Results

Polysomnographic sleep parameters confirmed that our subjects' sleep was within the normal range (Table 1). The proportion of SWS was 16.6 ± 1.3 % and of stage 2 sleep 55.7 ± 2.1 %. Figure 1 provides a comparison of EEG power between SWS and NonREM sleep stage 2. As expected power within the slow oscillation frequency band (~0.5 - 1.3 Hz) is distinctly higher during SWS than stage 2 sleep, and also the number of detected SOs is distinctly greater in SWS ($p<0.001$, Table 2). Power spectra of both stage 2 sleep and SWS show a clear peak for fast spindle activity, with a maximum over centro-parietal cortex regions. By contrast for slow spindle activity a clear peak was only visible in the grand mean power spectrum of SWS, with a maximum over the frontal cortex. This pattern was likewise apparent in the individual spectra from the 11 subjects (data not shown). The mean peak frequency (across subjects) was comparable between SWS (13.40 ± 0.11 Hz) and stage 2 sleep (13.46 ± 0.11 Hz) for fast spindles, but differed for slow spindles (10.23 ± 0.15 in SWS vs. 11.44 ± 0.12 Hz in stage 2 sleep, $p<0.01$; Figure 1 and Table 3). Density (per 30-sec interval) was generally lower for slow than fast spindles ($p<0.001$; Table 2). Because of the distinctly greater number of SO in SWS than stage 2 sleep and also because of the minor distinctiveness (in terms of power) during stage 2 sleep, we focussed the following analyses of temporal relationships between SOs and spindles on SWS.

Figure 2C shows the grand mean average of the SOs which were detected during SWS and exhibited the typical time course with a down-state of about 300-400 ms followed by an up-state of about 400-500 ms. In order to examine whether the occurrence of fast and slow spindles is specifically timed to the occurrence of these SO up- and down-states, in a first step, we averaged the original EEG signal time-locked to the detected fast and slow spindles, respectively (with the deepest, i.e., most negative trough in the filtered signal used as reference; Figure 2A). Comparing the average potential level during the 300-msec intervals preceding and following the spindle peak indicated strong and systematic slow potential shifts

underlying the two different types of spindles: Whereas this background potential level during fast spindles increased from -4.19 ± 1.87 µV (before spindle peak) to +3.63 ± 1.52 µV (after spindle peak, $p<0.001$), it strongly decreased from +1.77 ± 1.93 to -11.78 ± 2.08 µV ($p<0.001$) for slow spindles. In fact, whereas fast spindles appear to ride on the positive going upward potential shift of the SO, slow frontal spindles tend to coincide with the downward going negative SO shift. To examine the topography of this relationship, we averaged the slow potential shifts underlying spindles in groups of channels according to their anterior - posterior positions, i.e., for fast spindles separately across the central (C3, C1, Cz, C2, C4), centro-parietal (CP3, CP1, CP2, CP4) and parietal (P3, Pz, P4) leads, and for slow spindles separately for the frontal (F3, F1, Fz, F2, F4), fronto-central (FC3, FC1, FC2, FC4), and central (C1, Cz, C2) leads. Interestingly, this analysis revealed that the positive potential shifts underlying the fast spindles are larger the more posterior the fast spindles occur. Conversely, the negative potential shifts in the slow spindles become larger the more anterior the slow spindles occur (Figure 2B).

Event correlation histograms indicated a clear temporal relationship between the two types of spindles (Figure 3). Fast spindles were followed by an increase in slow spindle activity with a delay of ~500 ms ($p<0.001$, for comparing the 0.25…0.75-sec epoch with the -3.0…-2.5-sec epoch used as baseline reference). Slow spindles, conversely, were preceded (by ~500 ms) by a distinct increase in fast spindle activity ($p<0.001$, for -0.75…-0.25-sec epoch vs. baseline). In combination, these temporal relationships are consistent with a causal impact of fast centro-parietal spindles on slow frontal spindles, but do not support the opposite relation.

Event correlation histograms, in addition to the clear temporal relationship between the two kinds of spindles, indicated a consistent timing of these spindles during the SO cycle (Figure 4). As expected (Mölle et al., 2002) with reference to the negative half-wave peak of the SO, fast spindle activity was strongly suppressed around the SO down-state ($p<0.001$, for

-0.3…0.2 sec compared to baseline) and showed a pronounced increase during the transition to the up-state ($p<0.001$, for 0.4…0.9 sec compared to baseline). Interestingly, this strong increase in fast spindle activity during the up-state appears to be followed by a more prolonged (2-3 sec) period of slightly suppressed fast spindle activity ($p<0.01$). Fast spindle activity is also enhanced between ~1000-500 ms before the negative SO half-wave ($p<0.001$) although to a lesser degree than during the up-state following the SO down-state, which likely reflects up-state related activity of the preceding SO. Like fast spindle activity, slow spindle activity also shows two distinct maxima with reference to the negative half-wave peak of the SO which occurred, however, at times different from those of fast spindle activity (Figure 4 bottom). The first (and larger) maximum is reached immediately (~150 ms) before the negative SO peak ($p<0.01$, for -0.4…0.1 sec compared to baseline), which means that slow spindle activity is highest exactly during the transition into the SO down-state. The second maximum of slow spindle activity peaks ~1000 ms following the negative half-wave peak, i.e. ~500 ms following the pronounced increase in fast spindle activity associated with the SO up-state ($p<0.01$, for 0.75…1.25 sec compared to baseline).

These temporal relationships between spindles and SOs were further specified in time-frequency plots of spindle wavelet-power (± 1.2 sec around the negative SO peak; Figure 5), indicating for fast spindle activity (>12 Hz) the expected suppression during the SO down-state (around 0 sec) and distinct enhancements during both the preceding and following up-state. For slow spindle activity (<12 Hz) the plot confirms a strong transient enhancement during the transition into the down-state (between -0.2 and 0 sec) and a clear suppression during the transition into the following up-state (Figure 5B). Although seen at all 27 recording sites, the modulation of fast spindle activity is strongest in the middle centro-parietal channels and for slow spindle activity in the frontal channels, i.e., the respective sites of maximum spindle power (Figure 6).

We further explored the unexpected association of slow spindles with the transition into negative down-states of the SO applying correlation analyses (on mean spindle and SO measures in the 5 frontal EEG channels of interest). The density of slow spindles, i.e., the rate per 30 sec SWS, was only moderately correlated with the density of SOs in the prefrontal channels ($r = 0.27$, $p<0.05$) suggesting that slow spindles and SOs can occur independently of each other. To examine whether slow spindles if coinciding with a SO, could basically add to the negative amplitude of this oscillation we calculated correlations between the peak negativity of the prefrontal SO and the (root mean square) amplitude of concurrent slow frontal spindle activity. This correlation revealed to be significant ($p<0.05$) in all but one subject, but on average was rather low ($r = 0.14 \pm 0.04$).

Who influences whom in the slow oscillation cycle? Event correlation histograms indicated that fast spindles support the occurrence of slow spindles 500 ms later. To further examine to what extent the two spindle types also contribute to the emergence of the SO, we analyzed the relationship between spindle activity and SOs separately for four types of SOs: (i) SOs that were followed but not preceded by another SO, (ii) SOs that were preceded and followed by another SO, (iii) SOs that were preceded but not followed by another SO, and (iv) singular SOs that were neither preceded nor followed by another SO. The mean auto-event correlation histogram of all SOs (detected in an average channel representing the 8 fronto-central recordings, see Methods) indicated a clearly increased probability for an SO to be preceded and/or followed by another SO at about ±1.25 sec (Figure 7A). Also peak-to-peak amplitude of SOs preceded and followed by other SOs was significantly greater than for all other types of SOs (see Figure 7C for statistical comparisons). Interestingly, contrasting with the distribution of SO peak-to-peak amplitude the increase in fast spindle wavelet-power during the SO up-state was most pronounced not for the highest SO (followed and preceded by another SO), but for those SOs not preceded by any other SOs, i.e., the first SO in a sequence of SOs. The strong increase in fast spindle power during these 'initial' SOs, not

preceded by another SO, suggests a particular importance of this type of spindles for initiating further SO-slow spindle events. On the other hand, the increase in slow spindle wavelet-power during SO transitions into the down-state varied in parallel with the SO peak-to-peak amplitude, with these variations overall only approaching statistical significance (Figure 7C). This pattern does not speak for a substantial involvement of slow frontal spindles in the generation of SOs.

Discussion

We provide evidence for the existence of two different types of spindles during human NonREM sleep which do not only differ in frequency and topography but exhibit a unique temporal relationship to each other and to the slow oscillation (SO). The three main findings of our study are: (i) The fast spindles with a spectral peak at 13.4 Hz and a centro-parietal distribution precede by about 500 ms the slow spindles with a spectral peak at 10.2 Hz and a distribution clearly restricted to frontal cortical sites. (ii) Only the centro-parietal fast spindles show the expected synchronization to the depolarizing up-state of the SO with, a strong suppression of these spindles during the SO down-state. In contrast, slow frontal spindles are obviously associated with the transition into the down-state of the SO and, in the event correlation histograms revealed the highest probability shortly, i.e., 125 ms before the peak of the negative half-wave of the SO. (iii) Analysis of sequences of SOs indicated that power of fast spindles is largest for 'initial' SOs that are followed but not preceded by another SO, whereas amplitude of the SO itself was largest for 'middle' SOs that were preceded and followed by another SO. Altogether these findings show that the widely held concept of the depolarizing up-phase of the SO driving thalamic spindle generation accounts only for the fast centro-parietal spindles, but not for the slow frontal spindles occurring during cortical hyperpolarization (Contreras and Steriade, 1995; Destexhe et al., 1999; Timofeev and Bazhenov, 2005; Steriade, 2006). The fast centro-parietal spindles themselves appear to play

a regulatory role in the slow oscillation cycle in that they increase the likelihood of subsequent slow frontal spindles and simultaneously boost the hyperpolarizing down-phase of the subsequent SO.

Previous studies have suggested functional differences in fast centro-parietal and slow frontal spindles as revealed by their differential sensitivity to factors such as the duration of prior waking, pharmacological agents, age and intelligence (De Gennaro and Ferrara, 2003). The present data corroborate the concept of a distinct class of slow frontal spindles by revealing their differential involvement in the temporal evolution of the SO, thus pointing towards separate generating mechanisms for the two spindle phenomena. Studies of the generating mechanisms of spindles were performed mainly in cats and rats without distinguishing prefrontal spindles (Steriade, 2006). Those studies revealed a consistent association of spindles with the up-phase of the SO, reflecting the driving influence of depolarization and increased firing of cortico-thalamic projections on the generation of spindle oscillations in thalamo-neocortical feedback loops (Contreras and Steriade, 1995; Destexhe et al., 1999; Steriade, 2006). In contrast, surface-negative components of SOs corresponding with intracellular hyperpolarization were associated with silence in these corticofugal projections and suppressed spindle activity. The occurrence of slow frontal spindles during the hyperpolarizing down-phase precludes the same generating mechanism for these spindles. Although thalamic activity as a common source for slow and fast spindles cannot be excluded (Schabus et al., 2007), slow spindles could alternatively be considered primarily of cortical origin, developing in the aftermath of fading SO depolarization. This view would fit well with the idea that slow frontal spindles are functionally associated with cortico-cortical interactions whereas centro-parietal spindles are linked to activity in thalamo-cortical loops (Doran, 2003).

Characteristic for the slow frontal spindles is indeed their temporal proximity to and occurrence immediately before the down-state of the SO, i.e., at the up-to-down state

transition. Accordingly, averaging of slow spindles revealed that they were placed on a pronounced negative background potential shift towards hyperpolarization which contrasts with fast spindles residing on a slow positive, i.e., depolarizing potential shift. Interestingly, there was a small but very consistent correlation between slow spindle power and the peak negativity of the prefrontal SO. Likewise, analysis of sequences of SOs revealed that slow spindle power was maximal when the SO amplitude was also maximal, which was the case for 'middle' SOs that were preceded and followed by another SO. This pattern suggests that slow spindles once occurring during a SO, can significantly add to the hyperpolarizing SO down-state, which has been considered decisive for the further temporal evolution of the SO (Volgushev et al., 2006; Mölle and Born, 2009).. However, the observed pattern is equally consistent with the reverse relationship, such that the hyperpolarizing SO potential provides network conditions favoring the emergence of a slow spindle in prefrontal cortex.

A causal impact of the SO hyperpolarization on the generation of slow frontal spindles is in fact indicated by previous findings showing that slow frontal spindles are enhanced after transcranial application of slow potential fields oscillating at the SO frequency (0.75 Hz) (Marshall et al., 2006). The hyperpolarizing phase of the SO has been linked to several intrinsic currents in cortical neurons, i.e., mainly the activation of Ca^{2+}-dependent potassium currents, the inactivation of the persistent Na^{+} current and the activation of Na^{+}-dependent K^{+} current that together with activity-dependent synaptic depression induce a general disfacilitation of neuronal excitability (Contreras et al., 1996; Bazhenov et al., 2002; Timofeev and Bazhenov, 2005; Hill and Tononi, 2005; Destexhe et al., 2007). Slight displacements in the dynamics of these currents may predispose the network to the generation of slow spindles.

The analysis of trains of SOs revealed a remarkable pattern for the fast central-parietal spindles. Whereas amplitudes of the SO and slow spindles were maximal for 'middle' SOs that were preceded and followed by another SO, the centro-parietal spindles were indeed maximal

for 'initial' SOs starting a series of further SOs and minimal during SOs completing a series of SOs. This pattern suggests that fast spindles apart from being driven by the depolarizing SO up-state, themselves feed back to promote the generation of succeeding SOs. Overall our data reveal a loop-like scenario where fast centro-parietal spindles enhance both amplitude of subsequent SOs and the likelihood of a slow frontal spindle developing during transition into hyperpolarization of the subsequent SO. Emergent depolarization in this SO cycle, conversely, drives the generation of the next fast centro-parietal spindle.

Although our results reveal a clear temporal structure in the interplay between SOs and spindles, its function remains to be explored. Spindles coinciding with hippocampal sharp wave ripples have been proposed as a mechanism that facilitates the transfer of memory-related information from the hippocampus to the neocortex (Siapas and Wilson, 1998; Marshall and Born, 2007; Wierzynski et al., 2009). Spindles by promoting synaptic long term potentiation can support the long-term storage of memory-related information in neocortical networks (Rosanova and Ulrich, 2005). This view has been linked to the fast centro-parietal spindles occurring during the depolarizing phase of the SO. However, it is questionable whether slow frontal spindles that occur in the presence of background SO hyperpolarization can support synaptic plastic processes in a similar way. Several lines of evidence underline the particular importance of information transfer between hippocampus and prefrontal cortex for the sleep dependent system consolidation of memories, altogether suggesting that hippocampal aspects of a memory representation become preferentially transferred to the medial prefrontal cortex (Frankland and Bontempi, 2005; Takashima et al., 2006; Gais et al., 2007; Mölle and Born, 2009). It is tempting to speculate that slow spindles arising from just these prefrontal areas subserve a role specific to this transfer. Whatever the function, our data indicate that any future examination of spindles needs to account for the presence of two basically different types of spindles, i.e., slow frontal and fast centro-parietal spindles.

Material and Methods

Subjects and EEG recordings

Eleven healthy right-handed male volunteers (mean age: 25.8 years, range: 19-33 years) participated in the experiments. All participants were non-smokers, free of medication, and had no history of neurological or psychiatric disease. They slept seven to nine hours per night and reported no major disruptions of the sleep-wake cycle during the four weeks before experimentation. Participants were not allowed to ingest alcohol or caffeine during the day before the experimental night. To accustom subjects to sleeping under laboratory conditions, all subjects spent an adaptation night in the sleep laboratory, including the placement of electrodes, before the experiments proper. The experiments were approved by the ethics committee of the University of Lübeck. Written informed consent was obtained from all subjects prior to participating.

Experimental sessions started at 9.00 pm with preparing the subject for standard polysomnography and continuous EEG recordings during the subsequent night. Lights were turned off at 11 pm and sleep was permitted until 7 am, when subjects were awakened. Polysomnographical recordings as well as subjective reports obtained the next morning confirmed normal sleep in all subjects.

EEG recordings were obtained from 27 channels according to an extended 10-20-System (F3, F1, Fz, F2, F4, FC5, FC3, FC1, FC2, FC4, FC6, C5, C3, C1, Cz, C2, C4, C6, CP5, CP3, CP1, CP2, CP4, CP6, P3, Pz, P4; cap with Ag-AgCl ring electrodes; impedance <5 kOhm) and both mastoids (A1, A2) referenced to Cz. EEG signals were offline re-referenced to averaged A1 and A2. Additionally, horizontal and vertical eye movements and the electromyogram from the chin muscles were recorded with Ag-AgCl cup electrodes. The raw EEG signals were amplified by 10000, filtered between 0.05 and 100 Hz (plus 50 Hz notch), and digitized at 500 Hz per channel (SynAmps, 16-bit-ADC; Neuroscan, El Paso, TX, USA). Data were recorded and stored with Acquire software version 4.2 (Neuroscan, El Paso, TX,

USA) and analyzed using Spike2 software version 5 (Cambridge Electronic Design Limited, Cambridge, England) and Matlab (MathWorks Inc., Natick, USA).

Data analysis

Sleep stages (1, 2, 3, 4, and REM sleep), awake time, and movement artifacts were scored offline for 30-sec epochs according to standard criteria (Rechtschaffen and Kales, 1968). Stage 2 sleep corresponds to light non-REM sleep and stages 3 and 4 correspond to slow wave sleep (SWS). Whole night EEG data were additionally subjected to a first power analysis by fast Fourier transformations (FFT), performed on subsequent blocks of 4,096 data points (~8 sec of EEG data, 4 blocks per 30-sec epoch). Averages of power spectra across the whole night were calculated in all 27 EEG channels separately for NonREM stage 2 sleep and SWS (Figure 1).

Slow oscillations. Detection of SOs in NonREM sleep stage 2 and SWS was based essentially on a standard algorithm described elsewhere in detail (Mölle et al., 2002), and was limited to the 8 fronto-central channels that (during SWS) expressed the largest power in the SO frequency range, i.e., F3, F1, Fz, F2, F4, FC1, FC2, and Cz (Figure 1). In a first step, the EEG was low-pass filtered with 30 Hz and down sampled to 100 Hz. For identifying large SOs a low-pass filter of 3.5 Hz was applied to the EEG and time points of positive to negative zero crossings were computed in the resulting signal. Then the lowest and highest value between every two of these time points were detected (i.e., one negative and one positive peak between two succeeding positive to negative zero crossings). Intervals of positive to negative zero crossings with a length of 0.9 to 2 sec were marked as SO epochs if the corresponding negative peak amplitude was lower than -80 µV and the corresponding amplitude difference (positive peak minus negative peak) was at least 140 µV. Averages of original EEG potentials in a 2.6 sec window ±1.3 sec around the peak of the negative half-wave of all detected SOs were calculated.

Spindles. Spindles were identified during NonREM sleep stage 2 and SWS in the 12 fronto-central leads (slow spindles) and the 12 centro-parietal leads (fast spindles) that expressed the largest power in the respective slow (9-12 Hz) and fast spindle (12-15 Hz) frequency ranges. These were for slow spindles: F3, F1, Fz, F2, F4, FC3, FC1, FC2, FC4, C1, Cz, C2 and for fast spindles: C3, C1, Cz, C2, C4, CP3, CP1, CP2, CP4, P3, Pz, P4 (Figure 1). For each subject, in the spectra the peak frequency of slow and fast spindle activity was identified in the channels of interest. Subsequently, the EEG was first filtered with a band-pass of ± 1.5 Hz around this peak frequency of slow and fast spindle activity, respectively. For fast spindle activity in all subjects a clear peak in the power spectra was detectable. In subjects, where no discrete slow spindle peak was detectable (2 for SWS and 4 for stage 2 sleep), a band-pass of ± 1.5 Hz around the mean slow spindle peak frequency across the other nine subjects was used. After filtering a thresholding algorithm was applied that had proven effective in previous studies (Gais et al., 2002; Mölle et al., 2002) and was the same for detecting slow and fast spindles, respectively. First the root mean square (RMS) of the filtered signal was calculated at every sample point using a moving window of 0.2 sec. The resulting RMS signal was smoothed with a moving average of 0.2 sec. The threshold for spindle detection in the RMS signal was set to 1.5 standard deviations of the filtered signal (mean across the 12 fronto-central and 12 centro-parietal channels, respectively). A spindle was detected when the RMS signal remained above the threshold for 0.5 – 3 sec and the beginning and end of the spindle were marked at the threshold crossing points. For every detected spindle the peaks and troughs were detected as the maxima and minima of the filtered signal (between beginning and end of the spindle) and the deepest trough was designated as the "spindle peak" that represented the respective spindle in time, i.e., the time point taken for referencing event correlation histograms (see below).

To investigate the temporal relationships between slow spindles, fast spindles and SOs, four types of event correlation histograms of spindle activity were calculated using 10-

sec windows with 5-sec offsets and a bin size of 50 msec. The histograms were referenced to the spindle peaks or negative half-wave peaks of the SO, respectively. For “spindle activity” all detected spindle peaks and troughs of all detected spindles were taken. The first event correlation histogram calculated fast spindle activity referenced to the peak of slow spindles and the second histogram calculated, conversely, slow spindle activity around the peak of fast spindles. The third and fourth event correlation histogram calculated fast and slow spindle activity with reference to the negative half-wave peak of SOs.

In order to visualize how slow and fast spindle activity are organized by the SOs, we calculated time-frequency plots of power in all EEG channels in a time window ±2 sec around the negative peak of SOs. For this analysis SOs were detected using the same detection algorithm as specified above but using an "average" channel that was calculated by averaging (for every sample point) the potentials of the 8 fronto-central channels used in the original SO analysis. The calculation of time-frequency plots using Morlet wavelets was carried out in the Matlab toolbox for EEG/MEG-analysis “FieldTrip” (Donders Institute for Brain, Cognition and Behaviour, Nijmegen, Netherlands). Averages of the time-frequency plots across all detected SOs were calculated within and across all subjects. To evaluate the SO-related power changes, power values were normalized with respect to a baseline interval from -1.3 to -1.2 sec, expressing power for each frequency as relative increase or decrease with respect to power during the baseline.

A last analysis aimed at characterizing the role fast and slow spindles play in the initiation and within sequences of successive SOs. We first calculated auto-event correlation histograms for all detected SOs in the "average" channel as defined above. Then all detected SOs were classified according to whether or not another SO occurred before (between -2 to -0.5 sec) and/or after (between +0.5 to +2 sec) that SO (reference - negative half-wave peak), resulting in the following four groups: (i) SOs with only a succeeding SO, (ii) SOs with both preceding and succeeding SOs, (iii) SOs with only a preceding SO, and (iv) SOs without a

preceding or succeeding SO. For all four groups, the peak-to-peak amplitudes of the SOs and of the slow and fast spindle wavelet-power (between -0.3 and +0.8 sec around the SO negative half-wave peak) were determined.

Statistical comparisons relied on paired t-tests, unless specified otherwise. A p-value < 0.05 was considered significant.

Figure legends

Figure 1

EEG power during NonREM sleep

(A) Comparison of EEG power during stage 2 sleep and SWS. Average spectra were calculated across the whole night for all 27 EEG channels. Insets show enhanced views of spindle activity. Note, whereas there are clear peaks for both, slow and fast spindle activity during SWS, only fast spindle activity shows a clear peak during stage 2 sleep. Note also distinctly higher power in the SO frequency band (0.5 - 1.3 Hz) during SWS than stage 2 sleep.

(B) Maps indicating topography of power for the SO and the slow and fast spindle frequency ranges during SWS. Bold black dots indicate electrode positions of channels chosen for SO and slow and fast spindle detection.

Figure 2

Averaged fast and slow spindles and slow oscillations

(A) Grand mean averages (± SEM) of original EEG in (top) 12 centro-parietal channels across all detected fast spindles and (bottom) 12 fronto-central channels across all detected slow spindles. Spindles are averaged with reference to the deepest, i.e., most negative, trough in the filtered signal. Asterisks (and arrows) indicate a significant ($p<0.001$) positive and negative slow potential shift underlying fast and slow spindles, respectively, in the interval between 300 ms before to 300 ms after the spindle peak.

(B) Mean (± SEM) potential shifts underlying (top) fast spindles at central, centro-parietal and parietal electrodes and (bottom) slow spindles at frontal, fronto-central and central electrodes. Asterisks indicate a significant positive and negative slow potential shift, respectively (** $p<0.01$, * $p<0.05$).

(C) Grand mean averages of original EEG in 8 fronto-central channels across all detected SOs. Averaging was performed with reference to the negative half-wave peak of the SOs.

Figure 3

Temporal association between fast and slow spindles

Event correlation histogram (top) of fast spindle activity (i.e., all marked peaks and troughs in detected spindles) with reference to the peak (most negative trough) of slow spindles and (bottom) of slow spindle activity with reference to the peak of fast spindles. Insets show the respective reference spindle. Note, fast spindles are followed (with a 500 ms delay) by an increase in slow spindle activity and, conversely, slow spindles are preceded by an increase in fast spindle activity (500 ms before). Asterisks indicate a significant ($p<0.001$) increase in spindle activity in the indicated 0.5 sec interval (thin line) as compared to the 0.5 sec baseline interval (thick line).

Figure 4

Temporal association between slow oscillations and fast and slow spindle activity

Event correlation histogram (top) of slow spindle activity (i.e., all marked peaks and troughs in detected spindles) and (bottom) of fast spindle activity with reference to the negative peak of the SOs (shown in the insets). Note, strong increases in fast spindle activity before and after the negative SO downstate (coinciding with up-states) and strong increases in slow spindle activity coincide with the downward going negative phase of the SO. Asterisks indicate significant increases and decreases, respectively in spindle activity in the indicated intervals (thin lines) as compared to the baseline interval (thick line; *** $p<0.001$, ** $p<0.01$).

Figure 5

Time-frequency plots of wavelet-power during slow oscillations

(A) Time-frequency plots of wavelet-power in a time window of ± 1.2 sec and for frequencies of 5-20 Hz around the negative peak of the SO (0 sec) together with the SO as averaged from the original EEG (bottom) for all 27 recording channels.

(B) Enhanced views of the time-frequency plots in the frontal, central and parietal electrode. Note, strong enhancement in <12 Hz slow spindle wavelet-power during the transition into SO down-state (between -0.2 and 0 sec) most pronounced in frontal electrodes.

Figure 6

Scalp distributions of maximal spindle wavelet-power

(A) Scalp distributions of maximal slow (7-10 Hz, left) spindle wavelet-power (mean during the -0.2 to 0 sec-interval with reference to the negative SO peak) and of maximal fast (13-17 Hz, right) spindle wavelet-power (mean during 0.4 to 0.6 sec-interval).

(B) Mean wavelet-power of slow (left) and fast (right) spindle activity in frontal (F3, Fz, F4), central (C3, Cz, C4) and parietal (P3, Pz, P4) electrodes. Asterisks indicate significant ($p<0.001$) differences between mean wavelet-power in frontal and central electrodes and between central and parietal electrodes, respectively.

Figure 7

Analysis of sequences of slow oscillations

(A) Auto-event correlation histogram of all detected SOs in an average channel (calculated by averaging the potentials of the 8 fronto-central channels of interest). Shaded rectangles indicate time windows of increased probability of another SO preceding and/or following the actual SO.

(B) Averages of the original EEG (upper panels) and the wavelet-power for slow (7-10 Hz) and fast (13-17 Hz) spindle activity during SOs that were or were not followed and/or preceded by another SO. Averaging of SO was performed on the original unfiltered signal in the 8 fronto-central channels of interest. Fast spindle wavelet power is averaged for the 12 centro-parietal recording channels of interest, slow spindle wavelet power for the 12 fronto-central channels of interest. (Averages were calculated across all detected SOs and 11 subjects.) '-/after', 'before/after', 'before/-', '-/-' indicate presence or absence (-) of another SO before or after the target SO.

(C) Upper panel: Mean (+ SEM) peak-to-peak SO amplitudes (in the -0.2 to 0.7 sec interval) for the four types of SOs (across 8 fronto-central channels). Lower panels: Mean (+ SEM) amplitude (peak-to-peak wavelet-power in the -0.3 to 0.8 sec interval) of increase in fast spindle wavelet power (during SO up-state) and slow spindle wavelet power (during transition into SO down-state) for four types of SOs (averaged, respectively, across 12 centro-parietal and 12 fronto-central recording sites of interest; n=11). '-/a', 'b/a', 'b/-', '-/-' indicate presence or absence (-) of another SO before (b) or after (a) the target SO. Asterisks indicate significant differences in peak-to-peak SO amplitude and spindle wavelet-power, respectively between the different types of SOs (*** $p<0.001$, ** $p<0.01$, * $p<0.05$).

References

Anderer, P., Klosch, G., Gruber, G., Trenker, E., Pascual-Marqui, R.D., Zeitlhofer, J., Barbanoj, M.J., Rappelsberger, P., and Saletu, B. (2001). Low-resolution brain electromagnetic tomography revealed simultaneously active frontal and parietal sleep spindle sources in the human cortex. Neuroscience *103*, 581-592.

Bazhenov, M., Timofeev, I., Steriade, M., and Sejnowski, T.J. (2002). Model of thalamocortical slow-wave sleep oscillations and transitions to activated States. J. Neurosci. *22*, 8691-8704.

Buzsáki, G., and Draguhn, A. (2004). Neuronal oscillations in cortical networks. Science *304*, 1926-1929.

Contreras, D., and Steriade, M. (1995). Cellular basis of EEG slow rhythms: a study of dynamic corticothalamic relationships. J. Neurosci. *15*, 604-622.

Contreras, D., Timofeev, I., and Steriade, M. (1996). Mechanisms of long-lasting hyperpolarizations underlying slow sleep oscillations in cat corticothalamic networks. J. Physiol *494 (Pt 1)*, 251-264.

Czarnecki, A., Birtoli, B., and Ulrich, D. (2007). Cellular mechanisms of burst firing-mediated long-term depression in rat neocortical pyramidal cells. J. Physiol *578*, 471-479.

De Gennaro, L., and Ferrara, M. (2003). Sleep spindles: an overview. Sleep Med. Rev. *7*, 423-440.

Destexhe, A., Contreras, D., and Steriade, M. (1999). Spatiotemporal analysis of local field potentials and unit discharges in cat cerebral cortex during natural wake and sleep states. J. Neurosci. *19*, 4595-4608.

Destexhe, A., Hughes, S.W., Rudolph, M., and Crunelli, V. (2007). Are corticothalamic 'up' states fragments of wakefulness? Trends Neurosci. *30*, 334-342.

Doran, S.M. (2003). The dynamic topography of individual sleep spindles. Sleep Research Online *5*, 133-139.

Eschenko, O., Mölle, M., Born, J., and Sara, S.J. (2006). Elevated sleep spindle density after learning or after retrieval in rats. J. Neurosci. *26*, 12914-12920.

Frankland, P.W., and Bontempi, B. (2005). The organization of recent and remote memories. Nat. Rev. Neurosci. *6*, 119-130.

Gais, S., Albouy, G., Boly, M., Dang-Vu, T.T., Darsaud, A., Desseilles, M., Rauchs, G., Schabus, M., Sterpenich, V., Vandewalle, G., Maquet, P., and Peigneux, P. (2007). Sleep transforms the cerebral trace of declarative memories. Proc. Natl. Acad. Sci. U. S. A *104*, 18778-18783.

Gais, S., Mölle, M., Helms, K., and Born, J. (2002). Learning-dependent increases in sleep spindle density. J. Neurosci. *22*, 6830-6834.

Hill, S., and Tononi, G. (2005). Modeling sleep and wakefulness in the thalamocortical system. J. Neurophysiol. *93*, 1671-1698.

Marshall, L., and Born, J. (2007). The contribution of sleep to hippocampus-dependent memory consolidation. Trends Cogn Sci. *11*, 442-450.

Marshall, L., Helgadottir, H., Mölle, M., and Born, J. (2006). Boosting slow oscillations during sleep potentiates memory. Nature *444*, 610-613.

Massimini, M., Huber, R., Ferrarelli, F., Hill, S., and Tononi, G. (2004). The sleep slow oscillation as a traveling wave. J. Neurosci. *24*, 6862-6870.

Mölle, M., and Born, J. (2009). Hippocampus whispering in deep sleep to prefrontal cortex--for good memories? Neuron *61*, 496-498.

Mölle, M., Eschenko, O., Gais, S., Sara, S.J., and Born, J. (2009). The influence of learning on sleep slow oscillations and associated spindles and ripples in humans and rats. Eur. J. Neurosci. *29*, 1071-1081.

Mölle, M., Marshall, L., Gais, S., and Born, J. (2002). Grouping of spindle activity during slow oscillations in human non-rapid eye movement sleep. J. Neurosci. *22*, 10941-10947.

Mölle, M., Yeshenko, O., Marshall, L., Sara, S.J., and Born, J. (2006). Hippocampal sharp wave-ripples linked to slow oscillations in rat slow-wave sleep. J. Neurophysiol. *96*, 62-70.

Rechtschaffen, A., and Kales, A. (1968). A manual of standardized terminology, techniques and scoring system for sleep stages of human subjects (Bethesda, Maryland: US Department of Health, Education and Welfare).

Rosanova, M., and Ulrich, D. (2005). Pattern-specific associative long-term potentiation induced by a sleep spindle-related spike train. J. Neurosci. *25*, 9398-9405.

Schabus, M., Dang-Vu, T.T., Albouy, G., Balteau, E., Boly, M., Carrier, J., Darsaud, A., Degueldre, C., Desseilles, M., Gais, S., Phillips, C., Rauchs, G., Schnakers, C., Sterpenich, V., Vandewalle, G., Luxen, A., and Maquet, P. (2007). Hemodynamic cerebral correlates of sleep spindles during human non-rapid eye movement sleep. Proc. Natl. Acad. Sci. U. S. A *104*, 13164-13169.

Sejnowski, T.J., and Destexhe, A. (2000). Why do we sleep? Brain Res. *886*, 208-223.

Siapas, A.G., and Wilson, M.A. (1998). Coordinated interactions between hippocampal ripples and cortical spindles during slow-wave sleep. Neuron *21*, 1123-1128.

Steriade, M. (2006). Grouping of brain rhythms in corticothalamic systems. Neuroscience *137*, 1087-1106.

Steriade, M., Amzica, F., and Contreras, D. (1996). Synchronization of fast (30-40 Hz) spontaneous cortical rhythms during brain activation. J. Neurosci. *16*, 392-417.

Takashima, A., Petersson, K.M., Rutters, F., Tendolkar, I., Jensen, O., Zwarts, M.J., McNaughton, B.L., and Fernandez, G. (2006). Declarative memory consolidation in humans: a prospective functional magnetic resonance imaging study. Proc. Natl. Acad. Sci. U. S. A *103*, 756-761.

Terrier, G., and Gottesmann, C.L. (1978). Study of cortical spindles during sleep in the rat. Brain Res. Bull. *3*, 701-706.

Timofeev, I., and Bazhenov, M. (2005). Mechanisms and biological role of thalamocortical oscillations. In Trends in chronobiology research, F.H. Columbus, ed. (New York: Nova Science Publishers), pp. 1-47.

Tononi, G., and Cirelli, C. (2006). Sleep function and synaptic homeostasis. Sleep Med. Rev. *10*, 49-62.

Volgushev, M., Chauvette, S., Mukovski, M., and Timofeev, I. (2006). Precise long-range synchronization of activity and silence in neocortical neurons during slow-wave oscillations [corrected]. J. Neurosci. *26*, 5665-5672.

Werk, C.M., Harbour, V.L., and Chapman, C.A. (2005). Induction of long-term potentiation leads to increased reliability of evoked neocortical spindles in vivo. Neuroscience *131*, 793-800.

Wierzynski, C.M., Lubenov, E.V., Gu, M., and Siapas, A.G. (2009). State-dependent spike-timing relationships between hippocampal and prefrontal circuits during sleep. Neuron *61*, 587-596.

Table 1
Polysomnographic sleep parameter

Parameter	Mean ± SEM
TST	432.3 ± 9.7 min
Wake	2.8 ± 1.2 min
S1	1.5 ± 0.2 %
S2	55.7 ± 2.1 %
SWS	16.6 ± 1.3 %
REM	26.2 ± 1.9 %
SOL	3.9 ± 0.9 min

TST, total sleep time; S1 and S2, NonREM sleep stages 1 and 2; SWS, slow wave sleep; REM, rapid eye movement sleep; SOL, sleep onset latency. Percentages are given with reference to TST.

Table 2
Mean sleep spindle density (across 12 channels) and slow oscillation density (across 8 channels) during SWS and Stage 2 sleep in [number per 30 sec].

Subject	SWS slow spindles	SWS fast spindles	SWS SO	Stage 2 slow spindles	Stage 2 fast spindles	Stage 2 SO
1	1.16	2.23	2.74	1.69	2.29	0.61
2	1.25	2.78	3.80	2.36	2.86	0.40
3	1.57	2.79	3.51	2.71	3.22	1.27
4	2.49	2.85	3.52	2.43	3.04	1.30
5	2.12	2.82	0.83	2.18	2.81	0.43
6	1.15	3.10	1.06	2.19	3.49	0.21
7	2.41	2.67	2.62	2.02	3.17	0.46
8	1.00	1.78	1.64	1.75	2.93	0.39
9	1.48	2.34	4.13	2.01	2.62	0.86
10	2.11	2.20	1.94	2.11	2.66	0.82
11	2.01	2.28	3.97	2.37	2.74	0.82
Mean ± SEM	1.70 ± 0.16	2.53 ± 0.12	2.71 ± 0.36	2.16 ± 0.09	2.89 ± 0.10	0.69 ± 0.11

Table 3
Spindle peak frequencies in [Hz].

Subject	SWS slow spindles	SWS fast spindles	Stage 2 slow spindles	Stage 2 fast spindles
1	10.96	13.94	11.54	13.85
2	*	13.10	*	13.00
3	10.02	13.17	11.64	13.37
4	9.79	13.71	11.66	13.65
5	10.60	13.67	11.11	13.97
6	*	13.42	*	13.24
7	10.17	13.95	11.05	14.03
8	9.44	13.13	*	13.28
9	10.44	13.38	11.19	13.49
10	10.56	12.86	*	12.99
11	10.07	13.12	11.90	13.20
Mean ± SEM	10.23 ± 0.15	13.40 ± 0.11	11.44 ± 0.12	13.46 ± 0.11

* No peak detectable in the power spectra

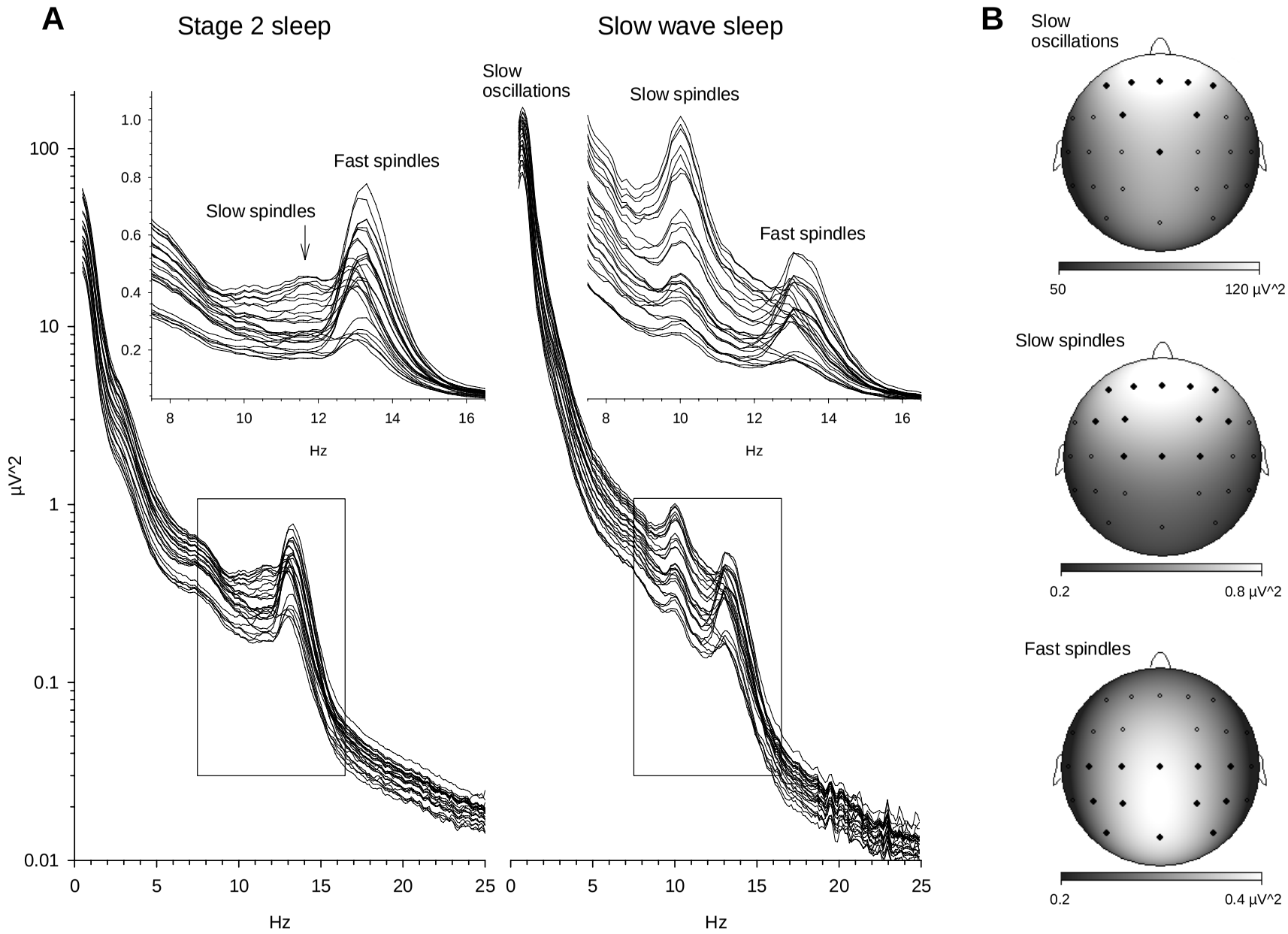
A
Stage 2 sleep
Slow wave sleep
Slow oscillations
Slow spindles
Fast spindles
Slow spindles
Fast spindles
μV^2
Hz
Hz
Hz
B
Slow oscillations
50
120 μV^2
Slow spindles
0.2
0.8 μV^2
Fast spindles
0.2
0.4 μV^2

Figure 1

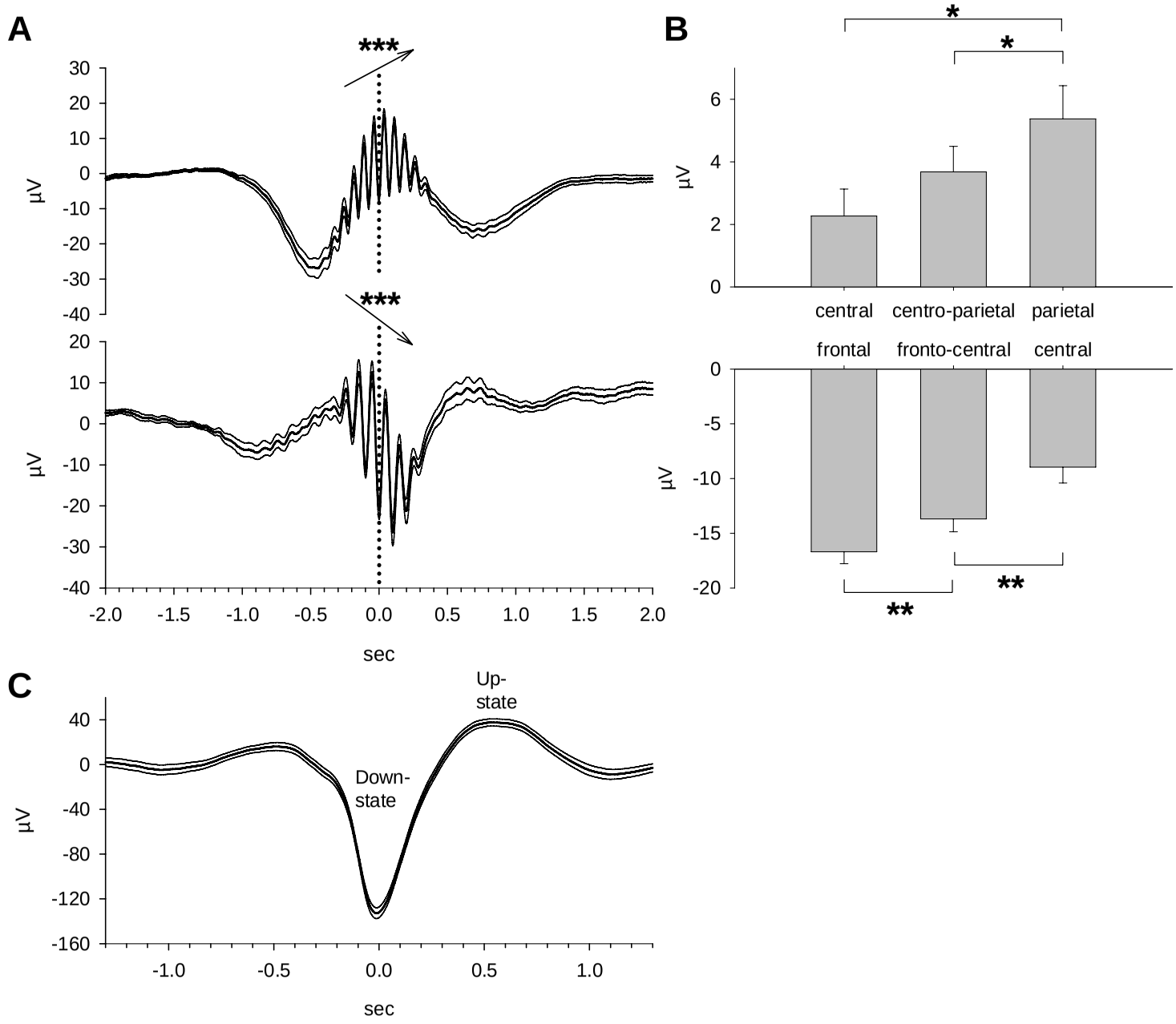
A
***
***
30
20
10
0
-10
-20
-30
-40
μV
-2.0
-1.5
-1.0
-0.5
0.0
0.5
1.0
1.5
2.0
sec
B
*
*
6
4
2
0
μV
central
centro-parietal
parietal
frontal
fronto-central
central
0
-5
-10
-15
-20
**
**
C
Up-
state
Down-
state
40
0
-40
-80
-120
-160
μV
-1.0
-0.5
0.0
0.5
1.0
sec

Figure 2

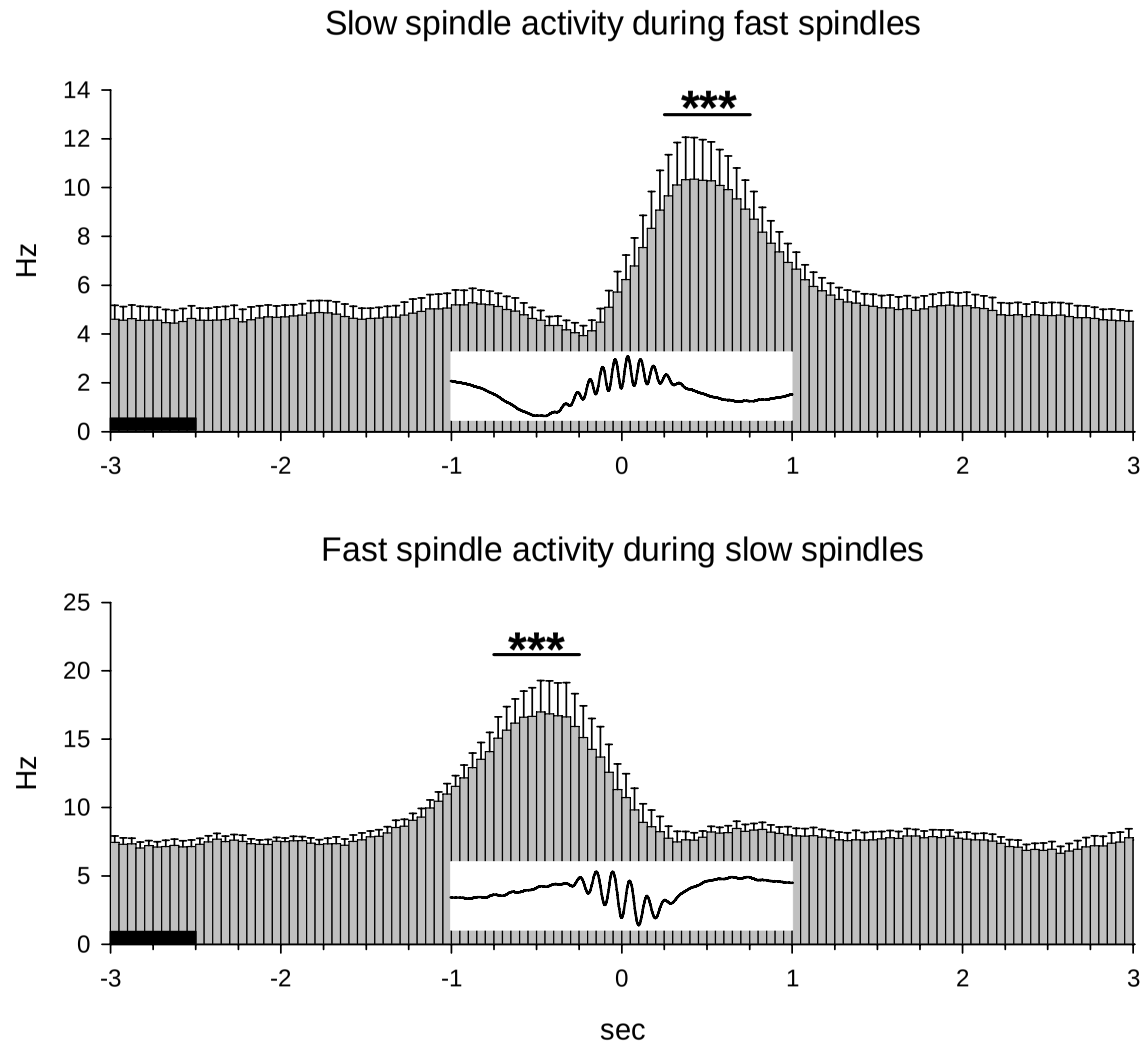
Slow spindle activity during fast spindles
***
Hz
14
12
10
8
6
4
2
0
-3
-2
-1
0
1
2
3
Fast spindle activity during slow spindles
***
Hz
25
20
15
10
5
0
-3
-2
-1
0
1
2
3
sec

Figure 3

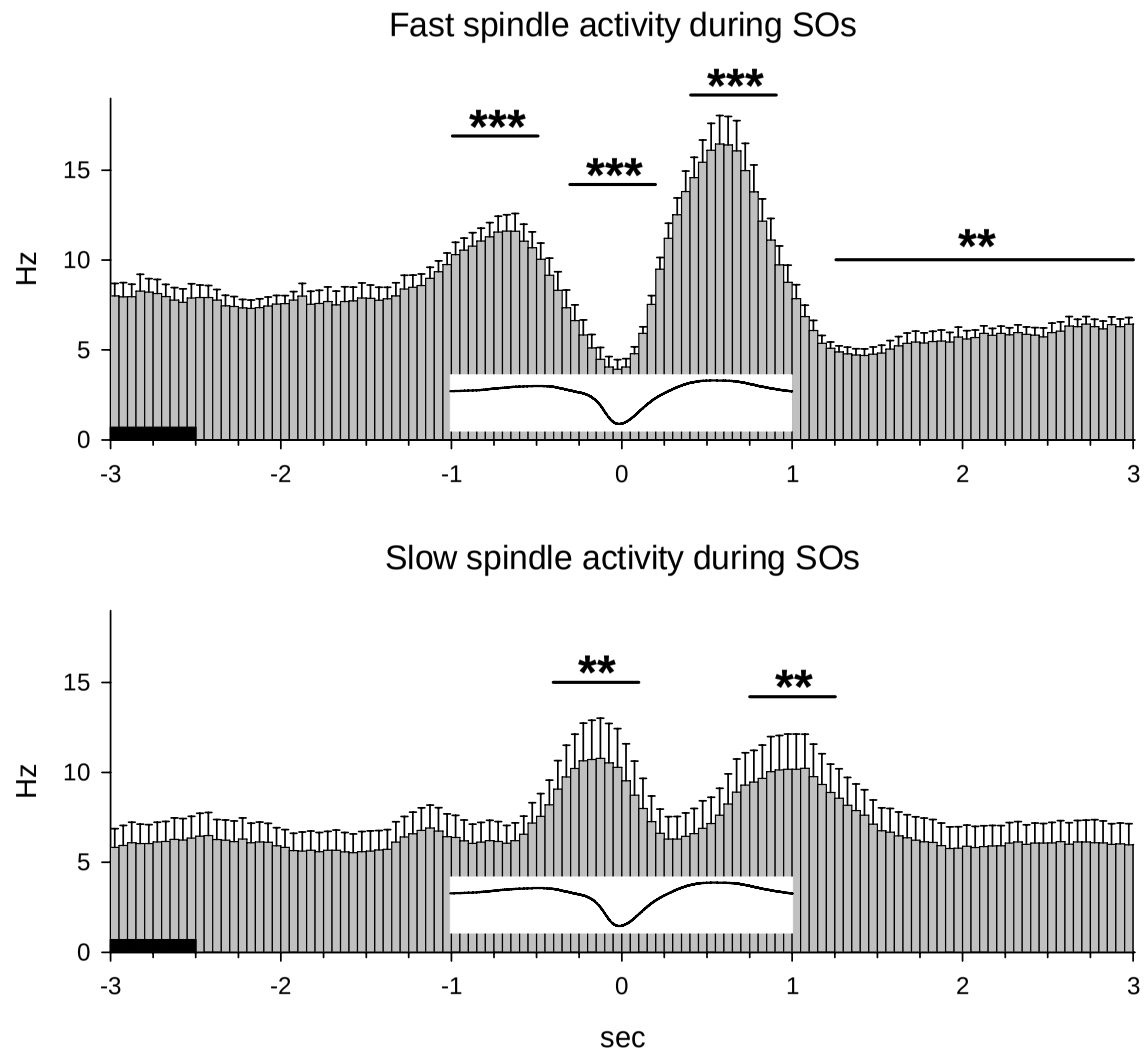
Fast spindle activity during SOs
***
***
***
**
Hz
15
10
5
0
-3
-2
-1
0
1
2
3
Slow spindle activity during SOs
**
**
Hz
15
10
5
0
-3
-2
-1
0
1
2
3
sec

Figure 4

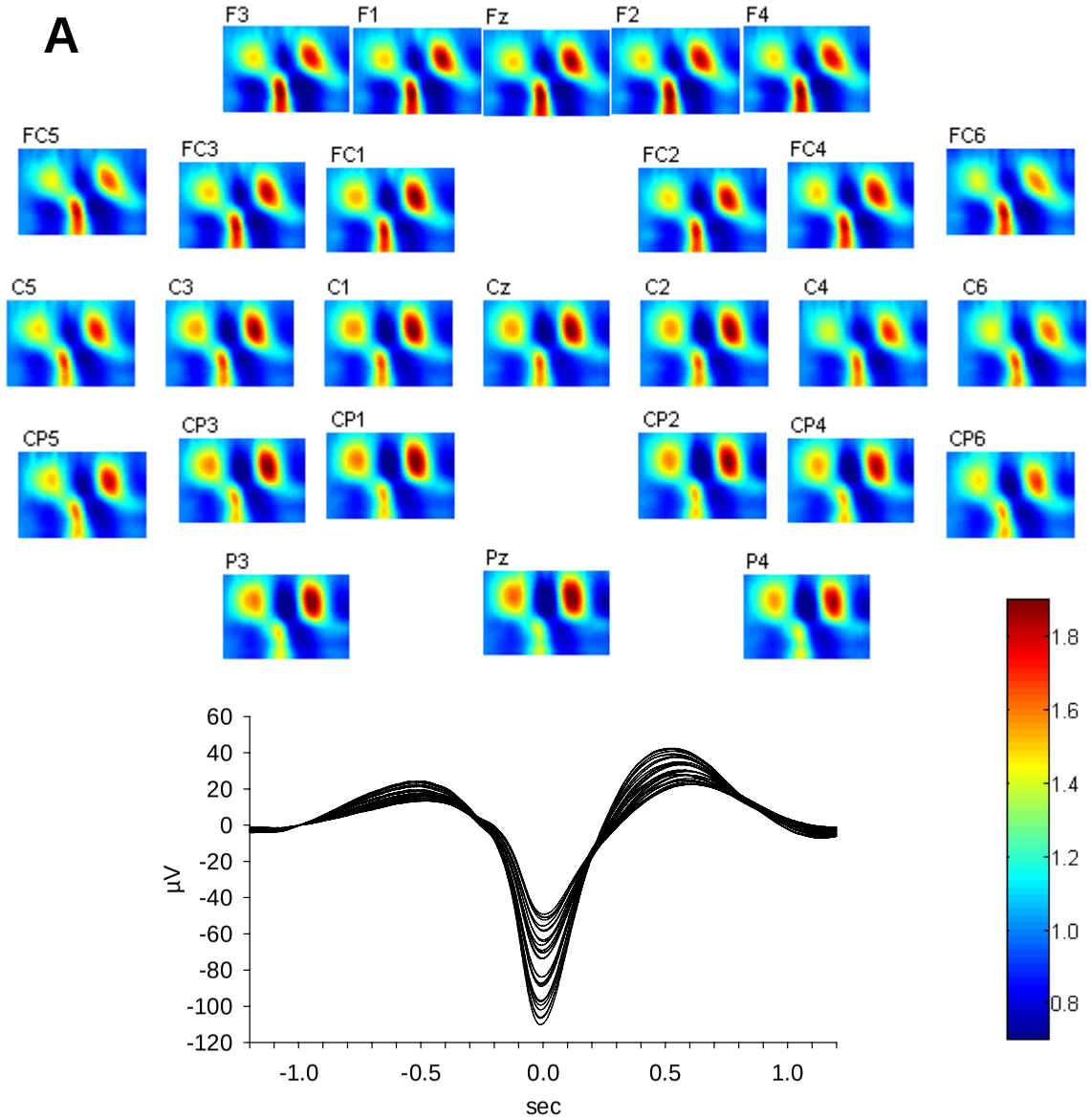
A
F3
F1
Fz
F2
F4
FC5
FC3
FC1
FC2
FC4
FC6
C5
C3
C1
Cz
C2
C4
C6
CP5
CP3
CP1
CP2
CP4
CP6
P3
Pz
P4
60
40
20
0
-20
-40
-60
-80
-100
-120
μV
-1.0
-0.5
0.0
0.5
1.0
sec
1.8
1.6
1.4
1.2
1.0
0.8

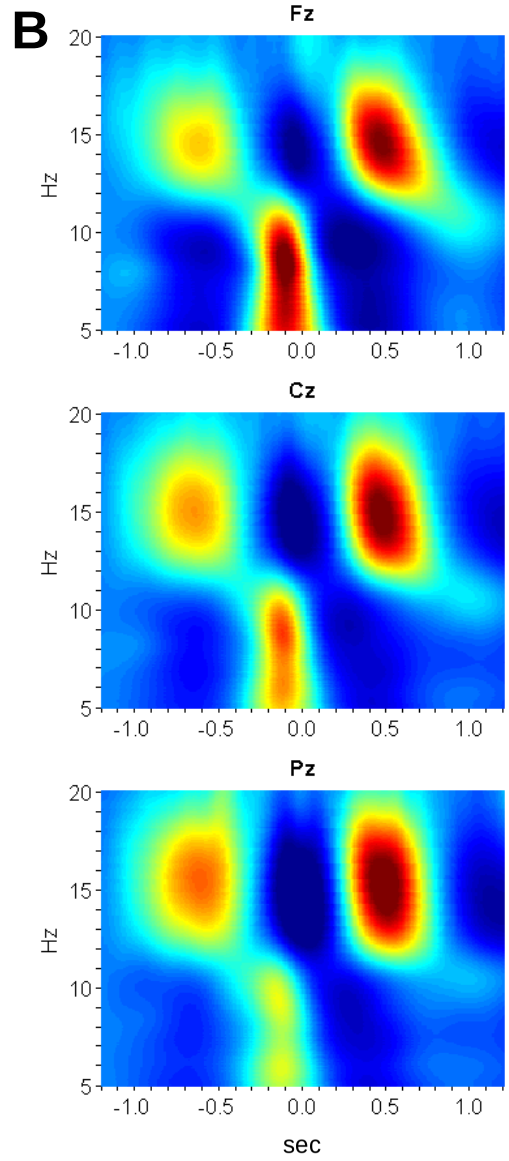
B
Fz
Cz
Pz
20
15
10
5
Hz
-1.0
-0.5
0.0
0.5
1.0
sec

Figure 5

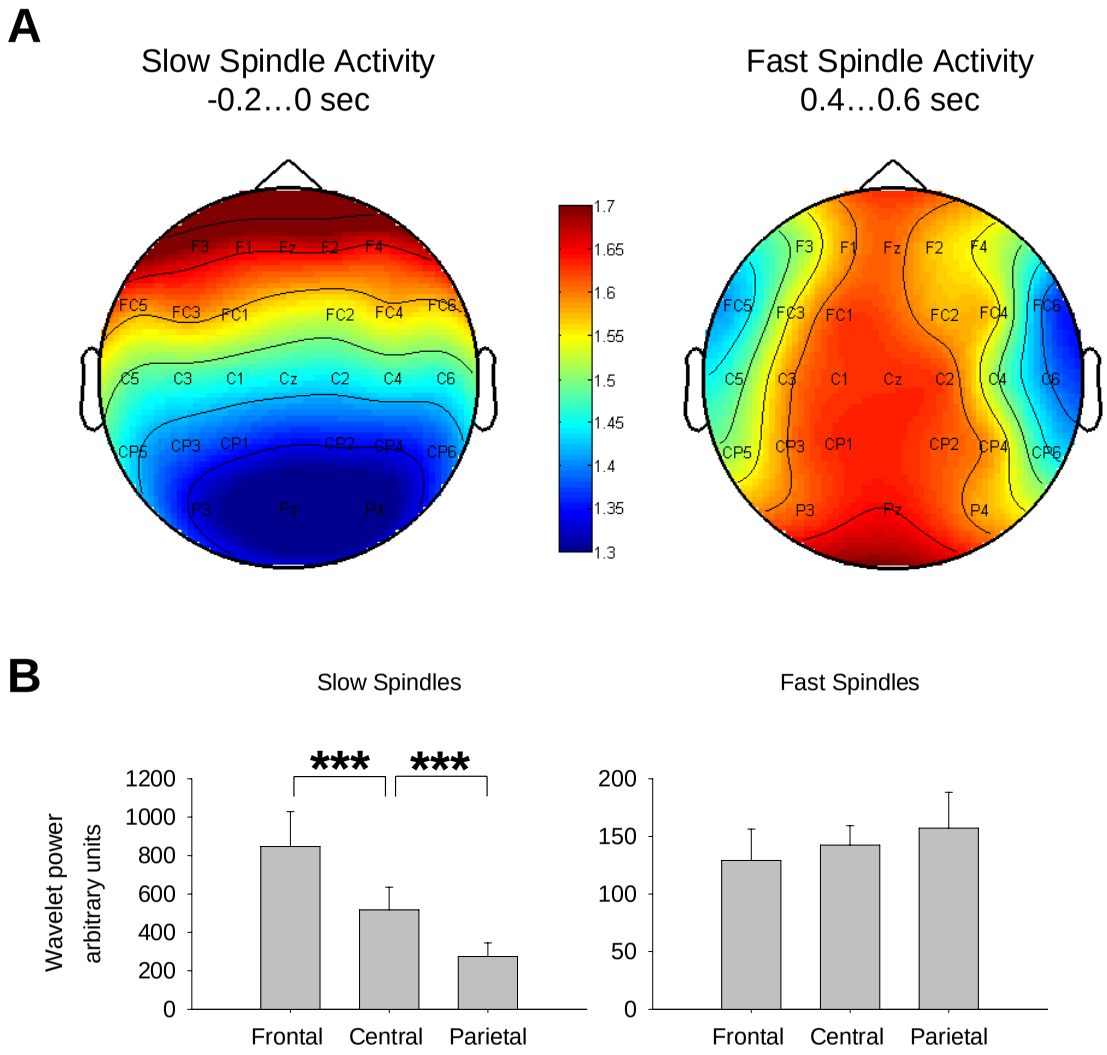
A
Slow Spindle Activity
-0.2…0 sec
Fast Spindle Activity
0.4…0.6 sec
F3 F1 Fz F2 F4
FC5 FC3 FC1 FC2 FC4 FC6
C5 C3 C1 Cz C2 C4 C6
CP5 CP3 CP1 CP2 CP4 CP6
P3 Pz P4
1.7
1.65
1.6
1.55
1.5
1.45
1.4
1.35
1.3
B
Slow Spindles
Fast Spindles
Wavelet power
arbitrary units
***
***
1200
1000
800
600
400
200
0
200
150
100
50
0
Frontal
Central
Parietal
Frontal
Central
Parietal

Figure 6

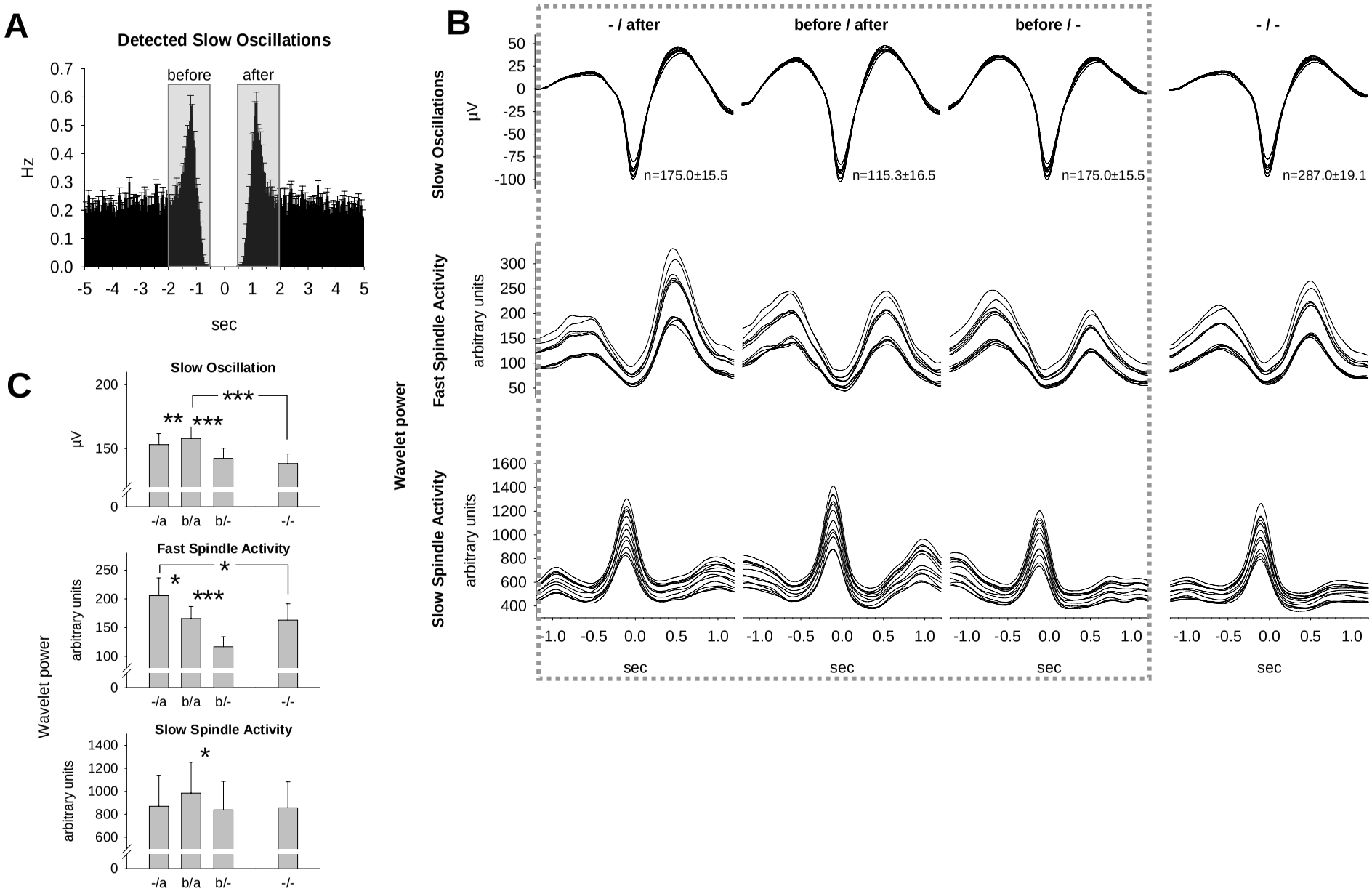
A
Detected Slow Oscillations
before
after
Hz
sec
B
- / after
before / after
before / -
- / -
Slow Oscillations
µV
n=175.0±15.5
n=115.3±16.5
n=175.0±15.5
n=287.0±19.1
Fast Spindle Activity
arbitrary units
Slow Spindle Activity
arbitrary units
Wavelet power
sec
C
Slow Oscillation
µV
Fast Spindle Activity
arbitrary units
Slow Spindle Activity
arbitrary units
Wavelet power
-/a
b/a
b/-
-/-

Figure 7

Paper IV

Title

Sleep spindles drive learning-specific hippocampo-neocortical reactivation

Authors

Til Ole Bergmann[1,*], Matthias Mölle[2], Jens Diedrichs[1], Jan Born[2], Hartwig Roman Siebner[1,3,4]

Affiliation

[1]*Department of Neurology, Christian-Albrechts University of Kiel, Germany*

[2]*Department of Neuroendocrinology, University of Lübeck, Germany*

[3]*Danish Research Center for Magnetic Resonance, Department of MR, Copenhagen University Hospital Hvidovre, Hvidovre, Denmark*

[4]*Institute of Neurology, Psychiatry and Senses, University of Copenhagen, Denmark*

Contact information

Til Ole Bergmann, Department of Neurology, Christian-Albrechts University of Kiel, Schittenhelmstrasse 10, D-24105 Kiel, Germany. Tel: +49 431 597 8823, fax: +49 431 597 8502, e-mail: t.bergmann@neurologie.uni-kiel.de

Running title: Spindle-related hippocampal-neocortical activation

SUMMARY

Newly acquired declarative memories are reactivated during NonREM sleep presumably to stimulate the hippocampo-to-neocortical transfer of memories for long-term storage. Thalamo-cortical spindles are thought to represent a key mechanism in this transfer by feeding reactivated hippocampal memory information into neocortical networks. To elaborate this hypothesis in humans, we recorded simultaneous EEG-fMRI during NonREM sleep after subjects had learned face-scene associations compared to a visuomotor control task. EEG-informed fMRI revealed conjoint hippocampal and neocortical activations that were time-locked to sleep spindles and were more strongly tuned by spindle amplitudes after learning than control. In the neocortex, increased spindle-related activity was restricted to face- and scene-selective visual cortex (fusiform and occipital face and parahippocampal place areas) engaged in prior learning. Learning performance before sleep further predicted the increase in spindle-related hippocampal activity. Together, our data provide first-time evidence for a learning-induced coactivation of hippocampal-neocortical memory representations time-locked to spindles during human sleep.

Highlights:

- EEG-fMRI during post-learning sleep reveals activation of declarative memory traces
- Activations are restricted to hippocampus and stimulus-specific neocortical sites
- Activations are time-locked to sleep spindles and increase with their amplitude
- Spindle-related hippocampal activation is predicted by prior learning performance

INTRODUCTION

It is a widely accepted idea that the hippocampus rapidly binds neocortical representations to integrated memory traces during the acquisition of declarative memories (Eichenbaum, 2000). During subsequent offline periods, the initially labile traces are conjointly reactivated in hippocampus and neocortex thereby promoting the formation of hippocampus-independent direct cortico-cortical connections (Buzsaki, 1989; Frankland and Bontempi, 2005; McClelland et al., 1995; Rasch and Born, 2007). This system consolidation process does not only lead to a reorganization of hippocampal-neocortical memory representations but is also thought to stabilize these memories making them resistant to decay and interference. As non-rapid eye movement (NonREM) sleep is accompanied by an almost complete suppression of incoming sensory information, this brain state provides an optimal environment for reactivating and reorganizing memory traces in the absence of interfering inputs. In fact, accumulated behavioral and neurophysiological evidence now strongly supports the beneficial role of sleep for memory consolidation (Born et al., 2006; Diekelmann et al., 2009; Maquet, 2001; Stickgold, 2005).

Thalamo-cortical sleep spindles during NonREM sleep (i.e. transient oscillatory patterns of 12-16 Hz with waxing and waning amplitude) are the candidate mechanism for mediating neuronal plasticity in the hippocampal-neocortical circuitry thus subserving processes of memory consolidation (Sejnowski and Destexhe, 2000; Steriade and Timofeev, 2003). Synchronized by the neocortical < 1 Hz slow oscillation (Steriade et al., 1993), spindles often occur time-locked to the sharp wave-ripples (> 100 Hz) which accompany memory trace reactivation in hippocampal networks (Clemens et al., 2007; Mölle et al., 2002; Mölle et al., 2006; Sirota et al., 2003; Steriade, 2006; Sutherland and McNaughton, 2000; Wierzynski et al., 2009).

Spindles may thus provide a fine-tuned temporal frame in which hippocampal ripples together with reactivated memory information become sandwiched into single spindle cycles which effectively feed the hippocampal memory information into selected neocortical circuits (Diekelmann and Born, 2010; Mölle and Born, 2009; Siapas and Wilson, 1998; Sirota et al., 2003; Wierzynski et al., 2009). The massive Ca^{2+} influx in neocortical pyramidal cells caused by thalamo-cortical spindles could set the stage for persistent synaptic changes mediating the long-term storage of hippocampal memory in the neocortex (Sejnowski and Destexhe, 2000). In fact, often an immediate increase in spindle number and amplitude has been observed after learning in humans (Clemens et al., 2005, 2006; Fogel and Smith, 2006; Gais et al., 2002; Schabus et al., 2004; Schabus et al., 2008).

Sleep spindles, unlike hippocampal ripples, can be easily investigated in the human scalp EEG (De Gennaro and Ferrara, 2003) and their neuronal correlates have even been described using event-related functional magnetic resonance imaging (fMRI) (Schabus et al., 2007). However, despite substantial evidence that spindles are temporarily linked to hippocampal memory replay and ripple activity, it has not been examined so far whether spindle associated neuronal activations indeed reflect neocortical reactivation of memories that were newly encoded prior to sleep. Positron emission tomography (PET) studies revealed reactivation of task-related brain activity in humans that occurred during rapid eye movement (REM) sleep after procedural learning and during slow wave sleep (SWS) after declarative learning (Maquet et al., 2000; Peigneux et al., 2004; Peigneux et al., 2003). However, these studies examined sleep stages in general and did not focus on specific electrophysiological phenomena like spindles that are particularly involved in the consolidation process.

Current models on sleep-dependent system memory consolidation make quite precise predictions about the very topography and timing of hippocampal-neocortical reactivation. It should (i) be spatially defined to those neocortical regions actually representing the encoded information (Frankland and Bontempi, 2005) and (ii) occur time-locked to thalamo-cortical spindle activity (Diekelmann and Born, 2010; Marshall and Born, 2007). This study explicitly aimed to test both predictions. (i) To dissociate the neocortical target sites of hippocampal reactivation, we designed a hippocampus-dependent associative learning task based on stimuli whose neocortical representations are well-localized, i.e., pictures of faces that activate the fusiform face area (FFA, Kanwisher et al., 1997) and occipital face area (OFA, Gauthier et al., 2000) and scenes that activate the parahippocampal place area (PPA, Epstein and Kanwisher, 1998). In the evening, subjects either performed the LEARNING task or a visuomotor CONTROL task that was matched for basal visual input and motor output but did not involve faces or scenes and did not require any form of associative learning (see **Figure 1** for experimental design and task description). (ii) During subsequent NonREM sleep, we simultaneously recorded fMRI and EEG with sufficiently high temporospatial resolution to test for changes in regional activity in the hippocampus and ventral visual neocortical areas during NonREM sleep that are time-locked to the expression of sleep spindles. We found that face-scene learning triggered conjoint activations in the hippocampus and stimulus specific neocortical areas (i.e., FFA, OFA, and PPA) during subsequent NonREM sleep. In line with the hypotheses, this hippocampal-neocortical co-activation was time-locked to the expression of sleep spindles and in its magnitude tightly linked to amplitude variations of discrete spindles.

RESULTS

Behavioral Data

At the end of the LEARNING task subjects successfully recalled on average 42 of the 48 cued associates. Response accuracy on immediate cued recall improved almost linearly across the four runs (run 1 to 4: 21.8 ± 6.3; 29.4 ± 7.3; 36.4 ± 6.9; 41.6 ± 6.8; **Figure 2**) as indicated by paired-sample t-tests (run 2-1: $T_8 = 4.65$, $P = 0.002$**;** run 3-2:$T_8 = 4.22$, $P = 0.003$**;** run 4-3:$T_8 = 5.96$, $P < 0.001$). Direct assignment of all picture pairs during the additional recognition task revealed that stimuli had not merely been associated with correct finger presses but in fact stimulus-stimulus associations had been learned (38.2 ± 6.1 correct pairs; **Figure 2**). Subjective sleepiness reported before task fMRI performance was comparable for LEARNING and CONTROL conditions (4.8 ± 1.2 vs. 5.2 ± 1.3; $P > 0.3$).

EEG

Sleep architecture in both EEG-fMRI sleep sessions was comparable (**Table 1**; no significant differences) as was the number of epochs in sleep stage 2 (LEARNING vs. CONTROL: 52 ± 21 vs. 57 ± 28; $P > 0.5$) and SWS (74 ± 25 vs. 66 ± 24; $P > 0.3$) that were included in the fMRI analysis. Sleep spindles during LEARNING and CONTROL sleep (**Figure 3**) did not differ in total number (LEARNING vs. CONTROL: 1043 ± 194 vs. 1020 ± 129), density (8.26 ± 0.90 vs. 8.35 ± 0.93 per 30 s), or amplitude (5.9 ± 1.6 µV vs. 6.0 ± 1.6 µV; $P > 0.4$ for all comparisons). LEARNING and CONTROL sleep EEG-fMRI sessions also did not differ regarding time spend in the MRI scanner (LEARNING vs. CONTROL: 111 ± 20 vs. 110 ± 19 min) or in number (3.3 ± 1.4 vs. 3.2 ± 2.2) or total duration (63 ± 10 vs. 61 ± 10 min) of analyzed NonREM segments ($P > 0.4$ for all comparisons). The same hold true for slow oscillations (**Table S1**). Taken together,

these analyses revealed no differences in any of the involved electrophysiological parameters that could have biased comparisons between LEARNING and CONTROL sessions within subsequent fMRI models.

fMRI

Learning-related Brain Activity during Wakefulness

Analyses of task-related activity during memory encoding and immediate recall before sleep localized neocortical representations specific for face and scene stimuli and determined the general LEARNING task-related brain activation pattern relative to that during the visuomotor CONTROL task (**Figure 4).** Face-specific activity was predominant bilaterally in the FFA and the amygdala (encoding and recall) as well as the OFA (recall), whereas scene-specific responses were located bilaterally in the PPA, the parieto-occipital sulcus/retrosplenial cortex region, as well as the transverse occipital and intraparietal sulcus (recall). General, stimulus-independent activity during memory encoding comprised bilateral hippocampus, precuneus, and inferior parietal cortex as well as left inferior, medial and superior frontal gyrus, and medial and superior temporal gyrus, whereas cued recall was generally associated with bilateral activation of the caudate nucleus, precuneus, and anterior cingulate cortex, as well as left medial frontal gyrus and inferior parietal cortex.

Spindle-related Brain Activity during NonREM sleep

A wide set of brain regions showed a modulation of regional activity levels during NonREM sleep depending on the temporal expression of sleep spindles (**Figure 5**). Spindle-related activations in bilateral thalamus, hippocampus and adjacent parahippocampal gyrus, ventral striatum, brainstem, inferior temporal cortex and several cortical regions near the vertex were principally associated with the

occurrence of spindles per se, independent of their respective amplitude (**Figure 5;** areas coded in red). In other brain regions, spindle-related activity covaried with the amplitude of discrete sleep spindles, including bilateral hippocampus, insula, anterior cingulate cortex, and supplementary motor area (**Figure 5;** areas coded in blue).

Increases of Spindle-related Brain Activity during NonREM sleep after Learning

Several brain regions showed enhanced spindle-related activation during NonREM sleep following LEARNING of face-scene associations compared to the visuomotor CONTROL task. Irrespective of spindle amplitude, the spindle-related activity level was higher in the left amygdala, the locus coeruleus, and the head of the caudate nucleus after LEARNING than CONTROL task performance (**Figure 6**; areas coded in red). However, the most important differences were observed when taking into account the spindle amplitude (**Figure 6**; areas coded in blue). Distinct areas in the right hippocampus, left PPA, right FFA, and bilateral OFA showed a stronger increase in regional activity with individual spindle amplitude after LEARNING of face-scene associations (see **Table 2** for peak voxels and statistical values). The neocortical increase of spindle amplitude-related activations was restricted to material-specific areas of the ventral visual processing stream which showed a strong overlap with learning-related neocortical activations as identified during prior learning (i.e., PPA, FFA, and OFA). This spatial overlap was clearly evident at the initial significance threshold of $P_{uncorr} < 0.001$. The specificity of overlapping activity was still present when lowering the threshold to $P_{uncorr} < 0.01$**.** At this threshold, the overlapping activity in the respective ventral visual cortical areas increased in extent, but no additional clusters emerged in other brain regions **(Figure 7)**. In PPA and FFA, the voxels showing a learning-specific increase in activation with spindle amplitude were located almost completely within the clusters of learning-related activation during

both memory encoding and recall. There was only a partial overlap of activation clusters in OFA, and this overlap was only present when considering recall but not encoding related activation. In contrast to the neocortical areas, no spatial overlap was found in the hippocampus. The hippocampal cluster showing a stronger activation with spindle amplitude during post-learning NonREM sleep was located posterior to the hippocampal cluster activated during memory encoding before sleep.

Correlational analyses investigated the link between individual learning performance and subsequent sleep spindle-related hippocampal activity. The better a subject performed on the LEARNING task before sleep (as indicated by the area under the learning curve, AULC; **Figure 2**), the more pronounced was the learning-specific increase in spindle amplitude-related hippocampal activity ($r = 0.81$, $p < 0.01$) and average sleep spindle amplitude ($r = 0.72$, $p < 0.05$; **Figure 8**).

DISCUSSION

Here we show for the first time that learning of face-scene associations triggers conjoint hippocampal-neocortical activation in subsequent NonREM sleep. Neuronal activity in right hippocampus as well as in neocortical regions specialized for processing of face and scene stimuli became more strongly coupled to the amplitude of single sleep spindles after LEARNING than after performance on a CONTROL task. Learning performance during wakefulness predicted the increase in hippocampal responsiveness to spindle amplitudes during subsequent sleep. These findings lend further support to the notion that sleep spindles represent a key mechanism for hippocampal-neocortical processing of recently acquired memory traces during sleep (Born et al., 2006; Diekelmann and Born, 2010; Marshall and Born, 2007; Sejnowski and Destexhe, 2000; Steriade and Timofeev, 2003).

Task-related brain activity during wakefulness

We deliberately used a paired associates LEARNING task that relied on the processing of face and scene stimuli in highly specialized neocortical sites of the ventral visual stream as well as on the hippocampus for storing the learned associations. Accordingly, the LEARNING task more strongly engaged memory related brain regions, such as hippocampus (Eichenbaum, 2000), precuneus, and lateral parietal areas (Wagner et al., 2005) relative to the visuomotor CONTROL task. As intended, the LEARNING task further particularly engaged the material-specific neocortical regions of interest in the ventral visual stream, i.e. FFA (Kanwisher et al., 1997), OFA (Gauthier et al., 2000), and PPA (Epstein and Kanwisher, 1998). This provided us with a priori information regarding the neocortical candidate regions expected to show a conjoint learning-specific activation with the hippocampus during subsequent sleep.

In line with previous work, face cues also evoked stronger activity in the amygdala (Adolphs and Spezio, 2006), whereas scene cues caused activation peaking in the parieto-occipital sulcus/retrosplenial cortex region (MacEvoy and Epstein, 2007; Maguire, 2001), the transverse occipital sulcus (Grill-Spector, 2003; Hasson et al., 2003; MacEvoy and Epstein, 2007), and the intraparietal sulcus (Grill-Spector, 2003).

Spindle-related brain activity independent of learning

In accordance to previous findings (Schabus et al., 2007), we observed spindle-related BOLD-activity independently of task condition in a set of brain regions including bilateral thalamus, brainstem, anterior cingulate cortex, supplementary motor area, insulae, and the hippocampus. A relevant new finding was that the

activity level in bilateral hippocampus and adjacent parahippocampal gyrus was consistently modulated by the particular amplitude of a sleep spindle. This finding tightly couples hippocampal network activity to the wide spread expression of thalamo-cortical spindles in the surface EEG. It also ties in well with results from intracranial recordings, suggesting a close temporal interaction of neocortical spindles and hippocampal ripples (Clemens et al., 2007; Mölle et al., 2009; Siapas and Wilson, 1998; Sirota et al., 2003; Wierzynski et al., 2009). Within an interactive framework of neocortical-hippocampal loops, emergent spindle activity might drive hippocampal ripples which in turn feed back into ongoing cycles of the thalamo-cortical spindle to effectively modulate the input to neocortical neurons (Mölle et al., 2009; Sirota et al., 2003).

The neurophysiological determinants of trial-by-trial variations in spindle amplitude as assessed by the human surface EEG remain yet to be fully clarified. In this context, it is interesting that thalamic activity levels were markedly enhanced during spindles per se, but hardly modulated by spindle amplitude. Although the thalamus is the core generator of sleep spindles (Steriade, 2003), thalamo-cortical spindle input can be amplified or suppressed by intracortical circuits (Contreras et al., 1997b; Kandel and Buzsaki, 1997). These local cortical mechanisms are a likely neural substrate contributing to the amplitude modulation of subsequent spindle events that are observed in surface EEG recordings.

Spindle-related activation in learning-related brain regions

Learning associations between faces and scenes altered spindle-related cortical activity. Our central hypothesis was that previous acquisition of hippocampus-dependent (declarative) memories should enforce the hippocampal-neocortical

dialogue, thus enhancing the interaction between hippocampal ripples and thalamo-cortical spindle input (Mölle et al., 2009; Sirota et al., 2003). If so, neuronal activity should become more tightly coupled to sleep spindles after learning specifically in those neocortical regions that represent the newly encoded information due to both the increased contribution of reentrant activity from the hippocampal system (Sirota et al., 2003) and increased responsiveness of cortical circuits to spindle input after synaptic potentiation (Werk et al., 2005).

Compared to the visuomotor control task, paired associative learning of face and scene cues specifically altered sleep spindle-related activity in those ventral visual areas that are specialized in the processing of faces and scenes. In accordance with our prediction, these neocortical regions became more strongly coupled to spindle amplitude variations after learning. Neocortical clusters showing increased activity with spindle amplitude in post-learning NonREM sleep closely corresponded to those engaged in prior learning.

Regardless of the learning context, the variation in spindle amplitude consistently modulated neuronal activity levels in the hippocampus during NonREM sleep. This general sensitivity of the hippocampus to fluctuations in spindle amplitude increased in the right hippocampus after paired associative learning. Furthermore, the strength of spindle-related hippocampal activation during NonREM sleep depended on individual encoding performance during prior wakefulness. Together with the learning-induced increase in material-specific visual areas, the spindle effects on hippocampal activity corroborate the view that sleep spindles generate a neural context which facilitates hippocampal-neocortical processing.

Only in a subset of task-related brain regions, regional activity became sensitized to spindle amplitudes after paired associative learning. In fact, the

increased responsiveness to spindle amplitudes was mainly restricted to those regions actually processing the newly encoded memory traces (i.e., the hippocampus linking stimulus-representations in FFA, PPA, and OFA). Other learning-related frontoparietal areas did not express such change in spindle-related activity, presumably because they subserve encoding and retrieval of memories rather than their actual storage. They therefore remain unchanged by learning and do not require any reactivation.

Additional clusters in left locus coeruleus, head of caudate nucleus, and the amygdala showed increased activation during sleep spindles after learning, independent of spindle amplitude. Although none of these clusters overlapped with those of task-related activity, adjacent parts of the caudate nuclei and the amygdalae were activated by prior learning. The caudate nucleus subserves stimulus-response learning (Packard and Knowlton, 2002) and strongly interacts with the hippocampal system (Poldrack and Rodriguez, 2004), which has also been demonstrated in the context of sleep-dependent memory reorganization (Orban et al., 2006). Likewise, the amygdala processes social stimuli, such as faces (Adolphs and Spezio, 2006) and is critically involved in the consolidation of emotional memories during sleep (Sterpenich et al., 2009).

Notably, the locus coeruleus constituting the major source of noradrenaline in the brain, has been rendered essential for learning-related plasticity (Sara, 2009) as well as its consolidation during sleep (Diekelmann and Born, 2010). Recordings in the rat showed not only that locus coeruleus bursts are entrained to the slow oscillation (Lestienne et al., 1997), but also that locus coeruleus firing is increased during SWS after olfactory learning (Eschenko and Sara, 2008). Thus, the increased activity of the locus coeruleus during spindles after learning well fits the idea of short

spindle-associated windows of cortical plasticity during SWS (Sejnowski and Destexhe, 2000; Steriade and Timofeev, 2003).

Conclusion

Our findings are compatible with the notion of a sleep-dependent hippocampal-neocortical dialogue that reactivates memory traces for the sake of redistribution from hippocampal to neocortical networks for long-term storage (Buzsaki, 1989; Diekelmann and Born, 2010; Frankland and Bontempi, 2005; McClelland et al., 1995). However, alternative explanations cannot be ruled out based on the correlational nature of our data. It is therefore possible, though unlikely in our understanding, that the observed spindle-related reactivations merely reflect a functionally meaningless epiphenomenon of previously potentiated synaptic connections which become more strongly recruited by unspecifically reverberating spindle activity. Foregoing pioneering PET studies have demonstrated increased regional cerebral blood flow in task-related brain regions during REM sleep after procedural learning of a *serial reaction time task* (Maquet et al., 2000; Peigneux et al., 2003) and during SWS after performance on a spatial navigation task (Peigneux et al., 2004). We now used combined EEG-fMRI recordings which have a superior temporospatial resolution compared with PET. Because of this and the employment of a paired associates learning task relying on the hippocampal binding of well-located neocortical representations, our results clearly extend existing data in two important aspects: (i) We provide first-time evidence that hippocampal activation during post-learning sleep is indeed accompanied by the reactivation of previously associated representations in the neocortex, supporting the idea of a hippocampal-neocortical memory reactivation. (ii) We demonstrate that declarative memory

reactivation is directly linked to the expression of individual sleep spindles rather than equally distributed throughout SWS.

EXPERIMENTAL PROCEDURES

Participants

Twenty-four healthy volunteers were recruited from the student population of the University of Kiel and participated in the experiments after they had given written informed consent. However, due to the adverse conditions of the MRI environment, only eleven out of fifteen subjects who initially passed the adaptation night also reached SWS in both experimental conditions, and two further data sets had to be excluded because of insufficient data quality (e.g., strong sweating artifacts). Data could therefore be successfully acquired from nine subjects (4 females, mean age: 25, range: 21-27 years). Experimental procedures conformed to the Declaration of Helsinki and were approved by the Ethics Committee of the University of Kiel. Participants were right-handed (Oldfield, 1971), free of medication, and had no history of neurological or psychiatric disease. They were instructed to restrict their sleep to 4 hours during the previous night and were not allowed to drink alcohol or caffeine during the day prior to each experimental night.

Experimental Design

Subjects were preselected according to whether or not they reached SWS during an ADAPTATION night with full EEG-fMRI recording inside the scanner. Anatomical images were acquired before the EEG cap was applied and subjects went to sleep. Successful participants were included in the actual experiment, taking part in two experimental conditions (LEARNING vs. CONTROL) which were separated by at least a

week and balanced in order across subjects. Procedures were identical in both experimental conditions except for the behavioral task itself (**Figure 1A**).

Subjects arrived in the lab around 7 pm, were instructed, and received a thorough training of the upcoming LEARNING or CONTROL task (**Figure 1B,C**). Around 8pm, the respective task-fMRI session started, lasting about 70 min, and in LEARNING nights followed by an additional recognition task outside the scanner (**Figure S1**). Then, EEG cap and bipolar electrodes were administered and coregistered to the individual anatomical image via frameless stereotactic neuronavigation. Around 11pm, subjects were again bedded in the MRI scanner to sleep for max. 2.5 h of continuous EEG-fMRI recording. Thereafter, subjects spent the rest of the night in the nearby sleep lab until they left the next morning.

To monitor potential differences in subjective sleepiness between experimental conditions, subjects filled out a German version of the Stanford Sleepiness Scale (Hoddes et al., 1973) before LEARNING and CONTROL tasks.

Behavioral Tasks

In the LEARNING task, subjects had to learn associations between pictures of faces and scenes while in the CONTROL task only basic visuomotor performance but no associative learning was required (both tasks performed during fMRI, **Figure 1**). An additional recognition task in the LEARNING condition (performed outside the scanner; **Figure S1**) emphasized the generation of specific stimulus-stimulus instead of mere stimulus-response category associations. See **Supplemental Experimental Procedures** for details.

The LEARNING task consisted of eight alternating runs of memory encoding and immediate recall (four each). During encoding runs, subjects had to learn pairs of consecutively presented pictures (pairs were combined of *male faces*, *female faces*,

urban scenes, *rural scenes*, and *scrambled images*, the latter considered as "nothing"). During recall runs, increasing memory strength was tested. All face and scene pictures were presented separately and subjects had to indicate the category of the paired associate by button press. No feedback of response accuracy was provided (**Figure 1B)**.

The CONTROL task was constructed in parallel, with two alternating types of simple monitoring tasks, matched to the LEARNING task regarding basic visual input (same but scrambled stimuli) and motor output (same buttons to press at the same time). Both tasks required a certain level of attention and information processing but no associative learning and no processing of faces and scenes (**Figure 1C)**.

In the recognition task, subjects had to choose the specific paired associate for each stimulus out of the complete set of possible stimuli. Again, no feedback of response accuracy was provided (**Figure S1)**..

Unless specified otherwise, data are reported as mean (M) ± standard deviation (SD). Statistical comparisons rely on two-sided paired t-tests with P-values < 0.05 considered significant.

Experimental Setting

During task-fMRI, subjects were laying on the MRI table, equipped with headphones for communication and noise protection, a mirror-display-combination for visual stimulus presentation, and a five-button box at the right hand for response collection (see **Supplemental Experimental Procedures** for technical details).

During subsequent sleep-EEG-fMRI, subjects wore light sleeping clothes and thoroughly inserted foam earplugs providing ~35 dB sound attenuation (*Ohropax Color*, Ohropax, Wehrheim, Germany). They were bedded comfortably on a mattress of viscoelastic foam (Tempur Deutschland, Steinhagen, Germany) superimposed on

the MRI table and were covered with a light blanket. A 3 cm layer of viscoelastic foam was further wrapped around the back part of the head inside of the head coil, stabilizing the head, providing additional noise protection, and preventing EEG electrodes from causing unpleasant pressure. EEG and bipolar amplifier, weighted with sandbags, were placed behind the head coil and in front of the feet, respectively, connected to a battery (behind the head coil) with power cables bypassing the center of the magnet. Recorded data was transmitted via fiber optic cables to a laptop (Inspiron 510m, Dell, Round Rock, TX, USA) outside the scanner room for saving. Subjects were equipped with an alarm bell to inform the experimenter at any time they wished to leave the scanner. Lights inside the scanner room were darkened with the stimulus display remaining active (picture of sky with cloudlets), which subjects reported to reduce the feeling of narrowness and helped to reduce anxiety in the case of sudden awakening from deep sleep.

EEG Data Acquisition

All electrophysiological recordings were performed with MRI compatible hardware. 32-channel EEG (10-20-system; Fp1, Fpz, Fp2, F7, F3, Fz, F4, F8, FC5, FC1, FC2, FC6, C3, Cz, C4, CP5, CP1, CP2, CP6, P7, P3, Pz, P4, P8, POz, O1, Oz, O2, T7, T8, TP9, TP10; referenced to FCz; ground ~1 cm below Oz) was obtained via a modified *BrainCap MR* electrode cap with Ag-AgCl ring electrodes and built-in 5 kOhm resistors (EasyCap, Munich, Germany) connected to a *BrainAmp MR plus* DC amplifier (BrainProducts, Munich, Germany). *Abralyt HiCl* electrode paste (Falk Minow Services, Herrsching, Germany) was used to ensure stable EEG recordings throughout the whole night. Additional recordings for polysomnography (PSG) such as vertical and horizontal electrooculogram (VEOG, HEOG), electromyogram (EMG) and electrocardiogram (ECG) were acquired via Ag-AgCl cup electrodes with built-in

15kOhm resistors and extra insulation of the leads (to prevent any heating of the skin) connected to a *BrainAmp ExG MR* bipolar amplifier (BrainProducts, Munich, Germany). Both amplifiers were powered by a rechargeable battery (*PowerPack*, BrainProducts, Munich, Germany). Skin resistance at EEG electrodes was kept below 5 kOhm by careful preparation of the skin with abrasive paste.

Data were recorded via *BrainVision Recorder V.1.10* software (BrainProducts, Munich, Germany) with a resolution of 0.5 µV/bit, analog-filtered (0.016-250 Hz), and digitized at a sampling rate of 5 kHz (synchronized with the MRI scanner clock to reduce variance of undersampled MRI gradient artifacts). A trigger signal from the MRI scanner marked the onset of each fMRI volume in the EEG recordings. Online MRI gradient and cardioballistic artifact correction via *BrainVision RecView V.1.2* software (BrainProducts, Munich, Germany) allowed monitoring of subjects' sleep stages.

Positions of EEG electrodes were coregistered to individual high-resolution T1-weighted anatomical images by means of frameless stereotaxy (TMS-Navigator, Localite, Sankt Augustin, Germany) to maintain exact positioning across conditions.

fMRI Data Acquisition

All measurements were performed on a 3 Tesla magnetic resonance tomograph (Philips Achieva, Philips Medical Systems, Best, The Netherlands) using an 8-channel SENSE head coil. High-resolution T1-weighted anatomical images were obtained using a standard MPRAGE sequence (TR = 7.7 ms, TE = 3.6 ms, flip angle = 8°, 170 sagittal slices, 1x1x1 mm voxel size, field of view = 224 x 224 mm). Functional MRI was conducted using echo planar imaging (EPI) sequences (TR = 2500 ms, TE = 37 ms, flip angle = 90°, FOV = 216 x 216 mm, 38 transversal slices, slice thickness = 3 mm, gap = 10%, in plane voxel size = 3.38 x 3.38 mm, continuous

slice acquisition order in bottom-up direction). While these parameters were identical for LEARNING and CONTROL task sessions, parameters for sleep sessions were slightly modified (TR = 2240 ms, TE = 30 ms) to ensure that residual gradient artifacts in the EEG, which are in the slice repetition frequency (here ~ 17 Hz), were beyond the frequency of sleep spindles (i.e., 10-16 Hz).

EEG Data Analysis

Preprocessing and fMRI artifact correction of the EEG data was done with *BrainVision Analyzer V. 2.0* software (BrainProducts, Munich, Germany). Slow oscillation and spindle detection was performed using *Spike2 V. 6.0* software (CED, Cambridge, UK).

MRI gradient artifacts were removed by using an adaptive average subtraction (Allen et al., 2000) with a moving average comprising both the previous and subsequent 50 volumes for each template subtraction. Afterwards, the EEG was downsampled to 250 Hz to reduce the computational effort of subsequent data processing and high-pass filtered (48 db/oct) at 0.1 Hz for EEG and 0.5 Hz for ECG. Then, ballistocardiographic artifacts were removed, also by means of template subtraction (based on an earlier algorithm by Allen et al., 1998). R-peaks in the ECG were identified semiautomatically based on their amplitude and correlation with a prototype ECG complex from the middle of the recoding. Global mean field power (GMFP) of all EEG channels was calculated time-locked to the R-peaks with GMFP peak latency determining the delay between the R-peak and the maximal ballistocardiographic EEG artifact. Then, taking into account this delay, moving averages comprising the 25 pulses before and after each artifact were subtracted individually for all channels. Comparing the frequency spectra as well as time-locked averages before and after artifact correction confirmed successful removal of both

gradient artifacts (except small residual artifacts at ~17 Hz) and ballistocardiographic artifacts. For sleep scoring and detection of sleep spindles and slow oscillations, EEG data was re-referenced to the average of electrodes TP9 and TP10 as surrogate for linked mastoids, not available in the MRI-compatible EEG cap.

For sleep scoring, EEG signals from C3 and C4, VEOG, HEOG, and EMG were filtered between 0.3 Hz and 35 Hz. Sleep stages were visually scored per 30-s epoch based on electrodes C3 and C4 according to standard criteria (Rechtschaffen and Kales, 1968) using *SchlafAus V. 1.4* software (by Steffen Gais; http://www.kfg.uni-luebeck.de).

Spindles were detected in all artifact-free 30-sec epochs of NonREM sleep in the 10 centro-parietal channels that expressed the largest power in the spindle frequency range (C3, Cz, C4, CP5, CP1, CP2, CP6, P3, Pz, P4). Peak frequency of fast spindle activity was identified in EEG power spectra of NonREM sleep, separately for each subject (13.6 ± 0.38 Hz; Mean ± SD). Subsequently, the EEG data were filtered using a band-pass of ± 1.5 Hz around this peak frequency. After filtering, a thresholding algorithm was applied that had proven to be effective in previous studies (Gais et al., 2002; Mölle et al., 2002). First, the root mean square (RMS) of the filtered signal was calculated at every sample point using a moving window of 0.2 sec. The resulting RMS signal was smoothed with a moving average of 0.2 sec. The threshold for spindle detection in the RMS signal was set to 0.8 standard deviations of the filtered signal (mean over the 10 centro-parietal channels). A spindle was detected if the RMS signal remained above the threshold for 0.5-3 sec and the beginning and end of the spindle were marked at the threshold crossing points. For every detected spindle the deepest trough was detected in the filtered signal. In order to include only the largest and most widespread spindles in the analysis an average RMS channel (across the RMS signals of the 10 centro-parietal

channels) was also calculated. The same thresholding algorithm for spindle detection was applied on this channel. If criteria for spindle detection were met in this average RMS channel, the number of EEG channels in which a spindle was simultaneously detected (i.e., between the beginning and end of the threshold crossings in the average RMS channel) was counted. Given that spindles appeared in at least 5 channels the peak time of the largest of these spindles was designated as the "spindle maximum" representing the respective spindle in time for further analysis. Peak times and corresponding RMS amplitudes (averaged across the 10 centro-parietal channels) of all detected spindles were extracted for subsequent singe-trial EEG-fMRI analysis (**Figure 3A**). Sleep spindles show a high degree of large-scale coherence across neocortical sites as a result of cortico-thalamic synchronization (Contreras et al., 1996, 1997a). As the applied spindle detection algorithm yielded only full blown and spatially wide spread spindles, the variability in spindle amplitude on the hemispherical surface provided reliable information about the temporal modulation of spindle amplitudes in the more inferiorly located areas of interest (i.e. FFA, OFA, and PPA) which are less strongly represented in the EEG signal.

Detection of slow oscillations in all artifact-free 30-sec epochs of NonREM sleep was based essentially on a standard algorithm described elsewhere in detail (Mölle et al., 2002). Slow oscillations were detected in an "average" channel that was calculated by averaging (at every sample point) the potentials of 12 (mainly fronto-central) channels which expressed the largest power in the slow oscillation frequency range during SWS (i.e., Fp1, Fpz, Fp2, F3, Fz, F4, FC1, FC2, Cz, CP1, CP2, and Pz). First, the EEG signal in the average channel was filtered between 0.16 Hz and 2.5 Hz. Then, time points of positive-to-negative zero crossings were computed in the resulting signal. In all intervals of positive-to-negative zero crossings with a length of 0.8 to 2 sec, the lowest and highest values were detected (i.e., one negative and one

positive peak between two succeeding positive-to-negative zero crossings). Subsequently, the average negative peak and the average negative-to-positive peak potentials were calculated and only those slow oscillations were finally included in the analysis whose (absolute) negative peak and negative-to-positive peak potentials were larger than 0.75 times the average. Negative peak times and corresponding negative-to-positive peak amplitudes (from the average channel) of all detected slow oscillations were extracted for subsequent singe-trial EEG-fMRI analysis (**Figure 3B**).

We applied relatively liberal amplitude criteria for both sleep spindle and slow oscillation detection in order to gain sufficient variance for subsequent explicit modeling of single-trial amplitudes in the fMRI analysis.

Unless specified otherwise, data are reported as mean (M) ± standard deviation (SD). Statistical comparisons rely on two-sided paired t-tests with P-values < 0.05 considered significant.

fMRI Data Analysis

fMRI data were converted from *DICOM* (tasks) and *Philips PAR/REC* (sleep) format to *NiFTI* using *MRIConvert V. 2.0, rev. 131* (by Jolinda Smith; http://lcni.uoregon.edu/~jolinda/MRIConvert) and *r2aGUI V. 2.4* (by Bas Neggers & Erno Hermans; http://r2agui.sourceforge.net/), respectively. NiFTI data was then preprocessed and analyzed using *SPM5, rev. 1782* (Wellcome Department of Cognitive Neurology, London, UK; http://www.fil.ion.ucl.ac.uk/spm) running on *Matlab 7.7.0.471, R2008b* (The MathWorks, Natick, MA, USA).

EPI images were preprocessed separately for task-fMRI, and sleep EEG-fMRI recordings but conjointly for LEARNING and CONTROL conditions. Images were slice timing corrected using slice 19 of 38 as a reference and all images were realigned to the mean EPI image using 4th order b-spline interpolation. T1-weighted images were

then coregistered to the mean EPI images and segmented using the tissue probability maps provided by SPM5 as a means to obtain normalization parameters transforming the images to the standard Montreal Neurological Institute (MNI) space. Thereby, normalized T1-weighted and EPI images could both be written (with 1 mm and 2 mm resolution, respectively) using the same spatial transformation while taking advantage of the high anatomical resolution of T1-weighted images. Normalized EPI images were spatially smoothed using a 8 mm full-width at half-maximum isotropic Gaussian kernel. For topographical interpretation and illustration purposes, a mean normalized T1-weighted image was calculated over all subjects.

Task-fMRI analyses were performed to determine the general LEARNING task-related brain activation pattern relative to that during the visuomotor CONTROL task and in particular to locate the material-specific neocortical representations of the learned face and scene stimuli. Separate first level models (single subject fixed-effects analyses) were calculated for memory encoding and immediate cued recall runs before sleep. In both models, the four runs each from LEARNING and CONTROL condition were set up as eight different runs. In the encoding model, nine event regressors (1^{st} stimulus: face/scene/nothing x 2^{nd} stimulus: face/scene/nothing; or the respective scrambled control trials) were modeled as stick functions convolved with the canonical hemodynamic response function (HRF). In the recall model, six event regressors (cue: face/scene x target: face/scene/nothing; or the respective scrambled control trials) were modeled as three second epochs convolved with the canonical HRF. Then separate LEARNING and CONTROL contrasts were specified, collapsing over runs and, in the encoding model, also pooling trials with merely reversed stimulus order. Thereby, either five (encoding: face-face, scene-scene, face-scene/scene-face, face-nothing/noting-face, scene-noting/noting-scene) or six (recall: face-face, face-scene, face-noting, scene-face, scene-scene, scene-noting) contrast

images (plus the same number for the matched control trials) were defined as input for the group analyses. On the second level (group random-effects analysis), two separate flexible factorial designs were specified for encoding and recall, comprising a SUBJECT factor (nine subjects, independent levels, equal variance), a TASK factor (LEARNING vs. CONTROL, dependent levels, equal variance), and a TRIAL TYPE factor (either five or six trial types, dependent levels, equal variance). Finally, differential contrasts were calculated, comparing LEARNING and CONTROL tasks separately for face- and scene-presenting trials to highlight stimulus-representing brain regions.

Single-trial sleep EEG-fMRI analyses (cf. Debener et al., 2006; Debener et al., 2005) aimed at (i) detecting brain regions in which the BOLD-signal actually depends on single-trial spindle amplitudes, thus comprising neurons particularly responsive to the thalamo-cortical sleep spindle and (ii) identifying those regions exhibiting stronger responsiveness after LEARNING than after CONTROL. On the first level (single subject fixed-effects analyses), continuous uninterrupted series of EPI volumes as revealed by the EEG analyses (see above) were concatenated within nights and entered as separate LEARNING and CONTROL runs into the model. To account for potential mean signal differences across concatenated EPI series, separate block regressors were included for each of them. Moreover, to avoid filter artifacts at discontinuities between concatenated EPI series, standard high-pass filtering was substituted by explicitly modeled regressor sets of cosine functions separately for each continuous EPI series (128 s high-pass filter sets generated by the SPM5 *spm_filter.m* function). For both conditions (LEARNING, CONTROL), BOLD-responses to individual sleep spindles were assessed by modeling an event regressor based on the spindle onsets from EEG analysis plus a parametrical modulator containing the individual spindle amplitudes. The same was done for individual slow oscillations and their amplitudes to account for any slow oscillation-related BOLD signal variation (Dang-Vu et al., 2008; Schabus

et al., 2007). All event and parametrical modulation regressors were further convolved with the canonical HRF as well as with its time and dispersion derivatives to model the unknown BOLD response to these electroencephalographic events as close as possible. Further nuisance regressors (not convolved with the HRF) modeled BOLD-signal changes induced by movement of the subject and its cardiac cycle. Movement regressors consisted of the six parameters estimated during realignment (translations in the x, y, and z directions and rotations around the x, y, and z axes) and their squares both of the current and, to account for spin history effects, the previous volume (24 regressors in total). Effects of changes in blood flow due to the cardiac cycle were modeled by convolution of the R-R interval from the ECG with a 5^{th} order set of sine and cosine functions (RETROICOR, Glover et al., 2000), resulting in 10 additional regressors. On the second level (group random-effects analysis), we first performed one-sample t-tests to reveal the main BOLD-correlates of sleep spindles independent of the experimental condition. Second, we calculated paired t-tests comparing the BOLD-response related to sleep spindles per se and their respective amplitudes during sleep after LEARNING and CONTROL tasks. Individual parameter estimates of the spindle amplitude-related learning effect for correlational analyses were extracted from the peak voxel of the hippocampal cluster (**Figure 6, Table 2**) using *rfxplot* (Gläscher, 2009).

ACKNOWLEDGEMENTS

This work was supported by the Deutsche Forschungsgemeinschaft (Project A6, SFB 654 'Plasticity and Sleep'). H.R.S. was supported by a structural grant from the Bundesministerium für Bildung und Forschung (01GO0511) to NeuroImageNord. We thank Olav Jansen for providing the MRI infrastructure, Kristoffer Madsen for helpful advices regarding the modeling of cardiac noise and explicit filter functions in first-

level fMRI analyses, and Oliver Granert for general computational assistance throughout data analyses.

REFERENCES

Adolphs, R., and Spezio, M. (2006). Role of the amygdala in processing visual social stimuli. Prog. Brain Res. *156*, 363-378.

Allen, P.J., Josephs, O., and Turner, R. (2000). A method for removing imaging artifact from continuous EEG recorded during functional MRI. Neuroimage *12*, 230-239.

Allen, P.J., Polizzi, G., Krakow, K., Fish, D.R., and Lemieux, L. (1998). Identification of EEG events in the MR scanner: the problem of pulse artifact and a method for its subtraction. Neuroimage *8*, 229-239.

Born, J., Rasch, B., and Gais, S. (2006). Sleep to remember. Neuroscientist *12*, 410-424.

Buzsaki, G. (1989). Two-stage model of memory trace formation: a role for "noisy" brain states. Neuroscience *31*, 551-570.

Clemens, Z., Fabo, D., and Halasz, P. (2005). Overnight verbal memory retention correlates with the number of sleep spindles. Neuroscience *132*, 529-535.

Clemens, Z., Fabo, D., and Halasz, P. (2006). Twenty-four hours retention of visuospatial memory correlates with the number of parietal sleep spindles. Neurosci. Lett. *403*, 52-56.

Clemens, Z., Mölle, M., Eross, L., Barsi, P., Halasz, P., and Born, J. (2007). Temporal coupling of parahippocampal ripples, sleep spindles and slow oscillations in humans. Brain *130*, 2868-2878.

Contreras, D., Destexhe, A., Sejnowski, T.J., and Steriade, M. (1996). Control of spatiotemporal coherence of a thalamic oscillation by corticothalamic feedback. Science *274*, 771-774.

Contreras, D., Destexhe, A., Sejnowski, T.J., and Steriade, M. (1997a). Spatiotemporal patterns of spindle oscillations in cortex and thalamus. J. Neurosci. *17*, 1179-1196.

Contreras, D., Destexhe, A., and Steriade, M. (1997b). Intracellular and computational characterization of the intracortical inhibitory control of synchronized thalamic inputs in vivo. J. Neurophysiol. *78*, 335-350.

Dang-Vu, T.T., Schabus, M., Desseilles, M., Albouy, G., Boly, M., Darsaud, A., Gais, S., Rauchs, G., Sterpenich, V., Vandewalle, G.*, et al.* (2008). Spontaneous neural activity during human slow wave sleep. Proc. Natl. Acad. Sci. U. S. A. *105*, 15160-15165.

De Gennaro, L., and Ferrara, M. (2003). Sleep spindles: an overview. Sleep Med Rev *7*, 423-440.

Debener, S., Ullsperger, M., Siegel, M., and Engel, A.K. (2006). Single-trial EEG-fMRI reveals the dynamics of cognitive function. Trends Cogn Sci *10*, 558-563.

Debener, S., Ullsperger, M., Siegel, M., Fiehler, K., von Cramon, D.Y., and Engel, A.K. (2005). Trial-by-trial coupling of concurrent electroencephalogram and functional magnetic resonance imaging identifies the dynamics of performance monitoring. J. Neurosci. *25*, 11730-11737.

Diekelmann, S., and Born, J. (2010). The memory function of sleep. Nat. Rev. Neurosci.

Diekelmann, S., Wilhelm, I., and Born, J. (2009). The whats and whens of sleep-dependent memory consolidation. Sleep Med Rev.

Eichenbaum, H. (2000). A cortical-hippocampal system for declarative memory. Nat. Rev. Neurosci. *1*, 41-50.

Epstein, R., and Kanwisher, N. (1998). A cortical representation of the local visual environment. Nature *392*, 598-601.

Eschenko, O., and Sara, S.J. (2008). Learning-Dependent, Transient Increase of Activity in Noradrenergic Neurons of Locus Coeruleus during Slow Wave Sleep in the Rat: Brain Stem-Cortex Interplay for Memory Consolidation? Cereb. Cortex.

Fogel, S.M., and Smith, C.T. (2006). Learning-dependent changes in sleep spindles and Stage 2 sleep. J. Sleep Res. *15*, 250-255.

Frankland, P.W., and Bontempi, B. (2005). The organization of recent and remote memories. Nat. Rev. Neurosci. *6*, 119-130.

Gais, S., Mölle, M., Helms, K., and Born, J. (2002). Learning-dependent increases in sleep spindle density. J. Neurosci. *22*, 6830-6834.

Gauthier, I., Tarr, M.J., Moylan, J., Skudlarski, P., Gore, J.C., and Anderson, A.W. (2000). The fusiform "face area" is part of a network that processes faces at the individual level. J. Cogn. Neurosci. *12*, 495-504.

Gläscher, J. (2009). Visualization of group inference data in functional neuroimaging. Neuroinformatics *7*, 73-82.

Glover, G.H., Li, T.Q., and Ress, D. (2000). Image-based method for retrospective correction of physiological motion effects in fMRI: RETROICOR. Magn. Reson. Med. *44*, 162-167.

Grill-Spector, K. (2003). The neural basis of object perception. Curr. Opin. Neurobiol. *13*, 159-166.

Hasson, U., Harel, M., Levy, I., and Malach, R. (2003). Large-scale mirror-symmetry organization of human occipito-temporal object areas. Neuron *37*, 1027-1041.

Hoddes, E., Zarcone, V., Smythe, H., Phillips, R., and Dement, W.C. (1973). Quantification of sleepiness: a new approach. Psychophysiology *10*, 431-436.

Kandel, A., and Buzsaki, G. (1997). Cellular-synaptic generation of sleep spindles, spike-and-wave discharges, and evoked thalamocortical responses in the neocortex of the rat. J. Neurosci. *17*, 6783-6797.

Kanwisher, N., McDermott, J., and Chun, M.M. (1997). The fusiform face area: a module in human extrastriate cortex specialized for face perception. J. Neurosci. *17*, 4302-4311.

Lestienne, R., Herve-Minvielle, A., Robinson, D., Briois, L., and Sara, S.J. (1997). Slow oscillations as a probe of the dynamics of the locus coeruleus-frontal cortex interaction in anesthetized rats. J. Physiol. Paris *91*, 273-284.

Lundqvist, D., Flykt, A., and Öhman, A. (1998). The Karolinska Directed Emotional Faces - KDEF. (CD ROM from Department of Clinical Neuroscience, Psychology section, Karolinska Institutet, ISBN 91-630-7164-9.).

MacEvoy, S.P., and Epstein, R.A. (2007). Position selectivity in scene- and object-responsive occipitotemporal regions. J. Neurophysiol. *98*, 2089-2098.

Maguire, E.A. (2001). The retrosplenial contribution to human navigation: a review of lesion and neuroimaging findings. Scand. J. Psychol. *42*, 225-238.

Maquet, P. (2001). The role of sleep in learning and memory. Science *294*, 1048-1052.

Maquet, P., Laureys, S., Peigneux, P., Fuchs, S., Petiau, C., Phillips, C., Aerts, J., Del Fiore, G., Degueldre, C., Meulemans, T.*, et al.* (2000). Experience-dependent changes in cerebral activation during human REM sleep. Nat. Neurosci. *3*, 831-836.

Marshall, L., and Born, J. (2007). The contribution of sleep to hippocampus-dependent memory consolidation. Trends Cogn Sci *11*, 442-450.

McClelland, J.L., McNaughton, B.L., and O'Reilly, R.C. (1995). Why there are complementary learning systems in the hippocampus and neocortex: insights from the successes and failures of connectionist models of learning and memory. Psychol. Rev. *102*, 419-457.

Mölle, M., and Born, J. (2009). Hippocampus whispering in deep sleep to prefrontal cortex--for good memories? Neuron *61*, 496-498.

Mölle, M., Eschenko, O., Gais, S., Sara, S.J., and Born, J. (2009). The influence of learning on sleep slow oscillations and associated spindles and ripples in humans and rats. Eur. J. Neurosci. *29*, 1071-1081.

Mölle, M., Marshall, L., Gais, S., and Born, J. (2002). Grouping of spindle activity during slow oscillations in human non-rapid eye movement sleep. J. Neurosci. *22*, 10941-10947.

Mölle, M., Yeshenko, O., Marshall, L., Sara, S.J., and Born, J. (2006). Hippocampal sharp wave-ripples linked to slow oscillations in rat slow-wave sleep. J. Neurophysiol. *96*, 62-70.

Oldfield, R.C. (1971). The assessment and analysis of handedness: the Edinburgh inventory. Neuropsychologia *9*, 97-113.

Orban, P., Rauchs, G., Balteau, E., Degueldre, C., Luxen, A., Maquet, P., and Peigneux, P. (2006). Sleep after spatial learning promotes covert reorganization of brain activity. Proc. Natl. Acad. Sci. U. S. A.

Packard, M.G., and Knowlton, B.J. (2002). Learning and memory functions of the Basal Ganglia. Annu. Rev. Neurosci. *25*, 563-593.

Peigneux, P., Laureys, S., Fuchs, S., Collette, F., Perrin, F., Reggers, J., Phillips, C., Degueldre, C., Del Fiore, G., Aerts, J.*, et al.* (2004). Are spatial memories strengthened in the human hippocampus during slow wave sleep? Neuron *44*, 535-545.

Peigneux, P., Laureys, S., Fuchs, S., Destrebecqz, A., Collette, F., Delbeuck, X., Phillips, C., Aerts, J., Del Fiore, G., Degueldre, C.*, et al.* (2003). Learned material content and acquisition level modulate cerebral reactivation during posttraining rapid-eye-movements sleep. Neuroimage *20*, 125-134.

Poldrack, R.A., and Rodriguez, P. (2004). How do memory systems interact? Evidence from human classification learning. Neurobiol. Learn. Mem. *82*, 324-332.

Rasch, B., and Born, J. (2007). Maintaining memories by reactivation. Curr. Opin. Neurobiol. *17*, 698-703.

Rechtschaffen, A., and Kales, A. (1968). A manual of standardized terminology, techniques and scoring system for sleep stages of human subjects (Washington, DC: United States Government Printing Office).

Sara, S.J. (2009). The locus coeruleus and noradrenergic modulation of cognition. Nat. Rev. Neurosci. *10*, 211-223.

Schabus, M., Dang-Vu, T.T., Albouy, G., Balteau, E., Boly, M., Carrier, J., Darsaud, A., Degueldre, C., Desseilles, M., Gais, S.*, et al.* (2007). Hemodynamic cerebral correlates of sleep spindles during human non-rapid eye movement sleep. Proc. Natl. Acad. Sci. U. S. A. *104*, 13164-13169.

Schabus, M., Gruber, G., Parapatics, S., Sauter, C., Klosch, G., Anderer, P., Klimesch, W., Saletu, B., and Zeitlhofer, J. (2004). Sleep spindles and their significance for declarative memory consolidation. Sleep *27*, 1479-1485.

Schabus, M., Hoedlmoser, K., Pecherstorfer, T., Anderer, P., Gruber, G., Parapatics, S., Sauter, C., Kloesch, G., Klimesch, W., Saletu, B., and Zeitlhofer, J. (2008). Interindividual sleep spindle differences and their relation to learning-related enhancements. Brain Res. *1191*, 127-135.

Sejnowski, T.J., and Destexhe, A. (2000). Why do we sleep? Brain Res. *886*, 208-223.

Siapas, A.G., and Wilson, M.A. (1998). Coordinated interactions between hippocampal ripples and cortical spindles during slow-wave sleep. Neuron *21*, 1123-1128.

Sirota, A., Csicsvari, J., Buhl, D., and Buzsaki, G. (2003). Communication between neocortex and hippocampus during sleep in rodents. Proc. Natl. Acad. Sci. U. S. A. *100*, 2065-2069.

Steriade, M. (2003). The corticothalamic system in sleep. Front. Biosci. *8*, d878-899.

Steriade, M. (2006). Grouping of brain rhythms in corticothalamic systems. Neuroscience *137*, 1087-1106.

Steriade, M., Nunez, A., and Amzica, F. (1993). A novel slow (< 1 Hz) oscillation of neocortical neurons in vivo: depolarizing and hyperpolarizing components. J. Neurosci. *13*, 3252-3265.

Steriade, M., and Timofeev, I. (2003). Neuronal plasticity in thalamocortical networks during sleep and waking oscillations. Neuron *37*, 563-576.

Sterpenich, V., Albouy, G., Darsaud, A., Schmidt, C., Vandewalle, G., Dang Vu, T.T., Desseilles, M., Phillips, C., Degueldre, C., Balteau, E.*, et al.* (2009). Sleep promotes the neural reorganization of remote emotional memory. J. Neurosci. *29*, 5143-5152.

Stickgold, R. (2005). Sleep-dependent memory consolidation. Nature *437*, 1272-1278.

Sutherland, G.R., and McNaughton, B. (2000). Memory trace reactivation in hippocampal and neocortical neuronal ensembles. Curr. Opin. Neurobiol. *10*, 180-186.

Wagner, A.D., Shannon, B.J., Kahn, I., and Buckner, R.L. (2005). Parietal lobe contributions to episodic memory retrieval. Trends Cogn Sci *9*, 445-453.

Werk, C.M., Harbour, V.L., and Chapman, C.A. (2005). Induction of long-term potentiation leads to increased reliability of evoked neocortical spindles in vivo. Neuroscience *131*, 793-800.

Wierzynski, C.M., Lubenov, E.V., Gu, M., and Siapas, A.G. (2009). State-dependent spike-timing relationships between hippocampal and prefrontal circuits during sleep. Neuron *61*, 587-596.

TABLES

Table 1: Sleep parameters for fMRI-EEG sleep sessions (M ± SD) in minutes and as percent of total sleep time (from first sleep onset to final awakening)

	Learning		Control	
	min	**%**	**min**	**%**
Sleep latency	1.7 ± 1.9		4.2 ± 5.6	
SWS latency	18.6 ± 10.6		21.3 ± 15.7	
Waking	7.4 ± 11.7	7.5 ± 11.7	3.7 ± 4.9	3.6 ± 5.1
Stage 1	2.3 ± 2.4	2.4 ± 2.5	2.3 ± 1.4	2.2 ± 1.4
Stage 2	50.1 ± 22.5	49.6 ± 16.5	51.0 ± 19.9	47.8 ± 11.8
SWS	35.8 ± 12.8	40.2 ± 21.7	45.4 ± 13.2	46.1 ± 15.9
Movement	0.2 ± 0.3	0.2 ± 0.3	0.3 ± 0.3	0.4 ± 0.5
Arousal events	6.7 ± 5.7		6.1 ± 4.4	
Total sleep	95.9 ± 19.7	100 ± 0	102.8 ± 25.0	100 ± 0

Table 2: Learning-dependent sleep spindle-related brain activity (BOLD-fMRI)

Brain Region	Side	Peak coordinates in mm			T-value
		X	Y	Z	
(A) LEARNING minus CONTROL sleep spindle events					
Head of caudate nucleus	L	-10	12	16	6.41
Amygdala	L	-22	0	-22	4.90
Locus coeruleus	L	-10	-30	-20	7.38
(B) LEARNING minus CONTROL sleep spindle amplitudes					
Hippocampus	R	32	-28	-12	6.14
Fusiform face area (FFA)	R	40	-46	-22	5.85
Parahippocampal place area (PPA)	L	-18	-42	-16	5.20
Occipital face area (OFA)	R	24	-82	-18	9.59
	L	-36	-74	-22	6.20

Only clusters with peak voxels significant at $P_{uncorr} < 0.001$ and cluster extent threshold > 5 voxels are reported; R = Right, L = Left

FIGURES

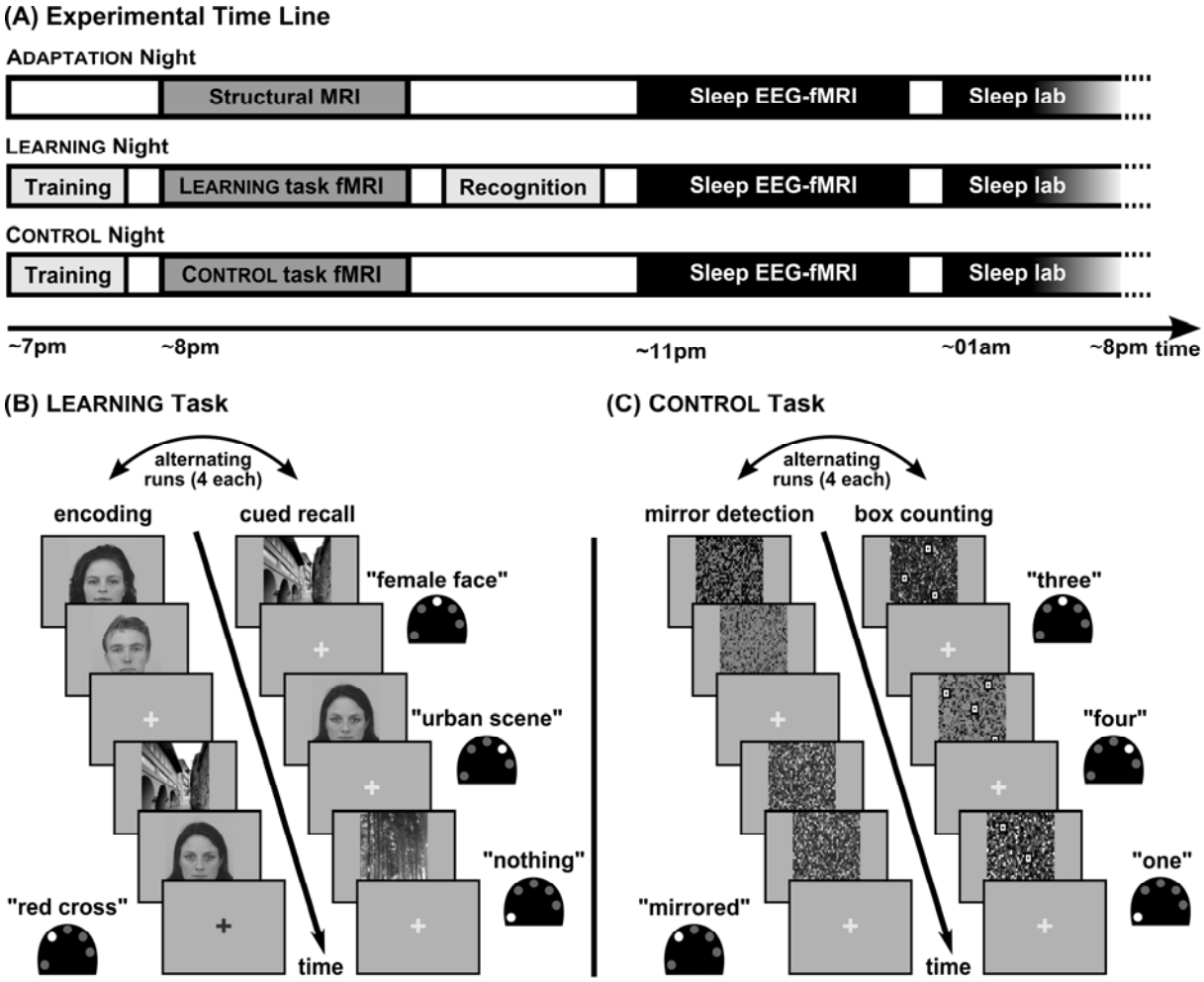

Figure 1: (A) Experimental time line (scaling not proportional). The ADAPTATION night was followed by LEARNING and CONTROL nights in balanced order separated by at least a weak. Initial training of the respective task outside the MRI was followed by the task fMRI session. Subjects then slept in the scanner for approx. the first sleep cycle, after which they continued their night in the adjacent sleep lab. In the LEARNING condition, fMRI tasks were additionally followed by a recognition task outside the MRI (**Figure S1**). **(B)** LEARNING task (alternating encoding and immediate cued recall runs, four of each): During encoding, pairs of pictures were presented in sequence (1.5 s each) separated by jittered inter-trial intervals (ITI) of 2-7 s showing a fixation cross. Subjects had to encode picture pairs and press a button when occasionally the cross turned red to preserve attention. During cued recall, pictures were presented separately (1.5 s each, 4-7 s ITI) and subjects had to indicate the missing associate by button press (“nothing”, “male face”, “female face”, “urban scene”, “rural scene”). **(C)** CONTROL task (alternating box counting and mirror detection runs, four of each): During mirror detection, pairs of scrambled pictures were presented in sequence (1.5 s each) separated by variable ITIs (2-7 s) with a fixation cross. Subjects had to monitor pictures carefully to hit a button when occasionally the second picture was a mirror image of the first to preserve attention. During box counting, scrambled pictures were presented separately (1.5 s each, 4-7 s ITI) and subjects had to indicate the number of superimposed box icons by button press (“one”, “two”, “three”, “four”, “five”). See **Supplemental Experimental Procedures** for details.

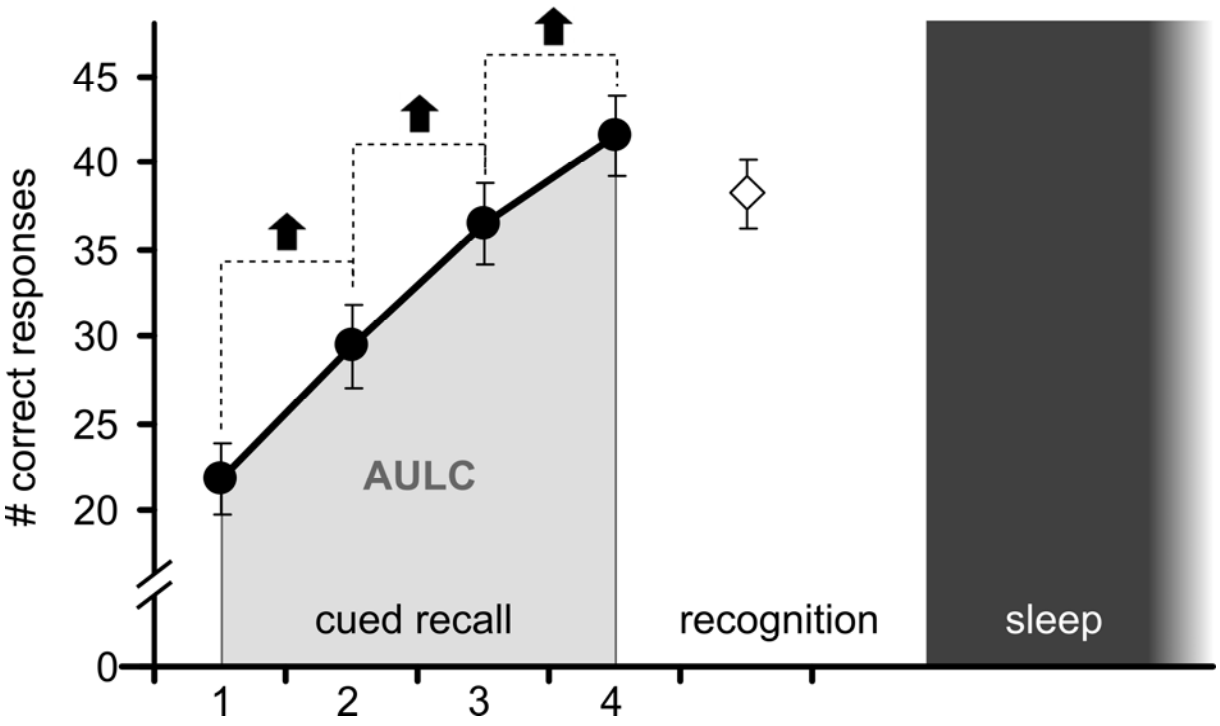

Figure 2: Learning curve depicting LEARNING task performance as number of correct responses (M ± SEM) for cued recall runs (black circles) and the recognition task (white diamond) before sleep. Recall performance increased after every encoding run during LEARNING (run 1-4) and subjects successfully allocated individual stimulus-stimulus associations in the recognition task. Arrows indicating significant increases with $p < 0.01$ (post-hoc two-sided paired t-tests). AULC = area under the learning curve.

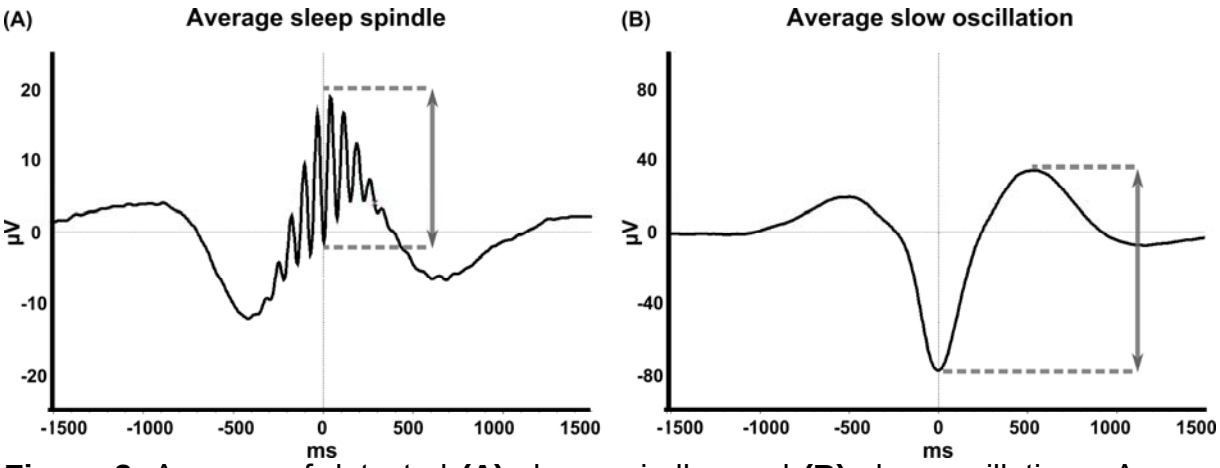

Figure 3: Average of detected **(A)** sleep spindles and **(B)** slow oscillations. Arrows indicate amplitudes as determined for single-trial EEG-fMRI analysis.

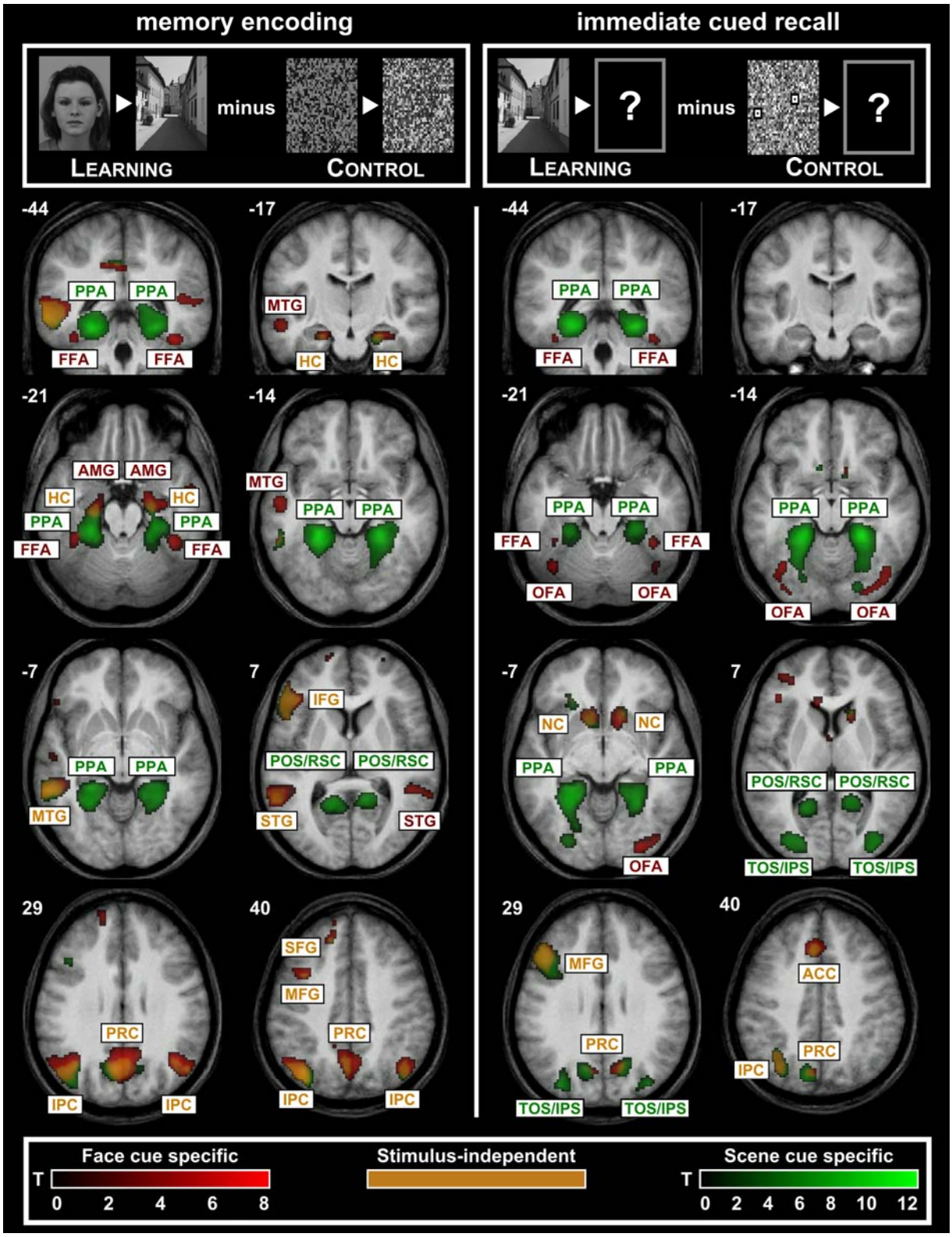

Figure 4: Selected brain areas showing a stronger activation during LEARNING than CONTROL task performance before sleep, separately for memory encoding (left panel) and immediate cued recall (right panel). Red and green clusters indicate face and scene cue specific activation, respectively, while orange shades indicate common stimulus-independent task-related activity (overlap of both clusters). ACC = anterior cingulate cortex, AMG = amygdala, FFA = fusiform face area, HC = hippocampus, IFG = inferior frontal gyrus, IPC = inferior parietal cortex, IPS = intraparietal sulcus, MFG = medial frontal gyrus, MTG = medial temporal gyrus, NC = head of caudate

nucleus, OFA = occipital face area, POS = parieto-occipital sulcus, PPA = parahippocampal place area, PRC = precuneus, RSC = retrosplenial cortex, STG = superior temporal gyrus, SFG = superior frontal gyrus, TOS = transverse occipital sulcus. Functional clusters are depicted on transversal slices (numbers indicate MNI coordinates in z direction) of the averaged T1-weighted image of all subjects. MNI (XYZ) coordinates are shown for coronal (Y) and transversal (Z) slices, respectively. Voxels are thresholded at $P_{uncorr} < 0.001$.

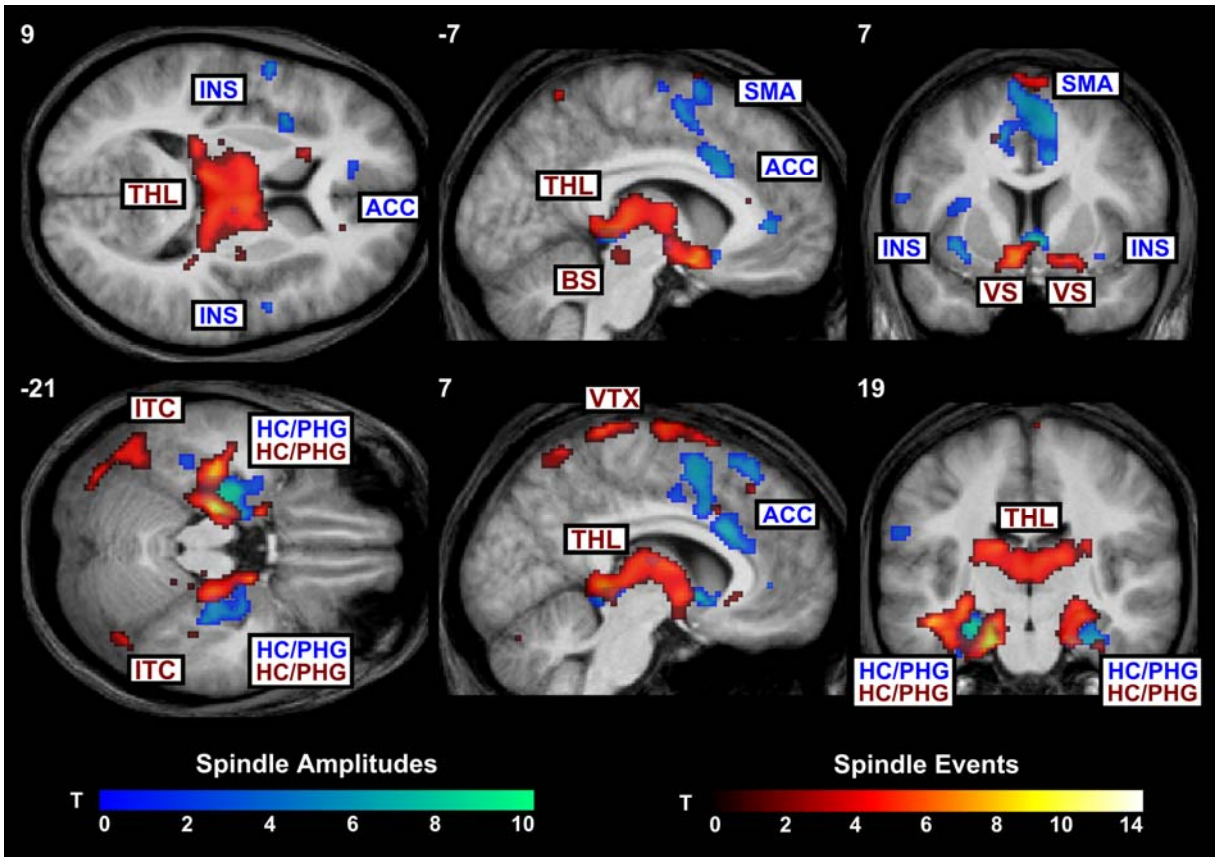

Figure 5: Wide spread brain areas showing increased BOLD-signal as a response to sleep spindles per se (event regressor; "hot" colors) or even dependent on their respective amplitudes (amplitude regressor; "cold" colors). ACC = anterior cingulate cortex, BS = brainstem, HC = hippocampus, INS = Insula, ITC = Inferior temporal cortex, SMA = supplementary motor area, PHG = parahippocampal gyrus, THL = thalamus, VS = ventral striatum, VTX = vertex. Functional clusters are depicted on the averaged T1-weighted image of all subjects. MNI (XYZ) coordinates are shown for transversal (Z), sagittal (X), and coronal slices (Y), respectively. Voxels are thresholded at $P_{uncorr} < 0.001$.

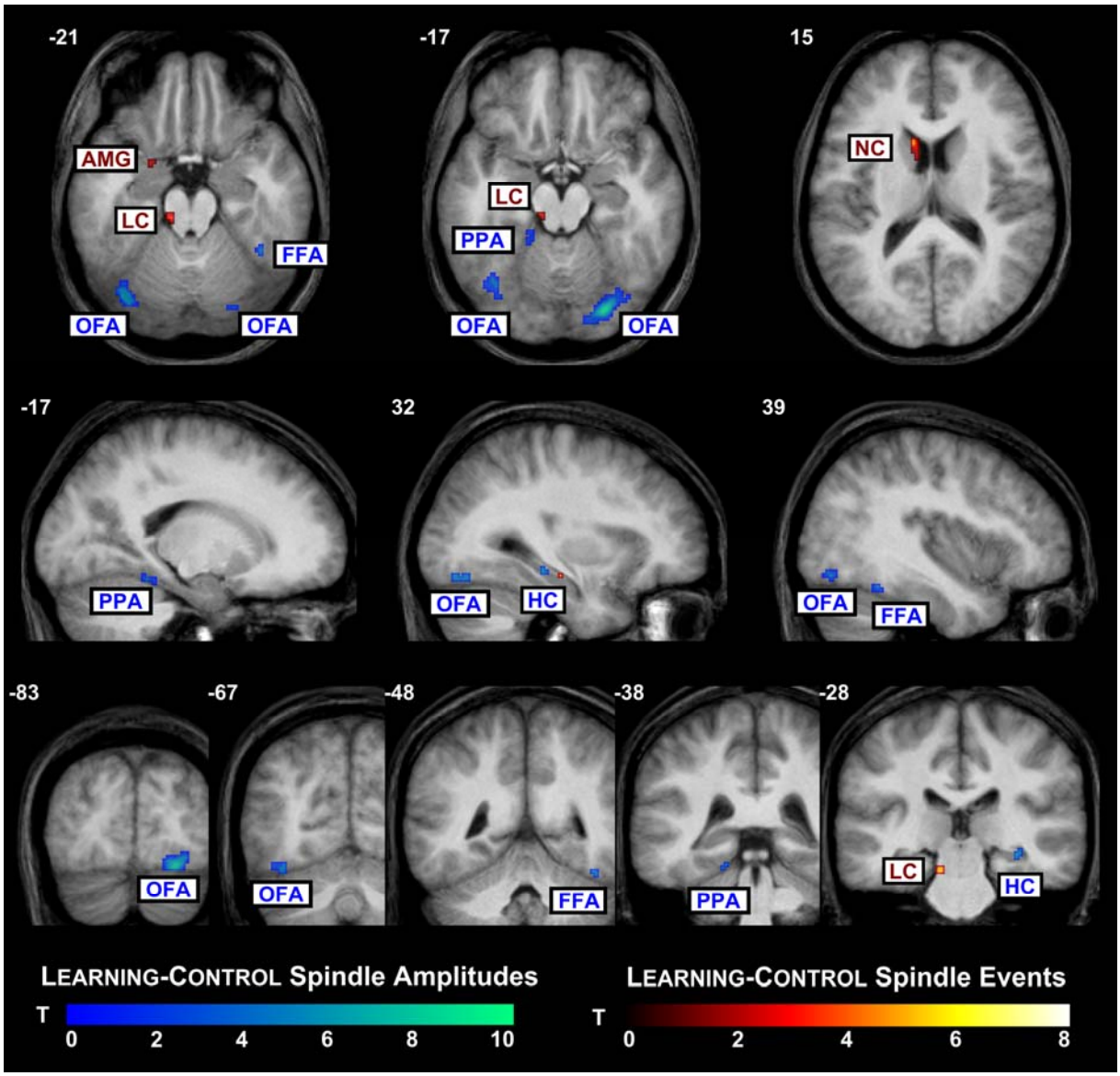

Figure 6: Circumscribed brain areas showing learning-specific (LEARNING minus CONTROL) spindles-effects (event regressor: "hot" colors"; amplitude regressor: "cold" colors). AMG = amygdala, LC = locus coeruleus, FFA = fusiform face area, HC = hippocampus, NC = Caudate nucleus, OFA = occipital face area, PPA = parahippocampal place area. Functional clusters are depicted on the averaged T1-weighted image of all subjects. MNI (XYZ) coordinates are shown for transversal (Z, upper row) sagittal (X, middle row), and coronal slices (Y, lower row), respectively. All voxels are significant at $P_{uncorr} < 0.001$ (only cluster > 5 voxels are labeled).

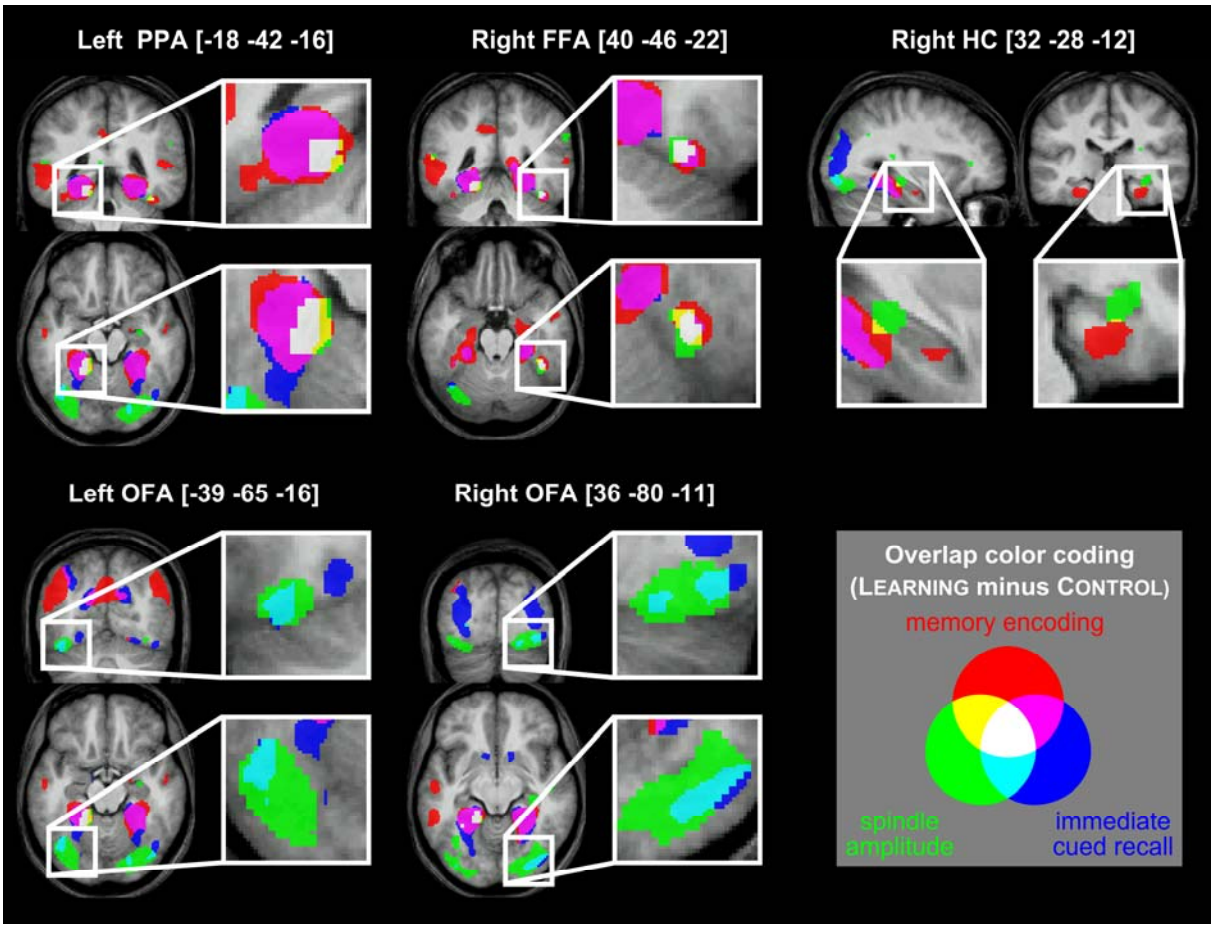

Figure 7: Overlap between learning-specific activations (LEARNING minus CONTROL) during memory encoding (red), immediate cued recall (blue) and spindle amplitude (green), with yellow, magenta, cyan, and white indicating respective overlaps (additive color blend). White boxes indicate zoom regions of interest. FFA = fusiform face area, HC = hippocampus, OFA = occipital face area, PPA = parahippocampal place area. Functional clusters are depicted on the averaged T1-weighted image of all subjects. MNI (XYZ) coordinates indicate the respective slice locations. Voxels from the main effects of task are thresholded at $P_{uncorr} < 0.001$, while differential spindle amplitude effects are thresholded at $P_{uncorr} < 0.01$ for illustration purposes and to demonstrate the high selectivity of activations (see text). All labeled clusters contain ≥ 5 voxels significant at $P_{uncorr} < 0.001$.

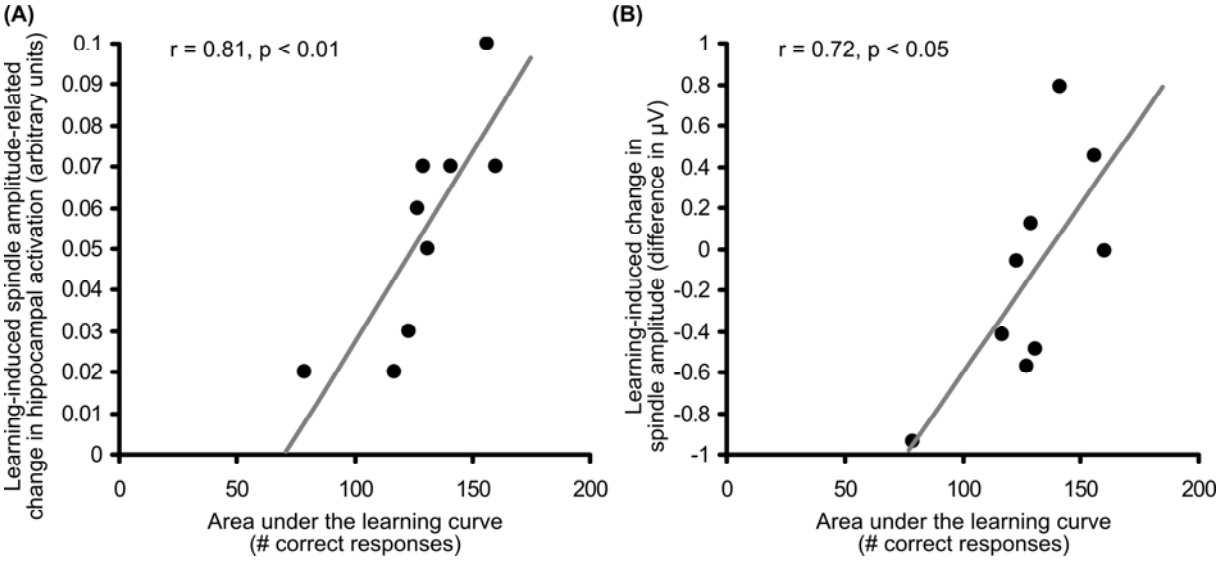

Figure 8: Scatter plots depict the positive relationship between individual learning success before sleep (area under the learning curve, AULC, across immediate recall runs; **Figure 2**) and subsequent individual change (LEARNING minus CONTROL) in spindle-related hippocampal activity (parameter estimates extracted from the hippocampal peak voxel at xyz = [32, -28, -12]; **Figure 6**) and sleep spindle amplitudes (as determined for single-trial EEG-fMRI analysis; **Figure 3**) during subsequent NonREM sleep: **(A)** AULC x hippocampal activity change ($r = 0.81$, $p < 0.01$), **(B)** AULC x spindle amplitude change ($r = 0.72$, $p < 0.05$).

SUPPLEMENTAL INFORMATION

SUPPLEMENTAL DATA

- **Figure S1:** Illustration of the recognition task
- **Table S1:** Statistical comparisons of slow oscillation parameters

SUPPLEMENTAL EXPERIMENTAL PROCEDURES

- **Behavioral Tasks:** Detailed description of LEARNING, CONTROL and recognition task procedures, including information about technical setting and generation of stimulus material.

SUPPLEMENTAL DATA

Figure S1: Recognition task. This task was performed outside the MRI scanner with a computer mouse on a laptop (15" display). In the upper middle frame, all face and scene stimuli were presented in consecutive (self-paced) trials. Subjects had to select the paired associate for every one of them by clicking on the respective image icon (or the scrambled icon if "nothing") in the surrounding (images were enlarged in the lower middle frame when moving the mouse cursor over the image icon).

Table S1: Statistical comparisons of slow oscillation parameters during sleep in LEARNING and CONTROL condition using two-sided paired t-tests. Data are given as mean ± SD.

Parameter	**LEARNING**	**CONTROL**	**P-value**
Total number of slow oscillations	958 ± 284	915 ± 253	P > 0.4
Density of slow oscillations (per 30 s)	7.54 ± 1.59	7.44 ± 1.63	P > 0.7
Amplitude of low oscillations	125.4 ± 23.7 µV	124.4 ± 31.9 µV	P > 0.9

SUPPLEMENTAL EXPERIMENTAL PROCEDURES

Behavioral Tasks

Technical details

All tasks were programmed using *E-Prime V. 1.1 SP3* (PST, Pittsburgh, PA, USA). Training and RECOGNITION task were performed on a laptop (15" display; Inspiron 510m, Dell, Round Rock, TX, USA). During task-fMRI (LEARNING and CONTROL tasks), visual stimulus presentation and response collection was accomplished using the *IFIS-SA fMRI System* (Invivo, Orlando, FL, USA). Visual stimuli were presented via a mirror-display-combination directly attached to the head coil (640 x 480 pixel resolution). Responses were recorded via a five-button box fixed to the right hand of the subjects. Communication of both devices with the control unit outside the scanner room was realized via fiber optic cables.

Stimulus Material

Stimulus material for all tasks consisted of grayscale images with 360 x 480 pixel resolution. Scrambled images were generated automatically by cutting the regular images in 40 x 40 (1600) pieces and rearranging them randomly. By this procedure it was ensured that no picture details were recognizable while very basic stimulus features like the distribution of brightness remained comparable.

For the LEARNING task, photographs of male faces, female faces, urban scenes, rural scenes, and scrambled versions of these pictures were used (**Figure 1B**; **Figure S1** for the complete set). A selection of photos of emotionally neutral *male faces* and *female faces* without prominent distinctive features (like scars, moles, pimples, etc.) were taken from the *Karolinska Directed Emotional Faces* (KDEF) database (Lundqvist et al., 1998). Pictures of either *urban scenes* (alleys lined by houses) or *rural scenes* (alleys lined by trees) not containing any prominent objects

(such as humans, animals, vehicles, signs, etc.) were taken from the internet. All pictures were reworked to match the specific presentation requirements. Paired associates were generated using all possible combinations of the stimulus categories *male face*, *female face*, *urban scene*, *rural scene*, and *nothing* (= scrambled image), including pairings within the same category. Pairs were constructed in a way that given a certain stimulus, the association with every stimulus category was equally likely.

For the CONTROL task, the scrambled face and scene pictures from the learning task were used. Additionally, certain pictures were replaced by their horizontal mirror image (reflecting the pixels around the central y-axis) and a set of scrambled images was created, containing one to five small black and white patterned boxes (45 x 60 pixel) on random positions (**Figure 1C**).

Training

Participants received training of the task on a laptop (15” display) directly prior to task-fMRI. Beside getting familiar with the task procedure, they had to learn the assignment of response keys (i.e., pressing five keys with the fingers of their right hand assigned to the five stimulus categories) until no mistakes were made anymore within 20 continuous trials.

Learning Task

The LEARNING task consisted of four iterations of memory encoding runs where subjects had to learn a set of picture pairs, each one followed by an immediate cued recall run where already learned associations were probed (**Figure 1B**).

During the memory encoding, a series of picture pairs was presented in pseudorandomized order, a pair consisting of two consecutive pictures on grey

background (1.5 s each). Pairs were separated by a time-jittered inter-trial interval (ITI) of 4.5 s average duration (2, 3, 4, 5, 6, or 7 s) in which a small black fixation cross appeared in the center of the screen. All 28 pairs to be learned were presented twice per run with inverted within-pair positions, making up a total of 56 learning trials plus eight trials with scrambled pairs (as low-level baseline) and eight null events (fixation cross only). Subjects were asked to remember the pairs as accurately as possible (neglecting the order of images within a pair and considering pictures paired with a scrambled image as solitary) and to visually imagine the two pictures together to improve their retention. It was emphasized that remembering the mere stimulus categories is insufficient, as assignment of exact individual pairings would be requested later on (recognition task). Additionally, they were instructed to respond with a button press of their right index finger when the fixation cross would turn red, which happened occasionally (nine times per run) for a second in the middle of an ITI to foster sustained attention.

During recall, all pictures of the encoding run were presented separately in pseudorandomized order for 1.5 s on grey background, separated by a time-jittered inter-trial interval of 5.5 s average duration (4, 5, 6, or 7 s). Both pictures of each pair were presented twice, except for pairs with scrambled images, where only the regular one was presented (as scrambled images could not be distinguished these were indicated to be paired with *nothing*), resulting in a total of 48 trials. Additionally, eight pauses of 15.5 s (fixation cross) were intermingled. Subjects were asked to retrieve the picture associated with the presented one as clearly as possible, and then to indicate its stimulus category (*nothing*, *male face*, *female face*, *urban scene*, *rural scene*) by pressing the corresponding of five buttons. Accuracy was strongly emphasized over speed and responses should also be made when only guessing was possible.

Together with a 10 s fixation cross at the beginning and end of each run, total run time was 9.3 min for encoding and 8 min for recall runs, resulting in a total scan time of 69.3 min.

Control Task

The CONTROL task consisted of four runs of MIRROR DETECTION alternating with four runs of box counting, controlling for visuomotor activity of the encoding and recall runs of the LEARNING task, respectively. In fact, exactly the same but scrambled stimuli were presented with identical order and timing, requiring responses with the same fingers at roughly the same time (**Figure 1C**).

During mirror detection, subjects had to watch pairs of scrambled pictures and respond with their right index finger when the second image was a horizontal mirror of the first one, which happened once in a while (corresponding to the red fixation cross events in the encoding run).

During box counting, one to five black and white patterned box icons were presented on top of scrambled images and subjects had to indicate the number of box icons by button press (corresponding to indicating the paired associate during the recall run).

Recognition Task

The recognition task was performed on a laptop (15” display) outside the MRI scanner (**Figure S1**). All face and scene pictures of the LEARNING task were sequentially presented in randomized order at the upper center of the screen. Using a computer mouse, subjects had to select the associated picture out of all others arranged as icons on both sides of the screen. Pictures could be enlarged at the

lower screen center by moving the mouse cursor over them. Indication of stimuli associated with “nothing” was done by clicking on a scrambled image icon.

Paper V

J Neurophysiol 102: 2303–2311, 2009.
First published August 19, 2009; doi:10.1152/jn.00437.2009.

Acute Changes in Motor Cortical Excitability During Slow Oscillatory and Constant Anodal Transcranial Direct Current Stimulation

Til Ole Bergmann,[1] Sergiu Groppa,[1] Markus Seeger,[1] Matthias Mölle,[2] Lisa Marshall,[2] and Hartwig Roman Siebner[1,3]

[1]*Department of Neurology, Christian-Albrechts University of Kiel;* [2]*Department of Neuroendocrinology, University of Lübeck, Lübeck, Germany; and* [3]*Danish Research Center for Magnetic Resonance, Department of Magnetic Resonance, Copenhagen University Hospital Hvidovre, Hvidovre, Denmark*

Submitted 20 May 2009; accepted in final form 14 August 2009

Bergmann TO, Groppa S, Seeger M, Mölle M, Marshall L, Siebner HR. Acute changes in motor cortical excitability during slow oscillatory and constant anodal transcranial direct current stimulation. *J Neurophysiol* 102: 2303–2311, 2009. First published August 19, 2009; doi:10.1152/jn.00437.2009. Transcranial oscillatory current stimulation has recently emerged as a noninvasive technique that can interact with ongoing endogenous rhythms of the human brain. Yet, there is still little knowledge on how time-varied exogenous currents acutely modulate cortical excitability. In ten healthy individuals we used on-line single-pulse transcranial magnetic stimulation (TMS) to search for systematic shifts in corticospinal excitability during anodal sleeplike 0.8-Hz slow oscillatory transcranial direct current stimulation (so-tDCS). In separate sessions, we repeatedly applied 30-s trials (two blocks at 20 min) of either anodal so-tDCS or constant tDCS (c-tDCS) to the primary motor hand area during quiet wakefulness. Simultaneously and time-locked to different phase angles of the slow oscillation, motor-evoked potentials (MEPs) as an index of corticospinal excitability were obtained in the contralateral hand muscles 10, 20, and 30 s after the onset of tDCS. MEPs were also measured off-line before, between, and after both stimulation blocks to detect any lasting excitability shifts. Both tDCS modes increased MEP amplitudes during stimulation with an attenuation of the facilitatory effect toward the end of a 30-s tDCS trial. No phase-locking of corticospinal excitability to the exogenous oscillation was observed during so-tDCS. Off-line TMS revealed that both c-tDCS and so-tDCS resulted in a lasting excitability increase. The individual magnitude of MEP facilitation during the first tDCS trials predicted the lasting MEP facilitation found after tDCS. We conclude that sleep slow oscillation-like excitability changes cannot be actively imposed on the awake cortex with so-tDCS, but phase-independent on-line as well as off-line facilitation can reliably be induced.

INTRODUCTION

Transcranial direct current stimulation (tDCS) was intensively used in animal studies and in vivo preparations in the 1960s (Bindman et al. 1964; Purpura and McMurtry 1965), but was reintroduced into neurophysiology approximately a decade ago (Nitsche and Paulus 2000; Priori et al. 1998). Since then, numerous studies have used this noninvasive stimulation technique to induce long-lasting bidirectional changes in the excitability of various human cortical areas (Nitsche et al. 2008). Because of its potential to change local excitability and promote cortical plasticity tDCS has also attracted increasing interest as a therapeutic tool (Fregni et al. 2007; Hummel and Cohen 2006). Most work focused on the hand area of the primary motor cortex ($M1_{HAND}$) since the excitability of the fast conducting corticospinal output neurons can easily be assessed by means of transcranial magnetic stimulation (TMS) of the cortex and measuring the amplitude of motor-evoked potentials (MEPs) in the contralateral hand muscles. Surface positive (anodal) tDCS of the $M1_{HAND}$ for merely 4 s has been shown to be sufficient to transiently increase motor cortical excitability (on-line tDCS effects), whereas surface negative (cathodal) tDCS has the opposite effect (Nitsche and Paulus 2000; Nitsche et al. 2003a, 2007).

There is evidence from early animal studies indicating that this on-line effect on cortical excitability during anodal and cathodal tDCS is induced by a shift in the neurons' membrane potential toward a more depolarized or hyperpolarized state, respectively (Bindman et al. 1964; Purpura and McMurtry 1965). Thereby, without directly eliciting action potentials, tDCS can modulate the spontaneous firing rates of neurons and cause long-lasting changes in synaptic strength (Gartside 1968b). Prolonged application of anodal and cathodal tDCS has resulted in long-lasting ($\leq$1 h) aftereffects on human $M1_{HAND}$ excitability (off-line tDCS effects) (Nitsche and Paulus 2000; Nitsche et al. 2007). These conditioning effects are probably mediated by *N*-methyl-D-aspartate receptors (Nitsche et al. 2003a) and depend on the modulation of protein synthesis (Gartside 1968a).

Whereas current strength is kept constant during classical constant tDCS (c-tDCS), researchers have recently started to use time-varied tDCS with oscillatory fluctuations in the induced tissue current. Anodal c-tDCS (Marshall et al. 2004) as well as anodal slow oscillation stimulation (Marshall et al. 2006a) were applied in a bilateral prefrontal montage during human nonrapid eye movement (NREM) sleep. The slow oscillation stimulation protocol was designed to mimic slow oscillations during sleep with a repetition rate of 0.75 Hz (Marshall et al. 2006a). Both stimulation modes enhanced endogenous slow oscillatory activity and facilitated the mnemonic function of these oscillations (Marshall and Born 2007). Notably, slow oscillation stimulation did not only facilitate endogenous slow oscillations but also appeared to phase-lock them to the exogenous stimulation (Marshall et al. 2006a). Theta-like 5-Hz oscillatory stimulation rather decreased slow oscillatory activity.

Recently, transcranial AC stimulation (tACS) with sinusoidally alternating polarities has been shown to modulate primary visual cortex excitability during wakefulness, as mea-

Address for reprint requests and other correspondence: T. O. Bergmann, Department of Neurology, Christian-Albrechts University Kiel, Schittenhelmstrasse 10, D-24105 Kiel, Germany (E-mail: t.bergmann@neurologie.uni-kiel.de).

sured by ratings and thresholds of tACS-induced phosphenes (Kanai et al. 2008). Here, the effectiveness of several stimulation frequencies to induce phosphenes was dependent on the currently predominant endogenous oscillation and was thus most effective in the beta range when eyes were open and in the alpha range when eyes were closed (but see Schwiedrzik 2009 for a critical comment). However, when testing the effect of different frequencies (1–45 Hz; applied over $M1_{HAND}$ during wakefulness), neither oscillatory tDCS (fixed anodal or cathodal polarity) nor tACS altered subsequent (off-line) $M1_{HAND}$ corticospinal excitability (MEPs) or spontaneous motor cortical electroencephalographic (EEG) activity (Antal et al. 2008).

These studies suggest that oscillatory transcranial stimulation can noninvasively shape endogenous cortical rhythms, thereby modifying ongoing internal processing modes of the brain. However, the underlying neuronal mechanisms are yet unknown. One important question is whether oscillating DC shifts can be directly imposed on the membrane of cortical neurons, given that this is the mechanism proposed for constant tDCS. Shifting the membrane potential repeatedly back and forth in an oscillating manner might be the basic principle by which oscillating transcranial stimulation can also take effect on endogenous rhythms.

We therefore probed the immediate impact of oscillating tDCS on the excitability of the fast-conducting corticospinal output neurons in the human $M1_{HAND}$. We applied either 0.8-Hz sinusoidally modulated anodal slow oscillatory tDCS (so-tDCS) or anodal c-tDCS to the left $M1_{HAND}$ and concurrently measured phase-dependent changes in MEP amplitude (on-line tDCS effects) in the contralateral hand muscles. MEP amplitudes were additionally measured before and after tDCS interventions (off-line tDCS effects). The experiments were performed during quiet wakefulness to maintain comparability with the majority of previous studies probing the effects of conventional c-tDCS on cortical excitability during this state of vigilance. We did not expect to trigger full-blown sleeplike slow oscillations (strong hyperpolarization followed by a rebound of massive synchronous firing), but hypothesized that so-tDCS might induce slow oscillatory changes in the membrane depolarization of idling motor neurons and thus cause slow oscillatory fluctuations in corticospinal excitability.

METHODS

Participants

Ten healthy right-handed male volunteers (mean age: 26.5 yr, range: 19–30 yr) participated in the experiments after they had given written informed consent. All participants were free of medication and had no history of neurological or psychiatric disease. Subjects were recruited from the student population of the University of Kiel. All of them were completely naïve toward the techniques of tDCS and TMS as well as regarding the detailed purpose of the study. Experimental procedures conformed to the Declaration of Helsinki and were approved by the Ethics Committee of the University of Kiel.

Experimental procedure

In a within-subject design, each participant underwent both slow oscillatory (0.8 Hz) and constant anodal tDCS to the left $M1_{HAND}$. The two stimulation modes were applied in separate experimental sessions performed ≥3 days apart and in randomized order. Participants were blinded to the type of tDCS and, despite the respective stimulation mode, experimental procedures were identical (Fig. 1). In both sessions, we repeatedly applied tDCS for 30 s. For monitoring and safety reasons the overall time of tDCS within a session was split into two consecutive blocks of 20.25 min. Each of the two on-line blocks consisted of thirty 30-s "tDCS trials" with anodal DC stimulation intermingled with five 30-s "tDCS-free trials" for use as a within-block baseline. Trials were separated by an intertrial interval (ITI) of about 5 s (Fig. 1).

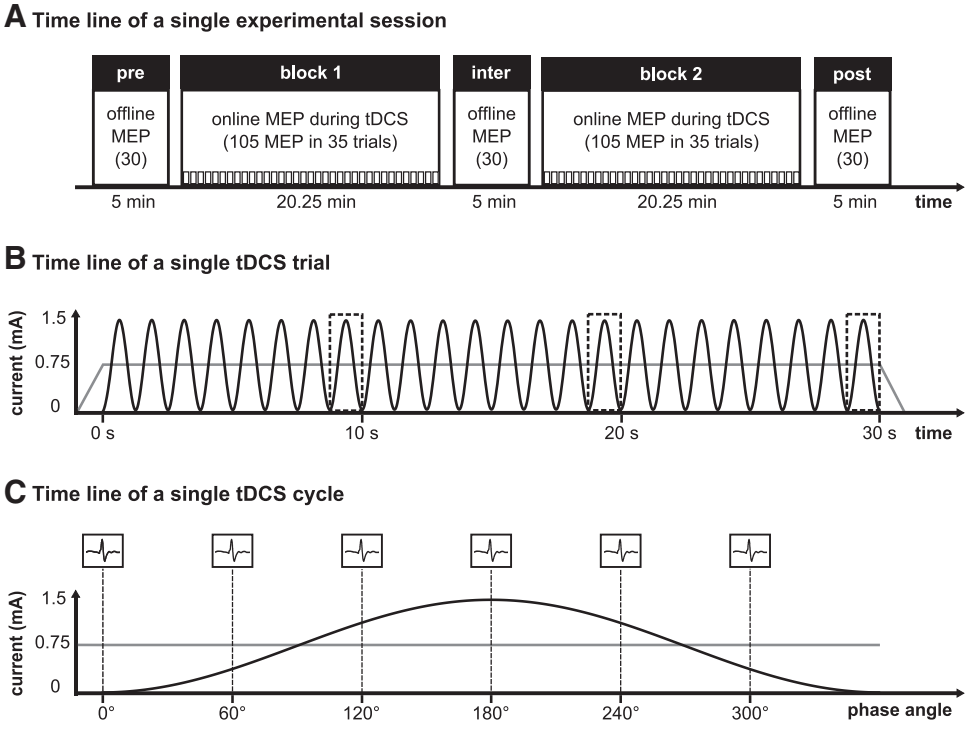

FIG. 1. Experimental procedure. *A*: slow oscillatory transcranial direct current stimulation (so-tDCS) and constant tDCS (c-tDCS) were applied in 2 experimental sessions on separate days. During one session 30 "off-line" motor-evoked potentials (MEPs) were measured before ("pre"), between ("inter"), and after ("post") 2 consecutive stimulation blocks. Each block consisted of 35 randomized trials (duration = 30 s, intertrial interval [ITI] = 5 s), 30 tDCS trials, and 5 tDCS-free trials. *B*: tDCS trials consisted of 30 s of anodal tDCS either slow oscillatory (0.8 Hz, 24 cycles, current range between 0 and 1.5 mA; black line) or constant (ramped up before and down after each trial for 1 s, constant current = 0.75 mA; gray line). Dashed rectangles indicate time windows of "on-line MEP" measurements. *C*: single-pulse transcranial magnetic stimulation (TMS) was applied over the left primary motor cortex (M1) to measure MEPs at different phase angles of the slow oscillatory cycle (black line) or corresponding time points during c-tDCS (gray line). During each trial only one of the 6 angles was probed in all 3 time windows.

Acute on-line effects of tDCS on the excitability of the corticospinal pyramidal neurons in the $M1_{HAND}$ were assessed by MEPs measured concurrently to the application of tDCS. Within each trial excitability of the $M1_{HAND}$ was probed by three single MEPs roughly 10, 20, and 30 s after stimulation onset or corresponding time points in tDCS-free trials (Fig. 1*B*). In the so-tDCS session MEPs were measured at various precisely defined phases of the slow oscillation (Fig. 1*C*). In one single trial all three MEPs were evoked at one of six different phase angles (0, 60, 120, 180, 240, and 300°; i.e., every 0.208 s with respect to the cycle onset) or corresponding time points during the c-tDCS session. Trials of different phase angles were applied semirandomized, that is, in consecutive groups each comprising all possible phase angles in randomized order, to guarantee a uniform distribution of phase angles over time. Off-line effects of tDCS on the excitability of the corticospinal neurons were assessed with single-pulse TMS as during tDCS. These MEP measurements were performed off-line before ("pre-tDCS"), between ("inter-tDCS"), and directly after ("post-tDCS") the stimulation blocks (Fig. 1*A*).

Transcranial DC stimulation

Anodal tDCS was applied through a bipolar montage of saline-soaked sponge electrodes (12 cm^2) using a battery-driven constant-current stimulator (Eldith DC-Stimulator, NeuroConn, Ilmenau, Germany). According to standard procedures (Nitsche and Paulus 2000), the center of the anode was placed directly above the "motor hot spot" of the first dorsal interosseus (FDI) muscle in the left $M1_{Hand}$, as identified by TMS before, whereas the cathode was fixed to the right forehead (Fig. 2*A*). In the c-tDCS trials the continuous-current strength of 0.75 mA (maximum current density: 0.0625 mA/cm^2) was slowly ramped up for 1 s before and ramped down for 1 s after each 30-s tDCS-trial (Fig. 1*B*) to avoid unpleasant sensations and the occurrence of retinal phosphenes. In the so-tDCS trials, 24 consecutive sinus waves with a cycle duration of 1.25 s (0.8 Hz) were generated. Current strength ranged from a minimum of 0 mA to a maximum of 1.5 mA (maximum current density: 0.125 mA/cm^2) (Fig. 1, *B* and *C*). Mean current density over time (0.0625 mA/cm^2) and total charge density per 30-s trial (1.875 C/cm^2) were thus equal for both stimulation modes (disregarding the short ramps in c-tDCS trials). The applied current is therefore both strong enough to be effective (Nitsche and Paulus 2000; Nitsche et al. 2007, 2008) and safe as being far below minimum values for inducing tissue damage (Nitsche et al. 2003b). Note, that the so-tDCS described earlier and the slow oscillation stimulation during sleep (Marshall et al. 2006b) differ in several parameters.

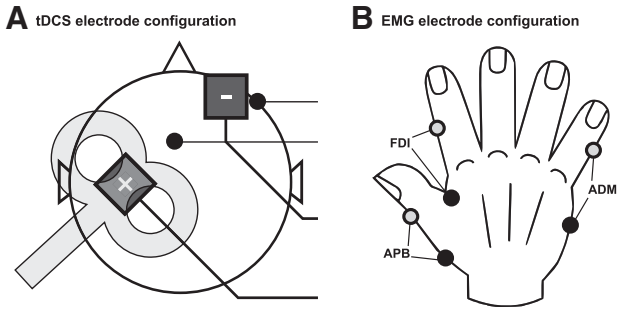

FIG. 2. Electrode configuration. *A*: the tDCS anode ("+") was placed directly over the representation of the first dorsal interosseus (FDI) muscle in the left $M1_{HAND}$, whereas the tDCS cathode ("−") was fixed on the right forehead. Recording electrodes (black circles) were placed both between stimulation sites and on the right lower lateral forehead to monitor the tDCS-induced current on the scalp. *B*: electromyographic (EMG) recordings were derived from the right FDI, abductor pollicis brevis (APB), and abductor digiti minimi (ADM) muscles using surface electrodes in bipolar belly-tendon montages (belly: dark gray; tendon: light gray).

Transcranial magnetic stimulation

Motor cortical excitability was assessed using single-pulse TMS over the left $M1_{HAND}$ while recording a surface electromyogram (EMG) from the contralateral proximal hand muscles (Fig. 2*B*). Single-pulse TMS over the left $M1_{HAND}$ was performed using a figure-of-eight–shaped "MC-B70" coil, with an outer diameter of 70 mm, connected to a MagPro-100 stimulator (MagVenture, Farum, Denmark). The magnetic stimulus had a monophasic pulse configuration with a width of about 70 μs (from onset to peak). The coil was positioned tangentially to the skull above the left $M1_{HAND}$ with the handle pointing backward and laterally at an angle of about 45° to the sagittal plane (Fig. 2*A*), inducing an electrical current in the brain tissue with a posterior–lateral to anterior–medial direction roughly perpendicular to the central sulcus. This current orientation is known to be optimal for evoking a motor response in the contralateral hand (Mills et al. 1992). The location and exact orientation at which stimuli at slightly suprathreshold intensity consistently yielded maximal MEPs in the contralateral FDI muscle were considered to constitute the "motor hot spot" and used for TMS of the $M1_{HAND}$ as well as for placement of the tDCS anode directly below the coil. The tDCS electrode cables were kept orthogonal to the main direction of the magnetic field to avoid retinal phosphenes, caused by induced currents in the electrode cables. TMS intensity (expressed as a percentage of maximum stimulator output) was adjusted at the beginning of each experimental session after positioning the coil above the tDCS electrode to elicit a mean peak-to-peak MEP amplitude between 0.5 and 0.75 mV in the relaxed contralateral FDI muscle and then remained constant throughout all measurements. Pre-, inter-, and post-tDCS off-line measurements consisted of 30 MEPs each (interstimulus interval [ISI] = 10 s, 5-min duration). The within-block baselines consisted of 15 MEP measurements per tDCS block (5 trials × 3 MEPs; ISI within trial = 10 s). On-line measurements consisted of 30 MEPs per phase angle (2 tDCS blocks × 5 trials × 3 MEPs; ISI within trial = 10 s).

Neuronavigation

We used frameless stereotaxy (TMS-Navigator, Localite, Sankt Augustin, Germany) based on a coregistered individual T1-weighted magnetic resonance image to navigate the TMS coil and to maintain its exact location and orientation throughout an experimental session. T1-weighted images were acquired some days before on a 3-Tesla magnetic resonance tomograph (Philips Achieva, Philips Medical Systems, Best, The Netherlands) using a standard MPRAGE sequence (repetition time = 7.7 ms, time to echo = 3.6 ms, flip angle = 8°, 170 sagittal slices, 1 × 1 × 1-mm voxel size, field of view = 224 × 224 mm).

Recordings

EMG activity was recorded from the right first dorsal interosseus (FDI), abductor pollicis brevis (APB), and abductor digiti minimi (ADM) muscles with Ag/AgCl surface electrodes using a bipolar belly-tendon montage (Fig. 2*B*). The raw EMG signals were amplified by 1,000 (D360, Digitimer, Welwyn Garden City, Herts, UK), filtered between 2 and 2,000 Hz (plus 50-Hz notch), and digitized at 5,000 Hz per channel (CED Power1401, 16-bit ADC; Cambridge Electronic Design [CED], Cambridge, UK). The administration of TMS pulses and EMG data recording, storage, and analyses were performed with Signal software (CED). Peak-to-peak amplitudes of each MEP (mV) were measured and mean MEP amplitudes were calculated for each condition using NuCursor software (Sobell Department of Motor Neuroscience and Movement Disorders, Institute of Neurology, Queen Square, London, UK).

Additionally, the tDCS-induced currents on the scalp were recorded with standard gold cup electrodes using a bipolar montage, with one

electrode placed between stimulation sites and the other one at the right lower lateral forehead (Fig. 2*A*) because this montage revealed the most stable signal (amplified by 300, filtered between 0.1 and 2,000 Hz).

Questionnaires

To additionally explore the potential effect of tDCS on subjective sleepiness, participants' subjective reports were gathered using a German version of the Stanford Sleepiness Scale (SSS) (Hoddes et al. 1973) before, after, and three times within each stimulation block. SSS ratings before and after tDCS blocks were reported orally, whereas those within blocks were reported by hand sign with the left hand (after 10, 20, and 30 trials) in TMS-free intervals.

After each session, participants completed a questionnaire asking for the unpleasantness of the experimental procedures in general and of the TMS and tDCS application in particular (ten-point rating scales ranging from "neutral" to "absolutely intolerable"). Participants were also asked to report any unpleasant sensations such as burning, pricking, tugging, itching, pressure, and pulsation during the stimulation (and, if applicable, to rate the severity on four-point rating scales) as well as any discomforts during and after the experiment such as headache, dizziness, nausea, or a feeling of pressure.

Data processing and statistical analyses

Unless specified otherwise, MEP values refer to those measured at the FDI muscle. For analyses of off-line tDCS effects, peak-to-peak amplitudes of off-line-MEPs from pre-, inter-, and post-tDCS measurements were first calculated for single trials and then averaged for each time point. Additionally, mean MEPs of tDCS-free trials within blocks 1 and 2 served as in-block off-line MEP measurement. For analyses of on-line tDCS effects, on-line-MEPs were processed analogously, but averaged separately, dependent on stimulation form, phase angle (or time-matched values for c-tDCS), and stimulation duration, i.e., time relative to stimulation onset. Subsequently, percentage deviations from mean MEPs of tDCS-free trials were calculated.

Repeated-measures ANOVAs were used to test for on-line and off-line tDCS effects on MEP amplitude. For on-line effects, the factors *stimulation mode* (so-tDCS, c-tDCS), *phase angle* (0, 60, 120, 180, 240, 300°), and *stimulation duration* (10, 20, 30 s) were included. Post hoc, a two-way ANOVA for *stimulation duration* was performed for tDCS-free trials only to exclude any within-trial baseline shifts (see RESULTS for rationale). Off-line effects were tested on the factors *stimulation mode* and *time* (pre-tDCS, within-block baseline 1, inter-tDCS, within-block baseline 2, post-tDCS). Greenhouse–Geisser (GG) correction for nonsphericity was applied where necessary, and ANOVAs were followed by post hoc two-sided paired-sample *t*-tests where applicable. To test for facilitatory on-line effects of anodal tDCS using the within-block baseline-adjusted data (with test values set to zero by definition), one-sided, one-sample *t*-tests were applied. Two-sided paired *t*-tests tested differences between the facilitatory effect of both stimulation modes. To test whether the initial facilitation of corticospinal excitability during tDCS (i.e., on-line effect) predicts the lasting increase in corticospinal excitability beyond the time of tDCS (i.e., off-line effect), linear regression analyses were applied using individually averaged on-line MEPs of the first 12 trials (2 of each phase angle) as independent variable and off-line MEPs of either inter- or post-tDCS measures as dependent variable (all adjusted to pre-tDCS baseline). Values of $P \leq 0.05$ were considered significant. Group data are given as means ± SE if not specified otherwise.

RESULTS

Neither TMS intensities (so-tDCS 81.60 ± 3.14%; c-tDCS 83.5 ± 3.07%) nor baseline MEP amplitudes (so-tDCS 0.70 ±

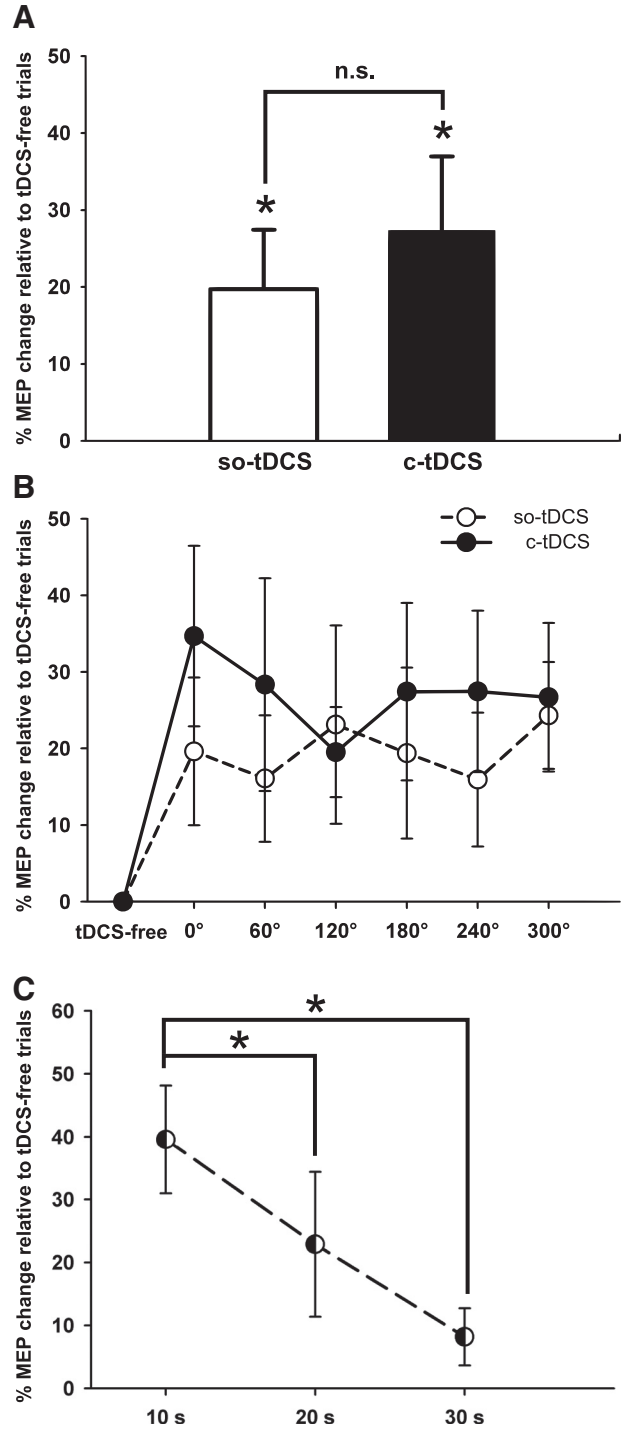

FIG. 3. On-line MEP effects. Means and SE are shown for percentage changes of on-line MEP amplitudes in the FDI muscle relative to tDCS-free trials constituting the in-block baseline. *A*: effects are displayed separately for so-tDCS and c-tDCS, with asterisks indicating significant ($P < 0.05$) differences from zero, and "n.s." indicating a nonsignificant ($P > 0.5$) direct comparison of both stimulation modes. *B*: effects of so-tDCS (open circles) and c-tDCS (closed circles) tDCS relative to stimulation-free test trials are depicted separately for the different phase angles (so-tDCS) or time-matched values (c-tDCS), respectively. *C*: facilitatory on-line tDCS effects (averaged over so-tDCS and c-tDCS) decreased within a 30-s trial relative to tDCS-free trials. Asterisks indicate significant ($P < 0.05$) differences from zero.

TABLE 1. *Online MEPs*

	Test Trial	Phase, deg					
		0	60	120	180	240	300
		A. Absolute MEP amplitudes in mV					
so-tDCS	0.99 ± 0.16	1.04 ± 0.16	1.01 ± 0.16	1.04 ± 0.14	1.03 ± 0.16	0.99 ± 0.14	1.05 ± 0.17
c-tDCS	0.86 ± 0.12	1.04 ± 0.17	0.98 ± 0.17	0.93 ± 0.13	0.97 ± 0.13	1.01 ± 0.21	0.98 ± 0.16
		B. Percentage change from test-MEP amplitudes					
so-tDCS	0 ± 0	20 ± 10	16 ± 8	23 ± 13	19 ± 11	16 ± 9	24 ± 7
c-tDCS	0 ± 0	35 ± 12	28 ± 14	20 ± 6	27 ± 12	27 ± 11	27 ± 10

Values are means ± SE, with respect to percentage change in MEP amplitude from tDCS-free in-block baseline at the FDI muscle. Values are displayed separately for different phase angles (so-tDCS) or time-matched values (c-tDCS), respectively. Note that percentage changes were first individually calculated and averaged afterward and that percentages of mean values would thus differ from the depicted values.

0.08 mV; c-tDCS 0.63 ± 0.07 mV) differed significantly between stimulation sessions ($P > 0.2$, paired-sample *t*-test).

On-line tDCS effects

All analyses regarding the on-line tDCS effect were performed on in-block baseline-adjusted MEP data (expressed as percentage change from tDCS-free trials) to control for any effects that may have built up over time.

We first tested whether anodal so-tDCS and c-tDCS exerted a facilitatory on-line effect on MEP amplitude. One-sided, one-sample *t*-tests revealed that MEPs were increased during anodal tDCS in general (collapsed over tDCS modes; mean 23%, $T_9 = 3.77$, $P = 0.002$) as well as during so-tDCS (mean 19%, $T_9 = 2.56$, $P = 0.015$) and c-tDCS (mean 27%, $T_9 = 2.84$, $P = 0.01$) per se (Fig. 3*A*). The acute facilitatory effect did not differ between stimulation modes ($P > 0.5$; two-sided paired *t*-test).

Next, we aimed to probe the phase dependence of on-line MEP facilitation during so-tDCS. Figure 3*B* and Table 1 depict the acute on-line MEP facilitation of both stimulation modes separately for all phase angles (or time-matched values in c-tDCS). Neither the two-way ANOVA for *stimulation mode* and *phase angle* nor a one-way ANOVA for *phase angle* during so-tDCS revealed any significant effects ($P > 0.5$). As can clearly be seen in Fig. 3*B*, a general facilitatory on-line effect was evident for both stimulation modes but there was no modulation by *phase angle* (i.e., acute current strength).

Because the presumed phase-dependent modulation of MEP size by means of so-tDCS might have needed some time to build up (e.g., due to slow phase-locking mechanisms), we additionally performed a three-way ANOVA for *stimulation mode*, *phase angle*, and *stimulation duration*. The only significant result, however, was a main effect of *stimulation duration* [$F_{(2,18)} = 4.49$, $P < 0.026$], which can be explained by a general decrease in MEP size from 10 to 20 s (40 vs. 23%; $T_9 = 2.30$, $P = 0.047$) as well as from 10 to 30 s (40 vs. 8%; $T_9 = 2.86$, $P = 0.019$) after tDCS onset. An additional two-way ANOVA for *stimulation mode* and *stimulation duration*, calculated exclusively for tDCS-free trials, revealed that within-block baseline MEPs did not change with increasing duration of the tDCS-free interval for any of the stimulation modes ($P > 0.3$). Thus the observed decrement of the facilitatory on-line effect seems indeed due to the in-trial duration of tDCS application (Fig. 3) and cannot be accounted for by mere shifts in within-block baseline.

Off-line tDCS effects

We then aimed to test for the off-line effects of both stimulation modes (Fig. 4). The ANOVA for *stimulation mode* and *time* revealed a main effect of *time* only [$F_{(4,36)} = 6.62$, $P = 0.004$, GG], whereas the main effect of *stimulation mode* and the interaction remained nonsignificant ($P > 0.4$). Due to the missing interaction, post hoc comparisons were performed on *time* levels only, averaged across *stimulation modes*. They revealed a continuous increase in MEP size from pre- to inter- to post-tDCS measurements (inter–pre: $T_9 = 3.01$, $P = 0.015$; post–inter: $T_9 = 8.98$, $P < 0.001$; post–-pre: $T_9 = 4.92$, $P < 0.001$), and also within-block MEPs were significantly increased from baseline (block 1–pre: $T_9 = 2.49$, $P = 0.034$; block 2–pre: $T_9 = 2.92$, $P = 0.017$).

Both anodal so-tDCS and c-tDCS had a strong facilitatory off-line effect on MEP amplitude that did not significantly differ between stimulation modes (about 39% after the first and 54% after the second 20-min block; Table 2).

Linear regression analyses

At an individual level, the amount of on-line facilitation of MEPs at the beginning of tDCS predicted later off-line effects of tDCS. The increase in MEP amplitudes during the first 12 trials of tDCS application relative to pre-tDCS baseline corre-

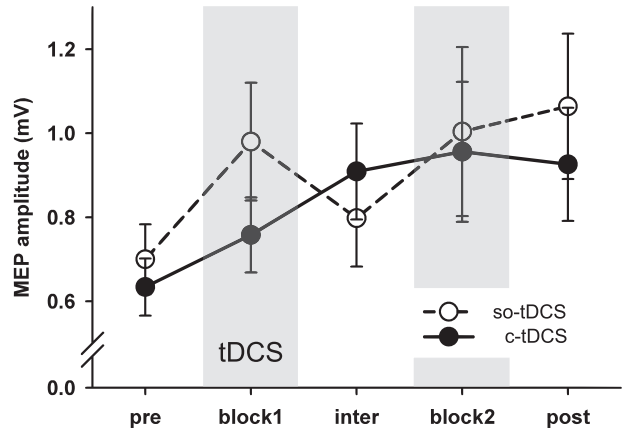

FIG. 4. Off-line MEP effects. Means and SE for off-line MEP amplitudes in the FDI muscle are shown for both stimulation modes: so-tDCS (open circles) and c-tDCS (filled circles). Off-line measurements before (pre), within (block1, block2), between (inter), and after (post) the 2 consecutive tDCS blocks are depicted.

TABLE 2. *Offline MEPs*

	Pre-tDCS Offline-MEP	Block 1 Test-MEP	Inter-tDCS Offline-MEP	Block 2 Test-MEP	Post-tDCS Offline-MEP
			A. Absolute MEP amplitudes in mV		
so-tDCS	0.70 ± 0.08	0.98 ± 0.14	0.80 ± 0.12	1.00 ± 0.20	1.06 ± 0.17
c-tDCS	0.63 ± 0.07	0.76 ± 0.09	0.91 ± 0.11	0.96 ± 0.17	0.93 ± 0.13
			B. Percentage change from baseline MEP amplitudes		
so-tDCS	0 ± 0	42 ± 20	22 ± 18	48 ± 24	55 ± 22
c-tDCS	0 ± 0	29 ± 19	55 ± 22	55 ± 22	52 ± 23

Values are means ± SE, with respect to percentage change in MEP amplitude from baseline (pre-tDCS) MEPs at the FDI muscle. Note that percentage changes were first individually calculated and averaged afterward and that percentage of mean values would thus differ from the depicted values.

lated with the facilitation of MEP amplitudes both after the first ($R^2 = 0.55$; $r = 0.74$, $P < 0.001$) and after the second tDCS block ($R^2 = 0.44$; $r = 0.66$, $P < 0.01$) as displayed in Fig. 5. This was also the case when MEP amplitudes during initial tDCS were calculated separately for 10-, 20-, and 30-s durations ($R^2 > 0.32$, $r > 0.57$, $P < 0.01$ for all analyses).

Topographical specificity of tDCS effects

Off-line MEP recordings in the APB and ADM muscles were available from only nine of ten subjects due to technical problems. To explore the topographical specificity of tDCS-effects, main analyses were performed independently for MEPs obtained from the APB and ADM muscles. The results of separate 2 × 5 two-way ANOVAs (*stimulation mode* × *time*) with appropriate post hoc *t*-tests mirrored the off-line tDCS effects in the FDI muscle (see Supplemental Table S1 for statistical details).[1] Likewise, one-sided, one-sample *t*-tests revealed phase-independent on-line facilitation of both stimulation modes in these muscles, whereas again no phase-dependent modulation was observed in separate 2 × 6 two-way ANOVAs (*stimulation mode* × *phase angle*) (see Supplemental Table S2 for statistical details). Taken together, these analyses confirm the main results found for the FDI muscle and demonstrate the expectably low topographical specificity of tDCS effects.

Sleepiness ratings

Because both c-tDCS and slow oscillation stimulation have been shown to enhance the amount of endogenous slow oscillatory cortical activity when applied during natural sleep (Marshall et al. 2004, 2006a), we also tested for any changes in participants' subjective sleepiness ratings. An ANOVA for *stimulation mode* and *time* (nine ratings: before, after, and three times within each of the two stimulation blocks) revealed a significant main effect of *time* only [$F_{(3.3,72)} = 9.12$, $P < 0.001$; GG] but no main effect of *stimulation mode* or interaction. As can be seen in Fig. 5, subjective sleepiness increased during tDCS blocks relative to tDCS-free periods as well as across the entire experiment similarly in both tDCS conditions.

Survey of potentially unpleasant sensations

Nine subjects completed the questionnaire (the first subject was questioned verbally and did not report any side effects). Tolerability of experimental procedures in general (mean ± SE: 2.89 ± 0.31) and of the TMS (mean ± SE: 2.11 ± 0.35) and tDCS (mean ± SE: 3.22 ± 0.49) application in particular was good and there was no difference between stimulation modes ($P > 0.16$, paired *t*-test). Participants also reported slight feelings of burning, pricking, tugging, itching, pressure, and pulsation during the tDCS application, which again did not differ between stimulation modes ($P > 0.2$, paired *t*-test). Two participants (one with both stimulation modes, the other with c-tDCS only) reported a light headache during the experiment, which had already decayed when they left the laboratory. Four participants (two with each stimulation mode) reported a feeling of pressure during the stimulation, which they ascribed to the fixation of sponge electrodes and neuronavigation markers on the head, not to the stimulation itself.

DISCUSSION

We found that anodal so-tDCS and c-tDCS over $M1_{HAND}$ were equally capable of inducing an increase in motor cortical excitability both during tDCS (on-line effect) and beyond the time of tDCS (off-line effect). At an individual level, the initial on-line facilitation of corticospinal excitability was predictive of the off-line effect on corticospinal excitability. The amount of enhancement in motor cortical excitability measured during so-tDCS did not vary with the phase of the applied current—not even between the minima and maxima of current strength—suggesting that anodal so-tDCS failed to induce sleeplike slow oscillatory changes at 0.8 Hz in $M1_{HAND}$ during wakefulness. The implication is that oscillatory excitability changes in a frequency that is inappropriate for the present brain state cannot be exogenously imposed on the cortex by means of oscillatory tDCS.

On-line tDCS effects

During ongoing stimulation both anodal so-tDCS and c-tDCS generally increased motor cortical excitability in the stimulated $M1_{HAND}$ relative to in-block tDCS-free trials and thus independently of any off-line effects developing concurrently. Although the effect of c-tDCS seemed to be slightly stronger (27% increase) than that of so-tDCS (19% increase), the difference was not significant (Fig. 3*A*).

Phase-locked analysis revealed that motor cortical excitability did not differ with respect to the phase angle of so-tDCS, not even between minimal (0 mA at 0°) and maximal (1.5 mA at 180°) current strength. Thus under the present experimental conditions exogenous DC currents with a sleeplike frequency of 0.8 Hz failed to induce measurable excitability changes in

[1] The online version of this article contains supplemental data.

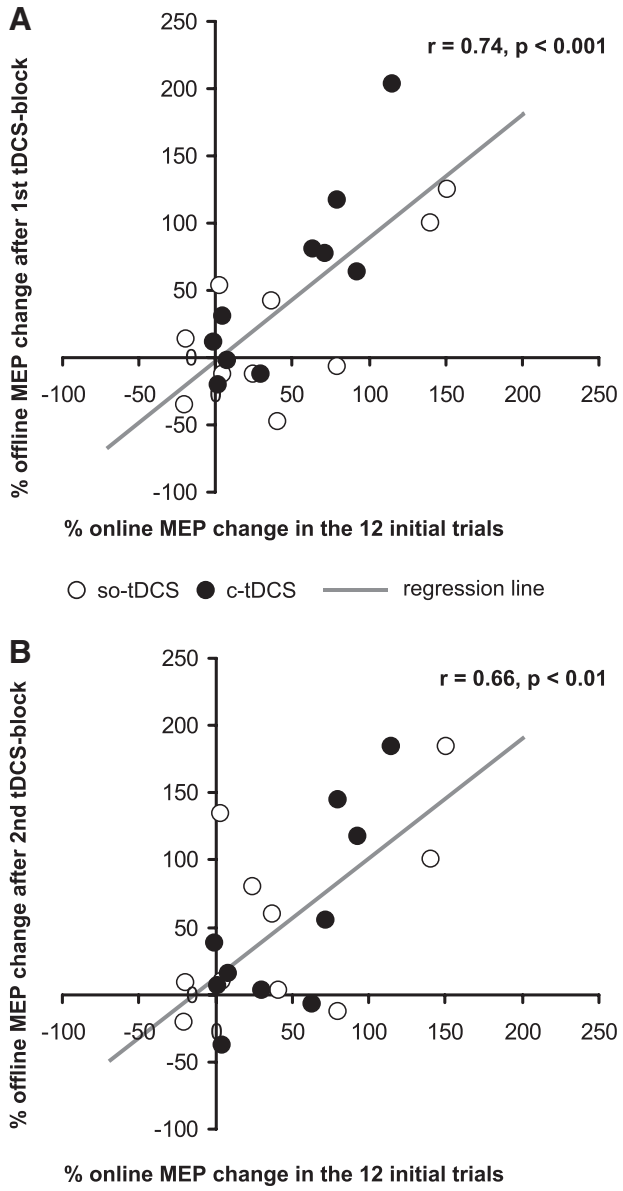

FIG. 5. Regression of off-line MEP effects on initial on-line MEP facilitation. Individual on-line facilitation of MEPs during the first 12 tDCS-trials (2 of each phase angle) of block 1 predicts later off-line MEP effects both (*A*) after the first ($R^2 = 0.55$; $r = 0.74$, $P < 0.001$) and (*B*) after the second tDCS-block ($R^2 = 0.44$; $r = 0.66$, $P < 0.01$). Both on-line and off-line MEPs were adjusted to pre-tDCS baseline. Scatterplots display data for both so-tDCS (open circles) and c-tDCS (filled circles) sessions for all subjects as well as linear regression lines (gray).

corticospinal $M1_{HAND}$ neurons. However, this absence in regulation of motor corticospinal excitability could be limited to the state of quiet wakefulness.

During NREM sleep, characterized by the occurrence of endogenous slow oscillations, corticospinal motor neurons in $M1_{HAND}$ might be more receptive for a slow oscillatory stimulation frequency of 0.8 Hz. This interpretation closely ties in with the findings of previous studies indicating a dependence of tDCS efficiency on the relationship between predominant endogenous EEG brain oscillations and frequency modulation of applied current (Kanai et al. 2008; Marshall et al. 2006a).

Spontaneous EEG rhythms reflect reverberating activity within reentrant neuronal circuits (such as the thalamocortical system). In addition, certain intrinsically defined properties of individual neurons may crucially contribute to the generation of membrane-voltage oscillators within a specific frequency (Hutcheon and Yarom 2000). These membrane properties are not fixed but subject to neuromodulatory modification (e.g., Lawrence 2008). Since slow oscillatory cortical activity at frequencies around 0.8 Hz is typically absent during wakefulness, but a dominant feature of NREM sleep (Steriade 2006), it is likely that wakefulness does not provide the appropriate neuronal milieu for the generation of slow oscillations. This explains why, in the present study, the cortical circuits in $M1_{HAND}$ showed no tendency to respond with excitability fluctuations to the externally imposed so-tDCS. Yet it remains to be tested whether time-varied exogenous DC currents that are tuned to the "preferred frequency" of the brain state at time of stimulation may induce phase-locked undulations in motor cortical excitability. Testing this hypothesis would require the measurement of phase-locked fluctuations in motor cortical excitability while applying *1*) so-tDCS during NREM sleep or *2*) "μ rhythm"-like 10-Hz oscillatory tDCS during relaxed wakefulness. Both approaches are challenging because *1*) TMS during sleep and EEG sleep monitoring during tDCS are technically highly demanding and *2*) 10-Hz oscillatory tDCS during wakefulness may be unpleasant and induce strong retinal phosphenes.

Interestingly, the facilitatory on-line tDCS effect was strongest after 10 s of stimulation and then strongly decayed within the subsequent 20 s of acute tDCS (Fig. 3*C*). This finding was somewhat surprising because the assumed shift in membrane potential was expected to build up with time. However, Priori and colleagues (1998) already hypothesized that neuronal elements in the motor cortex might adapt to and actively compensate for scalp DC-induced changes in the membrane potential. This potential compensatory mechanism, although sustained for the duration of stimulation, is quite short-lived because facilitatory effects recovered immediately after the 5-s ITI. The underlying sources of this regulatory mechanism apparently occurring at the cellular or network level are completely unknown, stressing the need for further research into

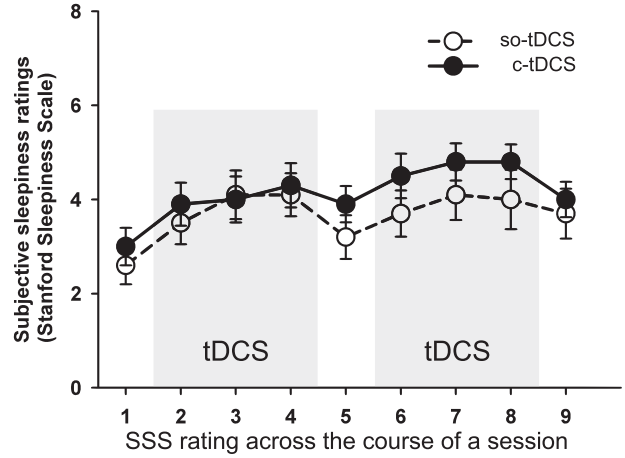

FIG. 6. Means and SE are shown for subjective sleepiness ratings on the Stanford Sleepiness Scale (SSS), with higher values indicating a stronger feeling of sleepiness. SSS ratings were obtained before, after, and 3 times within each stimulation block (indicated by gray frames). Subjective sleepiness increased across the course of a session similarly for both so-tDCS (open circles) and c-tDCS (closed circles).

the physiological responses acutely elicited by tDCS in the human cortex. This might include a thorough investigation of inhibitory processes across the time course of acute tDCS application, although Nitsche and colleagues (2005) reported no c-tDCS–induced changes in intracortical inhibition within 4-s epochs. In this context, the duration of a single tDCS epoch also appears to be of particular relevance. Although a similar on-line facilitation of MEP amplitudes (ranging from 20 to 50%) already emerges after 4 s of c-tDCS (Nitsche and Paulus 2000; Nitsche et al. 2003a, 2007), very brief c-tDCS epochs with a duration of 100 ms without ramps produce a less-consistent facilitation and require very high current densities to be efficient ($\leq$0.33 mA/cm^2) (Furubayashi et al. 2008).

Furthermore, early tDCS-induced on-line facilitation during the first dozen trials proved to be a good predictor for individual aftereffects after prolonged tDCS application. The predictive power of the initial on-line response to tDCS could be helpful in future studies to screen for responsive subjects or to probe stimulation efficacy before therapeutic application. Yet the neuronal underpinnings of this relationship are to be determined.

Off-line tDCS effects

Repeated application of tDCS also facilitated motor cortical excitability beyond the time of actual stimulation. Repeated measurements before, between, and after both stimulation blocks revealed a steady increase in excitability (about 39 and 54% after the first and second 20-min blocks, respectively), which was also roughly reflected by the within-block tDCS-free trials (Fig. 4). There was no significant difference in the amount of MEP facilitation between anodal so-tDCS and c-tDCS in the present study, indicating that both stimulation modes were equally effective in producing an excitability increase in corticospinal output neurons. In a separate series of experiments (S Groppa, TO Bergmann, C Siems, M Mölle, L Marshall, HR Siebner, unpublished data), we identified the mean current density over time (mA/cm^2) as an important variable determining the efficacy of so-tDCS to induce aftereffects in cortical excitability. Therefore we matched the mean current density over time between c-tDCS and so-tDCS in the present study. We wish to stress that this study was explicitly designed to compare the acute (on-line) effects of so- versus c-tDCS. Therefore variables influencing the efficacy of so-tDCS to induce long-lasting (off-line) effects on corticospinal excitability remain to be investigated.

Previous studies have always applied tDCS continuously (i.e., for several minutes) to induce lasting shifts in corticospinal excitability (Nitsche et al. 2008). In this study, tDCS was given continuously for only 30 s, with short breaks between consecutive tDCS applications. We also applied single-pulse TMS, both during and between tDCS trials. Despite the intermittent mode of tDCS and intermingled TMS measurements, the conditioning effect of tDCS gradually built up over time and reached a magnitude similar to that of conventional continuous tDCS. This implies that tDCS can be shortly interrupted or paired with occasional single TMS pulses without affecting the plasticity-inducing effects of tDCS. Since we applied single TMS pulses concurrently with tDCS, it is possible that the two types of stimulations had an additive influence on the off-line changes in MEP amplitude, for instance through a gating mechanism (Ziemann and Siebner 2008). This possibility needs to be explored more systematically in future studies.

A recent study by Antal and colleagues (2008) did not find any significant off-line effects in motor cortical excitability or spontaneous EEG recordings after application of oscillatory anodal tDCS to M1$_{HAND}$. We attribute this discrepancy with the present study to the significantly shorter stimulation durations (2–4 vs. 2 $\times$ 20 min) and lower current densities (maximum current density: 0.0156 vs. 0.125 mA/cm^2; mean current density: 0.0078 vs. 0.0625 mA/cm^2) that have been used by Antal and colleagues because it is unknown whether c-tDCS with these comparably weak parameters is able to induce plastic changes in the M1$_{HAND}$ either.

Subjective sleepiness

Subjective sleepiness ratings revealed that there were no stimulation-specific changes in subjective sleepiness. This was tested for because so-tDCS occurred in a frequency corresponding to that endogenously arising during NREM sleep. Independent of the stimulation mode, sleepiness apparently increased with session time as well as within stimulation blocks (Fig. 6). However, this effect is likely due to the participants' reduced motor activity and the monotonous sensory input associated with the experimental setting, rather than due to the stimulation itself. Because there was no sham stimulation, an unspecific tDCS effect on sleepiness cannot be ruled out in the present study.

Conclusions

To summarize, we found that acute motor cortical excitability is appreciably facilitated during both anodal so-tDCS and c-tDCS in general, but that there is no phase-locking of cortical excitability to the exogenously applied slow oscillation. With respect to the current literature we attribute this lack in phase dependence to the incompatibility of sleeplike 0.8-Hz stimulation and the present state of wakefulness. Moreover, acute facilitation effects rapidly decayed within 30 s of stimulation, but were totally renewed after a 5-s pause, suggesting the presence of fast regulatory mechanisms counteracting the induced DC shift.

GRANTS

This work was funded by the Deutsche Forschungsgemeinschaft Project A6/SFB 654 "Plasticity and Sleep." H. R. Siebner was supported by Bundesministerium für Bildung und Forschung Structural Grant 01GO0511 to NeuroImageNord.

REFERENCES

Antal A, Boros K, Poreisz C, Chaieb L, Terney D, Paulus W. Comparatively weak after-effects of transcranial alternating current stimulation (tACS) on cortical excitability in humans. *Brain Stimulation* 1: 97–105, 2008.

Bindman LJ, Lippold OC, Redfearn JW. The action of brief polarizing currents on the cerebral cortex of the rat (1) during current flow and (2) in the production of long-lasting after-effects. *J Physiol* 172: 369–382, 1964.

Fregni F, Freedman S, Pascual-Leone A. Recent advances in the treatment of chronic pain with non-invasive brain stimulation techniques. *Lancet Neurol* 6: 188–191, 2007.

Furubayashi T, Terao Y, Arai N, Okabe S, Mochizuki H, Hanajima R, Hamada M, Yugeta A, Inomata-Terada S, Ugawa Y. Short and long

duration transcranial direct current stimulation (tDCS) over the human hand motor area. *Exp Brain Res* 185: 279–286, 2008.

Gartside IB. Mechanisms of sustained increases of firing rate of neurones in the rat cerebral cortex after polarization: role of protein synthesis. *Nature* 220: 383–384, 1968a.

Gartside IB. Mechanisms of sustained increases of firing rate of neurons in the rat cerebral cortex after polarization: reverberating circuits or modification of synaptic conductance? *Nature* 220: 382–383, 1968b.

Hoddes E, Zarcone V, Smythe H, Phillips R, Dement WC. Quantification of sleepiness: a new approach. *Psychophysiology* 10: 431–436, 1973.

Hummel FC, Cohen LG. Non-invasive brain stimulation: a new strategy to improve neurorehabilitation after stroke? *Lancet Neurol* 5: 708–712, 2006.

Hutcheon B, Yarom Y. Resonance, oscillation and the intrinsic frequency preferences of neurons. *Trends Neurosci* 23: 216–222, 2000.

Kanai R, Chaieb L, Antal A, Walsh V, Paulus W. Frequency-dependent electrical stimulation of the visual cortex. *Curr Biol* 18: 1839–1843, 2008.

Lawrence JJ. Cholinergic control of GABA release: emerging parallels between neocortex and hippocampus. *Trends Neurosci* 31: 317–327, 2008.

Marshall L, Born J. The contribution of sleep to hippocampus-dependent memory consolidation. *Trends Cogn Sci* 11: 442–450, 2007.

Marshall L, Helgadottir H, Mölle M, Born J. Boosting slow oscillations during sleep potentiates memory. *Nature* 444: 610–613, 2006a.

Marshall L, Mölle M, Born J. Oscillating current stimulation–slow oscillation stimulation during sleep. (November 30, 2006). doi:10.1038/nprot.2006.299

Marshall L, Mölle M, Hallschmid M, Born J. Transcranial direct current stimulation during sleep improves declarative memory. *J Neurosci* 24: 9985–9992, 2004.

Mills KR, Boniface SJ, Schubert M. Magnetic brain stimulation with a double coil: the importance of coil orientation. *Electroencephalogr Clin Neurophysiol* 85: 17–21, 1992.

Nitsche MA, Cohen LG, Wassermann EM, Priori A, Lang N, Antal A, Paulus W, Hummel F, Boggio PS, Fregni F, Pascual-Leone A. Transcranial direct current stimulation: state of the art 2008. *Brain Stimulation* 1: 206–223, 2008.

Nitsche MA, Doemkes S, Karaköse T, Antal A, Liebetanz D, Lang N, Tergau F, Paulus W. Shaping the effects of transcranial direct current stimulation of the human motor cortex. *J Neurophysiol* 97: 3109–3117, 2007.

Nitsche MA, Fricke K, Henschke U, Schlitterlau A, Liebetanz D, Lang N, Henning S, Tergau F, Paulus W. Pharmacological modulation of cortical excitability shifts induced by transcranial direct current stimulation in humans. *J Physiol* 553: 293–301, 2003a.

Nitsche MA, Liebetanz D, Lang N, Antal A, Tergau F, Paulus W. Safety criteria for transcranial direct current stimulation (tDCS) in humans. *Clin Neurophysiol* 114: 2220–2222; author reply 2222–2223, 2003b.

Nitsche MA, Paulus W. Excitability changes induced in the human motor cortex by weak transcranial direct current stimulation. *J Physiol* 527: 633–639, 2000.

Nitsche MA, Seeber A, Frommann K, Klein CC, Rochford C, Nitsche MS, Fricke K, Liebetanz D, Lang N, Antal A, Paulus W, Tergau F. Modulating parameters of excitability during and after transcranial direct current stimulation of the human motor cortex. *J Physiol* 568: 291–303, 2005.

Priori A, Berardelli A, Rona S, Accornero N, Manfredi M. Polarization of the human motor cortex through the scalp. *Neuroreport* 9: 2257–2260, 1998.

Purpura DP, McMurtry JG. Intracellular activities and evoked potential changes during polarization of motor cortex. *J Neurophysiol* 28: 166–185, 1965.

Schwiedrzik CM. Retina or visual cortex? The site of phosphene induction by transcranial alternating current stimulation (Abstract). *Front Integr Neurosci* 3: 6, 2009.

Steriade M. Grouping of brain rhythms in corticothalamic systems. *Neuroscience* 137: 1087–1106, 2006.

Ziemann U, Siebner HR. Modifying motor learning through gating and homeostatic metaplasticity. *Brain Stimulation* 1: 60–66, 2008.

Supplemental material for

Acute changes in motor cortical excitability during slow oscillatory and constant anodal transcranial direct current stimulation

Til Ole Bergmann, Sergiu Groppa, Markus Seeger, Matthias Mölle, Lisa Marshall, Hartwig Roman Siebner

Supplemental Table 1: Statistical analyses of *offline tDCS-effects* for raw MEP data of FDI, APM and ADM muscles

	FDI			APB			ADM		
2x5 ANOVA (repeated measures)	**F**	**df**	**p**	**F**	**df**	**p**	**F**	**df**	**p**
stimulation mode	0.18	1,9	0.683	1.14	1,8	0.316	0.53	1,8	0.489
time	6.62	2.4, 21.3	**0.004***^{GG}	3.74	4,32	**0.013***	3.85	4,32	**0.012***
stimulation mode x time	0.94	4,36	0.451	0.15	4,32	0.960	0.34	2.5, 19.8	0.747^{GG}

Paired t-tests (two-sided)	**T**	**df**	**p**	**T**	**df**	**p**	**T**	**df**	**p**
block1 - pre	2.49	9	**0.034***	2.53	8	**0.035***	1.61	8	0.146
inter - pre	3.01	9	**0.015***	2.71	8	**0.027***	1.73	8	0.121
block2- pre	2.92	9	**0.017***	2.48	8	**0.038***	2.12	8	**0.06***
post - pre	4.92	9	**0.001***	3.42	8	**0.009***	2.57	8	**0.033***

Please note that APB and ADM data were only available from nine of ten subjects.
***** = significant with $p < 0.05$; GG = Greenhouse-Geisser correction for non-sphericity

Supplemental Table 2: Statistical analyses of *online tDCS-effects* for test-value adjusted MEP data from FDI, APM and ADM muscles

	FDI			APB			ADM		
One-sample T-test (one-sided)	**T**	**df**	**p**	**T**	**df**	**p**	**T**	**df**	**p**
tDCS (test-value-adjusted)	3.77	9	**0.002***	4.42	9	**0.001***	4.03	9	**0.001***
so-tDCS	2.56	9	**0.015***	3.14	9	**0.006***	3.59	9	**0.003***
c-tDCS	2.84	9	**0.010***	2.95	9	**0.008***	3.15	9	**0.006***
2x6 ANOVA (repeated measures)	**F**	**df**	**p**	**F**	**df**	**p**	**F**	**df**	**p**
stimulation mode	0.39	1,9	0.548	0.01	1,9	0.908	0.05	1,9	0.823
phase angle	0.33	5,45	0.894	0.62	3,26.6	0.608^{GG}	0.894	5,45	0.493
stimulation mode x phase angle	0.60	5,45	0.703	0.50	5,45	0.777	0.521	5,45	0.759

***** = significant with $p < 0.05$; GG = Greenhouse-Geisser correction for non-sphericity

Paper VI

Neuroscience 166 (2010) 1219–1225

SLOW-OSCILLATORY TRANSCRANIAL DIRECT CURRENT STIMULATION CAN INDUCE BIDIRECTIONAL SHIFTS IN MOTOR CORTICAL EXCITABILITY IN AWAKE HUMANS

S. GROPPA,[a]* T. O. BERGMANN,[a] C. SIEMS,[a] M. MÖLLE,[b] L. MARSHALL[b] AND H. R. SIEBNER[a,c]

[a]*Department of Neurology, Christian-Albrechts University, Kiel, Germany*

[b]*Department of Neuroendocrinology, University of Lübeck, Lübeck, Germany*

[c]*Danish Research Centre for Magnetic Resonance (DRCMR), Copenhagen University Hospital Hvidovre, Copenhagen, Denmark*

Abstract—Constant transcranial direct stimulation (c-tDCS) of the primary motor hand area ($M1_{HAND}$) can induce bidirectional shifts in motor cortical excitability depending on the polarity of tDCS. Recently, anodal slow oscillation stimulation at a frequency of 0.75 Hz has been shown to augment intrinsic slow oscillations during sleep and theta oscillations during wakefulness. To embed this new type of stimulation into the existing tDCS literature, we aimed to characterize the after effects of slowly oscillating stimulation (so-tDCS) on $M1_{HAND}$ excitability and to compare them to those of c-tDCS. Here we show that so-tDCS at 0.8 Hz can also induce lasting changes in corticospinal excitability during wakefulness. Experiment 1. In 10 healthy awake individuals, we applied c-tDCS or so-tDCS to left $M1_{HAND}$ on separate days. Each tDCS protocol lasted for 10 min. Measurements of motor evoked potentials (MEPs) confirmed previous work showing that anodal c-tDCS at an intensity of 0.75 mA (maximal current density 0.0625 mA/cm2) enhanced corticospinal excitability, while cathodal c-tDCS at 0.75 mA reduced it. The polarity-specific shifts in excitability persisted for at least 20 min after c-tDCS. Using a peak current intensity of 0.75 mA, neither anodal nor cathodal so-tDCS had consistent effects on corticospinal excitability. Experiment 2. In a separate group of ten individuals, peak current intensity of so-tDCS was raised to 1.5 mA (maximal current density 0.125 mA/cm2) to match the total amount of current applied with so-tDCS to the amount of current that had been applied with c-tDCS at 0.75 mA in Experiment 1. At peak intensity of 1.5 mA, anodal and cathodal so-tDCS produced bidirectional changes in corticospinal excitability comparable to the after effects that had been observed after c-tDCS at 0.75 mA in Experiment 1. The results show that so-tDCS can induce bidirectional shifts in corticospinal excitability in a similar fashion as c-tDCS if the total amount of applied current during the tDCS session is matched.

Key words: transcranial direct current stimulation, transcranial magnetic stimulation, motor cortex, neuronal plasticity.

*Corresponding author. Tel: +49-431-597-8823; fax: +49-431-597-8502.
E-mail address: s.groppa@neurologie.uni-kiel.de (S. Groppa).

Abbreviations: c-tDCS, constant current tDCS; EEG, electroencephalography; FDI, first dorsal interosseus; MEPs, motor evoked potentials; $M1_{HAND}$, primary motor hand area; so-tDCS, slowly oscillating transcranial direct current stimulation; tDCS, transcranial direct current stimulation; TMS, transcranial magnetic stimulation.

Transcranial direct current stimulation (tDCS) is a non-invasive stimulation technique to induce bidirectional shifts in excitability in the human cortex (Nitsche and Paulus, 2000). Its therapeutical use is currently under investigation (Nitsche et al., 2008). Most of the knowledge about the conditioning effects of tDCS on cortical excitability stems from electrophysiological studies in which a constant DC current was continuously applied to the primary motor hand area ($M1_{HAND}$) (Nitsche and Paulus, 2000, 2001; Nitsche et al., 2003b, 2008). In these studies, motor evoked potentials (MEPs) were elicited with single-pulse transcranial magnetic stimulation (TMS) before and after constant current tDCS (c-tDCS) and the time course of changes in MEP amplitude served as an index of the conditioning tDCS effects. Surface positive (anodal) c-tDCS of the $M1_{HAND}$ for several minutes is sufficient to increase motor cortical excitability, whereas several minutes of surface negative (cathodal) c-tDCS has the opposite effect (Nitsche et al., 2007; Nitsche and Paulus, 2000).

Recently several groups have started to use an oscillatory type of stimulation of tDCS or transcranial alternating current stimulation (Marshall et al., 2006; Antal et al., 2008; Kanai et al., 2008; Bergmann et al., 2009; Kirov et al., 2009). These studies used different types of current stimulation (DC in Antal et al., 2008; Marshall et al., 2006; Kirov et al., 2009 and AC in Antal et al., 2008; Kanai et al., 2008), but the rationale behind all these protocols with undulating current strength is to interact with endogenous oscillatory cortical activity. One such protocol involved cycles of ramp-like increases and decreases in current amplitude with a cycle rate of 0.75 Hz (Marshall et al., 2006, in press), and a bilateral prefrontal-mastoid electrode arrangement. Stimulation was given during early nocturnal non-rapid-eye-movement sleep. This intervention boosted the endogenous cortical slow oscillations characteristic for this period of sleep and enhanced the retention of sleep-dependent declarative memories (Marshall et al., 2006). During wakefulness the same stimulation protocol mainly increased the endogenous theta rhythm and facilitated declarative memory encoding when applied during learning (Kirov et al., 2009). The present study was designed to examine the conditioning effects of cathodal and anodal so-tDCS given over left $M1_{HAND}$ in the wake state on the corticospinal excitability and compare them to conventional c-tDCS. Although brain state, and specifics of stimulation protocol, for example region of stimulation differ between the present study and slow oscillation stimulation applied during sleep, the investi-

0306-4522/10 $ - see front matter © 2010 IBRO. Published by Elsevier Ltd. All rights reserved.
doi:10.1016/j.neuroscience.2010.01.019

gation of TMS-induced MEPs during wakefulness lends some advantages, while investigations conducted during wakefulness admit a limited temporal dynamics of electroencephalography (EEG), while during sleep the different stages should be taken into account. Secondly therefore, the assessment of motor cortical function within one session shows less response variability than between-session EEG analyses and also less variability than the assessment of sleep-dependent memory consolidation. Thirdly, there is a large body of existent literature to which results can be compared.

EXPERIMENTAL PROCEDURES

We performed two experiments using a common electrophysiological set-up. Experimental procedures had been approved by the Ethical Committee of the University of Kiel and all subjects gave written informed consent. Subjects had no history of neurological or psychiatric disease and were free of any acute or chronic CNS-affecting medication or illegal substances. Participants were comfortably seated in a reclining chair. They were asked to relax their hands and keep their eyes open. Auditory feedback of electromyographic activity in the target muscle was continuously provided to support complete relaxation. After each experimental session, participants filled out a questionnaire in which they were asked to report any unpleasant sensations like burning, pricking, tugging, itching, pressure and pulsation under the stimulation electrodes during the stimulation session. They were also asked to rate pain and unpleasantness of interventional tDCS on ten-point rating scales where ten corresponded to a maximal negative sensation and zero to no sensation at all.

Experiments I and II both used a within-subject design. Both experiments investigated effects of specific 10-min tDCS protocols on corticospinal excitability during the 20 min after the end of tDCS relative to pre-interventional baseline. tDCS and single-pulse TMS were both delivered to the left $M1_{HAND}$. To this end, suprathreshold single-pulse TMS was given to probe the excitability of the fast conducting corticospinal output neurons at rest before (baseline, T0), 5(T5), 10(T10) and 20(T20) minutes after each tDCS session.

Experiment 1

Ten right-handed healthy individuals (four males) with a mean age of 27 years (range 21–40) participated in Experiment 1. In four separate sessions, participants received one of four different tDCS protocols: anodal c-tDCS, cathodal c-tDCS, anodal so-tDCS or cathodal so-tDCS. The order of tDCS protocols was counterbalanced across participants. The current strength of c-tDCS was set at 0.75 mA, resulting in a maximal current density 0.0625 mA/cm^2. For so-tDCS, peak current strength was set at 0.75 mA and a cycle duration of 1.25 s, corresponding to a repetition rate of a sinus cycle of 0.8 Hz.

Experiment 2

A different group of 10 subjects (six males) with a mean age of 27 years (range 25–32) participated in this study. The effects of two so-tDCS protocols were tested on two separate days at least 1 week apart. In analogy to Experiment 1, anodal or cathodal so-tDCS was applied to left $M1_{HAND}$ for 10 min. The peak current strength was increased to 1.5 mA or a maximal current density of 0.125 mA/cm^2. Otherwise the settings of so-tDCS were identical to those used in Experiment 1. The order of anodal and cathodal so-tDCS was counterbalanced across participants.

Transcranial direct current stimulation

A commercial direct current stimulator was used for tDCS (Eldith DC-Stimulator, NeuroConn, Ilmenau, Germany). Using a bipolar arrangement, tDCS was applied through saline-soaked sponge electrodes (3×4 cm^2) with one electrode placed above the $M1_{HAND}$ and the other electrode over the right contralateral orbita (Fig. 1A). The sponge electrode targeting $M1_{HAND}$ was centred over the "motor hot spot" as revealed by single-pulse TMS (see below). The skin under both electrodes was prepared before the stimulation and a maximum impedance of 15 kΩ was controlled through the DC stimulator. Two types of tDCS were applied. The c-tDCS protocol consisted of a constant current at 0.75 mA (maximal current density of 0.625 mA/cm^2) which was continuously applied for 10 min. Beginning and end of stimulation were ramped up and down, respectively over 8 s to avoid peripheral sensory stimulation. The so-tDCS protocol involved a sinusoidal modulation of the anodal or cathodal current from zero to maximal intensity at a cycle rate of 0.8 Hz.

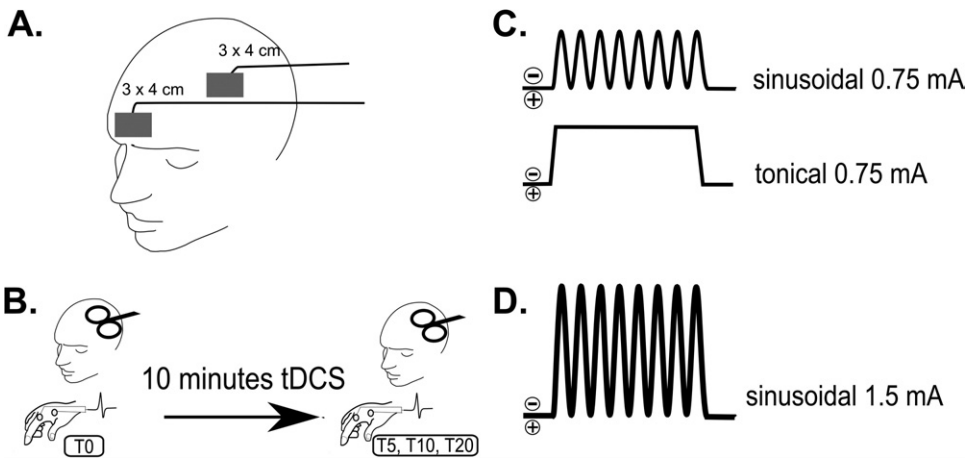

Fig. 1. Experimental setup. (A) Position and size of electrodes. The stimulation electrode is located on the left primary motor cortex and the reference electrode above the contralateral orbita. (B) 30 MEPs were collected before conditioning (T0), and 5-, 10, and 20 min afterwards (T5, T10, T20). (C) In Experiment 1 tDCS was given constantly at 0.75 mA or oscillatory at a peak intensity of 0.75 mA and a frequency of 0.8 Hz. (D) In Experiment 2, slow oscillatory tDCS was applied at a peak intensity of 1.5 mA and a frequency of 0.8 Hz. Note, in (C) and (D) no polarity was assigned to the types of tDCS.

Neuronavigated transcranial magnetic stimulation

TMS targeted the left $M1_{HAND}$ and the evoked motor response was recorded with surface EMG from contralateral first dorsal interosseus (FDI) muscle (Fig. 1). TMS was always given without the sponge electrodes used for tDCS being in place. Single magnetic pulses were applied through a figure-of eight coil (MC-B70) charged by a MagPro stimulator (MagVenture, Farum, Denmark). The stimuli had a monophasic waveform and elicited a maximum current in the tissue in the posterior-anterior direction. To determine the "motor hot spot" for positioning the coil we determined the site at which TMS evoked a maximal MEP in the right contralateral FDI muscle with the handle of the figure-of-eight coil pointing 45 degrees posterolaterally relative to the mid-sagittal line. Then, the motor threshold of the relaxed right FDI was determined by assessing the stimulus intensity required to evoke an MEP of 50 μV in at least five out of ten trials (Rossini et al., 1994). For MEP measurements, the stimulation intensity was adjusted to evoke MEPs of approximately 0.75 mV at baseline. This stimulus intensity ($SI_{0.75mV}$) was used to elicit MEPs throughout the experimental session. Excitability measurements were applied in blocks which consisted of thirty single pulse stimuli given on average every 4 s with a temporal jitter of $\pm$1.2 s. TMS measurements of corticospinal excitability were performed at baseline before tDCS (T0), at 5 min (T5), 10 min (T10) and 20 min (T20) after the end of tDCS (Fig. 1). MEPs were recorded from right FDI muscle with standard Ag–AgCl surface electrodes arranged in a belly-tendon montage. The raw EMG signals were amplified by 1000 (D360, Digitimer Ltd, Welwyn Garden City, Herts, UK), filtered between 2 and 2000 Hz (plus 50 Hz notch), and digitized at 5000 Hz per channel (CED Power1401, 16-bit-ADC; Cambridge Electronic Design, Cambridge, UK). Stimulus delivery and data recording were controlled using Signal Software (CED Power1401, 16-bit-ADC; Cambridge Electronic Design, Cambridge, UK). Peak-to-peak amplitudes of each MEP were analyzed offline using Nu Cursor software (Sobell Research Department of Motor Neuroscience and Movement Disorders, Institute of Neurology, University College of London, UK).

Frameless stereotaxy (TMS-Navigator, Localite, Sankt Augustin, Germany) was used to navigate the TMS coil, to maintain and reattain its exact location and orientation during the experimental session. Neuronavigation was based on coregistered individual T1-weighted magnetic resonance images of the whole brain which were acquired at 3 Tesla before the experiments (Philips Achieva, Philips Medical Systems, Best, The Netherlands). We used a standard MPRAGE sequence with an isotropic voxel resolution of 1 mm and sagittal slice orientation (TR=7.7 ms, TE =3.6 ms, flip angle=8°, 170 slices).

Statistical analyses

Statistical analyses were performed with SPSS software (Release 16.0, Copyright SPSS Inc, campus license). For all analyses, statistical threshold was set at $P<0.05$.

Experiment 1. The resting motor thresholds were compared in a one-factorial repeated-measures ANOVA with the within-subject factor type of tDCS (anodal c-tDCS at 0.75 mA, cathodal c-tDCS at 0.75 mA, anodal so-tDCS at peak intensity of 0.75 mA, cathodal so-tDCS at peak intensity of 0.75 mA). Differences in the subjective scores of pain and unpleasantness were assessed computing a one-factorial repeated-measures ANOVA with the within-subject factor type of tDCS. To test for tDCS induced changes in corticospinal excitability we performed a three-factorial repeated-measures ANOVA with the within-subject factors polarity (anodal vs. cathodal polarity), type of stimulation (constant current vs. slow oscillatory stimulation) and time of measurement (T0, T5, T10 and T20).

Experiment 2. Separate pair wise *t*-tests were performed to compare resting motor thresholds, subjective pain and unpleasantness scores in the anodal and cathodal so-tDCS session. Mean MEP amplitudes were analysed in a two-factorial repeated-measures ANOVA with the within-subject factors polarity (anodal vs. cathodal polarity) and time of measurement (T0, T5, T10 and T20).

Finally, we constructed an ANOVA model to compare anodal and cathodal c-tDCS at a constant current of 0.75 mA (Experiment 1) and anodal and cathodal so-tDCS at peak current strength of 1.5 mA (Experiment 2) with the within-subject factors polarity (anodal vs. cathodal polarity) and time of measurement (T0, T5, T10 and T20) and between-subject factor type of stimulation (constant current vs. slow oscillatory stimulation). If an ANOVA revealed significant main effects or interactions, the nature of these effects were explored with Fisher's LSD post hoc pair-wise comparisons ($P<0.05$; two-tailed; no adjustment for multiple comparisons).

RESULTS

None of the participants reported adverse effects during or after tDCS. Participants noticed no differences among the tDCS protocols that were applied in the two experiments. There were also no differences in subjective discomfort and subjective ratings for unpleasantness and pain perception (Table 1). The resting motor thresholds were comparable across sessions with no significant main effect of type of stimulation in the ANOVA.

Experiment 1

The continuous but not the slow-oscillatory type of stimulation produced a polarity-dependent bidirectional shift in corticospinal excitability (Fig. 2). This was confirmed by the ANOVA showing an interaction between the factors polarity and time [$F(3,24)=5.5285$, $P=0.005$] and among polarity, type and time [$F(3,24)=3.0578$, $P=0.047$]. There were no main effects of polarity, type of stimulation or the time of measurement. The post-hoc comparisons revealed an increase in MEP amplitude after anodal c-tDCS [T0–T10, $P=0.037$ and T0–T20, $P=0.002$] and a decrease in MEP amplitude after cathodal c-tDCS [T0–T5, $P<0.001$; T0–T10, $P=0.02$; T0–T20, $P<0.001$] (Fig. 2A). The individual

Table 1. Mean group values and standard deviation ($\pm$SD) for subjective ratings of unpleasantness and pain related to the tDCS protocols on a ten-point rating scale. A score of ten corresponds to maximal unpleasantness or pain. A score of zero equals no unpleasantness or pain

	Anodal c-tDCS 0.75 mA	Cathodal c-tDCS 0.75 mA	Anodal so-tDCS 0.75 mA	Cathodal so-tDCS 0.75 mA	Anodal so-tDCS 1.5 mA	Cathodal so-tDCS 1.5 mA
Unpleasantness	3.4±0.9	3.2±1.3	2.6±2.0	3.5±1.5	2.9±1.5	3.0±0.9
Pain	2.6±0.5	3.6±1.3	3.0±1.2	3.2±1.4	2.2±0.5	2.2±0.9

c-tDCS, constant current tDCS; so-tDCS, slow-oscillatory tDCS.

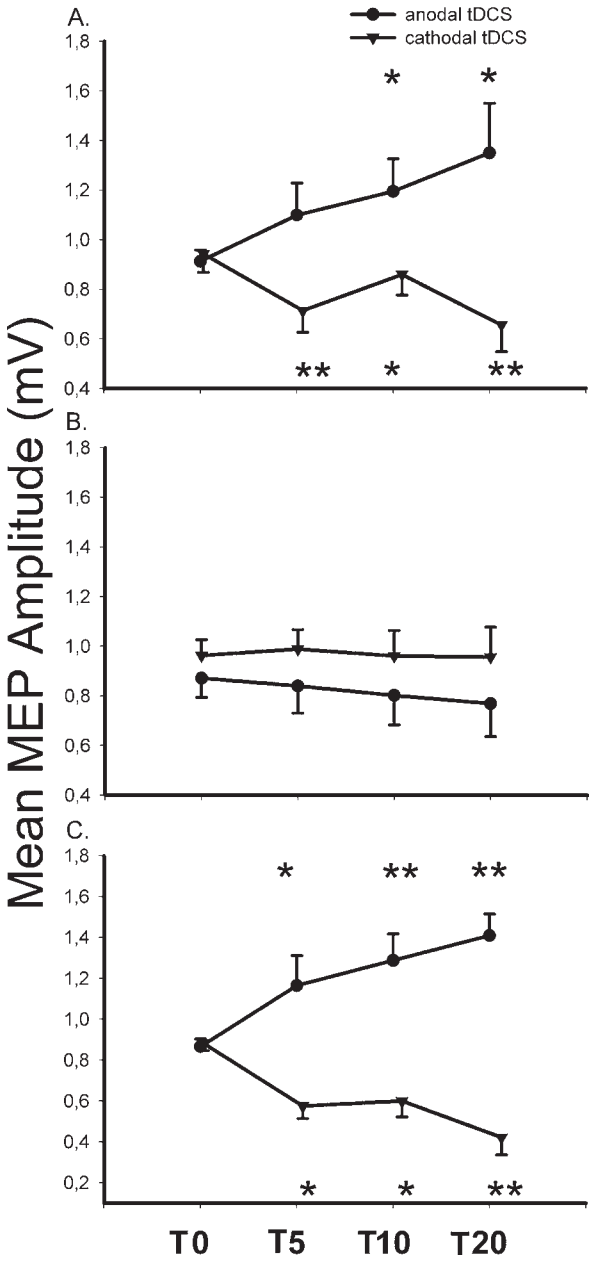

Fig. 2. Relative changes in mean MEP amplitudes after (A) constant current tDCS (c-tDCS) at a current intensity of 0.75 mA, (B) slow-oscillatory tDCS (so-tDCS) at peak intensity of 0.75 mA and (C) so-tDCS at peak intensity of 1.5 mA. The mean data given in panel A and B were acquired in the same group of subjects (Experiment 1), whereas the MEP amplitudes in panel C represent data from a different group of subjects (Experiment 2). Error bars indicate the standard error of the mean. T0, T5, T10 and T20 denote measurements at baseline, 5, 10 and 20 min after the conditioning paradigm. Asterisk indicates the significant level: * $P<0.05$, ** $P<0.005$.

increases in mean MEP amplitude after anodal c-tDCS ranged from 93% to 150% relative to baseline at 5 min after the end of stimulation. Individual decreases in mean MEP amplitudes ranged from 107% to 45% after cathodal c-tDCS at T5. In contrast, no changes in mean MEP amplitude occurred after so-tDCS at the peak intensity of 0.75 mA relative to pre-interventional baseline (Fig. 2B).

Experiment 2

When peak current strength of the slow oscillatory stimulation was increased to 1.5 mA, so-tDCS also induced a polarity-dependent polarity-specific shift in corticospinal excitability. The ANOVA revealed a main effect for the factor polarity [$F(1,5)=12.408$, $P=0.02$] and an interaction between time and polarity [$F(3,15)=21.075$, $P<0.001$]. Post-hoc comparisons showed higher MEP amplitudes after anodal so-tDCS at peak intensity of 1.5 mA [T0–T5, $P=0.009$; T0–T10, $P<0.001$; T0–T20, $P<0.001$] (Fig. 2C) and a reduction in mean MEP amplitude after cathodal so-tDCS at peak intensity of 1.5 mA [T0–T5, $P=0.003$; T0–T10, $P=0.010$; T0–T20, $P<0.001$] (Fig. 2C). At an individual level, the relative increases in mean MEP amplitude after anodal so-tDCS ranged from 80% to 170%. After cathodal so-tDCS, decreases in mean MEP amplitudes ranged from 101% to 40%.

The ANOVA model including the MEP data of the c-tDCS (0.75 mA) and so-tDCS (1.5 mA) sessions showed a significant main effect of polarity [$F(1,18)=43.167$, $P<0.001$] and a significant interaction between time and polarity [$F(3,54)=27,259$, $P<0.001$]. The continuous and slow oscillatory type of stimulation produced comparable after effects on MEP amplitudes. This was confirmed by the ANOVA which showed did not show any significant effect for the type of stimulation nor for the interaction between the type of stimulation, time of measurement, and polarity of tDCS.

DISCUSSION

The main finding of the present study is that a slow oscillatory type of stimulation can be as effective in inducing a polarity-dependent shift in motor cortical excitability as the conventional tonic type. Regardless of the mode of stimulation, anodal tDCS caused a lasting increase in excitability of the corticospinal output neurons, whereas cathodal tDCS resulted in a lasting reduction of corticospinal excitability. Critically, so-tDCS was only effective when the total amount of current that was applied during the tDCS session was matched to the current dose given during c-tDCS.

In the present experiment, anodal and cathodal c-tDCS served as control conditions. Ten minutes of anodal c-tDCS produced a consistent increase in MEP amplitudes. A switch in polarity reversed the direction of the excitability changes with a suppression of mean MEP amplitude after 10 min of cathodal c-tDCS. This polarity dependent shift in cortical excitability is in accordance with several previous studies (Nitsche and Paulus, 2000, 2001; Paulus, 2003; Siebner et al., 2004). It has been shown that the after effects of conventional c-tDCS critically depend on the intensity of tDCS. Using stimulation electrodes with an area of 35 cm^2, a five-minute session of anodal tDCS failed to induce an increase in corticospinal excitability when current intensity was reduced to 0.2 or 0.4 mA ($\sim$0.006 or $\sim$0.011 mA/cm^2) (Nitsche and Paulus, 2000). In contrast,

higher current intensities ranging from 0.6 to 1.0 mA (i.e. ~0.017 to ~0.029 mA/cm^2) increased motor cortical excitability. The higher the current intensity the stronger and longer was the tDCS induced MEP facilitation (Nitsche and Paulus, 2000). A similar response pattern emerged when the duration of anodal c-tDCS was systematically varied (Nitsche and Paulus, 2000). This implies that a minimal amount of current has to be injected into the cortex during c-tDCS conditioning to produce a consistent shift in corticospinal excitability.

In this study, we applied c-tDCS at a constant DC of 0.75 mA for 10 min. Using electrodes with an area of 12 cm^2 our c-tDCS protocol produced a current density of 0.0625 mA/cm^2 on the surface under stimulation electrodes. Due to the smaller stimulation electrodes the current density in our study was two to three times higher than the minimum current density which had been proven effective to induce lasting shifts in corticospinal excitability in the studies cited above. We chose this protocol because pilot experiments had shown that the total amount of current passing through the M1 was well above the threshold for changing corticospinal excitability. Indeed the c-tDCS protocol induced a consistent polarity-specific shift in corticospinal excitability which lasted for at least 20 min after the end of c-tDCS.

In striking contrast to c-tDCS, so-tDCS at a peak intensity of 0.75 mA failed to induce consistent shifts in motor cortical excitability. This does not exclude potential subthreshold effects on the excitability of intracortical inhibitory circuits which may have a lower modification threshold. At first glance, one might conclude that an oscillatory type of stimulation reduces the efficacy of tDCS to induce bidirectional changes in corticospinal excitability. There is however an alternative explanation. Due to the sinusoidal current modulation, the so-tDCS protocol applied only 50% of the total current during the 10 min of tDCS. Hence the inability of so-tDCS at 0.75 mA may also be explained by the reduced “total dose” of applied current relative to c-tDCS at 0.75 mA.

To resolve this ambiguity we performed a second experiment in which peak intensity of so-tDCS was increased from 0.75 to 1.5 mA while leaving the other parameters of tDCS unchanged. Since mean current intensity was 0.75 mA during so-tDCS, the total amount of current applied to M1 of the so-tDCS protocol in Experiment 2 was matched to the c-tDCS protocol of the first experiment. At a higher current intensity, so-tDCS produced a consistent polarity-specific shift in corticospinal excitability which did not differ from the excitability changes obtained with c-tDCS at 0.75 mA. We therefore conclude that so-tDCS and c-tDCS can induce similar effects on cortical excitability in awake subjects when the total current charge is matched. As former c-tDCS studies (Nitsche and Paulus, 2001; Nitsche et al., 2003a, 2007) have used an even lower current density (0.03 mA/cm^2) to successfully modulate $M1_{HAND}$ excitability, it is however possible that c-tDCS can already work at lower current densities than so-tDCS, which was not effective with at a mean current density of 0.03125 mA/cm^2 in the present study.

In good agreement with previous work using c-tDCS (Nitsche and Paulus, 2000), the direction of the excitability shift depends on the polarity of so-tDCS. Our results also suggest that the overall amount of current that is applied during the so-tDCS session determines whether or not the DC evokes a lasting shift in cortical excitability. However, we cannot exclude that other stimulation parameters beside total current charge may be important for the strength or duration of after effect, such as stimulation duration per se, electrode size, or distribution and depth of penetration of the electric field. Moreover, there might be differences in the duration of after effects between so-tDCS and c-tDCS beyond the investigated 20 min period, while within this time window excitability curves for c-tDCS and so-tDCS were highly similar.

When increasing the current intensity of tDCS, the higher current strength does not only increase the amount of polarization of a given neuron but also the depth of the polarizing effects in the stimulated cortical area (e.g. Miranda et al., 2009). Therefore it is conceivable that a stronger depth penetration of so-tDCS might have contributed to the observed cortical excitability changes after we had increased the current intensity from 0.75 to 1.5 mA, producing a maximal current density of 0.125 mA/cm^2. Alternatively, we could have had prolonged the duration of so-tDCS to match for total current charge, thereby matching the depth of penetration of the maximum electric field in the tissue between so-tDCS and c-tDCS (Nitsche et al., 2008). However, two considerations prompted us to increase the current intensity rather than using a longer stimulation period. We were concerned that the conditioning effects of tDCS may not depend on the total cortical charge but on the total charge applied in a given interval. If so, a longer stimulation duration would render the protocol less efficient. Moreover, a longer duration of so-tDCS might trigger homeostatic effects in the stimulated cortex that counteract the initial effects (Lang et al., 2004; Siebner et al., 2004). With regard to the after effects of tDCS, the relationship between stimulation duration and current strength is likely to be complex and might differ among c-tDCS, so-tDCS, or other types of tDCS.

Our findings reflecting the dependency on total charge are supported by recordings in the cat showing an approximately linear relation between the strength of the applied DC and changes in neuronal discharge frequency (Creutzfeldt et al., 1962). These assumptions are adequate for both anodal and cathodal currents which increase or decrease the spontaneous discharge rate, respectively. The work by Creutzfeldt et al. (1962) also revealed that a DC shift by an order of ten in comparison to the physiological DC shifts is needed to produce a measureable shift in cortical excitability. We suppose that these assumptions are in principal also valid for human studies. Modelling the current distribution shows that current density is determined by the gradient of the electric potential and is fairly uniform under the electrode (Miranda et al., 2006). While a different conductivity due to the skull between electrodes and tissue in human studies might change the uniformity of the field, the

physiological effects of the maximal current density should remain comparable. Furthermore, it is known that the current density in a conductor is proportional to the applied current, and it was reported that the amount of inward current through a dendritic membrane was larger when a more intense current was passed through a surface electrode (Landgren et al., 1962). Together with these studies on animals, the present results have important implications for the mechanistic interpretation of any change in brain function that can be observed after time-varying tDCS. Future studies applying time-varying tDCS protocols should be designed to be able to tease apart how much the temporal pattern of tDCS and the total amount of current injected into the cortex contribute to the observed change in brain function, such as a shift in cortical excitability, altered expression of oscillatory activity or a change in behaviour.

Beside the total amount and temporal modulation of the applied current, the present state of the stimulated neuronal networks at the time of tDCS appear to affect the immediate and lasting effects of tDCS, as indicated by early animal and recent human data (Creutzfeldt et al., 1962; Gorman, 1966; Kanai et al., 2008). Anodal polarization at rest might attenuate or eliminate surface-positive waves and enhance the surface-negative components of electrocortical potentials with cathodal polarization producing opposite changes whereas these effects disappear after habituation to the induced currents (Denney and Brookhart, 1962; Landau et al., 1964). Moreover, spectral power decrease in alpha and theta band and an increase in beta band after anodal stimulation was only observed at rest but not at during voluntary motor contraction (Pfurtscheller, 1970). Transcranial application of slowly oscillating DC at a rate of 0.75 Hz facilitates endogenous slow oscillations (0.5–1.5 Hz) and associated slow sleep spindles (8–12 Hz) when given during early nocturnal non-rapid-eye-movement sleep (Marshall et al., 2006). These effects were highly specific to the period and frequency of stimulation. A similar stimulation in the second half of the night caused no effects on sleep nor on subsequent memory recall, while a stimulation at a frequency of 5 Hz even induced a decrease in slow oscillation power but no effects on memory as well. All this data suggest an important interaction between stimulation frequency and the prevailing brain state (Marshall et al., 2006; Kirov et al., 2009). Therefore, the amount of current needed to modify cortical excitability with so-tDCS may well differ among functional states such as changes in the level of consciousness. For instance the cortex might become more susceptible to the conditioning effects of so-tDCS on cortical excitability during non-rapid eye movement sleep because of the spontaneous presence of cortical slow oscillations (Marshall et al., 2006). Based on the present data, we propose that both the temporal pattern of tDCS as well as the total amount of injected current determine the neuromodulatory effects of tDCS. We hypothesize that the relative influence of the two factors will significantly vary across different functional brain states. However, this hypothesis awaits experimental verification. While oscillatory current stimulation has been shown to interact with physiological processes of perception and memory, in the future it might also have therapeutical potential in disease states that are associated with a pathological change in oscillatory cortical activity such as Parkinson's disease or epilepsy by modulating pathological brain rhythms.

Acknowledgments—This work was funded by the Deutsche Forschungsgemeinschaft (Project A6, SFB 654 "Plasticity and Sleep"). H.R.S. was supported by a structural grant from the Bundesministerium für Bildung und Forschung (01GO0511) to NeuroImageNord.

REFERENCES

Antal A, Boros K, Poreisz C, Chaieb L, Terney D, Paulus W (2008) Comparatively weak after-effects of transcranial alternating current stimulation (tACS) on cortical excitability in humans. Brain Stimulat 1:97–105.

Bergmann TO, Groppa S, Seeger M, Molle M, Marshall L, Siebner HR (2009) Acute changes in motor cortical excitability during slow oscillatory and constant anodal transcranial direct current stimulation. J Neurophysiol 102:2303–2311.

Creutzfeldt O, Fromm GH, Kapp H (1962) Influence of transcortical D–C currents on cortical neuronal activity. Exp Neurol 5:436.

Denney D, Brookhart JM (1962) The effects of applied polarization on evoked electro-cortical waves in the cat. Electroencephalogr Clin Neurophysiol 14:885–897.

Gorman AL (1966) Differential patterns of activation of the pyramidal system elicited by surface anodal and cathodal cortical stimulation. J Neurophysiol 29:547–564.

Kanai R, Chaieb L, Antal A, Walsh V, Paulus W (2008) Frequency-dependent electrical stimulation of the visual cortex. Curr Biol 18:1839–1843.

Kirov R, Weiss C, Siebner HR, Born J, Marshall L (2009) Slow oscillation electrical brain stimulation during waking promotes EEG theta activity and memory encoding. Proc Natl Acad Sci U S A 106:15460–15465.

Landau WM, Bishop GH, Clare MH (1964) Analysis of the form and distribution of evoked cortical potentials under the influence of polarizing currents. J Neurophysiol 27:788–813.

Landgren S, Phillips CG, Porter R (1962) Cortical fields of origin of the monosynaptic pyramidal pathways to some alpha motoneurones of the baboon's hand and forearm. J Physiol 161:112–125.

Lang N, Nitsche MA, Paulus W, Rothwell JC, Lemon RN (2004) Effects of transcranial direct current stimulation over the human motor cortex on corticospinal and transcallosal excitability. Exp Brain Res 156:439–443.

Marshall L, Helgadottir H, Molle M, Born J (2006) Boosting slow oscillations during sleep potentiates memory. Nature 444:610–613.

Marshall L, Mölle M, Born J (in press) Oscillating current stimulation—slow oscillation stimulation during sleep. Nat Protoc; doi: 10.1038/nprot.2006.299.

Miranda PC, Faria P, Hallett M (2009) What does the ratio of injected current to electrode area tell us about current density in the brain during tDCS? Clin Neurophysiol 120:1183–1187.

Miranda PC, Lomarev M, Hallett M (2006) Modeling the current distribution during transcranial direct current stimulation. Clin Neurophysiol 117:1623–1629.

Nitsche M, Cohen LG, Wassermann EM, Priori A, Lang N, Antal A, Paulus W, Hummel F, Boggio PS, Fregni F, Pascual-Leone A (2008) Transcranial direct current stimulation: state of the art 2008. Brain Stimulat 1:206–223.

Nitsche MA, Doemkes S, Karakoese T, Antal A, Liebetanz D, Lang N, Tergau F, Paulus W (2007) Shaping the effects of transcranial direct

current stimulation of the human motor cortex. J Neurophysiol 97:3109–3117.

Nitsche MA, Fricke K, Henschke U, Schlitterlau A, Liebetanz D, Lang N, Henning S, Tergau F, Paulus W (2003a) Pharmacological modulation of cortical excitability shifts induced by transcranial direct current stimulation in humans. J Physiol 553:293–301.

Nitsche MA, Schauenburg A, Lang N, Liebetanz D, Exner C, Paulus W, Tergau F (2003b) Facilitation of implicit motor learning by weak transcranial direct current stimulation of the primary motor cortex in the human. J Cogn Neurosci 15:619–626.

Nitsche MA, Paulus W (2000) Excitability changes induced in the human motor cortex by weak transcranial direct current stimulation. J Physiol 527:633–639.

Nitsche MA, Paulus W (2001) Sustained excitability elevations induced by transcranial DC motor cortex stimulation in humans. Neurology 57:1899–1901.

Paulus W (2003) Transcranial direct current stimulation (tDCS). Suppl Clin Neurophysiol 56:249–254.

Pfurtscheller G (1970) Spectrum analysis of EEG: before, during and after extracranial stimulation in man [in German]. Elektromed Biomed Tech 15:225–230.

Rossini PM, Barker AT, Berardelli A, Caramia MD, Caruso G, Cracco RQ, Dimitrijevic MR, Hallett M, Katayama Y, Lucking CH (1994) Non-invasive electrical and magnetic stimulation of the brain, spinal cord and roots: basic principles and procedures for routine clinical application: report of an IFCN committee. Electroencephalogr Clin Neurophysiol 91:79–92.

Siebner HR, Lang N, Rizzo V, Nitsche MA, Paulus W, Lemon RN, Rothwell JC (2004) Preconditioning of low-frequency repetitive transcranial magnetic stimulation with transcranial direct current stimulation: evidence for homeostatic plasticity in the human motor cortex. J Neurosci 24:3379–3385.

(Accepted 9 January 2010)
(Available online 18 January 2010)